



Supplementary Materials for

Stereoselective amino acid synthesis by synergistic photoredox–pyridoxal radical biocatalysis

Lei Cheng¹, Dian Li¹, Binh Khanh Mai², Zhiyu Bo¹, Lida Cheng¹, Peng Liu^{2*} and Yang Yang^{1,3*}

Correspondence to: pengliu@pitt.edu; yang@chem.ucsb.edu

This PDF file includes:

Materials and Methods

Figs. S1 to S24

Tables S1 to S8

Table of Contents

I. General methods	3
II. General experimental and analytical procedure	7
III. Selected further results for reaction development	13
IV. DNA and protein sequences	20
V. Biocatalytic reactions using L-, D- and DL-serine and L-, L- <i>allo</i> - and DL-threonine	24
VI. Insights into enantiodivergent homophenylalanine synthesis	27
VII. Kinetic profile of the model reaction	29
VIII. Enantioconvergent nature of the biocatalytic transformation of (<i>rac</i>)-1p	33
IX. Radical trapping experiment and radical-derived byproduct identification	34
X. UV-Vis spectroscopic analysis	36
XI. X-ray crystal structures for the determination of absolute stereochemistry	38
XII. Synthesis and characterization of substrates	49
XIII. Synthesis and characterization of products	53
XIV HPLC calibration curves of amino acid products.....	73
XV. HPLC traces for Marfey's analysis	84
XVI. Computational studies and Marcus theory calculations	126
XVII. ^1H , ^{19}F and ^{13}C NMR spectra of compounds.....	244
References.....	297

I. General methods

General. All biocatalytic reactions were performed in a clear glass vial (13 × 100 mm, 8 mL, Fisherbrand) with magnetic stirring (500 rpm) using Heidolph Hei-Tec stir plates. Kessil LED PR160L-440 nm (max 45 W) was used as the visible light source. Unless otherwise noted, all chemicals and reagents were obtained from commercial suppliers (Sigma-Aldrich, VWR, Alfa Aesar, Combi-Blocks, AmBeed, Oakwood, and Enamine) and used without further purification. Silica gel chromatography was carried out using AMD Silica Gel 60, 230-400 mesh. ¹H and ¹³C NMR spectra were recorded on a Bruker 400 or 500 MHz instrument in DMSO-*d*₆, D₂O or methanol-*d*₄ (CD₃OD). ¹⁹F NMR and ¹¹B NMR spectra (where applicable) were recorded on a Bruker 400 or 500 MHz (¹H decoupled). Data for ¹H NMR are reported as follows: chemical shift (δ ppm), multiplicity (s = singlet, d = doublet, t = triplet, q = quartet, p = pentet, sext = sextet, m = multiplet, dd = doublet of doublets, dt = doublet of triplets, ddd = doublet of doublet of doublets, brs = broad singlet), coupling constant (Hz), integration. Sonication on a small scale was performed using a BioLogics ultrasonic homogenizer (model 150VT) equipped with a stepped microtip. Sonication on a large scale was performed using a Branson Digital Sonifier 450 Ultrasonic Processor. All IR spectra were recorded on a Thermo Scientific Nicolet iS5 spectrometer (iD5 ATR, diamond). High-resolution mass spectrometry data was obtained at the Mass Spectrometry Facilities at the University of California Santa Barbara and the University of California Irvine. High-resolution accurate mass (HRAM) ESI data was analyzed on a Waters LCT Premier mass spectrometer with a LEAP PAL autosampler with isocratic MeOH flow (no column; direct injection). Molecular formulas (MF) were validated by lock mass calibration to sodiated polyethylene glycol polymer or sodiated monoethyl ether polyethylene glycol polymer standards. High-resolution accurate mass (HRAM) EI data was acquired using a Waters LCT Premier time-of-flight (TOF) mass spectrometer. Masses of positively charged ions were calibrated using a methanol solution of polyethylene glycol or polyethylene glycol monomethyl ether as an internal standard. All samples were dissolved in methanol and were directly infused unless otherwise noted. Synthetic reactions were monitored by thin layer chromatography (TLC, Silicycle TLG-R10014BK-323 gel plates) using a UV-lamp or an appropriate TLC stain for visualization. UV-vis spectra were collected on a UV1800 Shimadzu spectrophotometer.

E. coli cells were grown using Luria-Bertani medium (LB) with 0.1 mg/mL ampicillin (LB_{amp}). Primer sequences for site-directed mutagenesis are provided below. T5 exonuclease, Phusion DNA polymerase, and *Taq* DNA ligase were purchased from New England Biolabs (NEB, Ipswich, MA). Potassium Phosphate Buffer (abbreviated as KPi buffer) was used as a buffering system for protein purification and storage unless otherwise specified.

Chromatography. Analytical reverse phase high performance liquid chromatography mass spectrometry (HPLC-MS) was carried out using a Shimazu-2040C 3D Plus with a 2020 MS detector and a Kromasil 100-5-C18 column (4.6 × 50 mm, 5 µm) with water (0.1% formic acid) and acetonitrile (0.1% formic acid) as the mobile phase. Yields were determined by calibration curves using 2-phenylbutyric acid as the internal standard. The enantiomeric ratios (e.r.'s) of non-canonical amino acid products were determined by Marfey's analysis as described below.

Reverse phase HPLC calibration curve development. Stock solutions of authentic products (80 mM in CH₃CN/1 M aq. HCl (v:v = 1:1)) and internal standard (2-phenylbutyric acid) (80 mM in CH₃CN/1 M aq. HCl (v:v = 1:1)) were freshly prepared. To a 1.5 mL microcentrifuge tube were added 50 µL of internal standard stock solution (4 µmol), 10, 20, 30, 40 and 50 µL of product stock solution was added to each tube, followed by the addition of 940, 930, 920, 910 and 900 µL CH₃CN/1 M aq. HCl to make the total volume to be 1 mL. The mixture was vortexed (20 s for 3 times) to ensure good mixing. The mixture was transferred to a 1.5 mL glass vial for HPLC analysis. The calibration curves detailed below plot product yield (y-axis) against the ratio of the peak area of the product to the peak area of the internal standard from HPLC analysis (x-axis). In the development of our calibration curves, care was taken such that the concentration of calibration curve samples was close to analyte samples. Compounds such as **3o** without strong UV-Vis absorption were first derived with Marfey's reagent under standard conditions, and the calibration curve was developed based on the UV-Vis absorption of derived products with different concentrations; care was taken such that the derivatization step in calibration curve development was carried out under similar conditions as analyte derivatization.

Cloning, site-directed mutagenesis. pET-22b (+) was used as the cloning and expression vector for *Pyrococcus furiosus* tryptophan synthase β-subunit variants, including L-*Pf*PLP^β, D-*Pf*PLP^β and related mutants described in this study (33, 51, 61, 62). Genes of PLP-dependent enzymes

were codon optimized and purchased from General Biol as plasmids using pET-22b(+) as the cloning vector. The gene of interest (GOI) was cloned into pET-22b(+) between restriction sites *Nde*I and *Xho*I and this construct has a C-terminal 6X His tag. Site-directed mutagenesis was carried out using the overlap extension polymerase chain reaction (PCR). The PCR products were digested with *Dpn*I, gel purified, and ligated using a Gibson mix prepared from 5X isothermal (ISO) reaction buffer (25% PEG-8000, 500 mM Tris-HCl pH 7.5, 50 mM MgCl₂, 50 mM DTT, 1 mM each of the dNTPs, and 5 mM NAD), T5 exonuclease, Phusion DNA polymerase, and *Taq* DNA ligase (63). The ligation mixture was used directly to transform electrocompetent *E. coli* strain *E. coli* BL21(DE3) cells (Lucigen).

Expression and purification of L-*PfPLP*^B and D-*PfPLP*^B. A single colony from LB_{amp} agar plate was picked using a sterile toothpick and cultured in LB_{amp} media (25 mL) at 37 °C and 230 rpm overnight. This preculture was used to inoculate a 1 L of TB_{amp} media in a 4 L Erlenmeyer flask, and the expression culture was incubated at 37 °C and 230 rpm for ca. 3 h, until the OD₆₀₀ reached ca. 2.0. The culture was cooled on ice for 20 min and induced with 1.0 mM isopropyl-β-D-thiogalactopyranoside (IPTG) (final concentration). Protein expression was conducted at 20 °C and 220 rpm for 20 h. *E. coli* cells were harvested by centrifugation at 4 °C and 4,500 g for 10 min using a Thermo Scientific Sorvall Lynx 6000 superspeed centrifuge. The cell pellet was then flash frozen with liquid nitrogen.

For protein purification, frozen cells were resuspended in HisTrap buffer A (25 mM KPi, 100 mM NaCl, 20 mM imidazole, pH 8.0, 2–3 mL/g of cell wet weight), following by the addition of the 10 mM PLP (stock solution in 50 mM, pH 8.0 KPi buffer) to a final concentration of 0.2 mM. The mixture was suspended and lysed by sonication using a Branson Digital Sonifier 450 Ultrasonic Processor. To pellet cell debris, lysates were centrifuged using a Lynx 6000 superspeed centrifuge (15,000 g, 60 min, 4 °C). L-*PfPLP*^B or D-*PfPLP*^B containing a C-terminal 6×His tag was purified with a Ni-NTA column (5 mL HisTrap HP, GE Healthcare, Piscataway, NJ) using an AKTA Start protein purification system (GE healthcare). Proteins were eluted on a linear gradient from Histrap buffer A (25 mM KPi, 100 mM NaCl, 20 mM imidazole, pH 8.0) to Histrap buffer B (25 mM KPi, 100 mM NaCl, 500 mM imidazole, pH 8.0) over 10 column volumes (CVs). Proteins eluted at approximately 100 mM imidazole. Fractions containing L-*PfPLP*^B or D-*PfPLP*^B were combined, followed by the addition of a PLP stock solution (10 mM PLP in 50 mM KPi

buffer, pH 8.0) to a final PLP concentration of 0.2 mM. The enzyme solution was concentrated and subjected to three rounds of buffer exchange using the storage buffer (buffer C, 50 mM KPi, pH 8.0) using ultracentrifugal filters (30 kDa molecular weight cut-off, Amicon Ultra, Sigma Millipore) to remove excess salt and imidazole. Protein concentration was measured with Nanodrop and normalized to ca. 50 mg/mL. Typically, 1 L of TB_{amp} expression culture provides 230 mg protein. Concentrated proteins were aliquoted and flash-frozen in liquid N₂ and stored at -80 °C until further use. If needed, 10% glycerol was added to the final storage buffer to enhance long-term protein stability upon storage.

II. General experimental and analytical procedure

General experimental procedure for synergistic photoredox and pyridoxal radical biocatalysis. L-*Pf*PLP β or D-*Pf*PLP β (ca. 50 mg/mL, 100 μ L) was allowed to thaw and kept on top of ice. In a Coy anaerobic chamber, the following stock solutions were prepared: alkyltrifluoroborate salt (200 mM in degassed DMSO), photocatalyst (13.3 mM in degassed DMSO), L-serine or L-threonine (500 mM in degassed 0.2 M KPi buffer, pH 7). To a 2-dram vial containing a stir bar were added the KPi buffer (200 mM, pH indicated below), 20 μ L RBF₃K stock solution, 24 μ L L-serine or 40 μ L L-threonine stock solution, 30 μ L photocatalyst stock solution, followed by ca. 34 μ L L-*Pf*PLP β or D-*Pf*PLP β solution (the specific volume of the enzyme stock solution is dependent on the concentration of the specific enzyme sample). With L-serine, the total reaction volume was 1.0 mL; the final concentrations of each reaction component are as follows: 4.0 mM RBF₃K, 12.0 mM L-serine, 0.04 mM L-*Pf*PLP β , and 0.4 mM photoredox catalyst. With L-threonine, the total reaction volume was 0.6 mL; the final concentrations of each reaction component are as follows: 6.7 mM RBF₃K, 33.3 mM L-threonine, 0.067 mM D-*Pf*PLP β , and 0.67 mM photoredox catalyst. The reaction vial was then sealed and removed from the Coy anaerobic chamber and submerged in a water bath at 50 °C. The reaction mixture was allowed to stir at 500 rpm and 50 °C and illuminated with a 45 W Kessil LED lamp for 12 h.

Yield determination. Upon completion, the reaction mixture was quenched with 1 mL of CH₃CN/1 M aq. HCl (v:v = 1:1). 50 μ L of a stock solution of 2-phenylbutyric acid (80 mM in CH₃CN/1 M aq. HCl) was then added as the internal standard. After vigorous mixing, ca. 1.0 mL of reaction mixture was transferred into a 1.5 mL Eppendorf tube and centrifuged at 15,000 rpm for 15 min. The solution was filtered through a 0.22 μ m PES membrane filter (diameter = 1.3 cm) and analyzed by LC-MS. The yield was determined by LC-MS using 2-phenylbutyric acid as a standard with the aid of calibration curves. The remaining reaction mixture was then used for the determination of enantiomeric ratio by Marfey's analysis as detailed below. A representative LC-MS analysis method is as follows: Kromasil 100-5-C18 column (4.6 \times 50 mm, 5 μ m), flow rate = 0.70 mL/min, hold at 5% CH₃CN (0.1% formic acid) in H₂O (0.1% formic acid) for 1.0 min, ramp up to 95% CH₃CN (0.1% formic acid) in H₂O (0.1% formic acid) over the course of 11.0 min, hold at 95% CH₃CN (0.1% formic acid) in H₂O (0.1% formic acid) for 1.0 min.

Enantiomeric ratio (e.r.) and diastereomeric ratio (d.r.) determination using our modified Marfey's analysis.

General method. Marfey's analysis is widely used to determine the stereochemical purity of amino acid products (64, 65). We developed a modified procedure for Marfey's analysis to reliably determine the enantio- and diastereomeric ratios of amino acid products described in this work. In our protocol, the ratio of Marfey's reagent to combined amino acid content in the reaction mixture is > 2:1 to ensure the complete conversion of biocatalytically formed, enantioenriched amino acids.

Note: Following this protocol is critical to correctly assaying the enantiopurity of enzymatically produced amino acids. An excess of Marfey's reagent is required. When the Marfey derivatization proceeds to only partial conversion, kinetic resolution of chiral amino acids oftentimes occurs, leading to an inaccurate estimation of enantiomeric ratios.

To a 1.5 mL glass vial were added 50 μ L (for L-serine) or 40 μ L (for L-threonine) of the reaction mixture as described above, 1 M aq. NaHCO₃ (100 μ L), DMSO (50 μ L) and a stock solution of Marfey's reagent, namely (S)-1-fluoro-2-4-dinitrophenyl-5-L-alanine amide ((S)-FDAA) or (R)-1-fluoro-2-4-dinitrophenyl-5-L-alanine amide ((R)-FDAA) (50 μ L, 20 mM in acetone). The vial was then placed in a microplate shaker and shaken at room temperature and 800 rpm for 8–12 h. The reaction mixture was diluted with 1:1 CH₃CN/1 M aq. HCl (800 μ L) to afford a clear solution and analyzed by LC-MS.

A representative LC-MS analysis method is as follows: Kromasil 100-5-C18 column (4.6 × 50 mm, 5 μ m), flow rate = 0.70 mL/min, hold at 5% CH₃CN (0.1% formic acid) in H₂O (0.1% formic acid) for 0.5 min, ramp up to 60% CH₃CN (0.1% formic acid) in H₂O (0.1% formic acid) over the course of 11.5 min, ramp up to 95% CH₃CN (0.1% formic acid) in H₂O (0.1% formic acid) over the course of 3.0 min, hold at 95% CH₃CN (0.1% formic acid) in H₂O (0.1% formic acid) for 1.0 min.

Determination of enantiomeric ratio (e.r.) of amino acids with one stereocenter. First, independently synthesized racemic amino acids using chemical methods (*vide infra*) were analyzed (**Fig. S1**). Before derivatization, enantiomers **L-3** ((S)-3) and **D-3** ((R)-3) were inseparable by achiral HPLC. After derivatization with Marfey's reagent, all the amino acids were

consumed as indicated by LC-MS analysis. Enantiomeric (*S*)-3 and (*R*)-3 were converted into diastereomeric (*S,R*)-3' and (*R,R*)-3', and these diastereomers could be easily separated by achiral HPLC. With racemic 3, the peak area ratios, $A((S,R)-3')/A((R,R)-3')$, were all found to be 50:50. This indicated that with an excess of Marfey's reagent, both the L- and the D-amino acid L-3 ((*S*)-3) and D-3 ((*R*)-3) were fully converted into the S_NAr product (*S,R*)-3' and (*R,R*)-3', respectively. Furthermore, it showed that diastereomeric (*S,R*-3' and (*R,R*)-3' had the same UV responding factor under appropriate wavelength (e.g., 330 nm). Together, these results indicated that the peak area ratio of derivatized diastereomer (*S,R*-3' and (*R,R*)-3', namely $A((S,R)-3')/A((R,R)-3')$, equals the enantiomeric ratio (e.r.) of 3, namely (*S*)-3 : (*R*)-3.

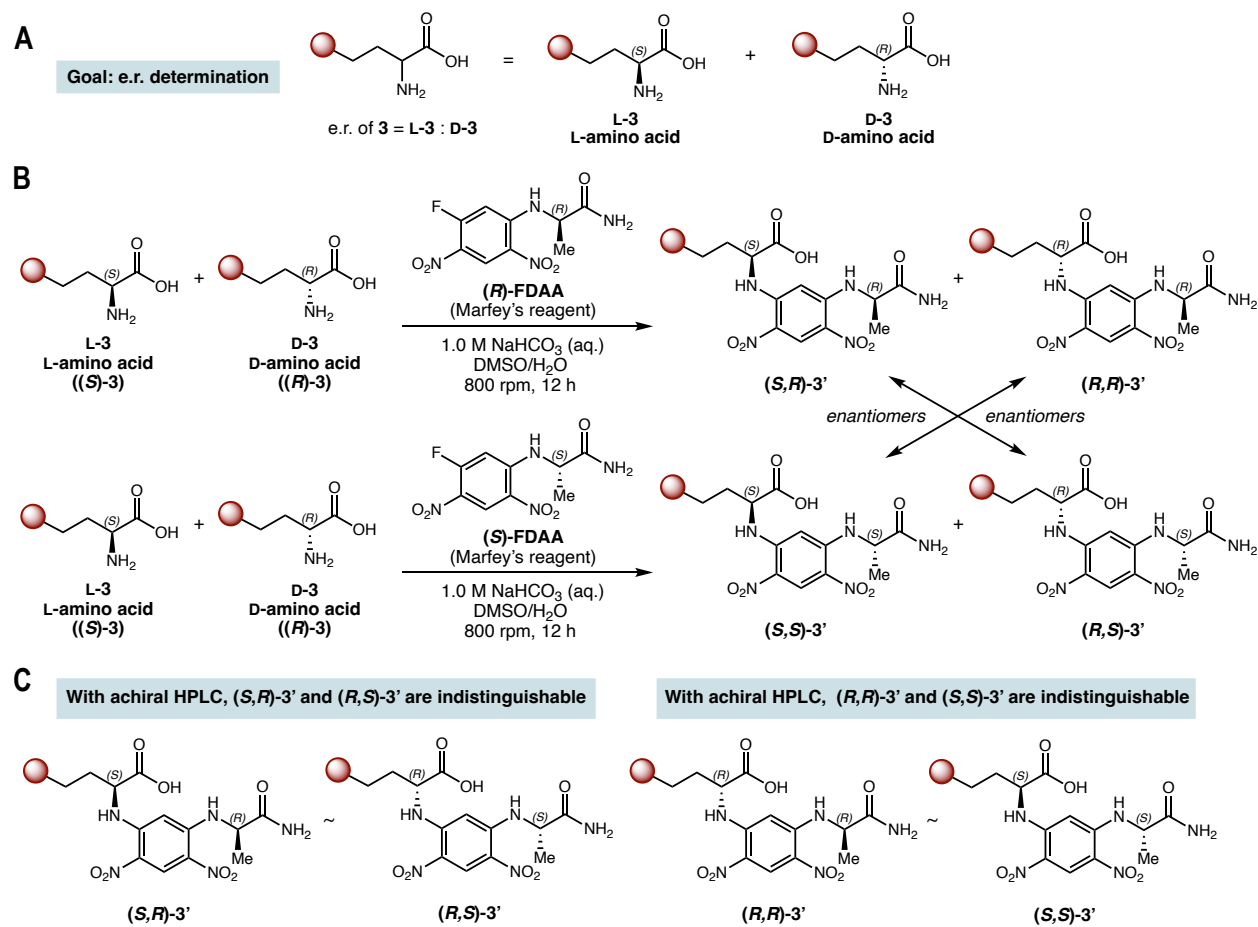


Fig. S1. Marfey's analysis with (*R*)- and (*S*)-FDAA: determination of enantiomeric ratio of amino acid products with one stereogenic center.

Second, to ensure the accuracy of our results, each biocatalytically produced, enantioenriched amino acid product **3** was derivatized with both (*R*)- and (*S*)-FDAA and analyzed by LC-MS (**Fig. S1(B)**). Using (*R*)-FDAA, (*S*)-**3** produces (*S, R*)-**3'** while (*R*)-**3** produces (*R, R*)-**3'**. Similarly, using (*S*)-FDAA, (*S*)-**3** produces (*S, S*)-**3'** and (*R*)-**3** produces (*R, S*)-**3'**. As (*S, R*)-**3'** and (*R, S*)-**3'** are enantiomers (**Fig. S1(B) and (C)**), they are indistinguishable by achiral HPLC analysis and have the same retention times. Similarly, (*R, R*)-**3'** and (*S, S*)-**3'** are enantiomers and they are thus indistinguishable by achiral HPLC analysis.

Using our protocol, for amino acids with a high L-content ((*S*)-**3**), when derivatized with (*R*)-FDAA, the first peak ((*S, R*)-**3'**) was found to be the major peak. The e.r. of **3** can be determined by the peak area ratio, namely $A((S, R)-3')/A((R, R)-3')$. Using (*S*)-FDAA for derivatization, the second peak ((*S, S*)-**3'**) was found to be the major peak, and the e.r. of **3** can also be determined by the peak area ratio, namely $A((S, S)-3')/A((R, S)-3')$. Importantly, in all our Marfey's analyses of enantioenriched amino acids, the measured e.r. of the amino acid product **3** with (*R*)- and (*S*)-FDAA were identical (*vide infra*). In other words, in all cases, $A((S, R)-3')/A((R, R)-3') = A((S, S)-3')/A((R, S)-3')$. Together, these results further ensured that no kinetic resolution was involved in our Marfey's analysis. Thus, the e.r. of **3** could be reliably determined.

Determination of absolute stereochemistry. The absolute stereochemistry of model reaction product homophenylalanine was determined by comparison with authentic enantiomerically pure L-homophenylalanine (*vide infra*). Further, the absolute stereochemistry of this product was ascertained by X-ray single crystal diffraction. The absolute stereochemistry of other non-canonical amino acid products was inferred by analogy to L-homophenylalanine.

Determination of diastereomeric ratio (d.r.) and enantiomeric ratio (e.r.) of amino acids with two stereocenters. The chemical synthesis of racemic amino acids ((*rac*)-**4**) requires multistep synthesis from commercially available starting materials and is thus nontrivial. To quickly determine both the diastereomeric and enantiomeric ratios of biocatalytically formed **4**, we used both (*R*)- and (*S*)-FDAA to derivatize the biocatalytically formed **4** (**Fig. S2**).

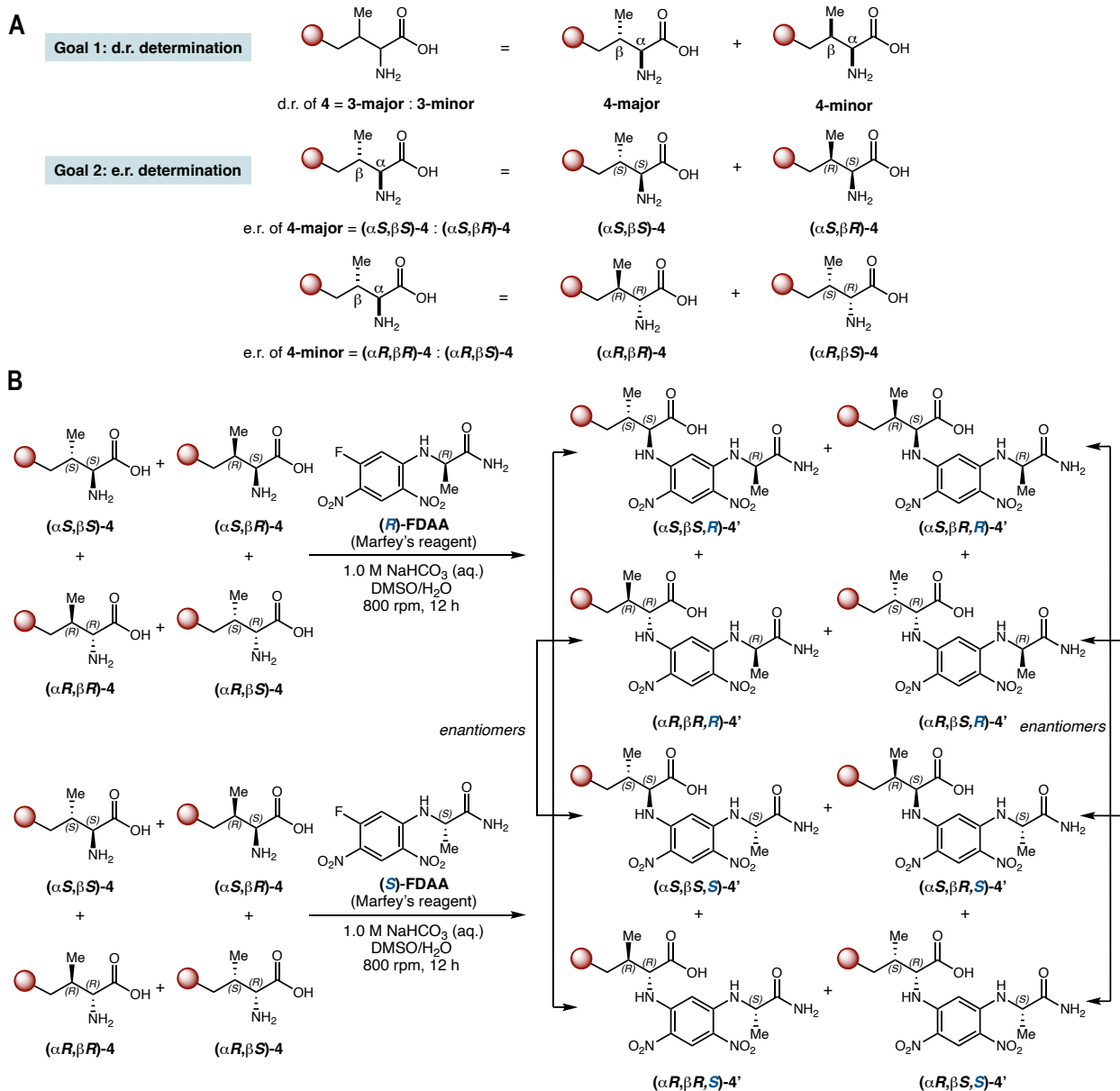


Fig. S2. Marfey's analysis with (*R*)- and (*S*)-FDAA: determination of enantiomeric and diastereomeric ratio of amino acid products with two stereogenic centers.

As can be seen from **Fig. S2**, using (*S*)-FDAA, ($\alpha S, \beta S$)-4 produces ($\alpha S, \beta S, S$)-4', which is the enantiomer of ($\alpha R, \beta R, R$)-4' derived from ($\alpha R, \beta R$)-4. Similarly, using (*S*)-FDAA, ($\alpha S, \beta R$)-4 produces ($\alpha S, \beta R, S$)-4', which is the enantiomer of ($\alpha R, \beta S, R$)-4' derived from ($\alpha R, \beta S$)-4. Using achiral HPLC analysis, enantiomers ($\alpha S, \beta S, S$)-4' and ($\alpha R, \beta R, R$)-4' are indistinguishable and thus have the same retention time and peak shape; enantiomers ($\alpha S, \beta R, S$)-4' and ($\alpha R, \beta S$,

R)-4' are indistinguishable and also have the same retention time. In other words, the retention time **(αR, βR, R)-4'** can be inferred from **(αS, βS, S)-4'**, and **(αR, βS, R)-4'** can be inferred from **(αS, βR, S)-4'**. Thus, through this Marfey's derivatization with *(R)*- and *(S)*-FDAA, four well resolved peaks corresponding to all the four isomers of biocatalytically formed **4**, including **(αS, βS)-4**, **(αS, βR)-4**, **(αR, βR)-4**, and **(αR, βS)-4**, are available without using a chemically prepared racemic mixture of **4**. **Diastereomeric ratio (d.r.)** and **enantiomeric ratio (e.r.)** were measured based on these 4 well resolved peaks.

General experimental procedure for preparative scale non-canonical amino acid synthesis. L- or D-*Pf*PLP^β (ca. 50 mg/mL, 1 mL/tube) was thawed from the -80 °C freezer and kept on ice. To a 100 mL round bottom flask, RBF₃K **1** (0.3 mmol), **2a** (0.9 mmol, 3 equiv, 94.5 mg) or **2b** (1.5 mmol, 5 equiv, 178.7 mg) and RhB (0.03 mmol, 10 mol%, 14.4 mg) were added in succession. Then, the flask was taken into a Coy anaerobic chamber, where 54.5 mL degassed KPi buffer (200 mM at indicated pH), 3 mL degassed DMSO (5% final volume) and 2.55 mL stock solution of L- or D-*Pf*PLP^β were added in succession. The total volume of scale-up reactions was 60.0 mL.

The flask was sealed and removed from the Coy anaerobic chamber, illuminated with 45 W Kessil Blue LED lamp(s) and stirred at 600 rpm and 50 °C for 12 h. The solution was concentrated under vacuum and purified directly on using a 10 g Biotage C18 Sfär cartridge with the aid of a Biotage Isolera instrument. Gradient: 0% to 20% MeCN (0.1% acetic acid) in H₂O (0.1% acetic acid) for 10 column volumes (CVs). Fractions were assessed for the presence of product by LC-MS. Those fractions that contained products were combined and concentrated with the aid of a rotary evaporator, providing the amino acid product as an HOAc adduct as a white solid. In some cases, drying this sample under high vacuum led to the complete loss of HOAc.

III. Selected further results for reaction development

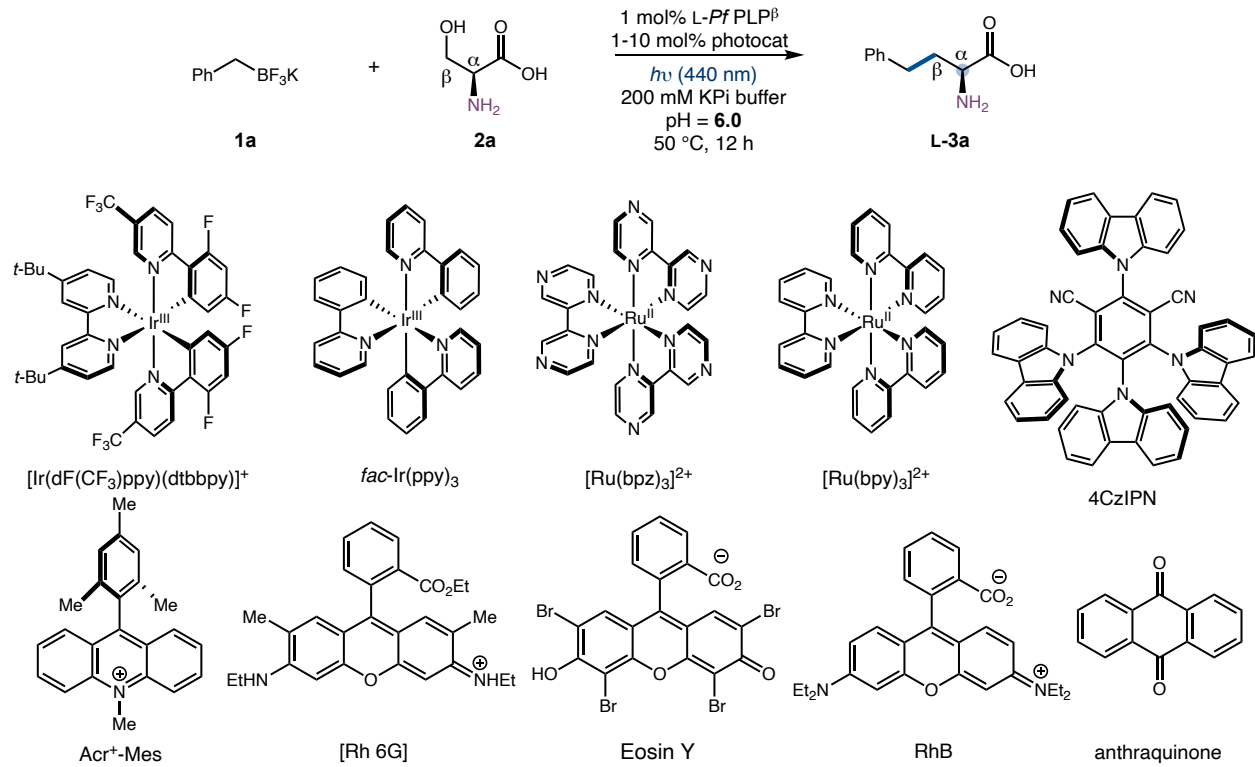
Table S1. Selected results on the evaluation of L-*PfPLP β* variants^a

entry	enzyme variant	yield of 3a (%)	e.r. of 3a
1	wt <i>PfTrpS</i> β-subunit P12L E17G I68V F274S T292S T321A	50	91:9
2	wt <i>PfTrpS</i> β-subunit P12L E17G I68V F274S T292S T321A L12P I16V F95L V384A (L-PfPLPβ)	73	93:7
3	L- <i>PfPLPβ</i> V68I L91P L161A V173E S274L A321T	26	75:25
4	L- <i>PfPLPβ</i> M139L N166D L212P	46	71:29
5	L- <i>PfPLPβ</i> M139L N166D L212P E104G	54	13:87
6	L- <i>PfPLPβ</i> E104G (D-PfPLPβ)	74	11:89
7	L- <i>PfPLPβ</i> M139L I165F N166D Y301H	13	95:5
8	L- <i>PfPLPβ</i> I165F	5	95:5
9	L- <i>PfPLPβ</i> Y301H	68	91:9
10	L- <i>PfPLPβ</i> M139L	37	86:14
11	L- <i>PfPLPβ</i> N166D	27	54:46
12	L- <i>PfPLPβ</i> M139L I165F N166D	<1%	45:55
13	L- <i>PfPLPβ</i> I165F N166D Y301H	15	95:5
14	L- <i>PfPLPβ</i> M139L I165F Y301H	14	95:5
15	L- <i>PfPLPβ</i> I165F Y301H	10	95:5
16	wt <i>CfTPL</i> ^b	0	-
17	<i>EcCysM</i> ^c	0	-
18	<i>EcCysK</i> ^c	0	-

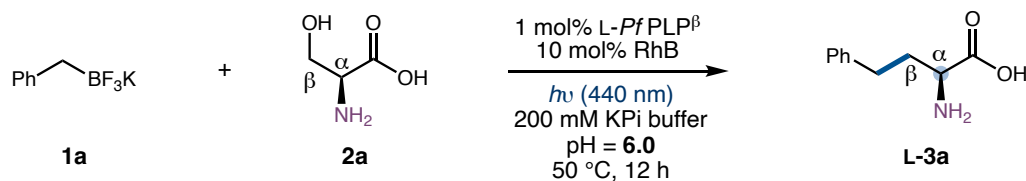
^a**1a** (4 mM), **2a** (20 mM), DMSO (5% v/v). ^b*Cf*TPL = tyrosine phenol lyase from *Citrobacter freundii*. Pyruvate and ammonium were used in lieu of serine when *Cf*TPL was used at basic pH.

^c *EcCysM* and *EcCysK* are *O*-acetylserine sulphhydrylase (OASS) from *E. coli*. *O*-acetylserine was used in lieu of serine at neutral pH.

Table S2. Selected results on the effect of photoredox catalysts



entry	photoredox catalyst	yield of 3a (%)	e.r. of 3a
1	[Ir(dF(CF ₃)ppy) ₂ (dtbbpy)](PF ₆) (1 mol%)	<1	65:35
2	<i>fac</i> -Ir(ppy) ₃ (1 mol%)	6	91:9
3	Ru(bpz) ₃ Cl ₂ (1 mol%)	1	80:20
4	Ru(bpy) ₃ Cl ₂ (1 mol%)	0	-
5	anthraquinone (10 mol%)	6	27:73
6	4CzIPN (10 mol%)	14	91:9
7	MesAcr (10 mol%)	26	80:20
8	Rh6G (10 mol%)	54	91:9
9	Eosin Y (10 mol%)	32	92:8
10	RhB (10 mol%)	73	93:7

Table S3. Control experiment results^a

entry	variation from the standard conditions	yield of 3a (%)	e.r. of 3a
1	none	73	93:7
2	No LED (440 nm)	0	--
3	No RhB	0	--
4	No L- <i>Pf</i> PLP β	0	--
5	5% PLP cofactor instead of L- <i>Pf</i> PLP β	0	--
6	390 nm LED instead of 440 nm	11	80:20
7	525 nm LED instead of 440 nm	49	92:8
8	3 equiv 2a	73	93:7

^a**1a** (4 mM), **2a** (20 mM), 1 mol% L-*Pf*PLP β , 10 mol% RhB, *hν*, 440 nm), 200 mM KPi buffer, pH 6.0, 50 °C, 12 h.

Table S4. Effects of photocatalyst loading

The reaction scheme illustrates the conversion of compound **1a** and compound **2a** to product **L-3a**. Compound **1a** (Ph-CH₂-BF₃K) reacts with compound **2a** (a chiral molecule with a central carbon atom labeled α, β, and NH₂) in the presence of 1 mol% L-PfPLP^β and x mol% RhB, under hν (440 nm) in 200 mM KPi buffer at pH = 6.0 and 50 °C for 12 h. The product **L-3a** is shown with a blue arrow pointing to the α-carbon.

entry	RhB loading	yield of 3a (%)
1	1 mol%	25
2	2 mol%	40
3	5 mol%	56
4	10 mol%	75
5	15 mol%	74
6	20 mol%	64
7 ^a	1 mol%	<1 (65:35 e.r.)
8 ^a	5 mol%	0.9 (65:35 e.r.)
9 ^a	10 mol%	4 (65:35 e.r.)

^a [Ir(dF(CF₃)ppy)₂(dtbbpy)](PF₆) was used in lieu of RhB.

As can be seen from Table S4, when organic photocatalysts such as RhB was used, a lower loading of RhB led to a reduced yield of **3a**. Increasing the RhB loading to 15 mol% provided a similar yield. Further increasing the RhB loading led to a lower yield of **3a**, presumably due to the mismatch of radical formation and consumption rates. When transition-metal photocatalysts such as [Ir(dF(CF₃)ppy)₂(dtbbpy)](PF₆) was used, much lower yields were observed. Increasing the loading of the photocatalyst resulted in small improvement in yield.

Table S5. Effects of **1a:**2a** ratio on the reaction outcome**

The reaction scheme illustrates the conversion of compound **1a** and compound **2a** to compound **L-3a**. Compound **1a** (Ph-CH₂-BF₃K) reacts with compound **2a** (a chiral molecule with a hydroxyl group at the beta position, an amino group at the alpha position, and a carboxylic acid group at the gamma position) in the presence of 1 mol% L-*Pf*PLP β , 10 mol% RhB, hν (440 nm), 200 mM KPi buffer, pH = 6.0, and 50 °C for 12 h. The product is compound **L-3a**, where the alpha-carbon of **2a** has been substituted with a phenyl group from **1a**.

entry	1a / 2a ratio	yield of 3a (%)
1	1:3	73
2	1:2	65
3	1:1	54
4	1.2:1	48
5	1.5:1	41

As can be seen from Table S5, the use of a 1:1 ratio of **1a** and **2a** led to a slightly reduced yield. Using an excess of **1a** resulted in further reduced yields, presumably due to the unmatched rates of photochemical radical generation and enzymatic radical consumption.

Table S6. Selected results on the pH effect on different enzyme variants

entry	enzyme variant	pH	yield of 3a (%)		e.r. of 3a
			L- <i>Pf</i> PLP $^{\beta}$	L- <i>3a</i>	
1	L- <i>Pf</i> PLP $^{\beta}$	6.0	73	93:7	
2	L- <i>Pf</i> PLP $^{\beta}$	6.5	77	86:14	
3	L- <i>Pf</i> PLP $^{\beta}$	7.0	76	77:23	
4	L- <i>Pf</i> PLP $^{\beta}$	8.0	71	49:51	
5	D- <i>Pf</i> PLP $^{\beta}$	6.0	74	11:89	
6	D- <i>Pf</i> PLP $^{\beta}$	6.5	82	8:92	
7	D- <i>Pf</i> PLP $^{\beta}$	7.0	79	6:94	
8	D- <i>Pf</i> PLP $^{\beta}$	8.0	73	5:95	
9	L- <i>Pf</i> PLP $^{\beta}$ M139L I165F N166D Y301H	6.0	13	95:5	
10	L- <i>Pf</i> PLP $^{\beta}$ M139L I165F N166D Y301H	6.3	47	95:5	
11	L- <i>Pf</i> PLP $^{\beta}$ M139L I165F N166D Y301H	6.5	56	94:6	
12	L- <i>Pf</i> PLP $^{\beta}$ M139L I165F N166D Y301H	7.0	67	89:11	
13	L- <i>Pf</i> PLP $^{\beta}$ M139L I165F N166D Y301H (1.5 mol%)	6.3	60	95:5	

IV. DNA and protein sequences

L-PfPLP β

DNA sequence

ATGTGGTCGGTGAATTGGTGGTCAGTACGTGCCAGAACGCTGGTGGACCCCTGAAAGAGC
TGGAAAAAGCTTACAAACGTTCAAAGATGACGAAGAATTCAATCGTCAGCTGAATTACTACCT
GAAAACCTGGGCAGGTGTCACCCACTGTACTACGCAAAACGCCTGACTGAAAAAATCGGT
GGTCTAAAGTCTACCTGAAACGTGAAGACCTGGTCACGGTGGTCACACAAGACCAACAACG
CCATCGGTCAAGGCAGTGCTGGCAAAGCTCATGGTAAAACCTCGTCTGATCGCTGAGACCAGGTGC
TGGTCAGCACGGCGTAGCGACTGCAATGGCTGGTCACTGCTGGCATGAAAGTGGACATTAC
ATGGGTGCTGAGGACGTAGAACGTAGAAAATGAACGTATTCCGTATGAAGCTGCTGGGTGCAA
ACGTAATTCCAGTTAACCTCGGTTCTCGCACCCCTGAAAGACGCAATCAACGAGGCTCTCGTGA
TTGGGTGGCTACTTTGAATACACCCACTACCTAATCGGTTCCGTGGTCGGTCCACATCCGTAT
CCGACCATCGTCGTGATTTCAGTCTGTTATCGTCGTGAGGCTAAAGCGCAGATCCTGGAGG
CTGAAGGTCACTGCCAGATGTAATCGTTGCTTGTGGTGGCTCTAACGCGATGGTAT
CTTTACCCGTTCGTGAACGACAAAAAGTTAACGCTGGTGGCGTTGAGGCTGGTGGTAAAGC
CTGGAATCTGGAAGCATTCCGCTAGCCTGAACGCAGGTCAAGGTTGGTGTGTCCCAGGCATGC
TGTCTACTTCTGCAGGACGAAGAAGGTCAAGCTGGTGGCGTTGAGGCTGGTGGTAAAGC
GGATTATCCAGGTGTTGGTCCAGAACACGCTTACCTGAAAAAAATTCAAGCGTGTGAATACGTG
GCTGTAACCGATGAAGAAGCACTGAAAGCGTCCATGAACGCTGGCTACCGAAGGTATCATCC
CAGCTCTGGAATCTGCGCATGCTGTGGCTTACGCTATGAAACTGGCTAAGGAAATGTCTCGTGA
TGAGATCATCATCGTAAACCTGTCGGTGGTGGACAAAGACCTGGATATTGTCCTGAAAGCG
TCTGGCAACGTGCTCGAGCACCACCACCACTGA

Protein sequence

MWFGEFGQYVPETLVGPLKELEKAYKRFKDDEEFNRQLNYYLKTWAGRPTPLYAKRLTEKIG
GAKVYLKREDLVHGGAHKTNNAIQQALLAKLMGKTRLIAETGAGQHGVATAMAGALLGMKVDIY
MGAEDVERQKMNVFRMKLLGANVIPNSGSRTLKDADNEALRDWVATFELYTHYLIGSVVGPHPY
PTIVRDFQSVIGREAKAQILEAEGQLPDVIVACVGGGSNAMGIFYPFVNDKKVKLGVVEAGGKG
LESGKHSASLNAGQVGVSHGMLSYFLQDEEGQIKPSHSIAPGLDYPVGVPHEAYLKKIQRAEYV

AVTDEEALKAFHELSRTEGIIPALESAHAVAYAMKLAKEMSRDEIIIVNLSGRGDKDLDIVLKA
SGNVLEHHHHHH

D-P β PLP β

DNA sequence

ATGTGGTCGGTGAATTGGTGGTCAGTACGTGCCAGAACGCTGGTGGACCCCTGAAAGAGC
TGGAAAAAGCTTACAAACGTTCAAAGATGACGAAGAATTCAATCGTCAGCTGAATTACTACCT
GAAAACCTGGGCAGGTCTCCAACCCCACGTACTACGCAAAACGCCTGACTGAAAAAATCGGT
GGTCTAAAGTCTACCTGAAACGTGAAGACCTGGTCACGGTGGTCACACAAGACCAACAACG
CCATCGGTCAAGGCAGTCTGGCAAAGCTCATGGTAAAACCTCGTCTGATCGCTGGCACCGGTGC
TGGTCAGCACGGCGTAGCGACTGCAATGGCTGGTCACTGCTGGCATGAAAGTGGACATTAC
ATGGGTGCTGAGGACGTAGAACGTCAAGAAATGAACGTATTCCGTATGAAGCTGCTGGTGCAA
ACGTAATTCCAGTTAACCTCGGTTCTCGCACCCCTGAAAGACGCAATCAACGAGGCTCTCGTGA
TTGGGTGGCTACTTTGAATACACCCACTACCTAACGTTCCGTGGTCGGTCCACATCCGTAT
CCGACCATCGTCGTGATTTCAGTCTGTTATCGTCGTGAGGCTAAAGCGCAGATCCTGGAGG
CTGAAGGTCACTGCCAGATGTAATCGTTGCTGTGGTGGCTCTAACGCGATGGTAT
CTTTACCCGTTCGTGAACGACAAAAAGTTAACGCTGGTGGCGTTGAGGCTGGTGGTAAAGC
CTGGAATCTGGTAAGCATTCCGCTAGCCTGAACGCAGGTCAAGGTTGGTGTGTCCCACATGGCATGC
TGTCTACTTCTGCAGGACGAAGAAGGTCAAGCTGGTGGCGTTGAGGCTGGTGGTAAAGC
GGATTATCCAGGTGGTCCAGAACACGCTTACCTGAAAAAAATTCAACGCGATGGTAT
GCTGTAACCGATGAAGAAGCACTGAAAGCGTCCATGAACGCTGGCTACCGAAGGTATCATCC
CAGCTCTGGAATCTGCGCATGCTGTGGCTTACGCTATGAAACTGGCTAAGGAAATGTCTCGTGA
TGAGATCATCATCGTAAACCTGTCTGGTGTGGTACAAAGACCTGGATATTGTCTGTGAAAGCG
TCTGGCAACGTGCTCGAGCACCACCACCACTGA

Protein sequence

MWFGEFGQYVPETLVGPLKELEKAYKRFKDDEFNRQLNYYLKTWAGRPTPLYAKRLTEKIG
GAKVYLKREDLVHGGAHKTNNAIQQALLAKLMGKTRLIAGTGAGQHGVATAMAGALLGMKVDIY
MGAEDVERQKMNVFRMKLLGANVIPNSGSRTLKDADNEALRDWVATFELYTHYLIGSVVGPHPY
PTIVRDFQSFIGREAKAQILEAEGQLPDVIVACVGGGSNAMGIFYPFVNDDKKVKLVGVEAGGKG

LESGKHSASLNAGQVGVSHGMLSYFLQDEEGQIKPSHSIAPGLDYPGVGPEHAYLKKIQRAEYV
AVTDEEALKAFHELSRTEGIIPALESAHAVAYAMKLAKEMSRDEIIIVNLSGRGDKDLDIVLKA
SGNVLEHHHHHH

L-P_fPLP^β M139L I165F N166D Y301H

DNA sequence

ATGTGGTCGGTGAATTGGTGGTCAGTACGTGCCAGAACGCTGGTGGACCCCTGAAAGAGC
TGGAAAAAGCTTACAAACGTTCAAAGATGACGAAGAATTCAATCGTCAGCTGAATTACTACCT
GAAAACCTGGGCAGGTGTCACCCCCACTGTACTACGCAAAACGCCTGACTGAAAAAATCGGT
GGTCTAAAGTCTACCTGAAACGTGAAGACCTGGTCACGGTGGTCACACAAGACCAACAACG
CCATCGGTCAAGGCAGTGCTGGCAAAGCTCATGGTAAAACCTCGTCTGATCGCTGAGACC GGTC
TGGTCAGCACGGCGTAGCGACTGCAATGGCTGGTCACTGCTGGCATGAAAGTGGACATTAC
ATGGGTGCTGAGGACGTAGAACGTCA GAAACTGAACGTATTCCGTATGAAGCTGCTGGTGCAA
ACGTAATTCCAGTTAACCTCGGTTCTCGCACCCCTGAAAGACGCATTGATGAGGCTCTCGTGA
TTGGGTGGCTACTTTGAATACACCCACTACCTAACCGTTCCGTGGTCGGTCCACATCCGTAT
CCGACCATCGTCGTGATTTCAGTCTGTTATCGGTGAGGCTAAAGCGCAGATCCTGGAGG
CTGAAGGTCA GCTGCCAGATGTAATCGTTGCTTGTTGGTGGCTCTAACCGCAGATGGTAT
CTTTACCGTTCGTGAACGACAAAAAGTTAACGCTGGTGGCGTTGAGGCTGGTGGTAAAGGC
CTGGAATCTGGTAAGCATTCCGCTAGCCTGAACGCAGGTCA GGGTGGTGTGTCCTGGCATGC
TGTCTACTTCTGCAGGACGAAGAAGGTCA GATCAAACCAAGCCACTCCATCGCACCAGGTCT
GGATCATCCAGGTGTTGGTCCAGAACACCGCTTACCTGAAAAAAATTCA CGGTGCTGAATACGTG
GCTGTAACCGATGAAGAAGCACTGAAAGCGTCCATGAACGTGAGCCGTACCGAAGGTATCATCC
CAGCTCTGGAATCTGCGCATGCTGTGGCTTACGCTATGAAACTGGCTAAGGAAATGTCTCGTGA
TGAGATCATCATCGTAAACCTGTCTGGTGTGGTACAAAGACCTGGATATTGTCCTGAAAGCG
TCTGGCAACGTGCTCGAGCACCACCACCACTGA

Protein sequence

MWFGEFGQYVPETLVGPLKELEKAYKRFKDDEFNRQLNYYLKTWAGRPTPLYAKRLTEKIG
GAKVYLKREDLVHGGAHKTNNAIQQALLAKLMGKTRLIAETGAGQHGVATAMAGALLGMKVDIY
MGAEDVERQKLNVFRMKLLGANVIPNSGSRTLKDAFDEALRDWVATFEYTHYLIGSVVGP HY
PTIVRDFQS VIGREAKAQILEAEGQLPDVIVACVGGGSNAMGIFYPFVNDDKKVKLVGVEAGGKG

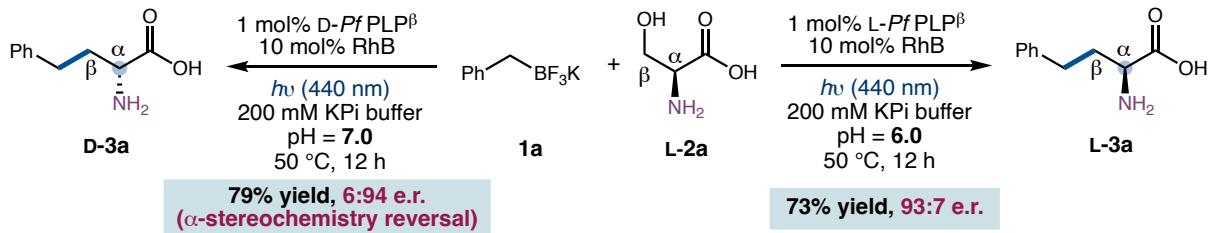
LESGKHSASLNAGQVGVSHGMLSYFLQDEEGQIKPSHSIAPGLDHPGVGPEHAYLKKIQRAEYV
 AVTDEEALKAFHELSRTEGIIPALESAHAVAYAMKLAKEMSRDEIIIVNLSGRGDKDLDIVLKA
 SGNVLEHHHHHH

Table S7. Selected primers used for the site-directed mutagenesis

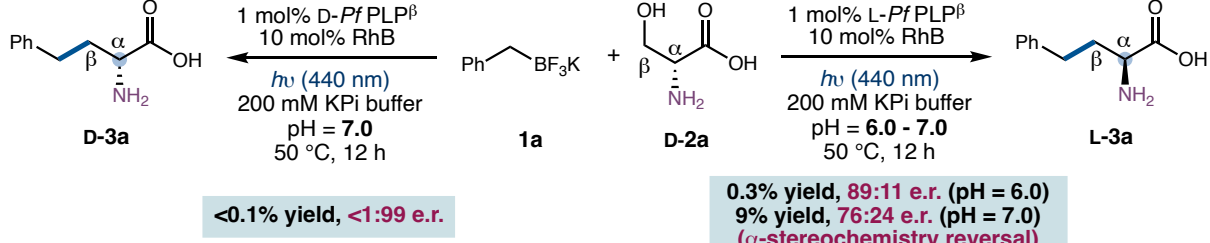
DNA template	primer name	primer sequence
L-PfPLP^β	E104G_fwd	GGTAAAACCTCGTCTGATCGCT GGCACCGGTGCTGG
	E104G_rev	CGATCAGACGAGTTTACCCATG
L-PfPLP^β	I165F_fwd	GGTTCTCGCACCTGAAAGACGCATTAAACGAGGCTC
	I165F_rev	GTCTTCAGGGTGCAGAACCGGAG
L-PfPLP^β	M139L_fwd	CTGAGGACGTAGAACGTCAGAAACT GAACGTATTCCG
	M139L_rev	CTGACGTTCTACGTCCCTCAGC
L-PfPLP^β	N166D_fwd	CTCGCACCTGAAAGACGCAAT CGATGAGGCTCTGCGTG
	N166D_rev	CTGACGTTCTACGTCCCTCAGC
L-PfPLP^β	Y301H_fwd	CTCCATCGCACCGAGTCTGGATCATCCAGGTGTTG
	Y301H_rev	CCAGACCTGGTGCATGGAG
L-PfPLP^β	L139M_fwd	CTGAGGACGTAGAACGTCAGAAA ATGAACGTATTCC
M139L I165F	L139M_rev	CTGACGTTCTACGTCCCTCAGC
N166D Y301H		
L-PfPLP^β	D166N_fwd	GGTTCTCGCACCTGAAAGACGCATTAAACGAGGCTC
M139L I165F	D166N_rev	CTGACGTTCTACGTCCCTCAGC
N166D Y301H		
L-PfPLP^β	H301Y_fwd	CTCCATCGCACCGAGTCTGGATTAT CCAGGTGTTG
M139L I165F	H301Y_rev	CCAGACCTGGTGCATGGAG
N166D Y301H		

V. Biocatalytic reactions using L-, D- and DL-serine and L-, L-*allo*- and DL-threonine

A



B



C

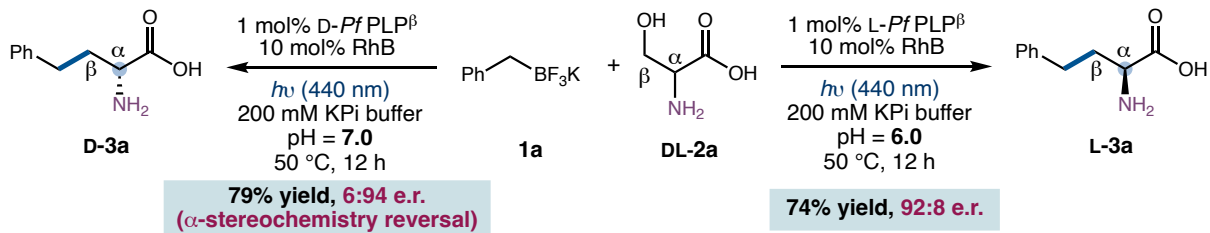


Fig. S3. Enantiodivergent biocatalytic synthesis of homophenylalanine using L-, D-serine and DL-serine

We evaluated the use of L-, D-serine and DL-serine under our enantiodivergent biocatalytic protocols, and our findings are detailed below (**Fig. S3**).

1. L-serine is the native substrate of *Pf*PLP β . Under our optimized conditions, L-*Pf*PLP β provided L-**3a** in 73% yield and 93:7 e.r., while D-*Pf*PLP β provided D-**3a** in 79% yield and 6:94 e.r. (**Fig. S3(A)**). Thus, L-*Pf*PLP β and D-*Pf*PLP β constitutes a pair of enantiodivergent biocatalysts.
2. D-amino acids are usually not accepted by PLP enzymes. Under our conditions, D-serine was found to be a viable substrate (**Fig. S3(B)**). Using L-*Pf*PLP β , at pH 6.0, D-serine provided L-**3a** in 0.3% yield and 89:11 e.r.. At pH 7.0, D-serine provided L-**3a** in 9% yield and 76:24 e.r.. Using D-*Pf*PLP β , at pH 7.0, D-serine provided D-**3a** in low yield but good enantiomeric ratio (<0.1% yield and <1:99 e.r.). The ability of *Pf*PLP β to convert D-serine is notable.

3. *PfPLP β* variants were able to convert racemic serine (DL-serine, (*rac*)-**2a**) into enantioenriched homophenylalanine with the same yields and enantioselectivities (Fig. S3(C)). Under our conditions, with (*rac*)-**2a**, L-*PfPLP β* provided **L-3a** in 74% yield and 92:8 e.r., while D-*PfPLP β* provided **D-3a** in 79% yield and 6:94 e.r. Thus, if needed, all the biocatalytic transformations described in this paper could be performed with DL-serine.

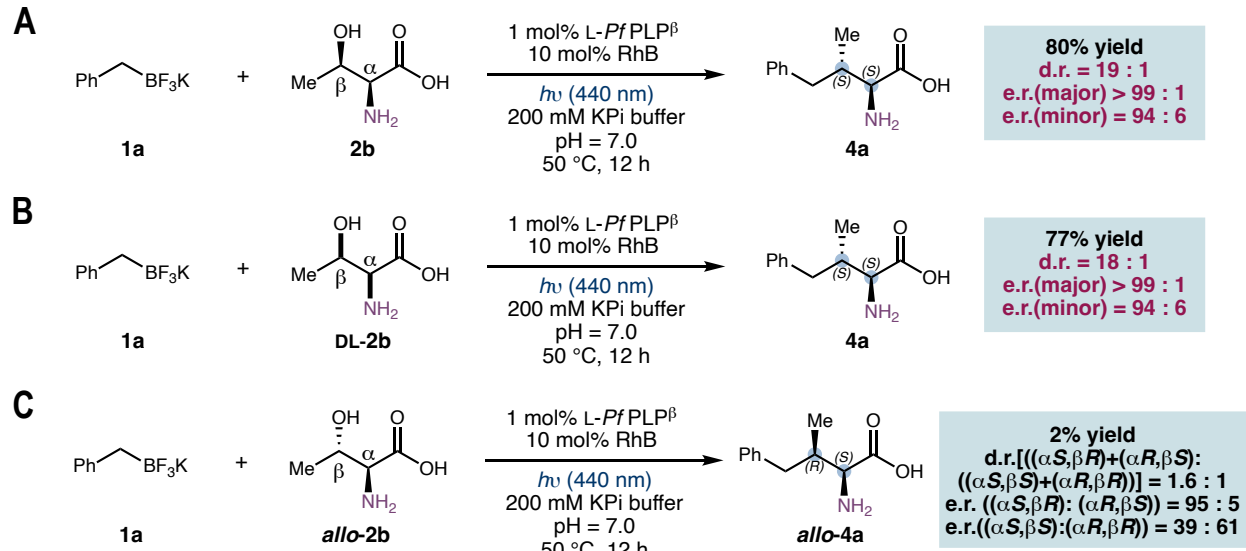


Fig. S4. Biocatalytic synthesis of **4a using L-, L-*allo*-threonine and DL-threonine.** The enatio- and diastereomeric ratios were determined by Marfey's analysis as described above.

We evaluated the use of L-, DL-threonine and L-*allo*-threonine using L-*PfPLP β* , and our findings are detailed below (Fig. S4).

1. L-*PfPLP β* could convert racemic threonine (DL-threonine, (*rac*)-**2b**) into diastereo- and enantioenriched **4** with almost the same yields and enantioselectivities as with L-threonine (**L-2b**, Fig. S4(A) and 4(B)). Under our conditions, with **L-2b**, L-*PfPLP β* provided **L-4a** in 80% yield, 19:1 d.r. and >99:1 e.r.. With (*rac*)-**2b**, L-*PfPLP β* provided **L-4a** in 77% yield 18:1 d.r. and >99:1 e.r.. Thus, if needed, all the biocatalytic transformations described in this paper could be performed with DL-threonine.

2. L-*PfPLP β* could also convert L-*allo*-threonine, the β -epimer of L-threonine, into the other major diastereomeric product, (α S, β R)-**4a**, in 2% yield, 1.6:1 d.r. and 95:5 e.r. (Fig. S4(C)). This result indicated the possibility of accessing this (α S, β R)-diastereomer through further protein engineering.

3. D-*PfPLP β* was found to be inactive toward threonine.

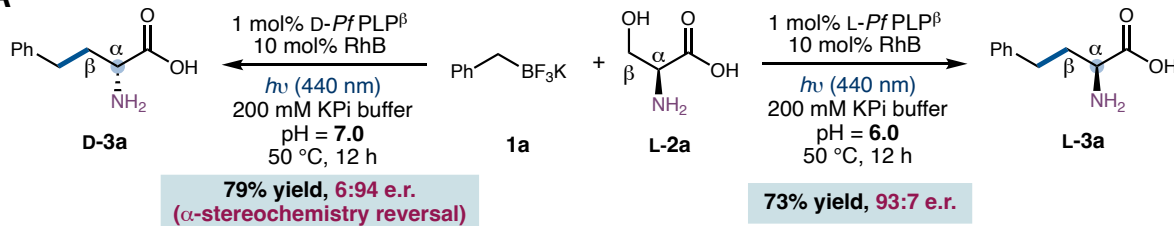
In the presence study, we opted to use L-serine and L-threonine for the vast majority of substrate scope study. Based on results detailed in **Fig. S3** and **Fig. S4**, DL-serine and DL-threonine furnished results very similar to that with L-serine and L-threonine. Thus, if needed, DL-serine and DL-threonine can be used in the same manner. As L-amino acids are abundantly available from nature, their costs are often comparable to, or even lower than, the racemic DL-amino acids. Specifically, while the costs of L-serine are comparable to that of DL-serine, L-threonine is uniformly less expensive than DL-threonine from all the suppliers we surveyed. In **Table S8**, we provide the costs of L-serine, DL-serine, L-threonine and DL-threonine from common suppliers as of 12/08/2022. Trade prices of serine and threonine are much lower from industrial suppliers.

Table S8. Costs of L-serine, DL-serine, L-threonine and DL-threonine (100 g) from common suppliers

supplier	L-serine	DL-serine	L-threonine	DL-threonine
Sigma-Aldrich	\$125	\$85.4	\$165	\$292
Combi-Blocks	\$40	/	\$40	\$60
Chem-Impex	\$25	\$47	\$18.5	\$90.6
Oakwood	\$22	\$40	\$40	/

VI. Insights into enantiodivergent homophenylalanine synthesis

A



B

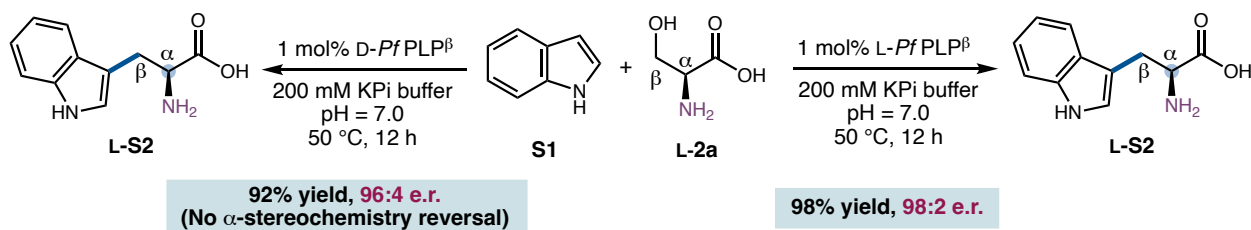


Fig. S5. Probing the origin of enantiodivergent dual photoredox and pyridoxal biocatalysis: evaluating L-PfPLP^β and D-PfPLP^β in their native function for tryptophan synthesis

In our synergistic photoredox and pyridoxal biocatalysis, L-PfPLP^β and D-PfPLP^β furnished complementary enantioselectivities (**Fig. S5(A)**). To gain further insights into factors governing the enantiopreference, we evaluated L-PfPLP^β and D-PfPLP^β in their native tryptophan synthesis reactions. Both L-PfPLP^β and D-PfPLP^β furnished L-tryptophan as the major enantiomeric product with excellent enantioselectivity, and no α-stereochemistry reversal was observed (**Fig. S5(B)**). This result indicated that the new radical pyridoxal enzymology is likely responsible for the observed α-stereochemistry reversal in homophenylalanine synthesis.

Experimental procedure for tryptophan synthesis. Under air, stock solutions of indole (80 mM in DMSO) and L-serine (500 mM in 200 mM KPi buffer, pH 7) were prepared. To a 2-dram vial containing a stir bar were added 876 μL of KPi buffer (200 mM, pH 7), 50 μL indole stock solution, 40 μL L-serine stock solution, and 34 μL L-PfPLP^β or D-PfPLP^β (50 mg/mL). The total reaction volume was 1.0 mL. The reaction mixture was then sealed and allowed to stir at 500 rpm and 50 °C for 12 h. Upon completion, the reaction mixture was quenched by the addition of 1 mL of CH₃CN/1 M aq. HCl (v:v = 1:1). 50 μL of a stock solution of 2-phenylbutyric acid (80 mM in CH₃CN/1 M

aq. HCl) was then added as the internal standard. The yield was determined by LC-MS analysis using a calibration curve. The enantioselectivity was determined by Marfey's analysis.

VII. Kinetic profile of the model reaction

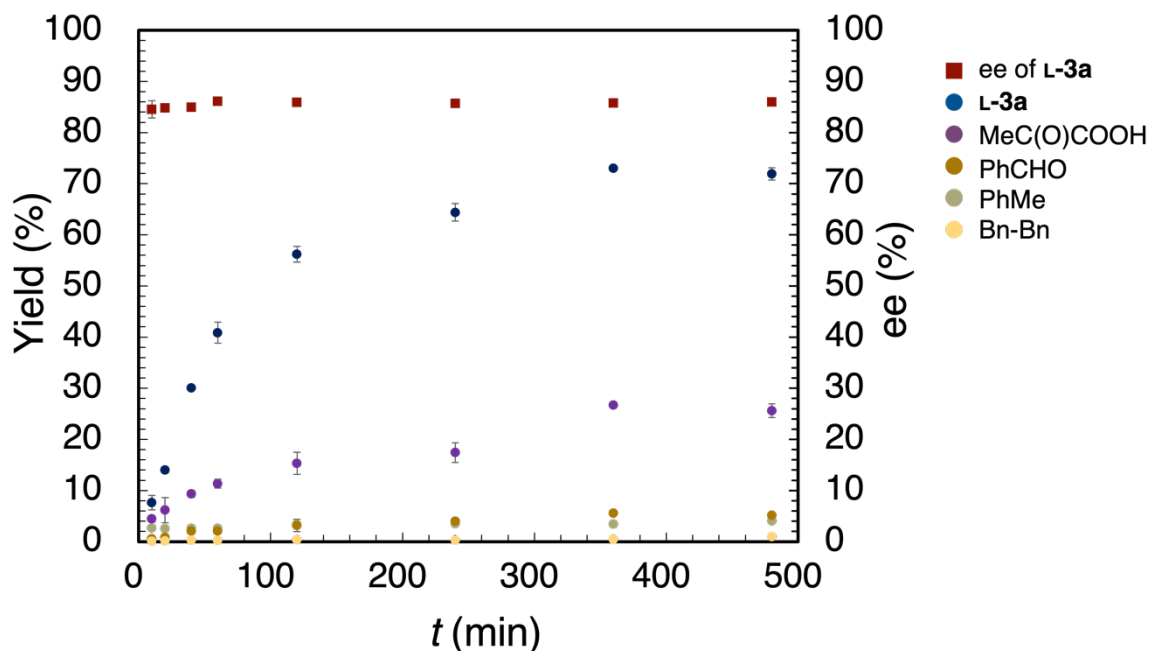
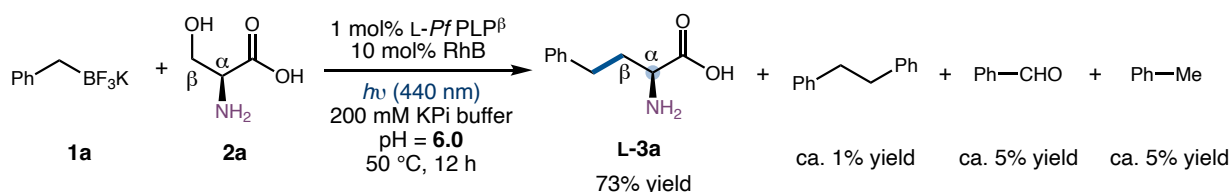
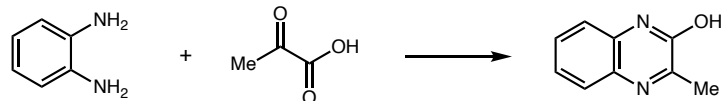


Fig. S6. Kinetic profile of the model reaction

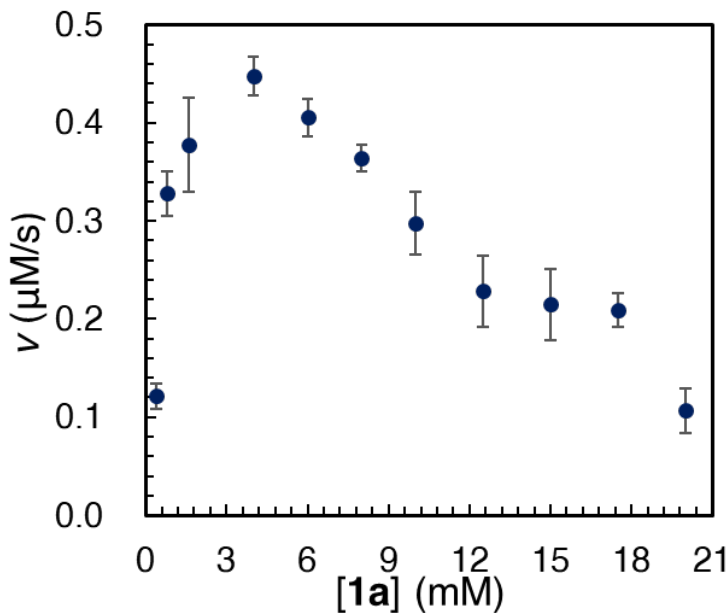
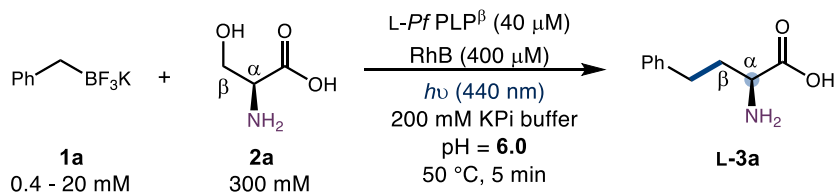
Experimental procedure. Following the general procedure, the model reaction was stopped and analyzed at 10, 20, 40, 60, 120, 240, 360 and 480 min. Yields and ee's were plotted as a function of time (Fig. S6). The yields of toluene, PhCHO and dibenzyl were determined by GC-MS analysis using dodecane as the internal standard.

Pyruvic acid formed from the deamination of serine was transformed into 3-methylquinoxalin-2-ol using *o*-phenylenediamine and analyzed by HPLC for yield determination (66). The derivation procedure is as follows: 75 μ L of a 16 mM solution of *o*-phenylenediamine in CH₃CN/4 M aq. HCl (v/v = 1:1) and 20 μ L reaction mixture were added into a 1 dram vial. 300 μ L CH₃CN/4 M aq. HCl (v/v = 1:1) was then added, and the mixture was allowed to stir at 40 °C for 3 h. Upon the complete conversion of pyruvic acid, the reaction mixture was diluted with

$\text{CH}_3\text{CN}/4$ M aq. HCl ($\text{v/v} = 1:1$). A stock solution of 2-Phenylbutyric acid was added as the internal standard and the yield of pyruvic acid was determined by LC-MS analysis.



As can be seen from **Fig. S6**, this dual catalytic reaction proceeded to completion in 360 min. The enantioselectivity did not change over the course of the reaction. In this optimized model reaction, the yield of the dibenzyl ($\text{Bn}-\text{Bn}$) side product was $<1\%$, indicating low degrees of undesired radical-radical homocoupling. Other side products derived from BnBF_3K included PhCHO (ca. 5%) and PhMe (ca. 5%). PhCHO is derived from further oxidation of the benzyl radical with the excited-state photocatalyst. PhMe is formed upon the protodeborylation of BnBF_3K . In general, when the dual catalytic process provided good yields, the side product profiles were similar to the model reaction. When the dual catalytic process provided a lower yield, a larger amount of one of these side products was observed.



Initial rate measurements. Steady-state kinetic studies were carried out using purified enzyme L-*Pf*PLP $^\beta$. Initial rates were determined using a concentration range from 0.4 mM to 20 mM BnBF₃K with an L-serine concentration of 300 mM. Previously, the KM value of serine of related *P. furiosus* tryptophan synthase variants was determined to be ca. 0.7 mM (33).

Stock solutions of **1a** in DMSO with varying concentrations were prepared by serial dilution (666.7 mM, 583.3 mM, 500 mM, 416.7 mM, 333.3 mM, 266.7 mM, 200 mM, 133 mM, 53.3 mM, 26.7 mM and 13.3 mM; this corresponded to a final concentration of 20 mM, 17.5 mM, 15 mM, 12.5 mM, 10 mM, 8 mM, 6 mM, 4 mM, 1.6 mM, 0.8 mM and 0.4 mM, respectively, when 15 μL of the stock solution was used for each reaction).

The initial rate measurements using L-*Pf*PLP $^\beta$ were performed in 475 μL KPi buffer (200 mM, pH 6.0) and 25 μL DMSO containing L-*Pf*PLP $^\beta$ (40 μM final concentration), RhB (400 μM final concentration), substrate **1a** (15 μL , 0.4 mM to 20 mM final concentration) and **2a** (300 mM final concentration) in a 2-dram vial containing a stir bar. The reaction vial was then sealed and removed

from the Coy anaerobic chamber and submerged in a water bath at 50 °C. The reaction mixture was allowed to stir at 500 rpm and 50 °C and illuminated with a 45 W Kessil LED lamp for 5 min. Following that, the reaction mixture was quenched with 0.5 mL of CH₃CN/1 M aq. HCl (v:v = 1:1). 20 µL of a stock solution of 2-phenylbutyric acid (50 mM in CH₃CN/1 M aq. HCl) was then added as the internal standard. After vigorous mixing, ca. 1.0 mL of reaction mixture was transferred into a 1.5 mL Eppendorf tube and centrifuged at 15,000 rpm for 15 min. The solution was filtered through a 0.22 µm PES membrane filter (diameter = 1.3 cm) and analyzed by LC-MS. The yield of the product was determined by LC-MS using 2-phenylbutyric acid as the internal standard.

Initial rates are shown below:

[1a] (mM)	[3a] (mM)	V (µM/s)
0.4	0.036	0.12 ± 0.01
0.8	0.098	0.33 ± 0.02
1.6	0.113	0.39 ± 0.03
4.0	0.134	0.45 ± 0.01
6.0	0.122	0.41 ± 0.01
8.0	0.109	0.36 ± 0.01
10.0	0.089	0.30 ± 0.02
12.5	0.069	0.25 ± 0.03
15.0	0.064	0.22 ± 0.03
17.5	0.063	0.21 ± 0.01
20.0	0.032	0.11 ± 0.02

In this preliminary enzyme kinetic study, the reaction rate increased as [**1a**] increased from 0.4 mM to 4.0 mM. Further increasing [**1a**] led to a decrease initial rate, indicating potential enzyme inhibition under these conditions.

VIII. Enantioconvergent nature of the biocatalytic transformation of (*rac*)-1p

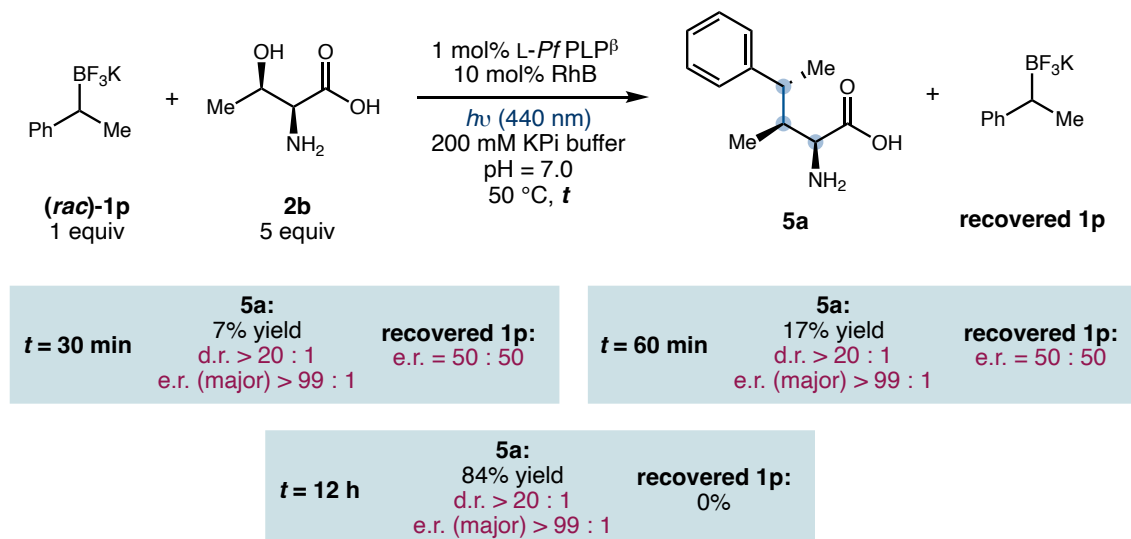


Fig. S7. Time course of the biocatalytic transformation of (*rac*)-1p and 2b.

To further understand the stereochemical course of the biotransformation of **1p**, the reaction was stopped at partial conversion, and the enantiomeric ratio of recovered **1p** was determined (Fig. S7). The e.r. of recovered **1p** was found to be 50:50, indicating no kinetic resolution was operative during the enantioconvergent transformation of **1p**.

Experimental procedure. Following the general procedure, the biocatalytic transformation of (*rac*)-1p was stopped and analyzed at 30 min and 60 min. The yields of the product **5a** were determined by LC-MS analysis. The enantioselectivity of the recovered starting material **1p** was determined using normal phase chiral HPLC. In this process, **1p** was oxidized using Oxone to provide the corresponding benzylic alcohol (**S3**). This oxidation is known to be a stereoretentive process (67). The benzylic alcohol was then extracted into EtOAc/hexanes and analyzed by chiral HPLC.

HPLC analysis conditions: Chiraldak IB-N5 column (4.6 mm × 25 cm, 5 micron), 97:3 hexanes: *i*-PrOH, 1.0 mL/min.

IX. Radical trapping experiment and radical-derived byproduct identification

When 3 equiv of TEMPO was added to the dual catalytic reaction, no standard product **3a** formed (**Fig. S8**). The radical trapping product **S4** ($m/z = 247$) was detected by mass spectrometry (**Fig. S9**). The yield of **S4** was determined by LC-MS analysis to be 14% using 2-phenylbutyric acid as an internal standard.

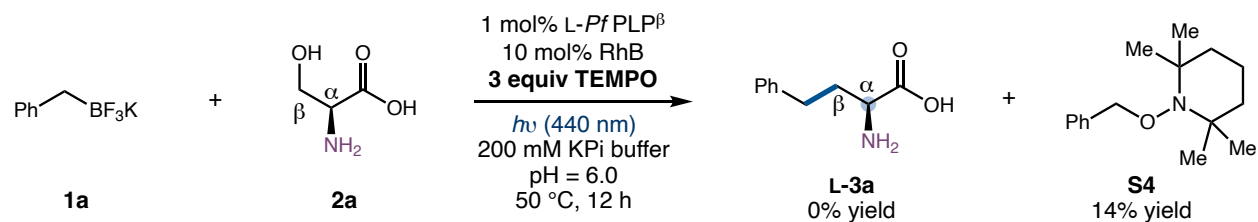


Fig. S8. Radical trapping with TEMPO.

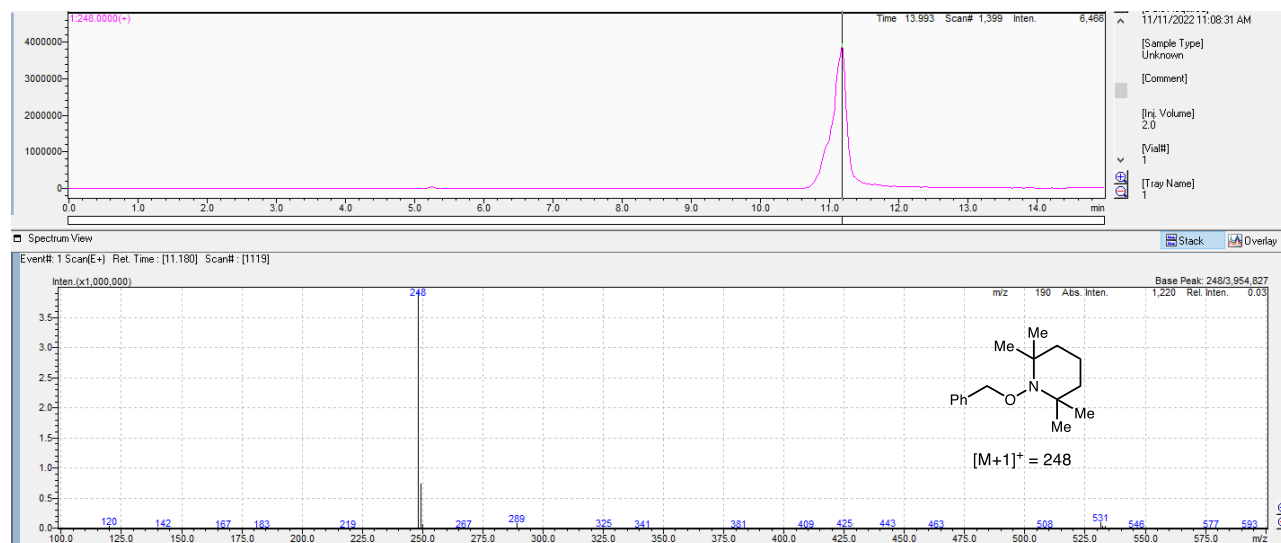


Fig. S9. Mass spectrometry of S4.

We also determined the side products for reactions with a modest yield (**Fig. S10**). For example, under current conditions, **3h** was formed in 37% yield and 6:94 e.r.. Dibenzyl **S5** ($m/z = 298$) was detected by GC-MS analysis. This dibenzyl side product is likely derived from the homocoupling of benzylic radical (**Fig. S11**). Together, these results are consistent with a radical mechanism.

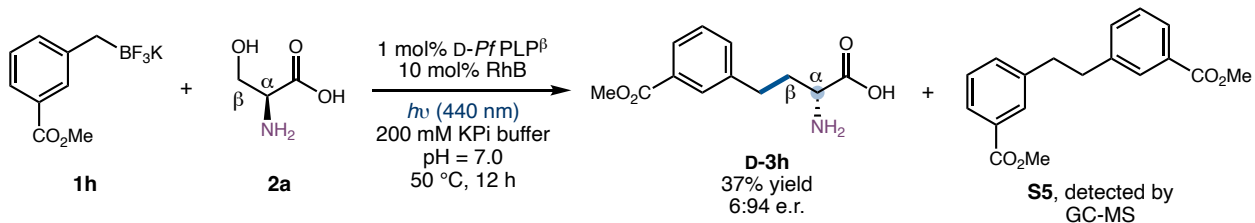


Fig. S10. Mass spectrometric analysis for radical-derived side product.

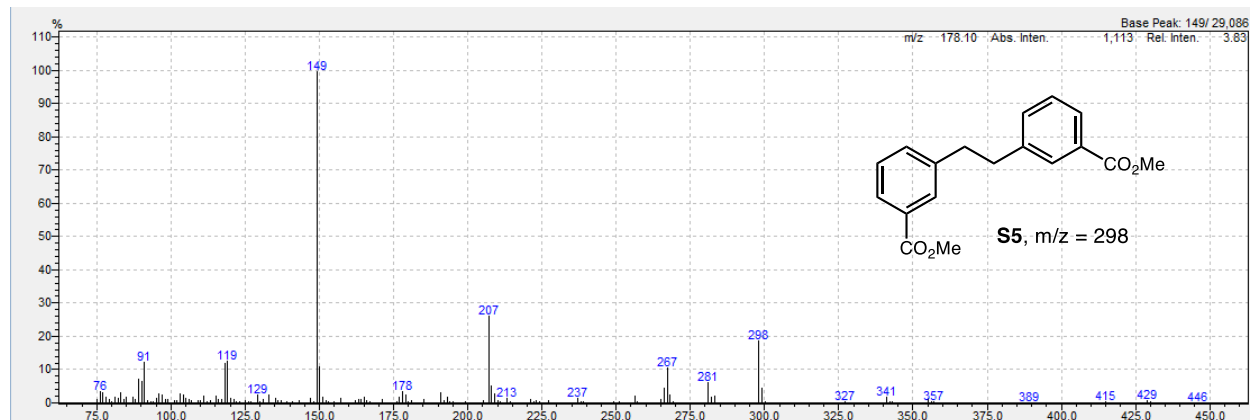


Fig. S11. GC-MS analysis of S5

Experimental procedure. The reaction of **1h** and **2a** using *D-PfPLP^B* was conducted under the standard conditions. Upon the completion of the reaction, 1 mL of 1:1 CH₃CN/1 M HCl (aq.) and 50 μL of a stock solution of 2-phenylbutyric acid (80 mM) were added. Half of the reaction mixture was used for LC-MS analysis to determine the yield and enantioselectivity of **3h**. The other half of the reaction mixture was extracted using EtOAc and the organic layer was analyzed by GC-MS.

Discussion: The relatively low yield of **3h** is due to the formation of homo-coupling product and protodeborylation product. These undesired products were observed by GC-MS analysis.

X. UV-Vis spectroscopic analysis

UV-Vis spectra (300–500 nm) were recorded on a Shimadzu UV1800 spectrophotometer using a quartz cuvette. In this UV-Vis spectroscopic analysis, 40 μ M L-*Pf*PLP $^{\beta}$ in 200 mM KPi buffer (pH 8.0) was used. Following literature procedure (1-2), thermostable enzyme samples were incubated at 75 °C for approximately 3 min to ensure that a stable temperature was reached and UV-Vis spectra were then recorded (**Fig. S12**). First, the UV-Vis spectrum of L-*Pf*PLP $^{\beta}$ was recorded. A strong absorption band at 412 nm is characteristic of the internal aldimine formed between the PLP cofactor and K82 of the protein scaffold (**VIII** in **Fig. 2(C)** of the manuscript). L-Serine was then added (12 mM in KPi buffer), and two new peaks emerged. Consistent with previous findings, the signal at 422 nm corresponds to the external aldimine (**IX** in **Fig. 2(C)**). The signal at 355 nm corresponds to the aminoacrylate intermediate (**XI** in **Fig. 2(C)**). Finally, BnBF $_3$ K was added (4 mM in KPi buffer/DMSO). Upon incubation, the UV-vis spectrum showed no emergence of new signals, suggesting that no strongly UV-Vis absorbing charge transfer (CT) complexes are involved between the benzyltrifluoroborate substrate and the covalent pyridoxal intermediates.

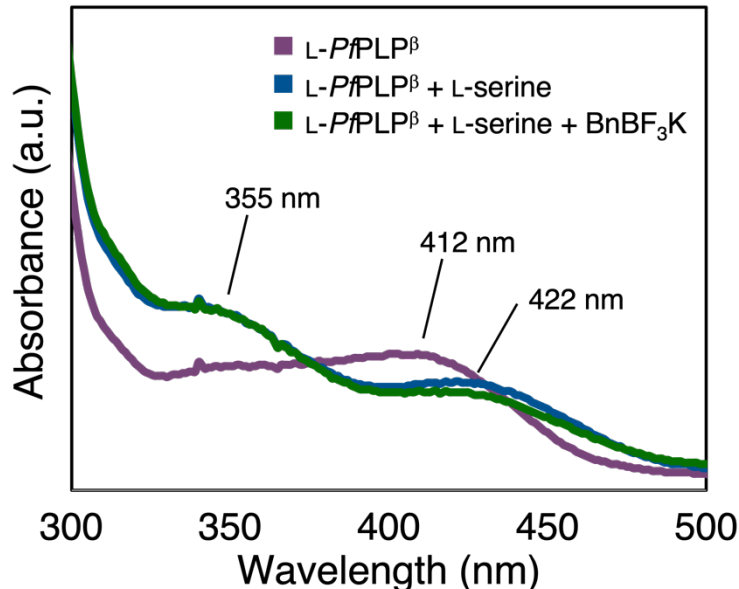


Fig. S12. UV-Vis spectra of the PLP enzyme in different states.

Furthermore, we also carried out UV-Vis spectroscopic analysis to probe if there is CT complex formation between the photocatalyst rhodamine B and the enzymatic intermediates (**Fig. S13**). A stock solution of RhB was added (40 μ M in KPi buffer/DMSO). The absorption spectrum of the mixture represented a linear combination of the absorption spectra of RhB and that of the enzymatic mixture. Thus, this analysis indicated that there is likely no formation of strongly UV-Vis absorbing CT complexes between the enzymatic intermediates and the RhB photocatalyst.

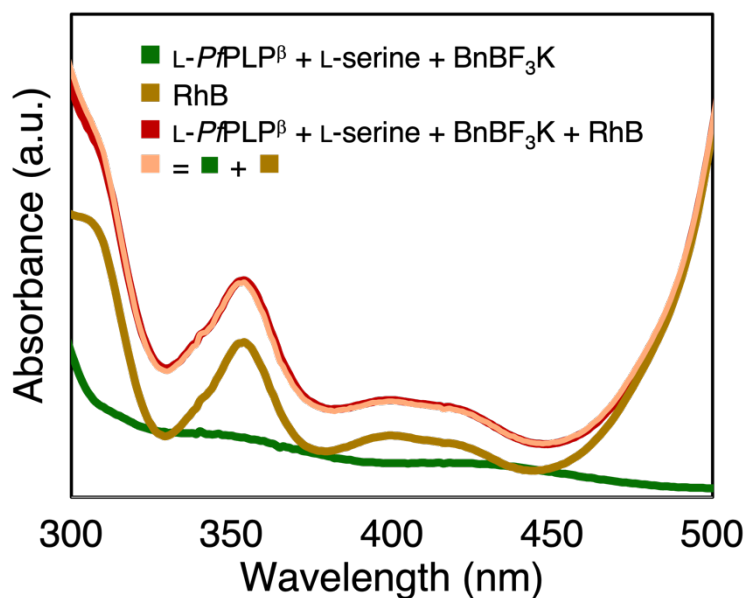


Fig. S13. UV-Vis spectra of the PLP enzyme, substrates and photocatalyst.

XI. X-ray crystal structures for the determination of absolute stereochemistry

The amino acid products (**3a**, **4a** and **5a**) were derivatized to the amide product **6** using 4-bromobenzoyl chloride for X-ray single crystal analysis.

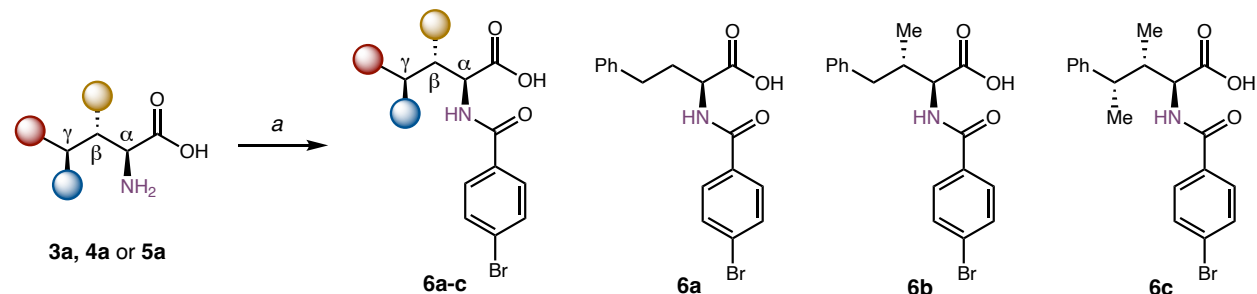


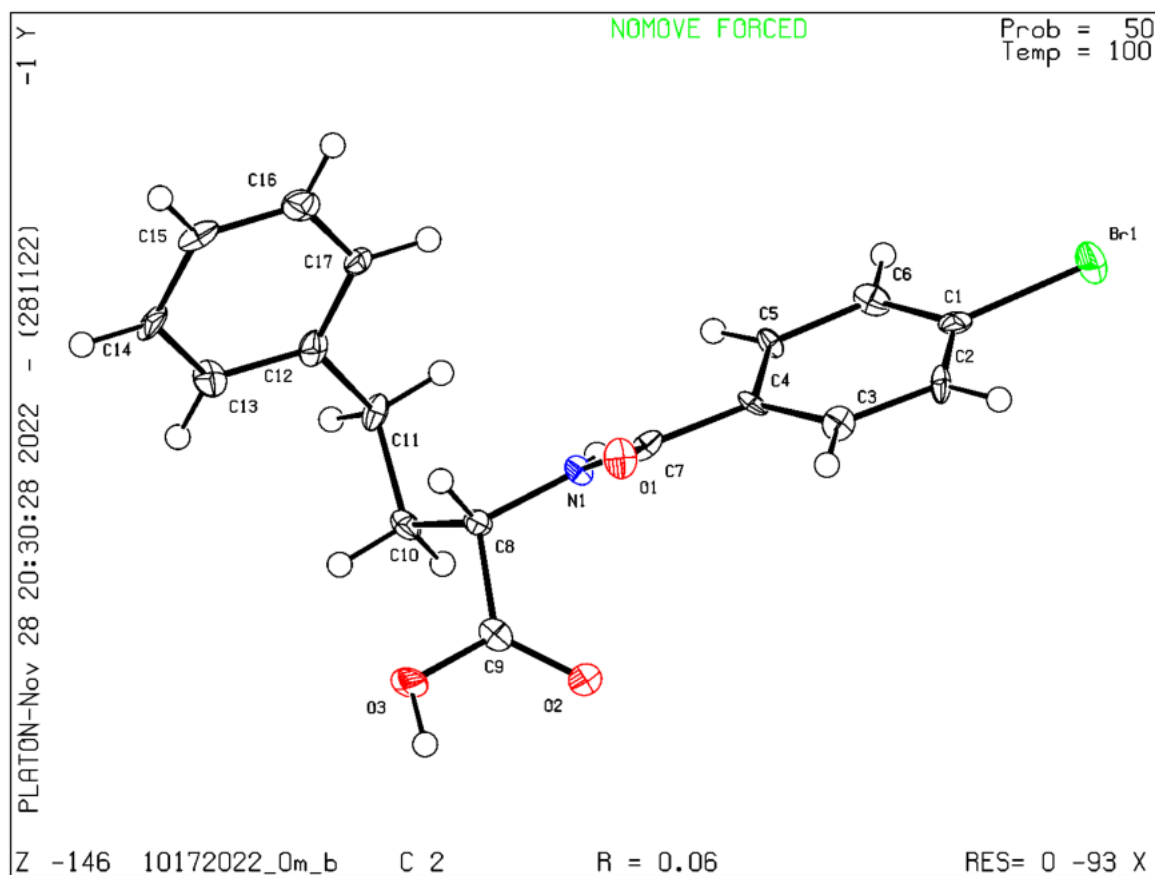
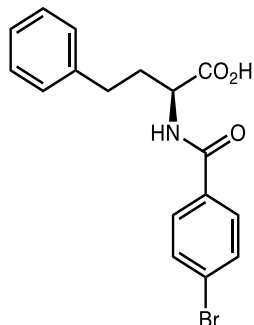
Fig. S14. Derivatization of amino acids for X-ray single crystal analysis.

Experimental procedure. At 0 °C, the amino acid was dissolved in 2 M NaOH (aq.) and a THF solution of 4-bromobenzoyl chloride (0.8 equiv) was added slowly (THF: H₂O = 1:1). The mixture was allowed to stir at room temperature for 3 h. 2 M HCl (aq.) was then added at 0 °C and the pH was adjusted to 2 with the aid of pH test paper. Then, EtOAc was added and the reaction mixture was extracted for two times with EtOAc. The organic layers were combined and dried over MgSO₄. The resulting product was concentrated under vacuum, and the resulting solid was directly used for crystallization. HPLC analysis of **6a** (IC column, hexanes: *i*-PrOH = 80:20, 1.0 mL/min) indicated >99:1 e.r., thus suggesting a minimal degree of racemization during this process (68).

For the crystallization of **6a** and **6b**, *n*-heptane/EtOAc (2:1) was used to dissolve the solids. The resulting solution was filtered through a PTFE membrane filter, and the filtrate was allowed to slowly evaporate at room temperature for several days to provide needle-shaped crystals suitable for XRD.

For **6c**, *n*-heptane/acetone (1:1) was used to provide needle-shaped crystals suitable for XRD.

(S)-2-(4-Bromobenzamido)-4-phenylbutanoic acid (6a) (CDCC 2220221)



Checkcif report:

Datablock: **10172022_0m_b**

Bond precision: C-C = 0.0136 Å Wavelength=0.71073

Cell: $a=18.817(4)$ $b=5.118(1)$ $c=18.362(4)$
 $\alpha=90$ $\beta=115.554(4)$ $\gamma=90$

Temperature: 100 K

Calculated

Reported

Volume	1595.4(6)	1595.4(6)
Space group	C 2	C 2
Hall group	C 2y	C 2y
Moiety formula	C17 H16 Br N O3	?
Sum formula	C17 H16 Br N O3	C17 H16 Br N O3
Mr	362.21	362.22
Dx,g cm-3	1.508	1.508
Z	4	4
Mu (mm-1)	2.588	2.588
F000	736.0	736.0
F000'	735.17	
h,k,lmax	22,6,22	22,6,22
Nref	3093[1732]	2963
Tmin,Tmax	0.856,0.879	0.593,0.745
Tmin'	0.460	

Correction method= # Reported T Limits: Tmin=0.593 Tmax=0.745

AbsCorr = MULTI-SCAN

Data completeness= 1.71/0.96 Theta(max)= 25.870

R(reflections)= 0.0561(2120) wR2(reflections)=
0.1150(2963)

S = 0.976 Npar= 199

The following ALERTS were generated. Each ALERT has the format

test-name_ALERT_alert-type_alert-level.

Click on the hyperlinks for more details of the test.

🟡 Alert level C

PLAT341_ALERT_3_C	Low Bond Precision on C-C Bonds	0.01359 Ang.
PLAT911_ALERT_3_C	Missing FCF Refl Between Thmin & STh/L=	0.600 11 Report

● Alert level G

<u>PLAT007_ALERT_5_G</u>	Number of Unrefined Donor-H Atoms	2 Report
<u>PLAT791_ALERT_4_G</u>	Model has Chirality at C8 (Sohnke SpGr)	S Verify
<u>PLAT883_ALERT_1_G</u>	No Info/Value for _atom_sites_solution_primary .	Please Do!
<u>PLAT912_ALERT_4_G</u>	Missing # of FCF Reflections Above STh/L= 0.600	15 Note
<u>PLAT941_ALERT_3_G</u>	Average HKL Measurement Multiplicity	3.6 Low
<u>PLAT978_ALERT_2_G</u>	Number C-C Bonds with Positive Residual Density.	0 Info

0 **ALERT level A** = Most likely a serious problem - resolve or explain

0 **ALERT level B** = A potentially serious problem, consider carefully

2 **ALERT level C** = Check. Ensure it is not caused by an omission or oversight

6 **ALERT level G** = General information/check it is not something unexpected

1 ALERT type 1 CIF construction/syntax error, inconsistent or missing data

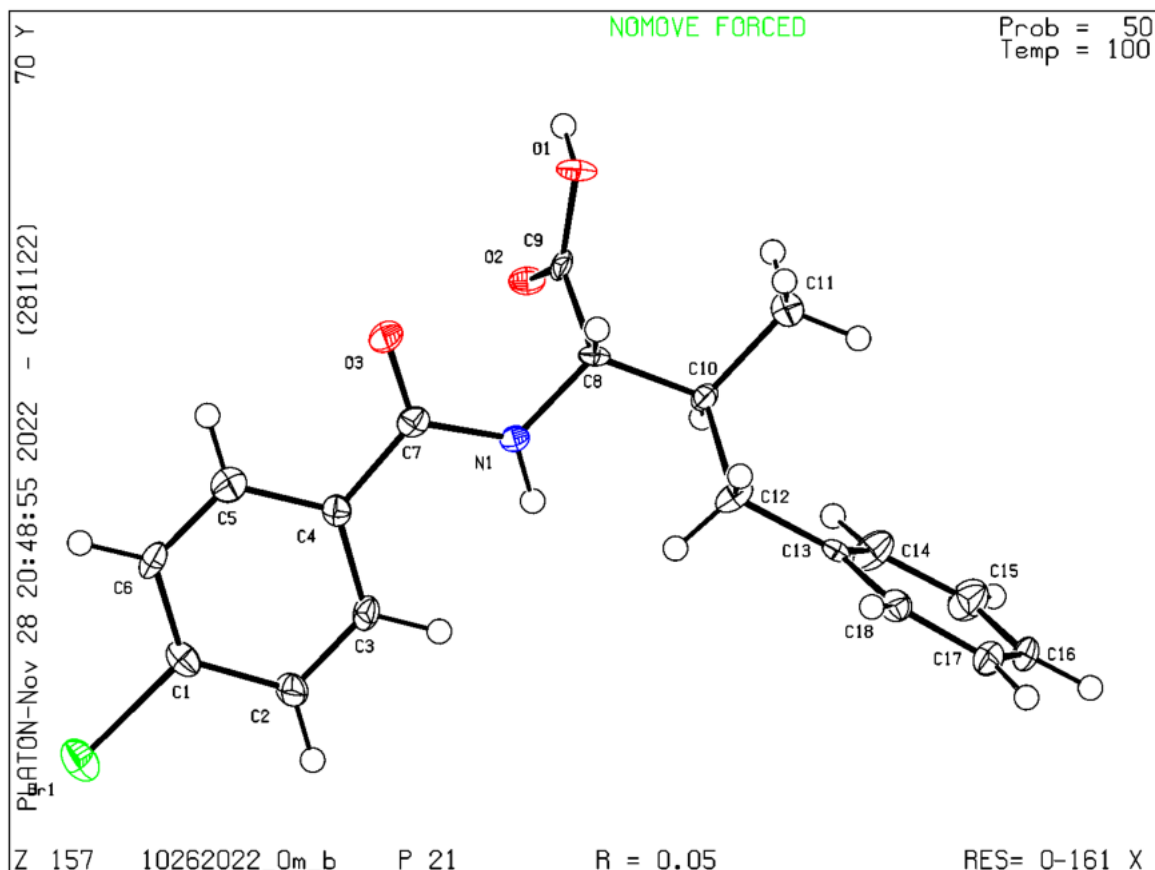
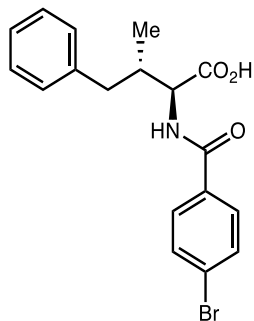
1 ALERT type 2 Indicator that the structure model may be wrong or deficient

3 ALERT type 3 Indicator that the structure quality may be low

2 ALERT type 4 Improvement, methodology, query or suggestion

1 ALERT type 5 Informative message, check

(2S,3S)-2-(4-Bromobenzamido)-3-methyl-4-phenylbutanoic acid (6b) (CDCC 2220222)



Checkcif report:

Datablock: 10262022_0m_b

Bond precision: C-C = 0.0103 Å Wavelength=0.71073

Cell: a=8.478(2) b=7.1807(18) c=13.544(4)
alpha=90 beta=96.347(13) gamma=90

Temperature: 100 K

Calculated

Reported

Volume	819.5(4)	819.5(4)
Space group	P 21	P 21
Hall group	P 2yb	P 2yb
Moiety formula	C18 H18 Br N O3	?
Sum formula	C18 H18 Br N O3	C18 H18 Br N O3
Mr	376.23	376.24
Dx,g cm-3	1.525	1.525
Z	2	2
Mu (mm-1)	2.522	2.522
F000	384.0	384.0
F000'	383.59	
h,k,lmax	10,8,16	10,8,16
Nref	3356[1817]	3324
Tmin,Tmax	0.641,0.882	0.575,0.745
Tmin'	0.598	

Correction method= # Reported T Limits: Tmin=0.575 Tmax=0.745

AbsCorr = MULTI-SCAN

Data completeness= 1.83/0.99 Theta(max)= 26.445

R(reflections)= 0.0504(2529) wR2(reflections)=
0.0954(3324)

S = 0.984 Npar= 213

The following ALERTS were generated. Each ALERT has the format

test-name_ALERT_alert-type_alert-level.

Click on the hyperlinks for more details of the test.

🟡 Alert level C

[PLAT341_ALERT_3_C](#) Low Bond Precision on C-C Bonds 0.01033 Ang.

● Alert level G

<u>PLAT007_ALERT_5_G</u>	Number of Unrefined Donor-H Atoms	1 Report
<u>PLAT791_ALERT_4_G</u>	Model has Chirality at C8 (Sohnke SpGr)	S Verify
<u>PLAT791_ALERT_4_G</u>	Model has Chirality at C10 (Sohnke SpGr)	S Verify
<u>PLAT883_ALERT_1_G</u>	No Info/Value for _atom_sites_solution_primary .	Please Do!
<u>PLAT912_ALERT_4_G</u>	Missing # of FCF Reflections Above STh/L= 0.600	6 Note
<u>PLAT941_ALERT_3_G</u>	Average HKL Measurement Multiplicity	3.8 Low
<u>PLAT978_ALERT_2_G</u>	Number C-C Bonds with Positive Residual Density.	0 Info

0 **ALERT level A** = Most likely a serious problem - resolve or explain

0 **ALERT level B** = A potentially serious problem, consider carefully

1 **ALERT level C** = Check. Ensure it is not caused by an omission or oversight

7 **ALERT level G** = General information/check it is not something unexpected

1 ALERT type 1 CIF construction/syntax error, inconsistent or missing data

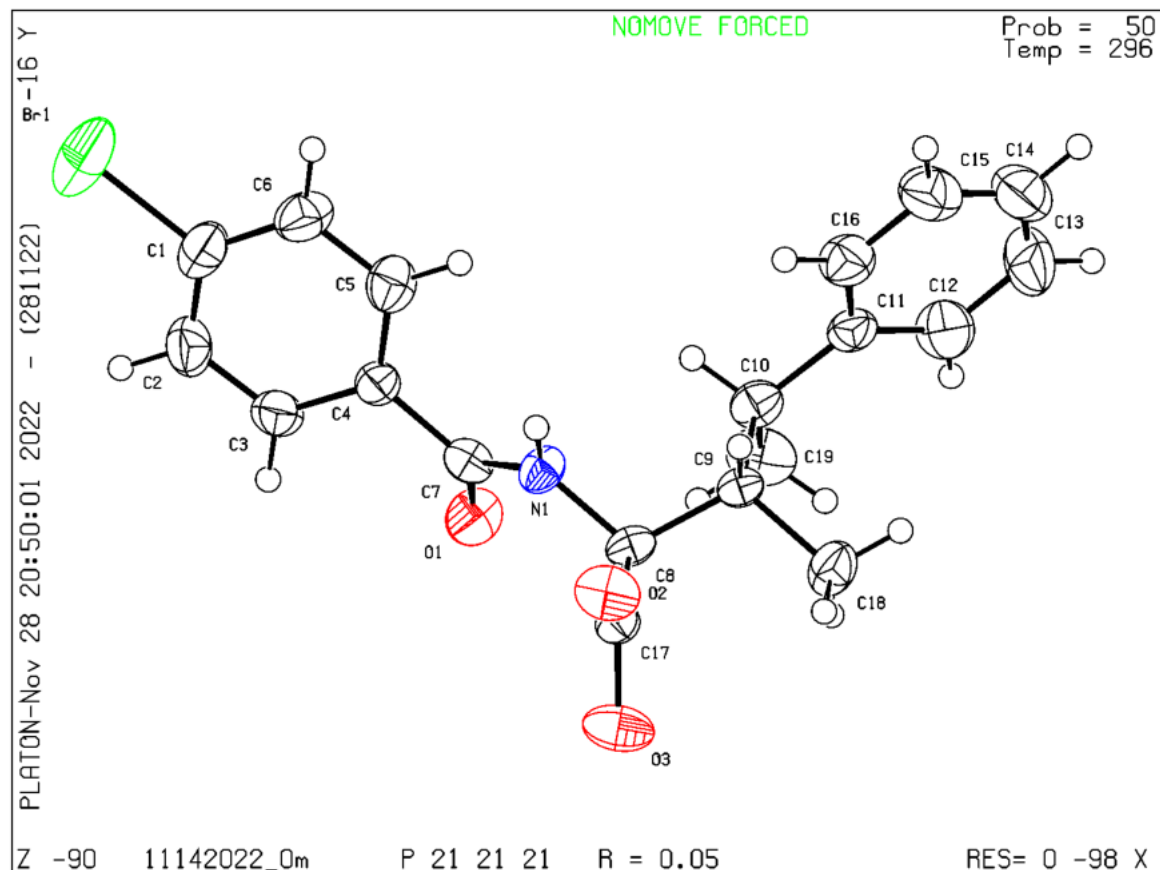
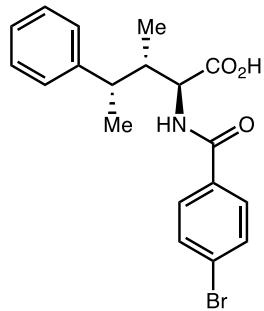
1 ALERT type 2 Indicator that the structure model may be wrong or deficient

2 ALERT type 3 Indicator that the structure quality may be low

3 ALERT type 4 Improvement, methodology, query or suggestion

1 ALERT type 5 Informative message, check

(2S, 3S, 4S)-2-(4-Bromobenzamido)-3-methyl-4-phenylpentanoic acid (6c) (CDCC 2220224)



Checkcif report:

Datablock: 11142022_0m

Bond precision: C-C = 0.0073 Å Wavelength=0.71073

Cell: a=7.4173(14) b=9.0592(17) c=26.459(5)
alpha=90 beta=90 gamma=90

Temperature: 296 K

Calculated

Reported

Volume	1777.9(6)	1777.9(6)
Space group	P 21 21 21	P 21 21 21
Hall group	P 2ac 2ab	P 2ac 2ab
Moiety formula	C19 H20 Br N O3	?
Sum formula	C19 H20 Br N O3	C19 H20 Br N O3
Mr	390.26	390.27
Dx,g cm-3	1.458	1.458
Z	4	4
Mu (mm-1)	2.328	2.328
F000	800.0	800.0
F000'	799.18	
h,k,lmax	8,10,31	8,10,31
Nref	3199[1868]	3169
Tmin,Tmax	0.756,0.792	0.614,0.745
Tmin'	0.497	

Correction method= # Reported T Limits: Tmin=0.614 Tmax=0.745

AbsCorr = MULTI-SCAN

Data completeness= 1.70/0.99 Theta(max)= 25.238

R(reflections)= 0.0466(1819) wR2(reflections)=
0.0607(3169)

S = 1.135 Npar= 219

The following ALERTS were generated. Each ALERT has the format

test-name_ALERT_alert-type_alert-level.

Click on the hyperlinks for more details of the test.

🟡 Alert level C

[PLAT242_ALERT_2_C](#) Low 'MainMol' Ueq as Compared to Neighbors of
Check

PLAT334 ALERT 2 C Small <C-C> Benzene Dist. C1 -C6 . 1.37
 Ang.
PLAT341 ALERT 3 C Low Bond Precision on C-C Bonds 0.00732 Ang.
PLAT911 ALERT 3 C Missing FCF Refl Between Thmin & STh/L= 0.600 12
 Report

● Alert level G

PLAT007 ALERT 5 G Number of Unrefined Donor-H Atoms 2 Report
PLAT791 ALERT 4 G Model has Chirality at C8 (Sohnke SpGr) S Verify

And 2 other PLAT791 Alerts

Less ...

PLAT791 ALERT 4 G Model has Chirality at C9 (Sohnke SpGr) S Verify
PLAT791 ALERT 4 G Model has Chirality at C10 (Sohnke SpGr) S Verify
PLAT883 ALERT 1 G No Info/Value for _atom_sites_solution_primary. Please Do!
PLAT941 ALERT 3 G Average HKL Measurement Multiplicity 3.9 Low
PLAT963 ALERT 2 G Both SHELXL WEIGHT Parameter Values Zero Please
 Check
PLAT965 ALERT 2 G The SHELXL WEIGHT Optimisation has not Converged Please
 Check
PLAT978 ALERT 2 G Number C-C Bonds with Positive Residual Density. 0 Info

- 0 **ALERT level A** = Most likely a serious problem - resolve or explain
- 0 **ALERT level B** = A potentially serious problem, consider carefully
- 4 **ALERT level C** = Check. Ensure it is not caused by an omission or oversight
- 9 **ALERT level G** = General information/check it is not something unexpected

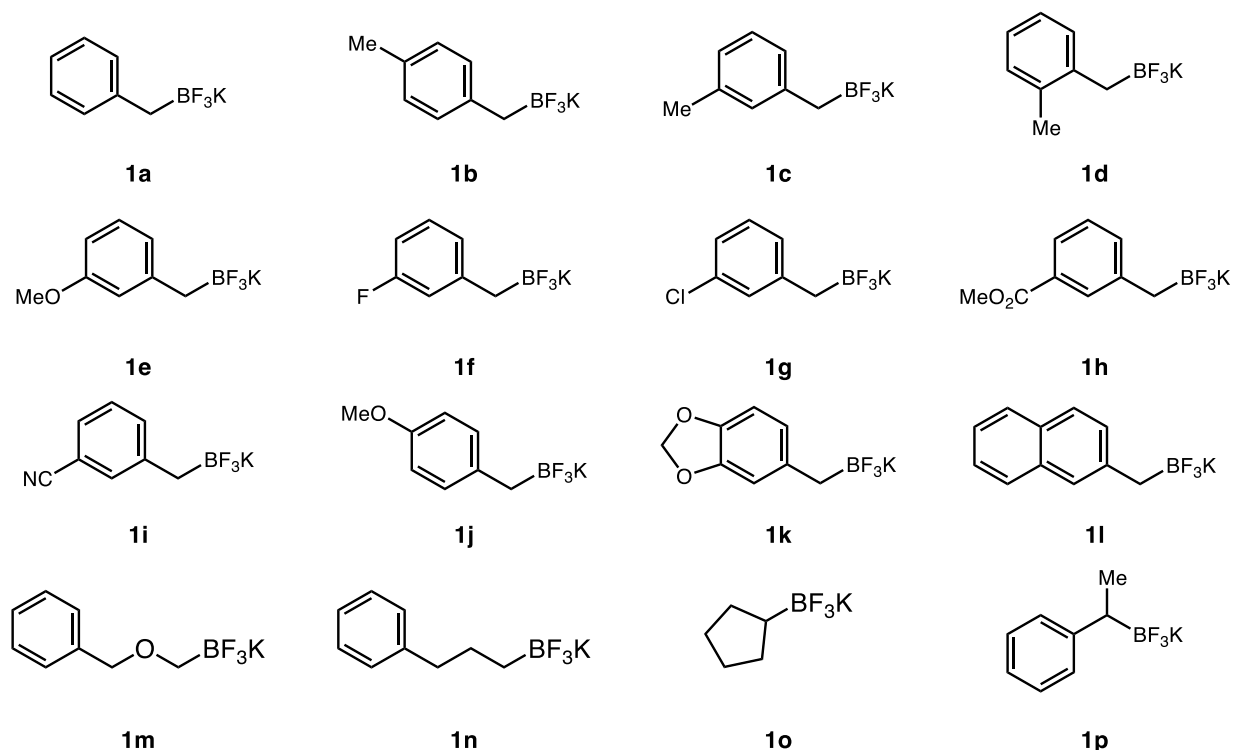
- 1 ALERT type 1 CIF construction/syntax error, inconsistent or missing data
- 5 ALERT type 2 Indicator that the structure model may be wrong or deficient

3 ALERT type 3 Indicator that the structure quality may be low

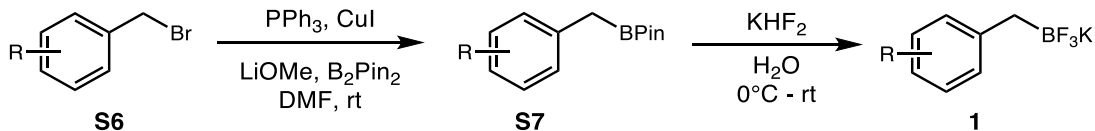
3 ALERT type 4 Improvement, methodology, query or suggestion

1 ALERT type 5 Informative message, check

XII. Synthesis and characterization of substrates



Compounds **1a–1b** and **1m–1o** were commercially available from Combi Blocks and they were used as received without further purification. Compounds **1c–1g**, **1j–1l**, and **1p** are known compounds (50, 69–71). Compounds **1h** and **1i** are unknown compounds. These alkyltrifluoroborate salts were synthesized according to **General procedures A, B, and C** as detailed below.

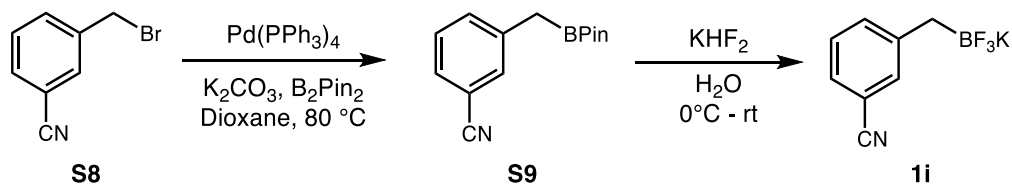


General procedure A. CuI (1.5 mmol, 10 mol%), PPh_3 (2.0 mmol, 13 mol%), LiOMe (30.0 mmol, 2.0 equiv) and bis(pinacolato)diboron (22.5 mmol, 1.5 equiv) were added to a 100 mL round-bottom flask. The flask was evacuated and backfilled with nitrogen (this process was repeated for 3 times). DMF (30 mL) and benzyl bromide (15.0 mmol, 1.0 equiv) were then added under nitrogen. The resulting mixture was allowed to stir at 25°C for 18 h. The reaction mixture was

then diluted with EtOAc (100 mL) and filtered through a silica plug. The filtrate was washed with brine (3×100 mL). The organic layer was dried over MgSO₄ and concentrated *in vacuo* with the aid of a rotary evaporator to provide the crude product, which was used directly for next step without further purification (72).

The crude product was dissolved in MeOH (50 mL) and cooled to 0 °C. Saturated aqueous KHF₂ (122 mmol, 8.1 equiv) was added dropwise over 30 min and the solution was allowed to warm to room temperature. The resulting suspension was concentrated under reduced pressure with the aid of a rotary evaporator. Pinacol and H₂O were azeotropically removed by resuspending the mixture in toluene (150 mL) and rotary evaporation at 40 °C. The remaining solid was dried under high vacuum and dissolved in hot acetone (3×100 mL) and filtered to remove inorganic salts. The filtrate was concentrated to a minimal volume (5–20 mL) and hexanes (500 mL) was added to provide a white solid. The solid product was isolated by filtration and washed with hexanes (50 mL) and CH₂Cl₂ (30 mL) to afford the desired benzyltrifluoroborate salt as analytically pure product (11).

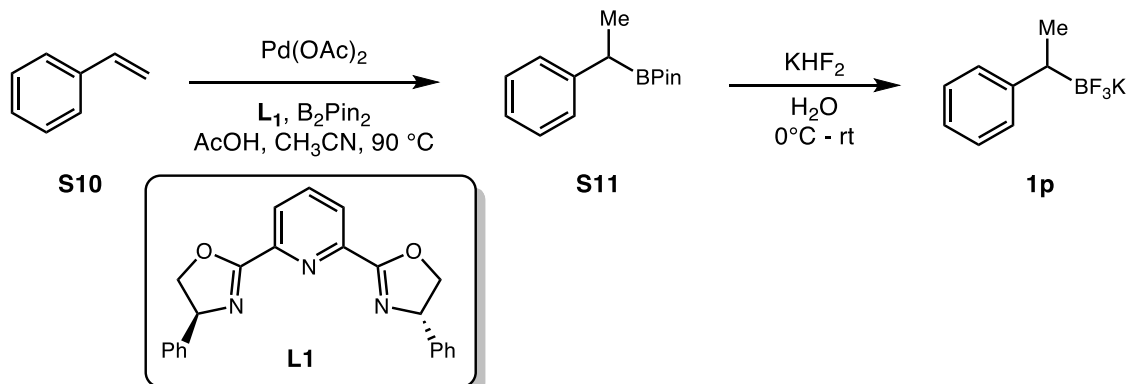
Compounds **1c–1h**, **1j–1l** were prepared according to general procedure A.



General procedure B. Pd(PPh₃)₄ (0.25 mmol, 5 mol%), bis(pinacolato)diboron (6.0 mmol, 1.2 equiv) and potassium carbonate (15 mmol, 3.0 equiv) were added to an oven-dried three-neck round bottom flask. The flask was evacuated and backfilled with nitrogen (this process was repeated for 3 times). The benzyl bromide substrate (5.0 mmol, 1.0 equiv) was added, followed by the addition of 1,4-dioxane (10 mL). The reaction mixture was heated to 80 °C for 6 h and then cooled to room temperature. The reaction mixture was filtered through a silica plug eluting with EtOAc (30 mL). The organic layer was washed with brine (3×30 mL), dried over MgSO₄, and concentrated *in vacuo* to provide the crude product, which was used directly for the next step without further purification (73).

Benzyltrifluoroborate salt preparation follows the same procedure as described in general procedure A.

Compound **1i** was prepared following general procedure B.



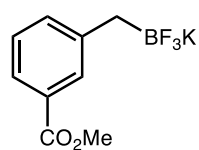
General procedure C. To a 100 mL round-bottom flask equipped with a stir bar were added $\text{Pd}(\text{OAc})_2$ (0.45 mmol, 7.5 mol%), styrene (6.0 mmol, 1.0 equiv), **L1** (0.45 mmol, 7.5 mol%), bis(pinacolato)diboron (9.0 mmol, 1.5 equiv), AcOH (10 mL), CH_3CN (20 mL). The vessel was evacuated and backfilled with nitrogen (this process was repeated for 3 times). The resulting reaction mixture was stirred at 90°C for 24 h. After the reaction proceeded to completion, it was cooled to room temperature, washed with sat. NaHCO_3 (aq.) and extracted with EtOAc (3×100 mL). The combined organic layers were washed with brine (100 mL), dried over MgSO_4 , concentrated *in vacuo* to provide the crude product, which was used directly for the next step without further purification (74).

Benzyltrifluoroborate salt preparation follows the same procedure as described in general procedure A.

Compound **1p** was prepared following this procedure.

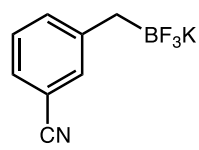
Characterization data for new trifluoroborate

Potassium trifluoro(3-(methoxycarbonyl)benzyl)borate (1h)



¹H NMR (400 MHz, DMSO-*d*₆) δ: 7.62 – 7.57 (m, 1H), 7.49 (dt, *J* = 7.4, 1.6 Hz, 1H), 7.25 – 7.13 (m, 2H), 3.79 (s, 3H), 1.52 (brs, 2H) ppm. ¹³C NMR (126 MHz, DMSO-*d*₆) δ: 167.5, 148.1 (q, *J* = 2.7 Hz), 134.0, 129.7, 128.9, 127.7, 123.6, 52.2 ppm. ¹⁹F NMR (376 MHz, DMSO-*d*₆) δ -137.04 ppm. ¹¹B NMR (128 MHz, DMSO-*d*₆) δ: 4.04 ppm. IR: 3003, 1707, 1420, 1354, 1223, 1091, 900, 530 cm⁻¹. HRMS (ESI) (m/z) for [M+K]⁺ C₉H₉BF₃K₂O₂ requires 294.9916, observed 294.9924.

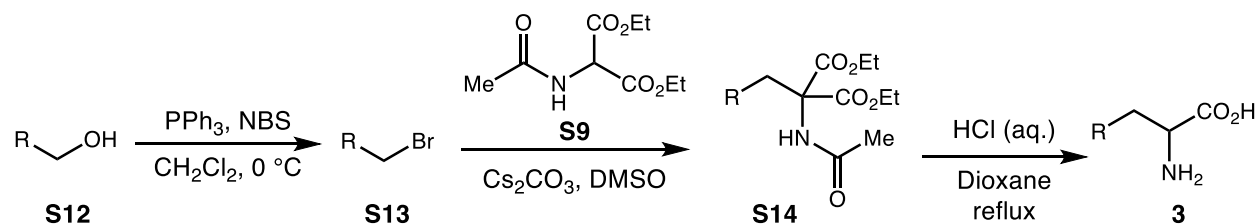
Potassium (3-cyanobenzyl)trifluoroborate (1i)



¹H NMR (400 MHz, DMSO-*d*₆) δ: 7.43 – 7.15 (m, 4H), 1.51 (brs, 2H) ppm. ¹³C NMR (126 MHz, DMSO-*d*₆) δ 149.4 (q, *J* = 2.6 Hz), 134.0, 131.9, 128.6, 126.4, 120.2, 110.4 ppm. ¹⁹F NMR (376 MHz, DMSO-*d*₆) δ: -137.36 ppm. ¹¹B NMR (128 MHz, DMSO-*d*₆) δ: 3.65 ppm. IR: 3000, 1705, 1422, 1355, 1217, 1090, 783, 530 cm⁻¹. HRMS (ESI) (m/z) for [M+K]⁺ C₈H₆BF₃K₂N requires 261.9814, observed 261.9821.

XIII. Synthesis and characterization of products

Compound **3a** was commercially available and directly used without further purification. Reference compounds **3b–3g**, **3i–3o** were synthesized using **general procedure D**. Amino acids **3h**, **4a–4e** and **5a**, *including their racemates*, are difficult to synthesize using chemical methods. Thus, preparative biocatalytic synthesis was used to provide these products using **general experimental procedure for preparative scale non-canonical amino acid synthesis** as described above.



General procedure D. This procedure was modified from previously described procedure (75, 76). The alcohol (10 mmol, 1.0 equiv) was dissolved in CH_2Cl_2 (60 mL) and the solution was cooled to 0 °C using ice bath under nitrogen. Triphenylphosphine (15 mmol, 1.5 equiv) was added in one portion and the resulting solution was stirred at 0 °C for 10 min. N-bromosuccinimide (15 mmol, 1.5 equiv) was then added into the solution slowly in several portions over 5 min and the mixture was allowed to stir at 0 °C for another 30 min. After the completion of the reaction as indicated by TLC analysis, the reaction solution was concentrated *in vacuo* and purified by column chromatography with the aid of a Biotage Isolera to afford the bromide product.

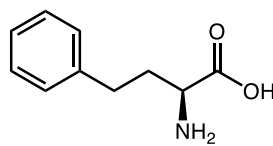
To a solution of diethyl acetamidomalonate (14.4 mol, 2.0 equiv) in DMSO (30 mL) was added Cs_2CO_3 (18.0 mol, 2.5 equiv) at 0 °C. The reaction solution was stirred at rt for 1 h. The alkyl bromide (7.2 mol, 1.0 equiv) was added to the reaction mixture at room temperature and the reaction mixture was stirred at 65 °C for 8 h. Upon the completion of this reaction, the mixture was added into ice water (80 mL) and stirred for 1 h. The precipitate was filtered and dried under vacuum to give the alkylation product as an off-white solid, which was used directly for the next step without further purification.

A suspension of this crude product (5.00 mmol, 0.2 M) in 1:1 of aq. HCl (6.0 M solution for **3b–3d**, **3f**, **3g**, **3i**, **3l**, **3n**, **3o**; 3.0 M solution for **3e**, **3j**, **3k**, **3m**) and 1,4-dioxane was heated to reflux for 12 h. Upon the completion of the reaction as indicated by TLC analysis, the reaction

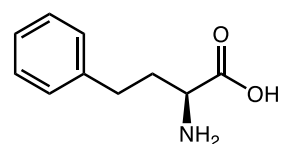
mixture was concentrated *in vacuo* with the aid of a rotary evaporator and the residue was recrystallized from methanol and diethyl ether. The solid amino acid product was collected by filtration. In many cases, this collected solid was found to be analytically pure. It can be further purified by C18 silica gel chromatography with the aid of a Biotage Isolera if needed.

Characterization data for non-canonical amino acids

2-Amino-4-phenylbutanoic acid (**3a**)



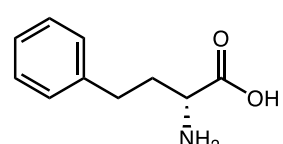
¹H NMR (500 MHz, D₂O) δ: 7.26 – 7.20 (m, 2H), 7.19 – 7.11 (m, 3H), 3.95 (t, *J* = 6.3 Hz, 1H), 2.73 – 2.57 (m, 2H), 2.20 – 2.01 (m, 2H) ppm. ¹³C NMR (126 MHz, D₂O) δ: 171.7, 139.9, 128.8, 128.4, 126.6, 52.2, 31.4, 30.2 ppm. Spectral data match those reported previously (77).



L-3a was prepared according to general procedure using L-*PfPLP*^β. **L-3a** was derivatized using (S)-FDAA and analyzed by LC-MS.

Yield: run 1: 78%; run 2: 71%; run 3: 70%; average yield: 73%.

Enantioselectivity: run 1: 93:7 e.r.; run 2: 93:7 e.r.; run 3: 92:8 e.r.; average e.r.: 93:7.

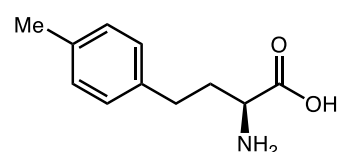


D-3a was prepared according to general procedure using D-*PfPLP*^β. **D-3a** was derivatized using (S)-FDAA and analyzed by LC-MS.

Yield: run 1: 80%; run 2: 81%; run 3: 77%; average yield: 79%.

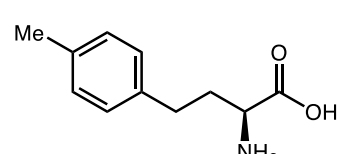
Enantioselectivity: run 1: 6:94 e.r.; run 2: 6:94 e.r.; run 3: 6:94 e.r.; average e.r.: 6:94.

2-Amino-4-(p-tolyl) butanoic acid (**3b**)



Purified by C18 silica using Biotage [10 g Biotage C18 Sfär cartridge, 0–25% MeCN (0.1% acetic acid) in H₂O (0.1% acetic acid) over 10 CV] to afford the product as a white solid.

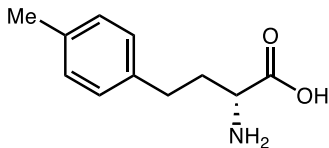
¹H NMR (500 MHz, D₂O) δ: 7.11 – 7.06 (m, 4H), 3.96 (t, *J* = 6.3 Hz, 1H), 2.70 – 2.55 (m, 2H), 2.19 – 2.11 (m, 4H), 2.09 – 2.01 (m, 1H) ppm. ¹³C NMR (126 MHz, D₂O) δ: 171.7, 136.8, 136.6, 129.3, 128.4, 52.2, 31.5, 29.8, 19.9 ppm. IR: 3301, 2946, 2831, 1675, 1452, 1416 cm⁻¹. HRMS (ESI) (m/z) for [M+Na]⁺ C₁₁H₁₅NNaO₂ requires 216.0995, observed 216.0994.



L-3b was prepared according to general procedure using L-*PfPLP*^β M139L I165F N166D Y301H (1.5 mol%) in KPi buffer (pH 6.3). **L-3b** was derived with (S)-Marfey's reagent and analyzed by LC-MS.

Yield: run 1: 63%; run 2: 62%; run 3: 61%; average yield: 62%.

Enantioselectivity: run 1: 98:2 e.r.; run 2: 98:2 e.r.; run 3: 98:2 e.r.; average e.r. 98:2.

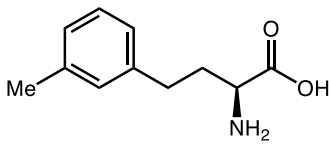


D-3b was prepared according to general procedure using L-*Pf*PLP β (1 mol%) in KPi buffer (pH 7). **D-3b** was derivatized using (S)-Marfey's reagent and analyzed by LC-MS.

Yield: run 1: 69%; run 2: 71%; run 3: 70%; run 4: 73%; average yield: 71%.

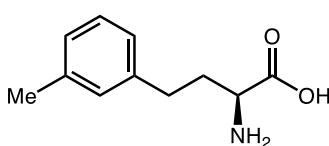
Enantioselectivity: run 1: 3:97 e.r.; run 2: 3:97 e.r.; run 3: 3:97 e.r.; run 4: 3:97 e.r.; average e.r.: 3:97.

2-Amino-4-(m-tolyl) butanoic acid (**3c**)



Purified by C18 silica using Biotage [10 g Biotage C18 Sfär cartridge, 0–25% MeCN (0.1% acetic acid) in H₂O (0.1% acetic acid) over 10 CV] to afford the product as a white solid.

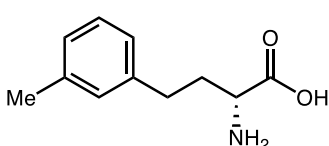
¹H NMR (500 MHz, D₂O) δ : 7.31 – 7.24 (m, 1H), 7.18 – 7.08 (m, 3H), 4.07 (t, *J* = 6.3 Hz, 1H), 2.83 – 2.67 (m, 2H), 2.31 (s, 3H), 2.30 – 2.14 (m, 2H) ppm. ¹³C NMR (126 MHz, D₂O) δ : 171.9, 140.1, 139.0, 129.1, 128.8, 127.2, 125.4, 52.4, 31.6, 30.2, 20.3 ppm. IR: 3319, 2946, 2831, 1663, 1446, 1416 cm⁻¹. HRMS (ESI) (m/z) for [M+Na]⁺ C₁₁H₁₅NNaO₂ requires 216.0995, observed 216.0997.



L-3c was prepared according to general procedure L-*Pf*PLP β (1 mol%) in KPi buffer (pH 6). **L-3c** was derived with (S)-Marfey's reagent and analyzed by LC-MS.

Yield: run 1: 71%; run 2: 76%; run 3: 76%; average yield: 74%.

Enantioselectivity: run 1: 89:11 e.r.; run 2: 88:12 e.r.; run 3: 88:12 e.r.; average e.r. 88:12.

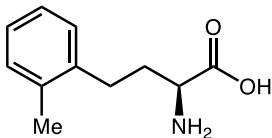


D-3c was prepared according to general procedure using L-*Pf*PLP β (1 mol%) in KPi buffer (pH 7). **D-3c** was derivatized using (S)-Marfey's reagent and analyzed by LC-MS.

Yield: run 1: 59%; run 2: 69%; run 3: 59%; average yield: 62%.

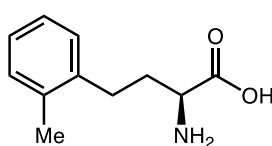
Enantioselectivity: run 1: 3:97 e.r.; run 2: 3:97 e.r.; run 3: 3:97 e.r.; average e.r.: 3:97.

2-Amino-4-(o-tolyl) butanoic acid (3d)



Purified by C18 silica using Biotage [10 g Biotage C18 Sfär cartridge, 0–25% MeCN (0.1% acetic acid) in H₂O (0.1% acetic acid) over 10 CV] to afford the product as a white solid.

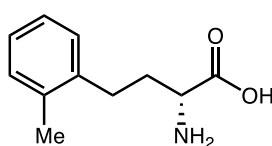
¹H NMR (500 MHz, D₂O) δ: 7.12 – 7.00 (m, 4H), 4.02 (t, *J* = 6.1 Hz, 1H), 2.70 – 2.52 (m, 2H), 2.13 (s, 3H), 2.09 – 1.92 (m, 2H) ppm. ¹³C NMR (126 MHz, D₂O) δ: 171.6, 138.2, 136.4, 130.4, 128.8, 126.8, 126.3, 52.5, 30.2, 27.8, 18.0 ppm. IR: 3301, 2940, 2831, 1657, 1446, 1410 cm⁻¹. Spectral data match those reported previously (78).



L-3d was prepared according to general procedure using L-*Pf*PLP^B (1 mol%) in KPi buffer (pH 6). **L-3d** was derived with (S)-Marfey's reagent and analyzed by LC-MS.

Yield: run 1: 63%; run 2: 74%; run 3: 70%; average yield: 69%.

Enantioselectivity: run 1: 56:44 e.r.; run 2: 56:44 e.r.; run 3: 56:44 e.r.; average e.r.: 56:44.

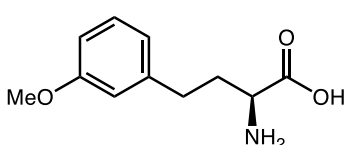


D-3d was prepared according to general procedure using D-*Pf*PLP^B (1 mol%) in KPi buffer (pH 7). **D-3d** was derived with (S)-Marfey's reagent and analyzed by LC-MS.

Yield: run 1: 58%; run 2: 50%; run 3: 50%; average yield: 53%.

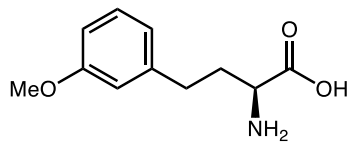
Enantioselectivity: run 1: 4:96 e.r.; run 2: 4:96 e.r.; run 3: 4:96 e.r.; average e.r.: 4:96.

2-Amino-4-(3-methoxyphenyl) butanoic acid (3e)



Purified by C18 silica using Biotage [10 g Biotage C18 Sfär cartridge, 0–25% MeCN (0.1% acetic acid) in H₂O (0.1% acetic acid) over 10 CV] to afford the product as a white solid.

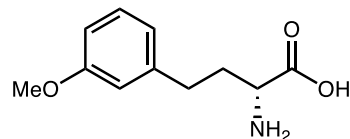
¹H NMR (500 MHz, D₂O) δ: 7.10 (t, *J* = 7.8 Hz, 1H), 6.75 – 6.64 (m, 3H), 3.89 (t, *J* = 6.3 Hz, 1H), 3.60 (s, 3H), 2.64 – 2.49 (m, 2H), 2.13 – 1.94 (m, 2H) ppm. ¹³C NMR (126 MHz, D₂O) δ: 171.6, 158.9, 141.7, 129.9, 121.2, 114.1, 112.0, 55.2, 52.2, 31.2, 30.2 ppm. IR: 3325, 2946, 2831, 1657, 1452, 1410 cm⁻¹. HRMS (ESI) (m/z) for [M+Na]⁺ C₁₁H₁₅NNaO₃ requires 232.0944, observed 232.0941.



L-3e was prepared according to general procedure using L-*Pf*PLP^β (1 mol%) in KPi buffer (pH 6). **L-3e** was derived with (*S*)-Marfey's reagent and analyzed by LC-MS.

Yield: run 1: 63%; run 2: 64%; run 3: 59%; average yield: 62%.

Enantioselectivity: run 1: 93:7 e.r.; run 2: 93:7 e.r.; run 3: 92:8 e.r.; average e.r.: 93:7.

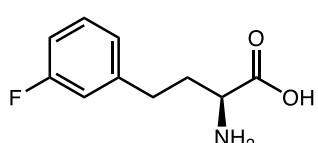


D-3e was prepared according to general procedure using D-*Pf*PLP^β (1 mol%) in KPi buffer (pH 7). **D-3e** was derived with (*S*)-Marfey's reagent and analyzed by LC-MS.

Yield: run 1: 74%; run 2: 80%; run 3: 74%; average yield: 76%.

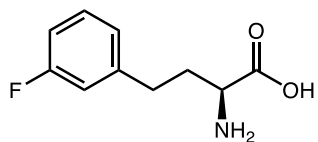
Enantioselectivity: run 1: 4:96 e.r.; run 2: 4:96 e.r.; run 3: 4:96 e.r.; average e.r.: 4:96.

2-Amino-4-(3-fluorophenyl) butanoic acid (3f)



Purified by C18 silica using Biotage [10 g Biotage C18 Sfär cartridge, 0–25% MeCN (0.1% acetic acid) in H₂O (0.1% acetic acid) over 10 CV] to afford the product as a white solid.

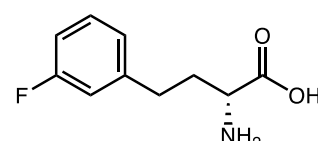
¹H NMR (400 MHz, MeOD) δ: 7.38 – 7.26 (m, 1H), 7.10 – 7.04 (m, 1H), 7.04 – 6.88 (m, 2H), 3.98 (t, *J* = 6.3 Hz, 1H), 2.91 – 2.70 (m, 2H), 2.32 – 2.08 (m, 2H) ppm. ¹³C NMR (126 MHz, MeOD) δ: 170.2, 163.0 (d, *J* = 244.5 Hz), 142.7 (d, *J* = 7.3 Hz), 130.1 (d, *J* = 8.3 Hz), 123.9 (d, *J* = 2.7 Hz), 114.8 (d, *J* = 21.3 Hz), 112.9 (d, *J* = 21.2 Hz), 52.0, 31.9, 30.4 ppm. ¹⁹F NMR (376 MHz, MeOD) δ: -115.33 ppm. IR: 3340, 2947, 2841, 1590, 1489, 1453, 1255 cm⁻¹. HRMS (ESI) (m/z) for [M+Na]⁺ C₁₀H₁₂FNNaO₂ requires 220.0744, observed 220.0742.



L-3f was prepared according to general procedure using L-*Pf*PLP^β (1 mol%) in KPi buffer (pH 6). **L-3f** was derived with (*S*)-Marfey's reagent and analyzed by LC-MS.

Yield: run 1: 70%; run 2: 67%; run 3: 60%; average yield: 65%.

Enantioselectivity: run 1: 92:8 e.r.; run 2: 92:8 e.r.; run 3: 91:9 e.r.; average e.r.: 92:8.

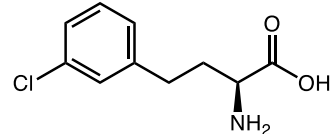


D-3f was prepared according to general procedure using D-*Pf*PLP^β (1 mol%) in KPi buffer (pH 7). **D-3f** was derived with (*S*)-Marfey's reagent and analyzed by LC-MS.

Yield: run 1: 89%; run 2: 84%; run 3: 95%; average yield: 89%.

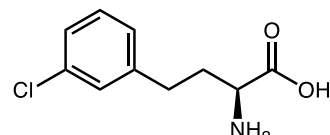
Enantioselectivity: run 1: 6:94 e.r.; run 2: 6:94 e.r.; run 3: 4:96 e.r.; average e.r.: 5:95.

2-Amino-4-(3-chlorophenyl) butanoic acid (**3g**)



Purified by C18 silica using Biotage [10 g Biotage C18 Sfär cartridge, 0–25% MeCN (0.1% acetic acid) in H₂O (0.1% acetic acid) over 10 CV] to afford the product as a white solid.

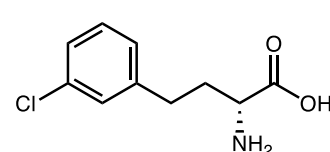
¹H NMR (400 MHz, MeOD) δ: 7.43 – 7.32 (m, 2H), 7.32 – 7.20 (m, 2H), 4.05 (t, *J* = 6.2 Hz, 1H), 2.96 – 2.75 (m, 2H), 2.38 – 2.14 (m, 2H) ppm. ¹³C NMR (126 MHz, MeOD) δ: 171.5, 143.6, 135.4, 131.2, 129.5, 127.9, 127.7, 53.4, 33.3, 31.8 ppm. IR: 3307, 2940, 2831, 1657, 1446, 1410 cm⁻¹. HRMS (ESI) (m/z) for [M+H]⁺ C₁₀H₁₃ClNO₂ requires 214.0629, observed 214.0627.



L-3g was prepared according to general procedure using L-*P*fPLP^β (1 mol%) in KPi buffer (pH 6). **L-3g** was derived with (S)-Marfey's reagent and analyzed by LC-MS.

Yield: run 1: 66%; run 2: 67%; run 3: 65%; average yield: 66%.

Enantioselectivity: run 1: 95:5 e.r.; run 2: 95:5 e.r.; run 3: 95:5 e.r.; average e.r.: 95:5.

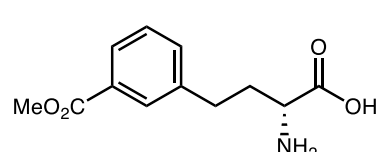


D-3g was prepared according to general procedure using D-*P*fPLP^β (1 mol%) in KPi buffer (pH 7). **D-3g** was derived with (S)-Marfey's reagent and analyzed by LC-MS.

Yield: run 1: 56%; run 2: 55%; run 3: 56%; average yield: 56%.

Enantioselectivity: run 1: 5:95 e.r.; run 2: 4:96 e.r.; run 3: 4:96 e.r.; average e.r.: 4.5:95.5.

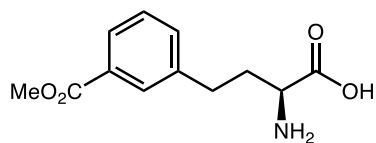
(R)-2-Amino-4-(3-(methoxycarbonyl) phenyl) butanoic acid (**3h**)



The product was prepared using enzymatic reactions (general procedure E) and purified by C18 silica using Biotage [10 g Biotage C18 Sfär cartridge, 0–25% MeCN (0.1% acetic acid) in H₂O (0.1% acetic acid) over 10 CV] to afford the product as a white solid.

¹H NMR (500 MHz, D₂O) δ: 7.74 – 7.67 (m, 2H), 7.40 (dt, *J* = 7.7, 1.5 Hz, 1H), 7.30 (t, *J* = 7.7 Hz, 1H), 3.95 (t, *J* = 6.3 Hz, 1H), 3.75 (s, 3H), 2.78 – 2.61 (m, 2H), 2.20 – 2.03 (m, 2H) ppm. ¹³C NMR (126 MHz, D₂O) δ: 171.6, 169.2, 140.3, 133.7, 129.6, 129.1, 128.9, 127.5, 52.6, 52.1, 31.1,

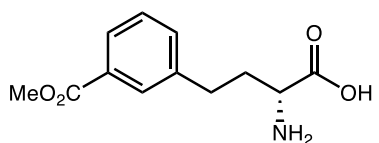
30.0 ppm. IR: 3022, 2972, 2867, 1720, 1608, 1505, 1436 cm^{-1} . HRMS (ESI) (m/z) for $[\text{M}+\text{H}]^+$ $\text{C}_{12}\text{H}_{16}\text{NO}_4$ requires 238.1074, observed 238.1076. $[\alpha]_D^{23} = -11.7$ ($c = 0.4$, MeOH).



L-3h was prepared according to general procedure using L-*Pf*PLP $^\beta$ (1 mol%) in KPi buffer (pH 7). **L-3h** was derived with (S)-Marfey's reagent and analyzed by LC-MS.

Yield: run 1: 25%; run 2: 22%; run 3: 21%; average yield: 23%.

Enantioselectivity: run 1: 96:4 e.r.; run 2: 95:5 e.r.; run 3: 96:4 e.r.; average e.r. 96:4.

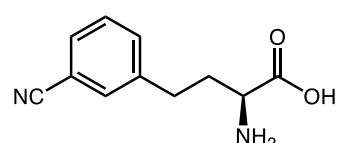


D-3h was prepared according to general procedure using D-*Pf*PLP $^\beta$ (1 mol%) in KPi buffer (pH 7). **D-3h** was derived with (S)-Marfey's reagent and analyzed by LC-MS.

Yield: run 1: 42%; run 2: 36%; run 3: 35%; average yield: 37%.

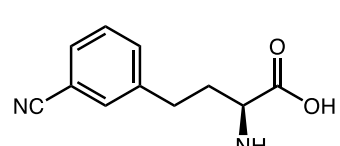
Enantioselectivity: run 1: 6:94 e.r.; run 2: 5: 95e.r.; run 3: 6:94 e.r.; average e.r.: 6:94.

2-Amino-4-(3-cyanophenyl) butanoic acid (3i)



Purified by C18 silica using Biotage [10 g Biotage C18 Sfär cartridge, 0–25% MeCN (0.1% acetic acid) in H₂O (0.1% acetic acid) over 10 CV] to afford the product as a white solid.

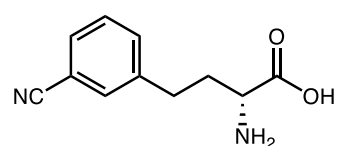
¹H NMR (400 MHz, D₂O) δ : 7.92 – 7.55 (m, 3H), 7.54 – 7.45 (m, 1H), 4.05 (t, $J = 6.2$ Hz, 1H), 2.96 – 2.75 (m, 2H), 2.38 – 2.14 (m, 2H) ppm. ¹³C NMR (126 MHz, D₂O) δ : 172.0, 141.2, 133.7, 132.1, 130.6, 129.5, 119.7, 111.1, 52.4, 31.1, 30.0 ppm. IR: 3306, 2940, 2835, 1658, 1453, 1416 cm^{-1} . HRMS (ESI) (m/z) for $[\text{M}+\text{H}]^+$ $\text{C}_{11}\text{H}_{13}\text{N}_2\text{O}_2$ requires 205.0972, observed 205.0977.



L-3i was prepared according to general procedure using L-*Pf*PLP $^\beta$ (1 mol%) in KPi buffer (pH 6). **L-3i** was derived with (S)-Marfey's reagent and analyzed by LC-MS.

Yield: run 1: 55%; run 2: 58%; run 3: 59%; average yield: 57%.

Enantioselectivity: run 1: 98:2 e.r.; run 2: 97:3 e.r.; run 3: 97:3 e.r.; average e.r.: 97:3.

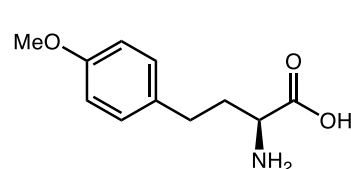


D-3i was prepared according to general procedure using D-*Pf*PLP $^\beta$ (1 mol%) in KPi buffer (pH 7). **D-3i** was derived with (S)-Marfey's reagent and analyzed by LC-MS.

Yield: run 1: 54%; run 2: 52%; run 3: 53%; average yield: 53%.

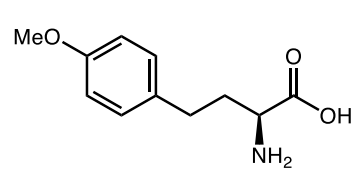
Enantioselectivity: run 1: 4:96 e.r.; run 2: 4:96 e.r.; run 3: 4:96 e.r.; average e.r. 4:96.

2-Amino-4-(4-methoxyphenyl) butanoic acid (**3j**)



Purified by C18 silica using Biotage [10 g Biotage C18 Sfär cartridge, 0–25% MeCN (0.1% acetic acid) in H₂O (0.1% acetic acid) over 10 CV] to afford the product as a white solid.

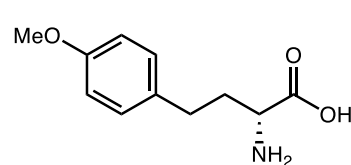
¹H NMR (500 MHz, D₂O) δ: 7.17 – 7.10 (m, 2H), 6.88 – 6.82 (m, 2H), 3.96 (t, *J* = 6.3 Hz, 1H), 3.69 (s, 3H), 2.69 – 2.56 (m, 2H), 2.20 – 2.01 (m, 2H) ppm. ¹³C NMR (126 MHz, D₂O) δ: 171.8, 157.4, 132.6, 129.6, 114.2, 55.4, 52.2, 31.6, 29.4 ppm. Spectral data match those reported previously (79).



L-3j was prepared according to general procedure using L-*Pf*PLP^β (1.0 mol%) in KPi buffer (pH 6). The reactions were conducted in triplicates. **L-3j** was derived with (S)-Marfey's reagent and analyzed by LC-MS.

Yield: run 1: 67%; run 2: 61%; run 3: 64%; average yield: 64%.

Enantioselectivity: run 1: 96:4 e.r.; run 2: 97:3 e.r.; run 3: 96:4 e.r.; average e.r.: 96:4.

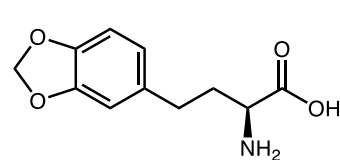


D-3j was prepared according to general procedure using D-*Pf*PLP^β (1 mol%) in KPi buffer (pH 7). **D-3j** was derived as diastereoisomers using (S)-Marfey's reagent and analyzed by LC-MS.

Yield: run 1: 77%; run 2: 79%; run 3: 80%; average yield: 79%.

Enantioselectivity: run 1: 1:99 e.r.; run 2: 2:98 e.r.; run 3: 1:99 e.r.; average e.r.: 1.5:98.5.

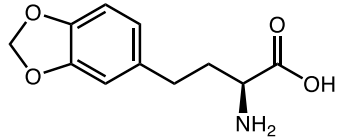
2-Amino-4-(benzo[d][1,3]dioxol-5-yl)butanoic acid (**3k**)



Purified by C18 silica using Biotage [10 g Biotage C18 Sfär cartridge, 0–25% MeCN (0.1% acetic acid) in H₂O (0.1% acetic acid) over 10 CV] to afford the product as a white solid.

¹H NMR (500 MHz, D₂O) δ: 6.67 – 6.61 (m, 2H), 6.60 – 6.56 (m, 1H), 5.73 (s, 2H), 3.90 (t, *J* = 6.3 Hz, 1H), 2.67 – 2.45 (m, 2H), 2.12 – 1.93 (m, 2H) ppm. ¹³C NMR (126 MHz, D₂O) δ: 171.6, 147.0, 145.4, 133.7, 121.4, 108.8, 108.4, 100.8, 52.1, 31.6, 30.0 ppm.

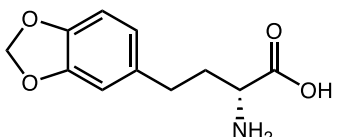
IR: 3319, 2946, 2831, 1663, 1446, 1416 cm^{-1} . HRMS (ESI) (m/z) for $[\text{M}+\text{Na}]^+$ $\text{C}_{11}\text{H}_{13}\text{NNaO}_4$ requires 246.0737, observed 246.0742.



L-3k was prepared according to general procedure using L-*Pf*PLP $^\beta$ M139L I165F N166D Y301H (2.0 mol%) in KPi buffer (pH 7). **L-3k** was derived with (S)-Marfey's reagent and analyzed by LC-MS.

Yield: run 1: 44%; run 2: 41%; run 3: 41%; average yield: 42%.

Enantioselectivity: run 1: 95:5 e.r.; run 2: 95:5 e.r.; run 3: 95:5 e.r.; average e.r.: 95:5.

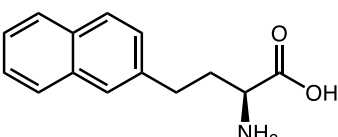


D-3k was prepared according to general procedure using D-*Pf*PLP $^\beta$ (1 mol%) in KPi buffer (pH 7). **D-3k** was derived with (S)-Marfey's reagent and analyzed by LC-MS.

Yield: run 1: 32%; run 2: 33 %; run 3: 32%; average yield: 32%.

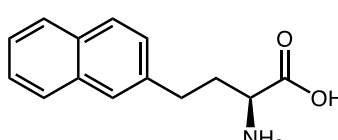
Enantioselectivity: run 1: 4:96 e.r.; run 2: 5:95 e.r.; run 3: 5:95 e.r.; average e.r.: 5:95.

2-Amino-4-(naphthalen-2-yl)butanoic acid (3l)



Purified by C18 silica using Biotage [10 g Biotage C18 Sfär cartridge, 0–25% MeCN (0.1% acetic acid) in H₂O (0.1% acetic acid) over 10 CV] to afford the product as a white solid.

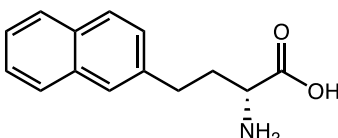
¹H NMR (500 MHz, MeOD) δ : 7.85 – 7.77 (m, 3H), 7.74 – 7.70 (m, 1H), 7.51 – 7.37 (m, 3H), 4.03 (t, J = 6.3 Hz, 1H), 3.06 – 2.88 (m, 2H), 2.41 – 2.21 (m, 2H) ppm. ¹³C NMR (126 MHz, MeOD) δ : 171.7, 138.7, 135.1, 133.8, 129.4, 128.6, 128.5, 127.8, 127.7, 127.2, 126.6, 53.5, 33.4, 32.2 ppm. Spectral data match those reported previously (80).



L-3l was prepared according to general procedure using L-*Pf*PLP $^\beta$ M139L I165F N166D Y301H (2.0 mol%) in KPi buffer (pH 7). **L-3l** was derived with (S)-Marfey's reagent and analyzed by LC-MS.

Yield: run 1: 44%; run 2: 45%; run 3: 52%; average yield: 47%.

Enantioselectivity: run 1: 91:9 e.r.; run 2: 90:10 e.r.; run 3: 91:9 e.r.; average e.r.: 90:10.

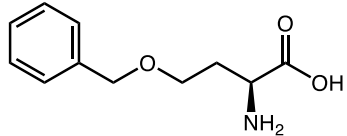


D-3l was prepared according to general procedure using D-*Pf*PLP $^\beta$ (1 mol%) in KPi buffer (pH 7). **D-3l** was derived with (S)-Marfey's reagent and analyzed by LC-MS.

Yield: run 1: 28%; run 2: 22%; run 3: 23%; average yield: 24%.

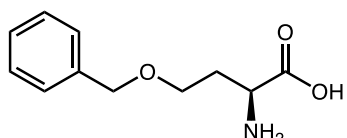
Enantioselectivity: run 1: 2:98 e.r.; run 2: 2:98 e.r.; run 3: 2:98 e.r.; average e.r. 2:98.

O-benzyl-L-homoserine (3m)



Purified by C18 silica using Biotage [10 g Biotage C18 Sfär cartridge, 0–25% MeCN (0.1% acetic acid) in H₂O (0.1% acetic acid) over 10 CV] to afford the product as a white solid.

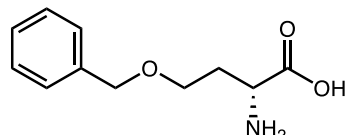
¹H NMR (400 MHz, D₂O) δ: 7.51 – 7.38 (m, 5H), 4.59 (s, 2H), 3.89 – 3.84 (m, 1H), 3.78 – 3.70 (m, 2H), 2.29 – 2.06 (m, 2H) ppm. ¹³C NMR (126 MHz, D₂O) δ: 174.0, 137.3, 128.7, 128.4, 128.3, 73.0, 67.0, 53.5, 29.9 ppm. IR: 3319, 2946, 2831, 1657, 1446, 1416 cm⁻¹. HRMS (ESI) (m/z) for [M+Na]⁺ C₁₁H₁₅NNaO₃ requires 232.0944, observed 232.0950.



L-3m was prepared according to general procedure using L-P*f*PLP^β (2.0 mol%) in KPi buffer (pH 7). **L-3m** was derived with (S)-Marfey's reagent and analyzed by LC-MS.

Yield: run 1: 6%; run 2: 6%; run 3: 5%; average yield: 6%.

Enantioselectivity: run 1: 96:4 e.r.; run 2: 95:5 e.r.; run 3: 96:4 e.r.; average e.r.: 96:4.

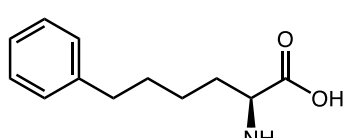


D-3m was prepared according to general procedure using D-P*f*PLP^β (1 mol%) in KPi buffer (pH 7). **D-3m** was derived with (S)-Marfey's reagent and analyzed by LC-MS.

Yield: run 1: 5%; run 2: 4%; run 3: 3%; average yield: 4%.

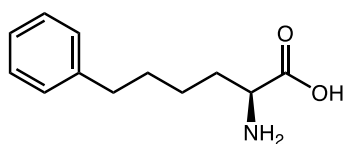
Enantioselectivity: run 1: 87:13 e.r.; run 2: 89:11 e.r.; run 3: 88:12 e.r.; average e.r.: 88: 12.

2-amino-6-phenylhexanoic acid (3n)



Purified by C18 silica using Biotage [10 g Biotage C18 Sfär cartridge, 0–25% MeCN (0.1% acetic acid) in H₂O (0.1% acetic acid) over 10 CV] to afford the product as a white solid.

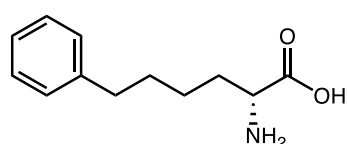
¹H NMR (400 MHz, D₂O) δ: 7.28 – 7.22 (m, 2H), 7.20 – 7.12 (m, 3H), 3.96 (t, *J* = 6.3 Hz, 1H), 2.54 (t, *J* = 7.5 Hz, 2H), 1.95 – 1.77 (m, 2H), 1.63 – 1.51 (m, 2H), 1.43 – 1.20 (m, 2H) ppm. ¹³C NMR (126 MHz, D₂O) δ: 171.8, 142.5, 128.4, 125.8, 52.6, 34.3, 29.9, 29.3, 23.5 ppm. Spectral data match those reported previously (18).



L-3n was prepared according to general procedure using L-*Pf*PLP β (2.0 mol%) in KPi buffer (pH 7). **L-3n** was derived with (S)-Marfey's reagent and analyzed by LC-MS.

Yield: run 1: 16%; run 2: 15%; run 3: 15%; average yield: 15%.

Enantioselectivity: run 1: 72:28 e.r.; run 2: 70:20 e.r.; run 3: 71:29 e.r.; average e.r.: 71:29.



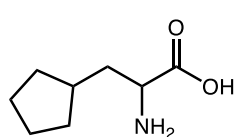
D-3n was prepared according to general procedure using D-*Pf*PLP β (1 mol%) in KPi buffer (pH 7). **D-3n** was derived with (S)-Marfey's reagent and analyzed by LC-MS.

Yield: run 1: 2.0%; run 2: 2.2%; run 3: 2.1%; average yield: 2.1%.

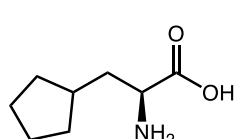
Enantioselectivity: run 1: 5:95 e.r.; run 2: 4:96 e.r.; run 3: 6:94 e.r.; average e.r.: 5:95.

2-amino-3-cyclopentylpropanoic acid (**3o**)

Crystallization using MeOH and Et₂O to afford the product as a white solid.



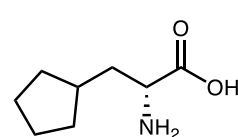
¹H NMR (500 MHz, MeOD) δ : 3.91 (dd, *J* = 7.4, 5.9 Hz, 1H), 2.06 – 1.94 (m, 2H), 1.94 – 1.80 (m, 3H), 1.75 – 1.64 (m, 2H), 1.66 – 1.55 (m, 2H), 1.26 – 1.14 (m, 2H) ppm. ¹³C NMR (126 MHz, MeOD) δ : 172.2, 53.5, 37.9, 37.2, 33.4, 33.3, 26.0, 25.8 ppm. IR: 3325, 2940, 2831, 1651, 1452, 1422 cm⁻¹. HRMS (ESI) (m/z) for [M+H]⁺ C₈H₁₆NO₂ requires 158.1176, observed 158.1176.



L-3o was prepared according to general procedure using L-*Pf*PLP β (2.0 mol%) in KPi buffer (pH 7). **L-3o** was derived with (S)-Marfey's reagent and analyzed by LC-MS.

Yield: run 1: 4%; run 2: 4%; run 3: 4%; average yield: 4%.

Enantioselectivity: run 1: 88:12 e.r.; run 2: 88:12 e.r.; run 3: 89:11 e.r.; average e.r.: 88:12.

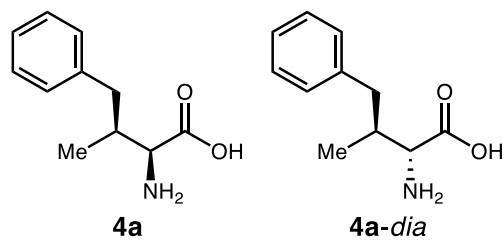


D-3o was prepared according to general procedure using D-*Pf*PLP β (1 mol%) in KPi buffer (pH 7). **D-3o** was derived with (S)-Marfey's reagent and analyzed by LC-MS.

Yield: run 1: 8%; run 2: 9 %; run 3: 7%; average yield: 8%.

Enantioselectivity: run 1: 32:68 e.r.; run 2: 32:68 e.r.; run 3: 32:68 e.r.; average e.r.: 32:68.

(2*S*, 3*S*)-2-amino-3-methyl-4-phenylbutanoic acid (4a**)**

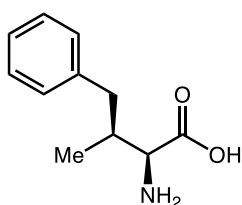


NMR d.r. = 20 : 1 (**4a** : **4a-dia**)

Compound **4a** was prepared using biocatalytic methods following the general procedure. The reaction mixture was purified by C18 silica using Biotage [10 g Biotage C18 Sfär cartridge, 0–25% MeCN (0.1% acetic acid) in H₂O (0.1% acetic acid) over 10 CV] to afford the product as a white solid. Two diastereomers were present (d.r. =

20:1) in this product.

¹H NMR (500 MHz, D₂O) for major diastereomer (**4a**) δ: 7.18 – 7.13 (m, 2H), 7.11 – 7.06 (m, 3H), 3.82 (d, *J* = 3.3 Hz, 1H), 2.64 (dd, *J* = 13.6, 6.7 Hz, 1H), 2.44 (dd, *J* = 13.6, 8.7 Hz, 1H), 2.28 – 2.20 (m, 1H), 0.78 (d, *J* = 7.0 Hz, 3H) ppm; for minor diastereomer (**4a-dia**) δ: 7.18 – 7.13 (m, 2H), 7.11 – 7.06 (m, 3H), 3.84 (d, *J* = 3.2 Hz, 1H), 2.64 (dd, *J* = 13.6, 6.7 Hz, 1H), 2.44 (dd, *J* = 13.6, 8.7 Hz, 1H), 2.28 – 2.20 (m, 1H), 0.73 (d, *J* = 6.7 Hz, 3H) ppm. ¹³C NMR (101 MHz, D₂O) δ: 170.8, 139.1, 129.1, 128.6, 126.6, 56.3, 38.0, 36.2, 13.9 ppm. IR: 3398, 3029, 2970, 1731, 1629, 1497, 1457, 1229 cm⁻¹. [α]_D²³ = +26.2 (*c* = 1.0, MeOH). The absolute and relative stereochemistry of the major stereoisomer of **4a** was determined by derivation and crystallization, see part X for details. Spectral data match those reported previously (54).



(2*S*, 3*S*)-**4a** was prepared according to general procedure using L-*P*fPLP^B (1.0 mol%) in KPi buffer (pH 7). (2*S*, 3*S*)-**4a** was derived with (*S*)- and (*R*)-Marfey's reagent which were then analyzed by LC-MS.

Yield: run 1: 81%; run 2: 78%; run 3: 81%; average yield: 80%.

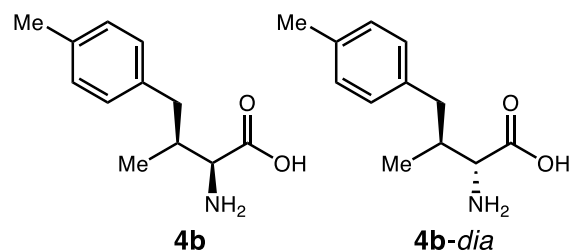
Diastereoselectivity and enantioselectivity determination: For preparative scale biocatalytic reactions, the diastereoselectivity was found to be 20:1 based on ¹H NMR analysis; For analytical scale reactions, the diastereoselectivity and enantioselectivity of **4a** were determined by LC-MS.

Diastereomeric ratio by LC-MS: run 1: 0.3:95.0:4.5:0.2; run 2: 0.2:94.9:4.7:0.2; run 3: 0.3:94.6:4.8:0.2.

Diastereoselectivity by LC-MS (*A*₂+*A*₄)/(*A*₁+*A*₃): run 1: 20:1 d.r.; run 2: 19:1 d.r.; run 3: 19:1 d.r.; average d.r.: 19:1.

Enantioselectivity of major diastereomer diastereomer by LC-MS A_2/A_4 : run 1: >99:1 e.r.; run 2: >99:1 e.r.; run 3: >99:1 e.r.; average e.r.: >99:1; **minor diastereomer A_3/A_1 :** run 1: 93:7 e.r.; run 2: 96:4 e.r.; run 3: 93:7 e.r.; average e.r.: 94:6.

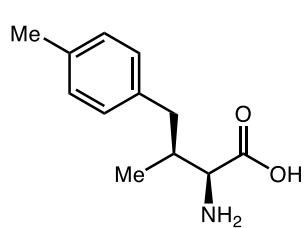
(2*S*, 3*S*)-2-amino-3-methyl-4-(p-tolyl)butanoic acid (4b**)**



NMR d.r. = 12.5 : 1 (**4b** : **4b-dia**)

Compound **4b** was prepared using biocatalytic methods following the general procedure. The reaction mixture was purified by C18 silica using Biotage [10 g Biotage C18 Sfär cartridge, 0–25% MeCN (0.1% acetic acid) in H₂O (0.1% acetic acid) over 10 CV] to afford the product as a white solid.

Two diastereomers were present (d.r. = 12.5:1). ¹H NMR (500 MHz, D₂O) for major diastereomer (**4b**) δ: 7.11 – 7.02 (m, 4H), 3.90 – 3.86 (m, 1H), 2.67 (dd, *J* = 13.6, 6.7 Hz, 1H), 2.51 – 2.43 (m, 1H), 2.34 – 2.23 (m, 1H), 2.16 (s, 3H), 0.85 (d, *J* = 6.9 Hz, 3H) ppm; for minor diastereomer (**4b-dia**) δ: 7.11 – 7.02 (m, 4H), 3.92 – 3.90 (m, 1H), 2.67 (dd, *J* = 13.6, 6.7 Hz, 1H), 2.51 – 2.43 (m, 1H), 2.34 – 2.23 (m, 1H), 2.16 (s, 3H), 0.80 (d, *J* = 6.7 Hz, 3H) ppm. ¹³C NMR (101 MHz, D₂O) for major diastereomer (**4b**) δ: 170.9, 136.6, 136.0, 129.2, 129.1, 56.4, 37.5, 36.2, 19.9, 13.9 ppm; for minor diastereomer (**4b-dia**) δ: 170.9, 136.6, 136.0, 129.2, 129.1, 56.4, 37.5, 35.7, 19.9, 13.2 ppm. IR: 3424, 2971, 2922, 1735, 1602, 1515, 1229 cm⁻¹. HRMS (ESI) (m/z) for [M+Na]⁺ C₁₂H₁₇NNaO₂ requires 230.1151, observed 230.1157. [α]_D²³ = +11.8 (c = 1.5, MeOH).



(2*S*, 3*S*)-**4b** was prepared according to general procedure using L-*PfPLP*^B (1.0 mol%) in KPi buffer (pH 7). (2*S*, 3*S*)-**4b** was derived with (*S*)- and (*R*)-Marfey's reagent which were then analyzed by LC-MS.

Yield: run 1: 74%; run 2: 74%; run 3: 78%; average yield: 75%.

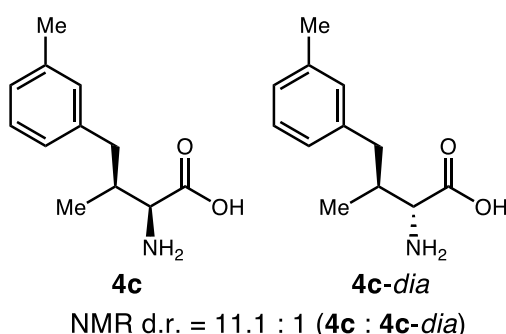
Diastereoselectivity and enantioselectivity determination: For preparative scale biocatalytic reactions, the diastereoselectivity was found to be 12.5:1 based on ¹H NMR analysis. For analytical scale reactions, the diastereoselectivity and enantioselectivity were determined by LC-MS.

Diastereomeric ratio by LC-MS: run 1: 0.2:92.7:7.1:0.1; run 2: 0.1:92.6:7.2:0.1; run 3: 0.2:92.6:7.2:0.1.

Diastereoselectivity by LC-MS ($A_2+A_4)/(A_1+A_3)$: run 1: 13:1 d.r.; run 2: 13:1 d.r.; run 3: 13:1 d.r.; average d.r.: 13:1.

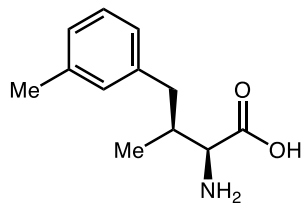
Enantioselectivity of major diastereomer diastereomer by LC-MS A_2/A_4 : run 1: >99:1 e.r.; run 2: >99:1 e.r.; run 3: >99:1 e.r.; average e.r.: >99:1; **minor diastereomer A_3/A_1 :** run 1: 97:3 e.r.; run 2: 98:2 e.r.; run 3: 98:2 e.r.; average e.r.: 98:2.

(2*S*, 3*S*)-2-amino-3-methyl-4-(m-tolyl)butanoic acid (**4c**)



Compound **4c** was prepared using biocatalytic methods following the general procedure. The reaction mixture was purified by C18 silica using Biotage [10 g Biotage C18 Sfar cartridge, 0–25% MeCN (0.1% acetic acid) in H₂O (0.1% acetic acid) over 10 CV] to afford the product as a white solid. Two diastereomers were present (d.r. = 12.5:1). ¹H NMR (500 MHz, D₂O) for

major diastereomer (**4c**) δ: 7.27 (t, *J* = 7.4 Hz, 1H), 7.17 – 7.07 (m, 2H), 4.02 (d, *J* = 3.3 Hz, 1H), 2.82 (dd, *J* = 13.6, 6.6 Hz, 1H), 2.60 (dd, *J* = 13.6, 8.8 Hz, 1H), 2.49 – 2.38 (m, 1H), 2.30 (s, 3H), 0.98 (d, *J* = 6.9 Hz, 3H) ppm; for minor diastereomer (**4c-dia**) δ: 7.27 (t, *J* = 7.4 Hz, 1H), 7.17 – 7.07 (m, 2H), 4.04 – 4.03 (m, 1H), 2.82 (dd, *J* = 13.6, 6.6 Hz, 1H), 2.60 (dd, *J* = 13.6, 8.8 Hz, 1H), 2.49 – 2.38 (m, 1H), 2.30 (s, 3H), 0.94 (d, *J* = 6.0 Hz, 3H) ppm. ¹³C NMR (126 MHz, D₂O) for major diastereomer (**4c**) δ: 171.1, 139.3, 138.8, 129.9, 128.7, 127.3, 126.2, 56.5, 37.9, 36.3, 20.3, 14.0 ppm; for minor diastereomer (**4c-dia**) δ: 171.6, 139.0, 138.9, 129.7, 128.8, 127.3, 126.1, 56.7, 38.0, 35.7, 20.3, 13.3 ppm. IR: 3393, 3021, 2965, 2919, 1729, 1608, 1490, 1230 cm⁻¹. HRMS (ESI) (m/z) for [M+Na]⁺ C₁₂H₁₇NNaO₂ requires 230.1151, observed 230.1153. [α]_D²³ = +20.7 (c = 1.0, MeOH).



(*2S, 3S*)-**4c** was prepared according to general procedure using L-*Pf*PLP^B (1.0 mol%) in KPi buffer (pH 7). (*2S, 3S*)-**4c** was derived with (*S*)- and (*R*)-Marfey's reagent which were then analyzed by LC-MS.

Yield: run 1: 75%; run 2: 73%; run 3: 74%; average yield: 74%.

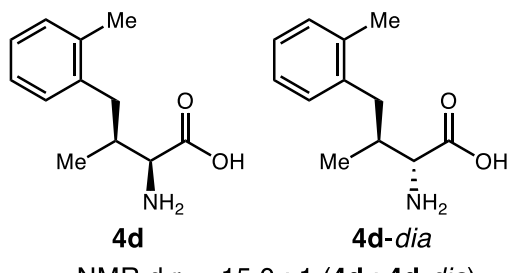
Diastereoselectivity and enantioselectivity determination: For preparative scale biocatalytic reactions, the diastereoselectivity was 11.1:1 based on ¹H NMR; For analytical scale reactions, the diastereoselectivity and enantioselectivity were determined by LC-MS.

Diastereomeric ratio by LC-MS: run 1: 1.0:90.3:8.4:0.3; run 2: 0.9:90.6:8.2:0.3; run 3: 1.0:90.3:8.4:0.3.

Diastereoselectivity by LC-MS (*A*₂+*A*₄)/(*A*₁+*A*₃): run 1: 10:1 d.r.; run 2: 10:1 d.r.; run 3: 10:1 d.r.; average d.r.: 10:1.

Enantioselectivity of major diastereomer diastereomer by LC-MS *A*₂/*A*₄: run 1: >99:1 e.r.; run 2: >99:1 e.r.; run 3: >99:1 e.r.; average e.r.: >99:1; **minor diastereomer *A*₃/*A*₁:** run 1: 90:10 e.r.; run 2: 90:10 e.r.; run 3: 89:11 e.r.; average e.r.: 90:10.

(*2S, 3S*)-2-amino-3-methyl-4-(o-tolyl)butanoic acid (**4d**)

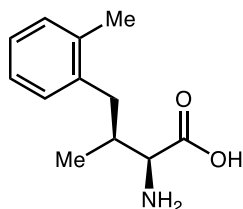


NMR d.r. = 15.0 : 1 (**4d** : **4d-dia**)

Compound **4d** was prepared using biocatalytic methods following the general procedure. The reaction mixture was purified by C18 silica using Biotage [10 g Biotage C18 Sfar cartridge, 0–25% MeCN (0.1% acetic acid) in H₂O (0.1% acetic acid) over 10 CV] to afford the product as a white solid. Two diastereomers were

present in the white solid. ¹H NMR (500 MHz, D₂O) for major diastereomer (**4d**) δ: 7.28 – 7.17 (m, 4H), 4.07 (d, *J* = 3.2 Hz, 1H), 2.86 (dd, *J* = 13.7, 5.6 Hz, 1H), 2.63 (dd, *J* = 13.7, 9.6 Hz, 1H), 2.50 – 2.39 (m, 1H), 2.29 (s, 3H), 0.99 (d, *J* = 7.0 Hz, 3H) ppm; for minor diastereomer (**4d-dia**) δ: 7.28 – 7.17 (m, 4H), 4.05 (d, *J* = 3.7 Hz, 1H), 2.86 (dd, *J* = 13.7, 5.6 Hz, 1H), 2.63 (dd, *J* = 13.7, 9.6 Hz, 1H), 2.50 – 2.39 (m, 1H), 2.30 (s, 3H), 0.94 (d, *J* = 6.8 Hz, 3H) ppm. ¹³C NMR (126 MHz, D₂O) for major diastereomer (**4d**) δ: 171.3, 137.3, 137.1, 130.5, 130.3, 126.9, 126.0, 57.1, 35.0, 34.6, 18.4, 14.0 ppm; for minor diastereomer (**4d-dia**) δ: 171.8, 137.2, 137.0, 130.6, 130.0, 127.0,

126.1, 57.3, 35.6, 34.5, 18.5, 13.2 ppm. IR: 3014, 2974, 2876, 1730, 1588, 1495, 1222 cm^{-1} . HRMS (ESI) (m/z) for $[\text{M}+\text{Na}]^+$ $\text{C}_{12}\text{H}_{17}\text{NNaO}_2$ requires 230.1151, observed 230.1157. $[\alpha]_D^{23} = +31.3$ ($c = 1.0$, MeOH).



(2S, 3S)-4d was prepared according to general procedure using L-*Pf*PLP^B (1.0 mol%) in KPi buffer (pH 7). (2S, 3S)-4d was derived with (S)- and (R)-Marfey's reagent which were then analyzed by LC-MS.

Yield: run 1: 78%; run 2: 79%; run 3: 80%; average yield: 79%.

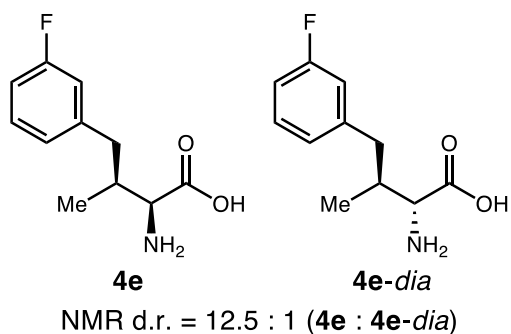
Diastereoselectivity and enantioselectivity determination: For preparative scale biocatalytic reactions, the diastereoselectivity was 15.0: 1 based on ¹H NMR; For analytical scale reactions, the diastereoselectivity and enantioselectivity were determined by LC-MS.

Diastereomeric ratio by LC-MS: run 1: 0.1:93.2:6.7:0.1; run 2: 0.1:92.8:6.9:0.2; run 3: 0.1:93.1:6.5:0.2.

Diastereoselectivity by LC-MS ($A_2+A_4)/(A_1+A_3)$: run 1: 14:1 d.r.; run 2: 13:1 d.r.; run 3: 14:1 d.r.; average d.r.: 14:1.

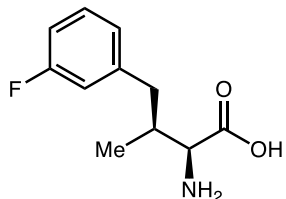
Enantioselectivity of major diastereomer diastereomer by LC-MS A_2/A_4 : run 1: >99:1 e.r.; run 2: >99:1 e.r.; run 3: >99:1 e.r.; average e.r.: >99:1; **minor diastereomer A_3/A_1 :** run 1: 98:2 e.r.; run 2: 98:2 e.r.; run 3: 98:2 e.r.; average e.r.: 98:2.

(2S, 3S)-2-amino-4-(3-fluorophenyl)-3-methylbutanoic acid (4e)



Compound 4e was prepared using enzymatic reactions (general procedure F) and purified by C18 silica using Biotage [10 g Biotage C18 Sfär cartridge, 0–25% MeCN (0.1% acetic acid) in H₂O (0.1% acetic acid) over 10 CV] to afford the product as a white solid. Two diastereomers were present in the white solid. ¹H NMR (500 MHz, D₂O) for major diastereomer (4e) δ : 7.23 – 7.17 (m, 1H), 6.97 – 6.85 (m, 3H), 3.88 (d, $J = 3.3$ Hz, 1H), 2.72 (dd, $J = 13.7, 7.0$ Hz, 1H), 2.54 (dd, $J = 13.6, 8.5$ Hz, 1H), 2.38 – 2.26 (m, 1H), 0.85 (d, $J = 6.9$ Hz, 3H) ppm; for minor

diastereomer (**4e-dia**) δ : 7.20 (td, $J = 7.9, 6.2$ Hz, 1H), 6.98 – 6.83 (m, 3H), 3.91 (d, $J = 3.1$ Hz, 1H), 2.72 (dd, $J = 13.7, 7.0$ Hz, 1H), 2.54 (dd, $J = 13.6, 8.5$ Hz, 1H), 2.38 – 2.26 (m, 1H), 0.81 (d, $J = 6.4$ Hz, 3H) ppm. ^{13}C NMR (126 MHz, D₂O) for major diastereomer (**4e**) δ : 170.8, 162.6 (d, $J = 243.1$ Hz), 141.7 (d, $J = 7.4$ Hz), 130.2 (d, $J = 8.5$ Hz), 125.0 (d, $J = 2.7$ Hz), 115.8 (d, $J = 21.1$ Hz), 113.3 (d, $J = 20.9$ Hz), 56.2, 37.8, 36.0, 13.9 ppm; for minor diastereomer (**4e-dia**) δ : 171.4, 162.7 (d, $J = 243.2$ Hz), 141.3 (d, $J = 7.5$ Hz), 130.3 (d, $J = 8.6$ Hz), 125.0 (d, $J = 2.7$ Hz), 115.8 (d, $J = 21.1$ Hz), 113.4 (d, $J = 21.1$ Hz), 56.6, 37.8, 35.5, 13.3 ppm. ^{19}F NMR (376 MHz, D₂O) for major isomer δ : -114.16 ppm; for minor isomer δ : -113.98 ppm. IR: 3016, 2971, 2878, 1731, 1590, 1489 cm⁻¹. HRMS (ESI) (m/z) for [M+H]⁺ C₁₁H₁₅FNO₂ requires 212.1081, observed 212.1087. $[\alpha]_D^{23} = +27.4$ ($c = 0.5$, MeOH).



(2*S*, 3*S*)-**4e** was prepared according to general procedure using L-*Pf*PLP^B (1.0 mol%) in KPi buffer (pH 7). (2*S*, 3*S*)-**4e** was derived with (*S*)- and (*R*)-Marfey's reagent which were then analyzed by LC-MS.

Yield: run 1: 85%; run 2: 85%; run 3: 81%; average yield: 83%.

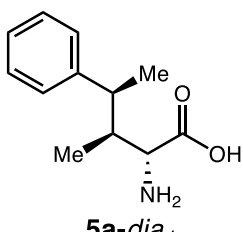
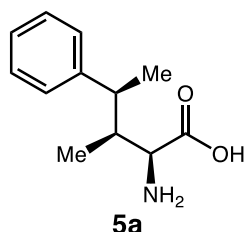
Diastereoselectivity and enantioselectivity determination: For preparative scale biocatalytic reactions, the diastereoselectivity was 12.5:1 based on ^1H NMR; For analytical scale reactions, the diastereoselectivity and enantioselectivity were determined by LC-MS.

Diastereomeric ratio by LC-MS: run 1: 0.2:91.4:8.3:0.1; run 2: 0.2:91.6:8.1:0.1; run 3: 0.1:91.6:8.2:0.1.

Diastereoselectivity by LC-MS (A_2+A_4)/(A_1+A_3): run 1: 11:1 d.r.; run 2: 11:1 d.r.; run 3: 11:1 d.r.; average d.r.: 11:1.

Enantioselectivity of major diastereomer diastereomer by LC-MS A_2/A_4 : run 1: >99: 1 e.r.; run 2: >99: 1 e.r.; run 3: >99: 1 e.r.; average e.r.: >99: 1; **minor diastereomer A_3/A_1 :** run 1: 98:2 e.r.; run 2: 98:2 e.r.; run 3: 99:1 e.r.; average e.r.: 98:2.

(2*S*, 3*S*, 4*S*)-2-amino-4-(3-fluorophenyl)-3-methylbutanoic acid (5a**)**

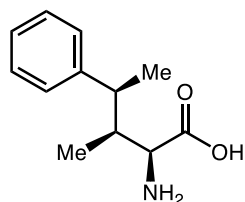


NMR d.r. = > 20 : 1 (**5a** : **5a-dia₁**)

Compound **4d** was prepared using enzymatic reactions (general procedure F) and purified by C18 silica using Biotage [10 g Biotage C18 Sfär cartridge, 0–25% MeCN (0.1% acetic acid) in H₂O (0.1% acetic acid) over 10 CV] to afford the product as a white solid. Two major diastereoisomers contained in the white solid.

¹H NMR (500 MHz, D₂O) major (**5a**) δ: 7.46 – 7.37 (m, 4H), 7.35 – 7.30 (m, 1H), 3.69 (d, *J* = 2.7 Hz, 1H), 3.06 – 2.96 (m, 1H), 2.31 – 2.21 (m, 1H), 1.27 (d, *J* = 7.0 Hz, 3H), 1.13 (d, *J* = 6.8 Hz, 3H) ppm; minor (**5a-dia**) δ: 7.47 – 7.36 (m, 4H), 7.37 – 7.28 (m, 1H), 3.63 (d, *J* = 2.6 Hz, 1H), 3.07 – 2.94 (m, 1H), 2.33 – 2.20 (m, 1H), 1.32 (d, *J* = 6.4 Hz, 3H), 1.10 (d, *J* = 6.9 Hz, 3H) ppm.

¹³C NMR (126 MHz, D₂O) δ: 170.7, 145.4, 128.8, 127.6, 126.8, 55.0, 41.5, 40.9, 19.4, 11.5 ppm. IR: 3033, 2972, 2876, 2760, 1729, 1603, 1514 cm⁻¹. HRMS (ESI) (m/z) for [M+Na]⁺ C₁₂H₁₇NNaO₂ requires 230.1151, observed 230.1157. [α]_D²³ = +39.0 (*c* = 0.87, MeOH). The absolute configuration **5a** was determined by derivation and crystallization, see part X for details.



(2*S*, 3*S*, 4*S*)-**5a** was prepared according to general procedure using L-*Pf*PLP^β (1.0 mol%) in KPi buffer (pH 7). (2*S*, 3*S*, 4*S*)-**5a** was derived with (*S*)- and (*R*)-Marfey's reagent which were then analyzed by LC-MS.

Yield: run 1: 86%; run 2: 81%; run 3: 85%; average yield: 84%.

Diastereoselectivity and enantioselectivity determination: For preparative scale biocatalytic reactions, the diastereoselectivity was >20:1 based on ¹H NMR; For analytical scale reactions, the diastereoselectivity and enantioselectivity were determined by LC-MS.

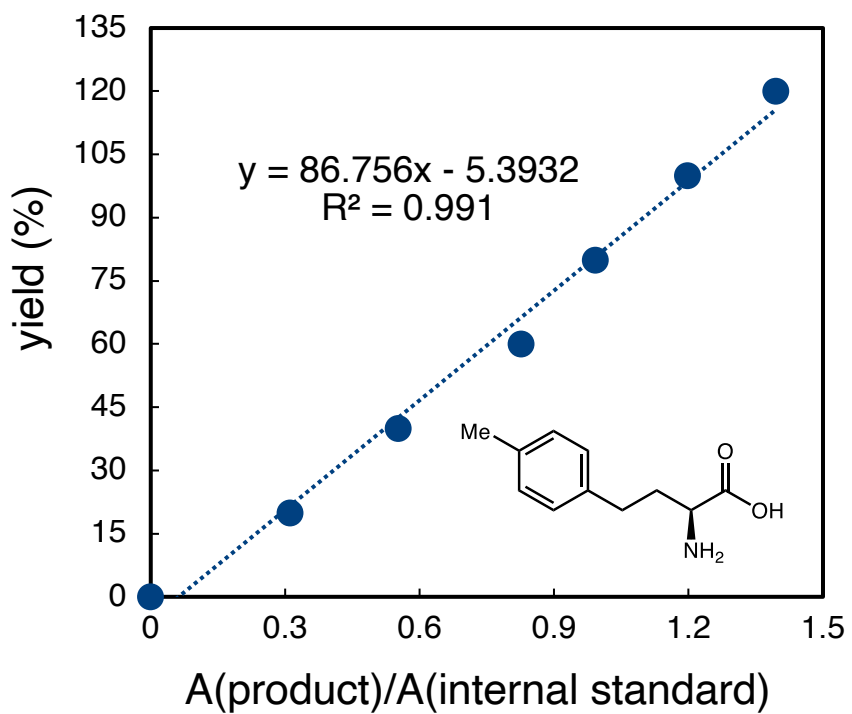
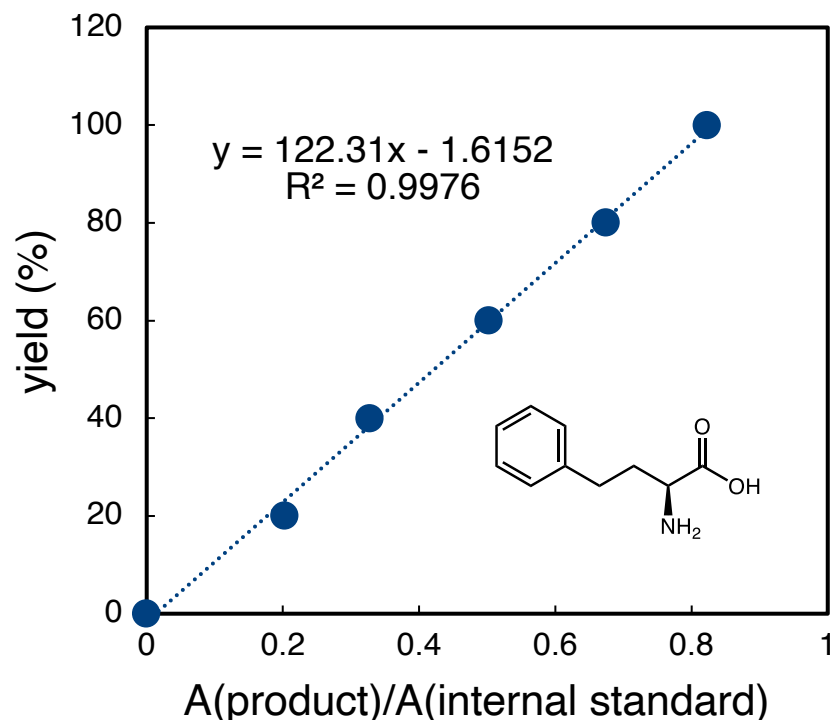
Stereoisomeric ratio by LC-MS: run 1: 0.1:97.3:2.5:0.1; run 2: 0.1:97.3:2.4:0.1; run 3: 0.1:97.3:2.5:0.1.

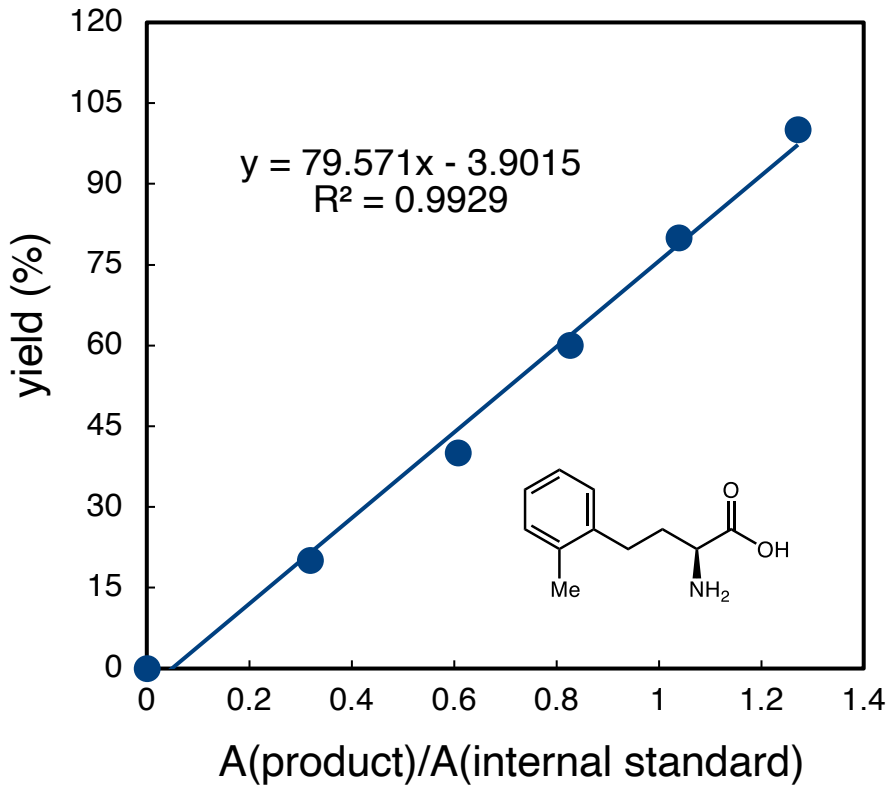
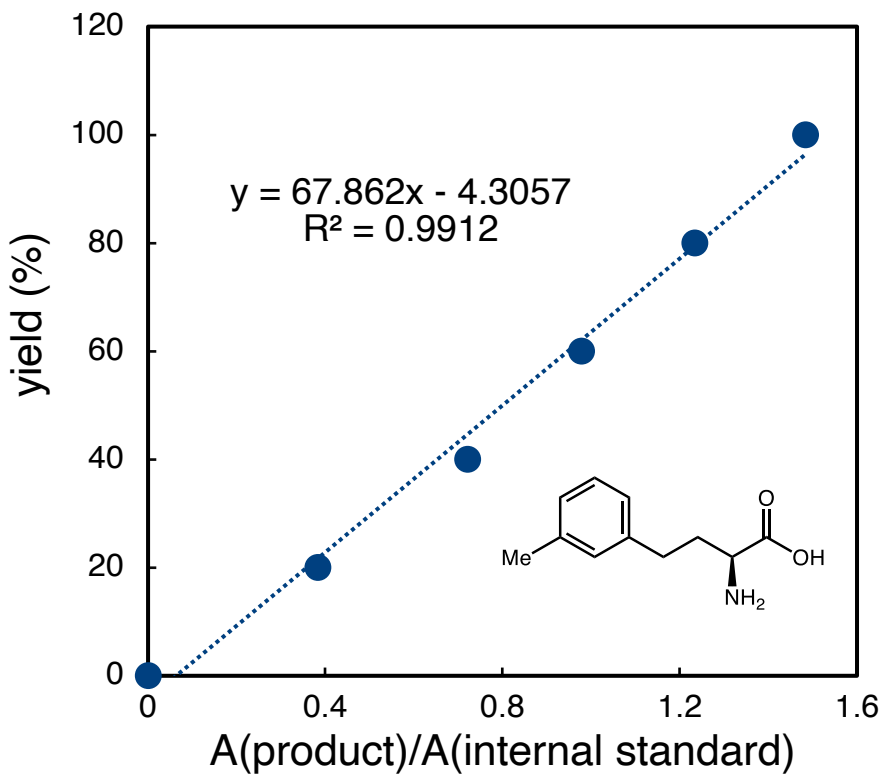
Diastereoselectivity by LC-MS (A₂+A₄)/(A₁+A₃): run 1: 38:1 d.r.; run 2: 38:1 d.r.; run 3: 37:1 d.r.; average d.r.: 38:1.

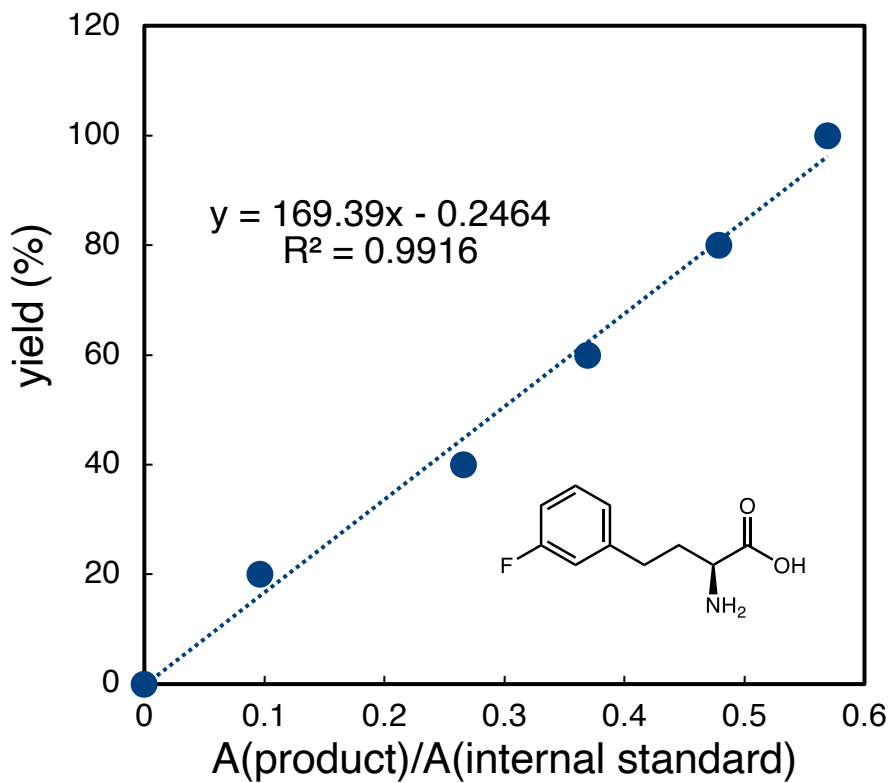
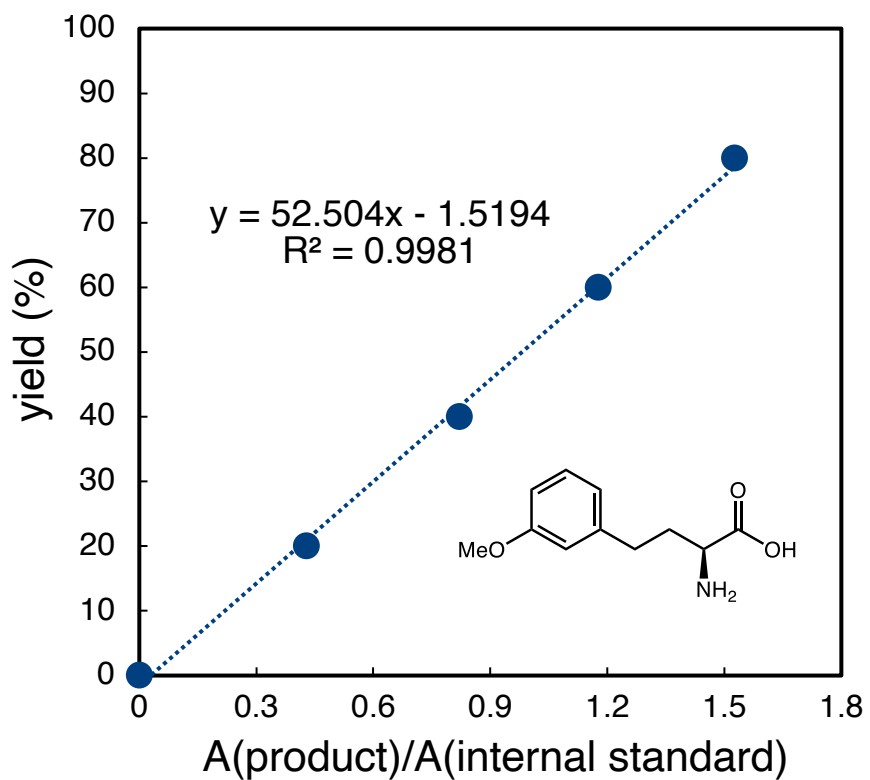
Enantioselectivity of major diastereomer by LC-MS A_2/A_4 : run 1: >99:1 e.r.; run 2: >99:1 e.r.; run 3: >99:1 e.r.; average e.r.: >99:1; **minor diastereomer** A_3/A_1 : run 1: 95:5 e.r.; run 2: 95:5 e.r.; run 3: 95:5 e.r.; average e.r.: 95:5.

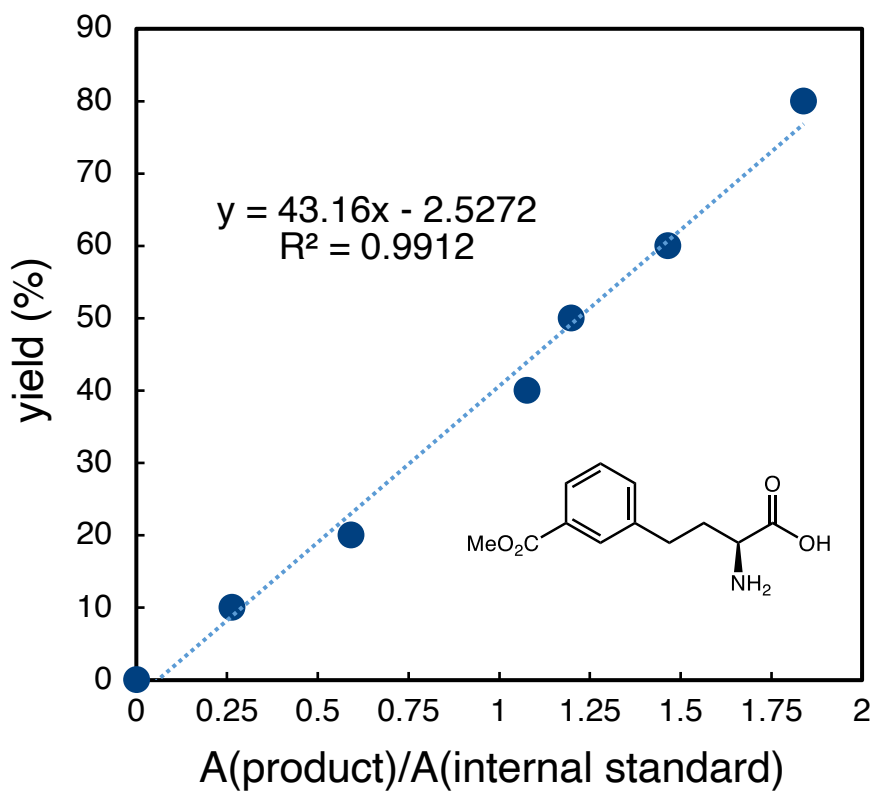
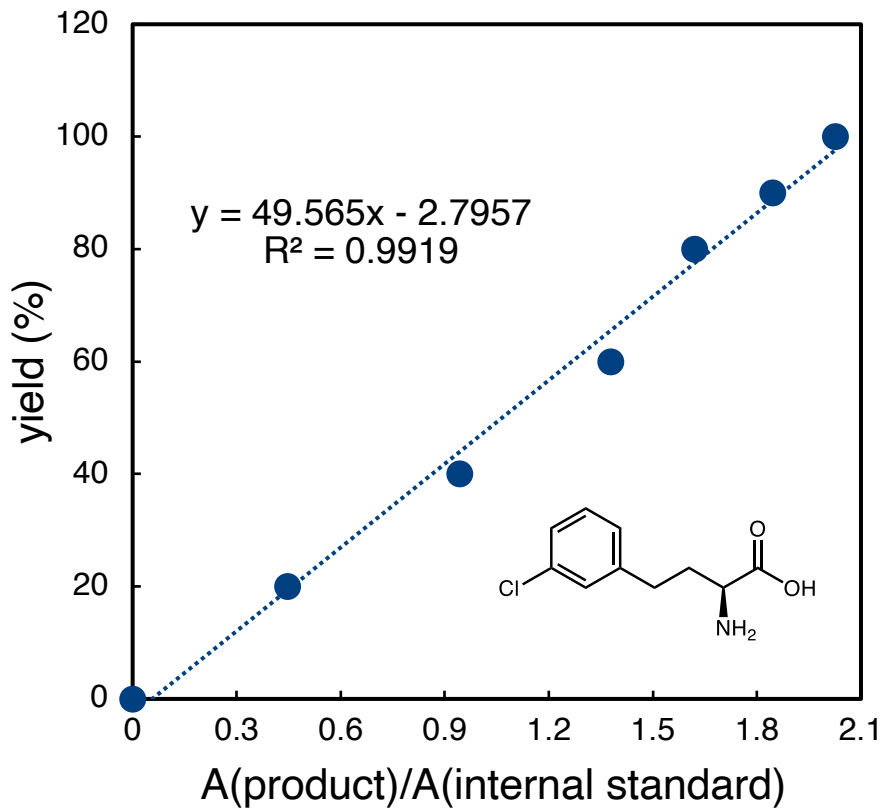
In principle, Marfey's analysis of **5a** could afford a total of 8 diastereomers. For non-stereoselective reactions, in principle, all these 8 peaks could be resolved in LC-MS analysis. With our enzymatic sample of highly diastereo- and enantioenriched **5a**, only 2 peaks were present after derivatization with (*S*)-FDAA. Similarly, only 2 peaks were present after derivatization with (*R*)-FDAA. The diastereomeric ratio of **5a** was primarily determined by ^1H NMR analysis (ca. 38:1), which is consistent with our assignment and diastereomeric ratio determined by Marfey's analysis (ca. 38:1). The enantiomeric ratio was determined by Marfey's analysis.

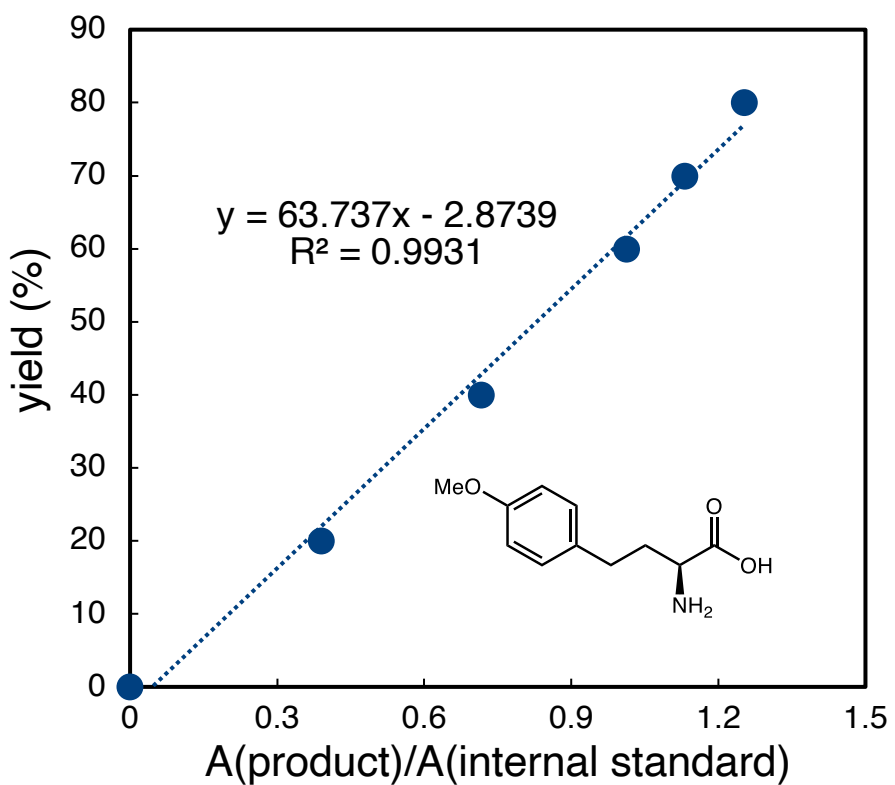
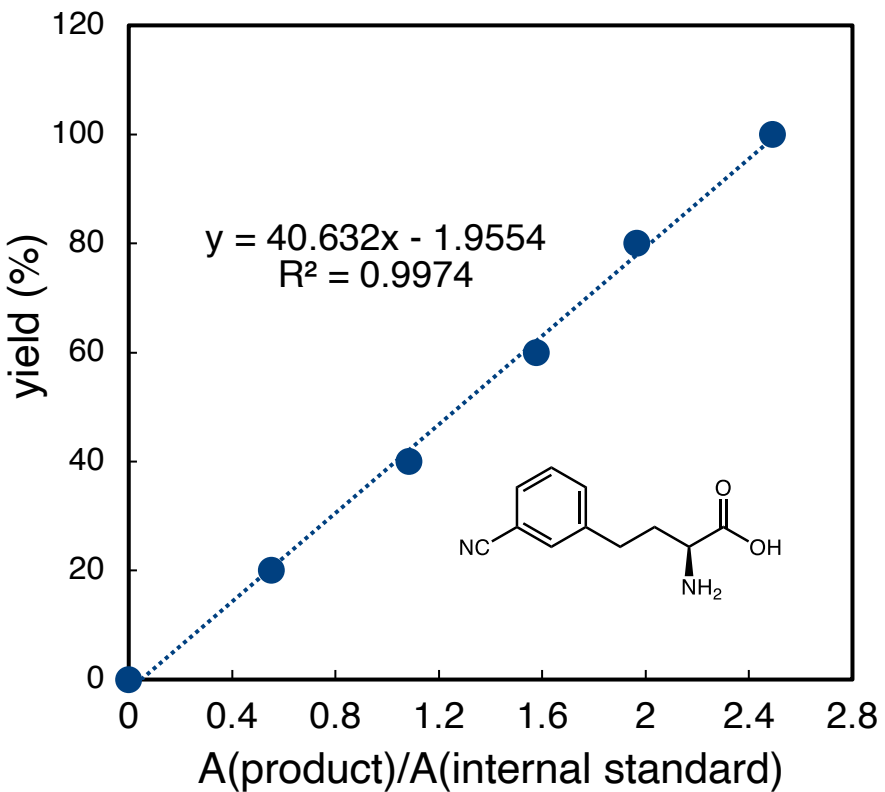
XIV HPLC calibration curves of amino acid products

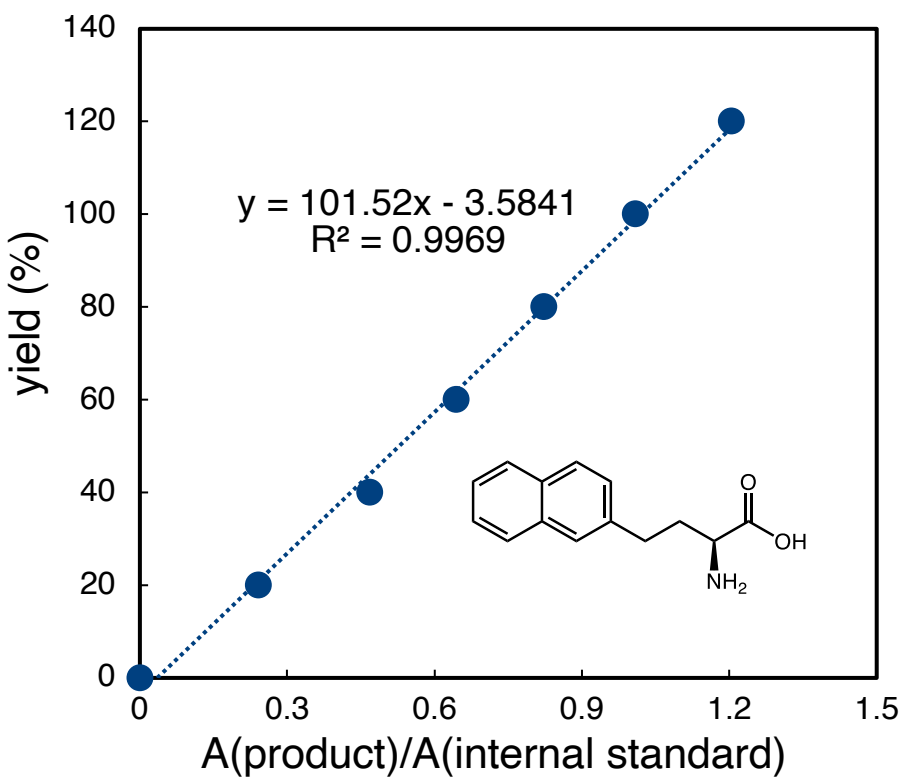
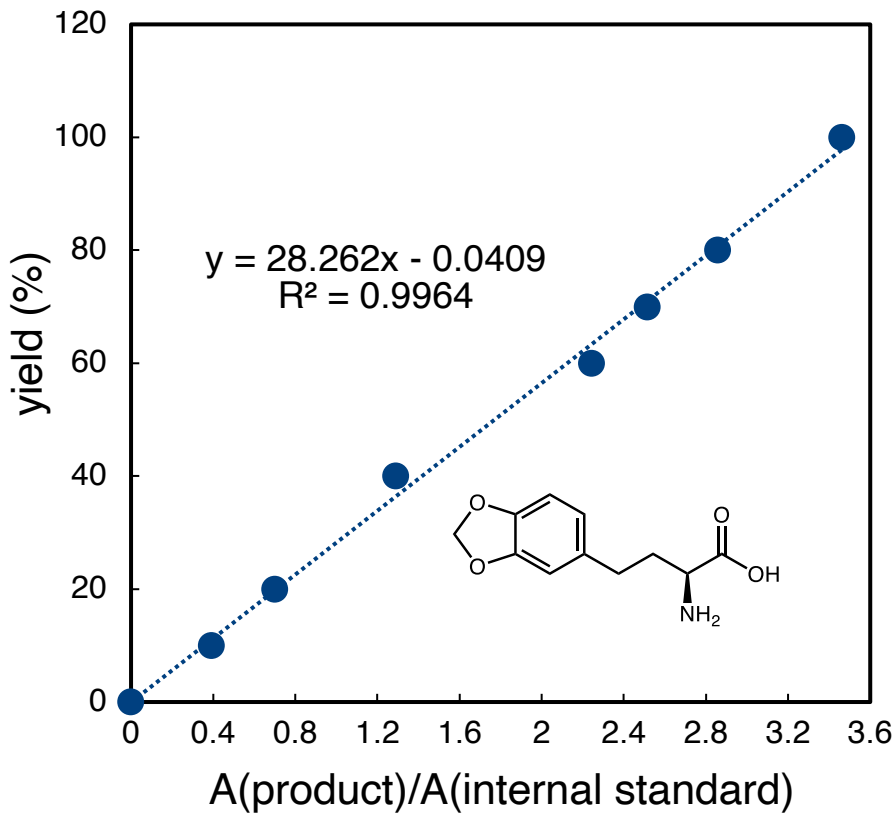


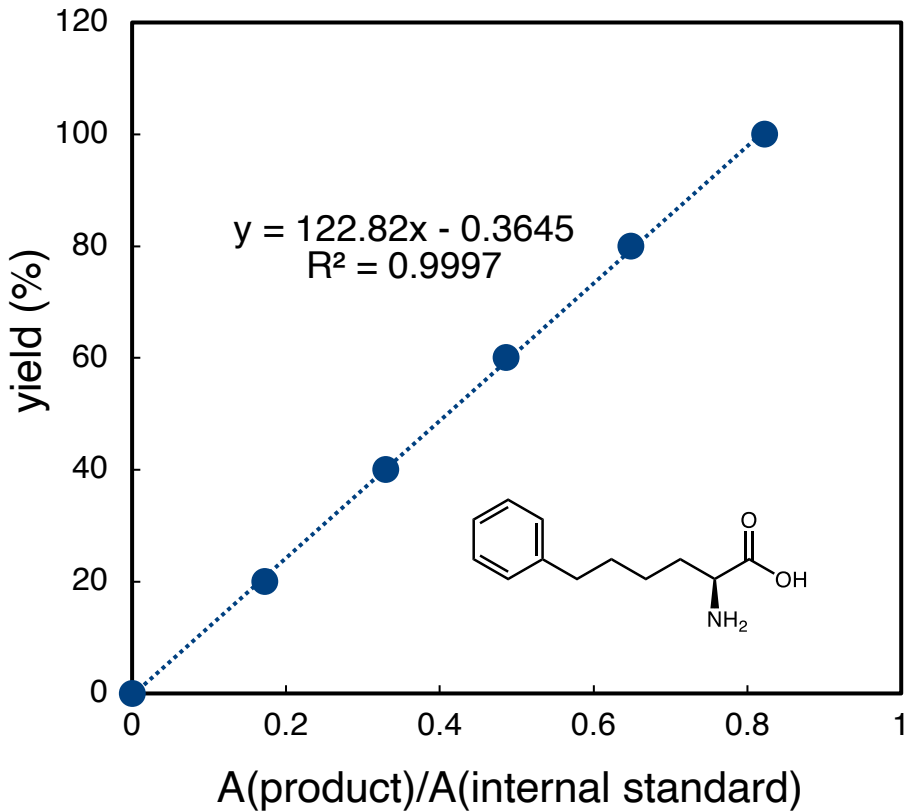
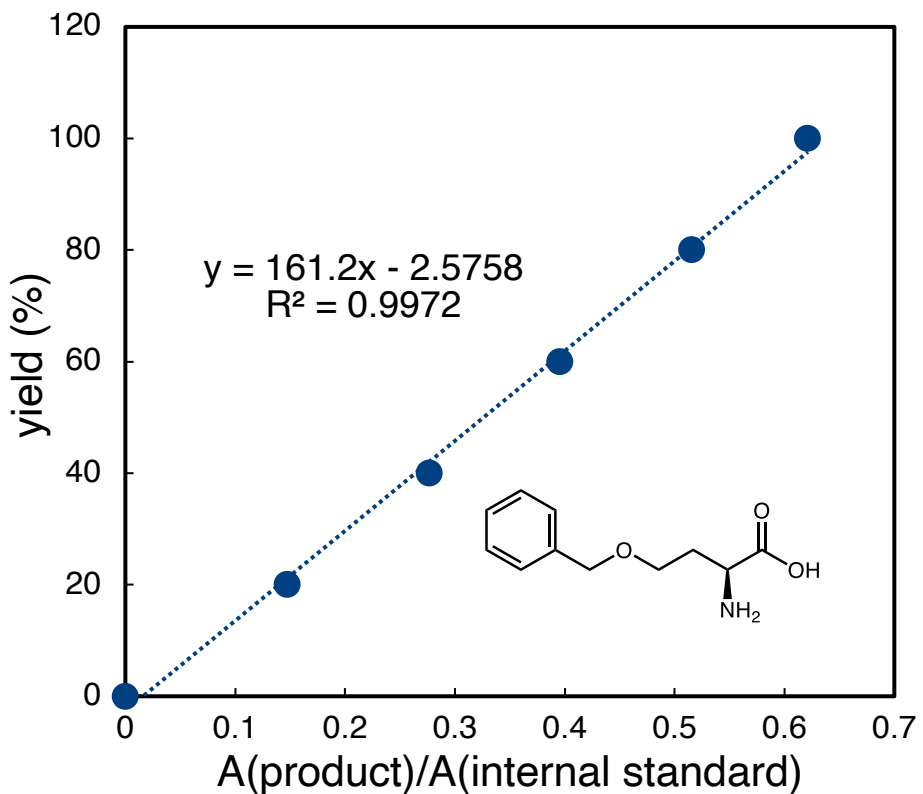


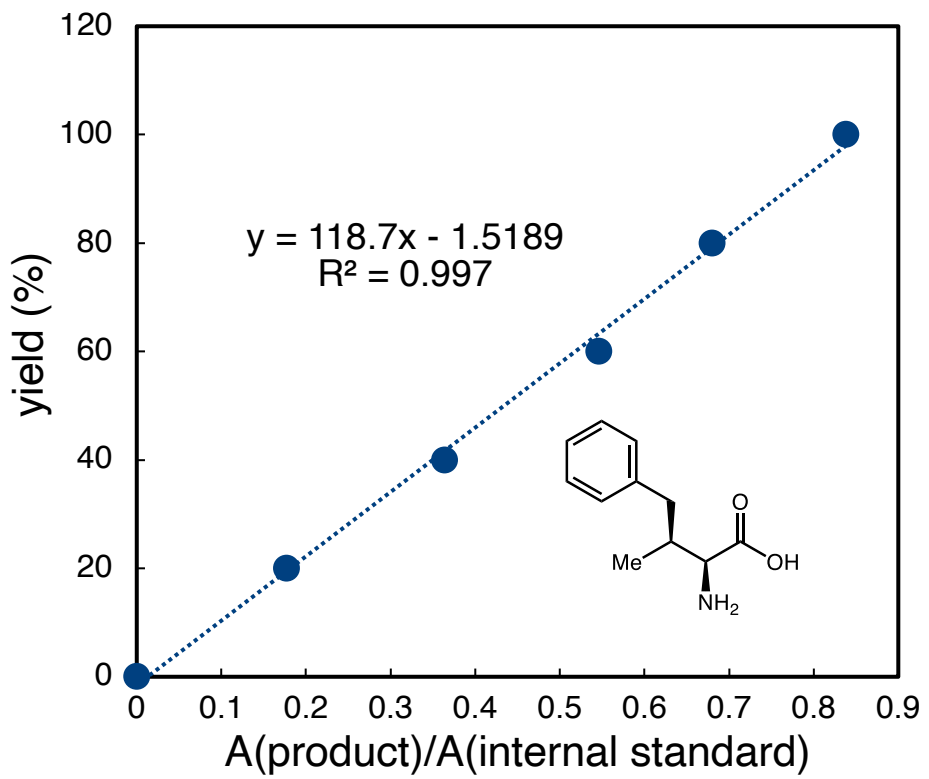
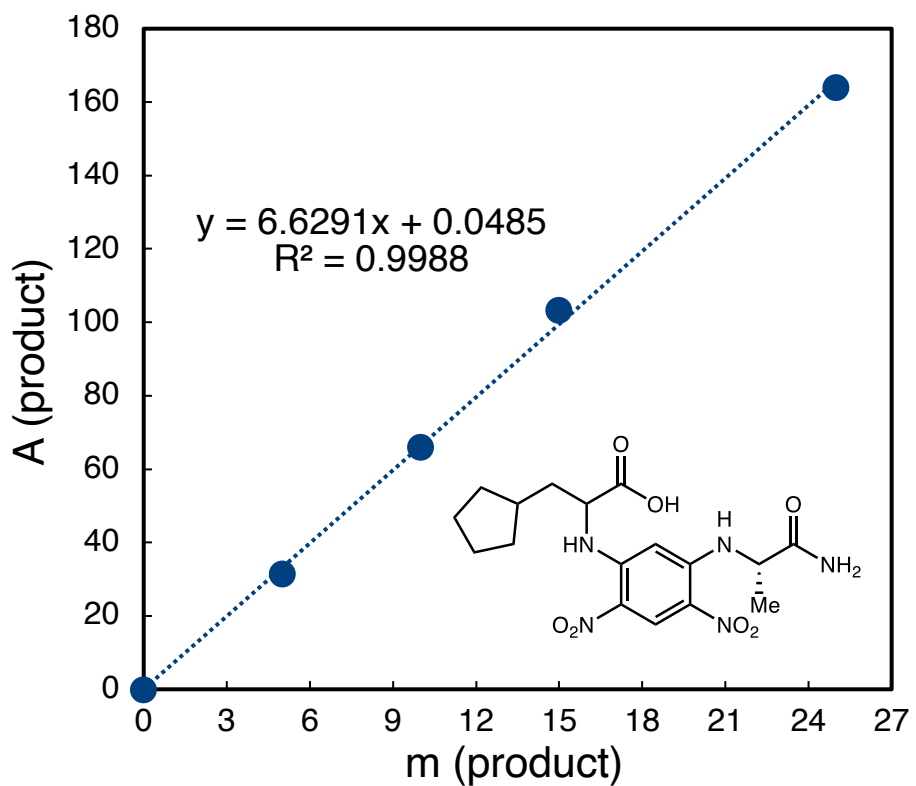


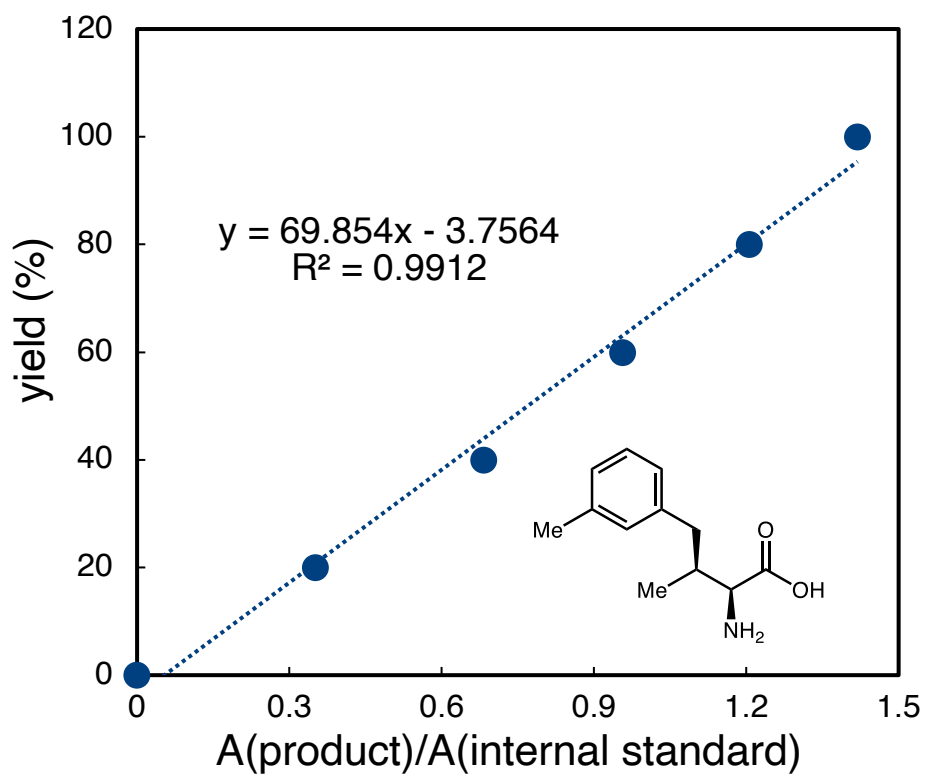
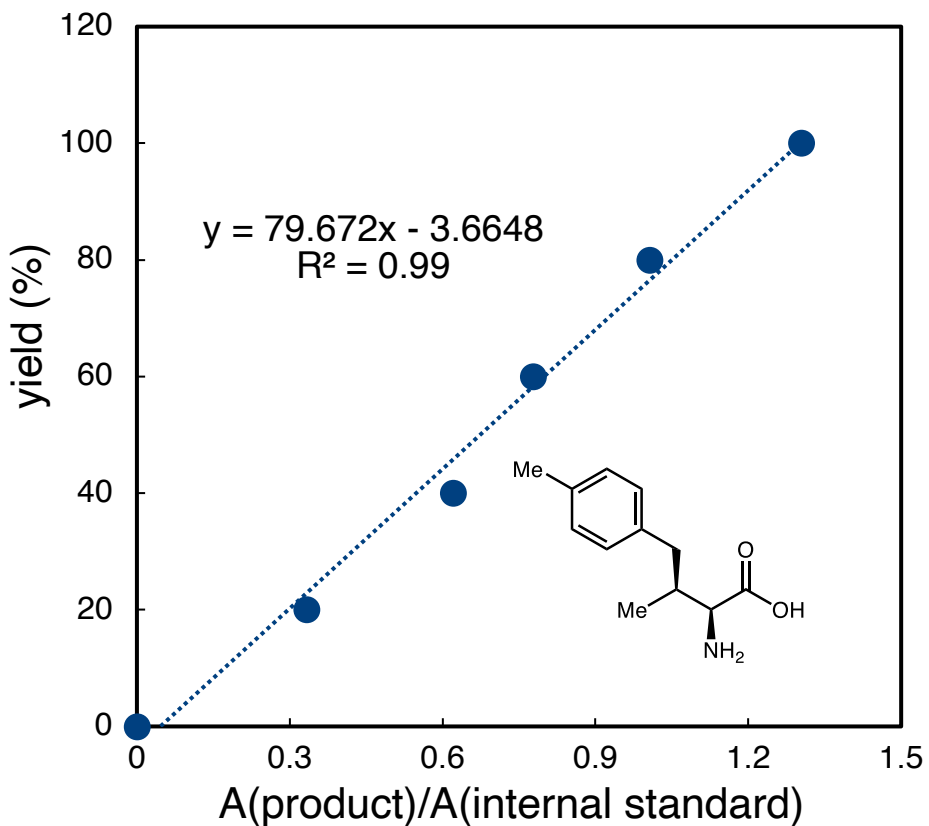


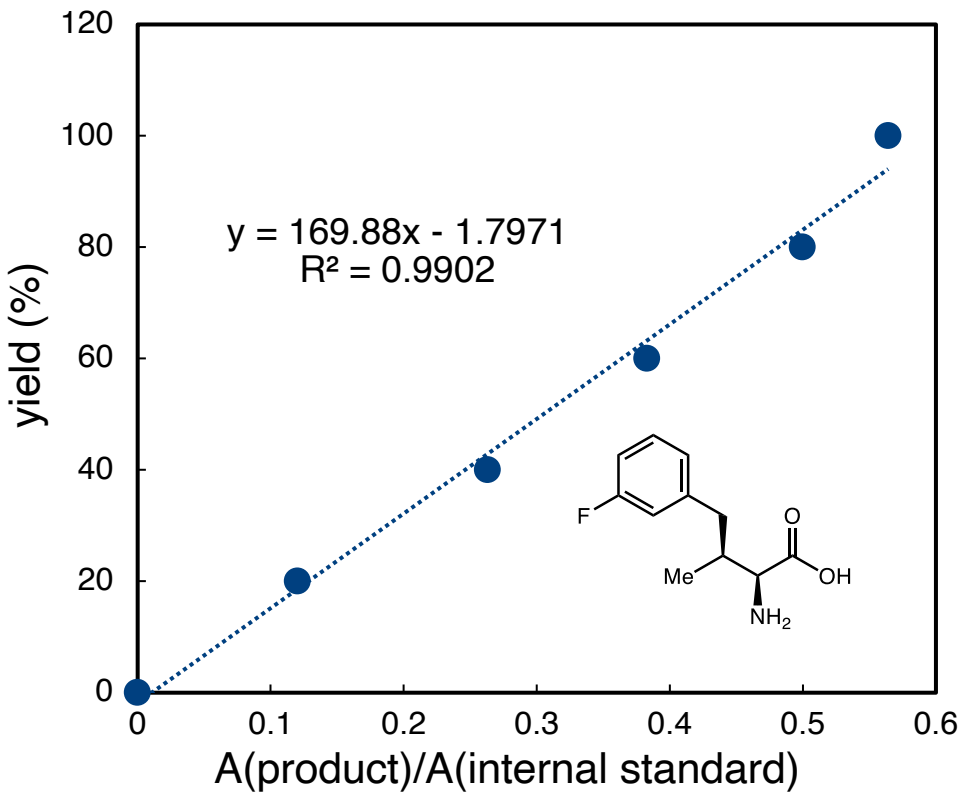
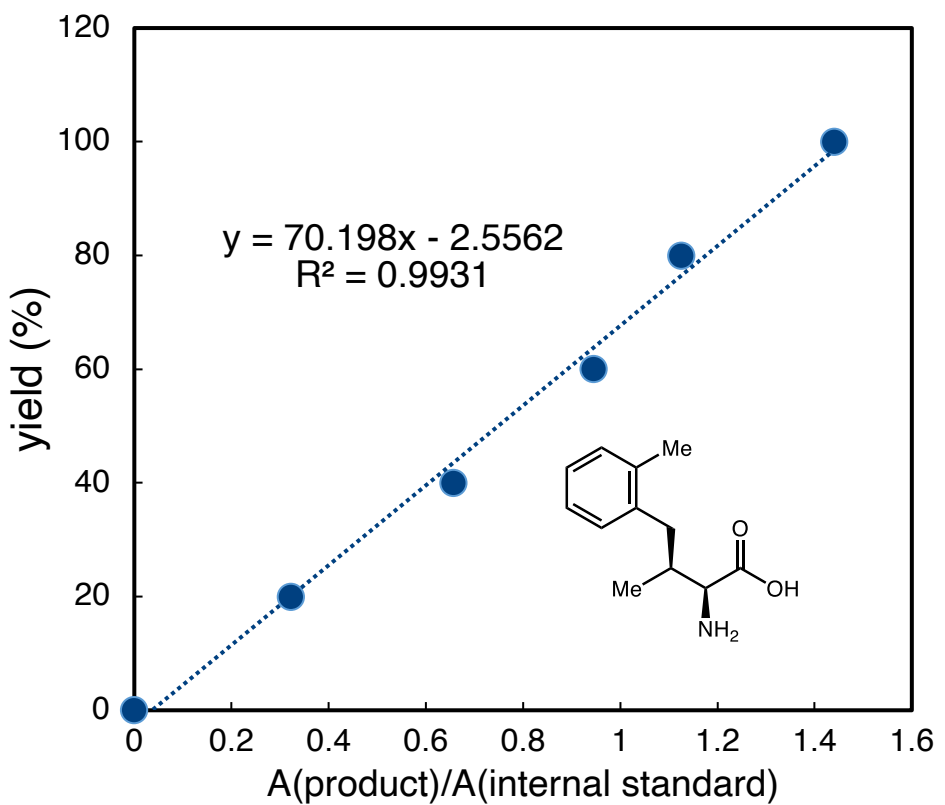


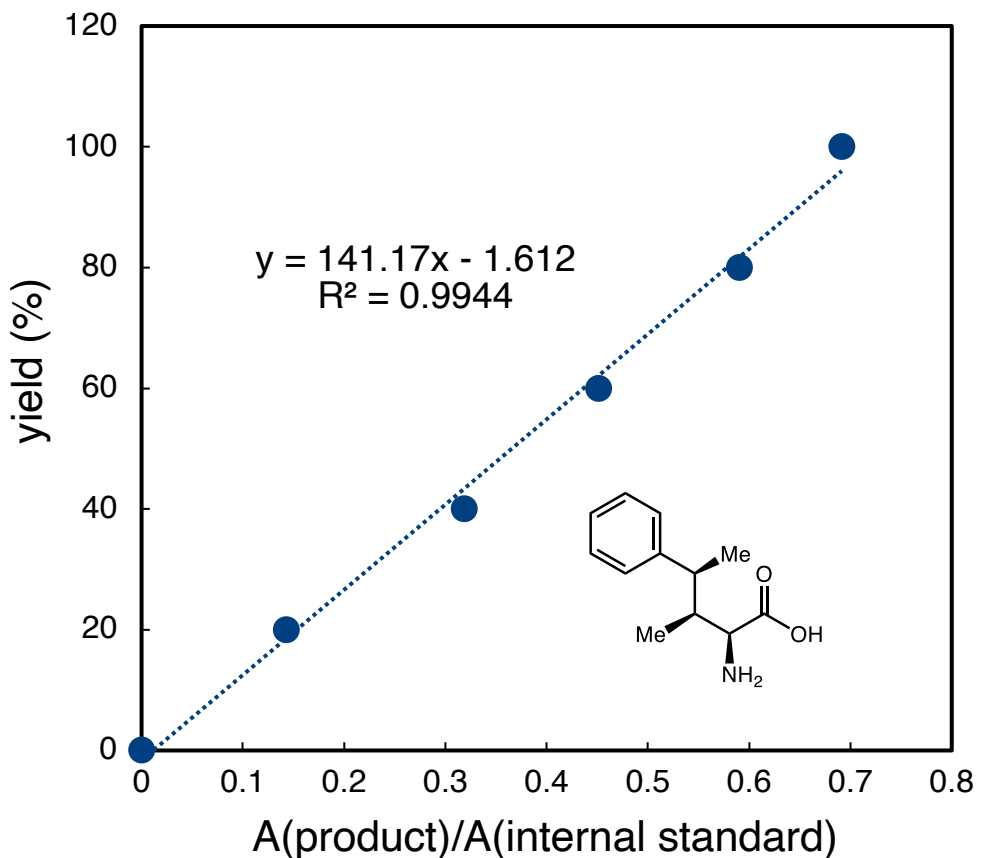








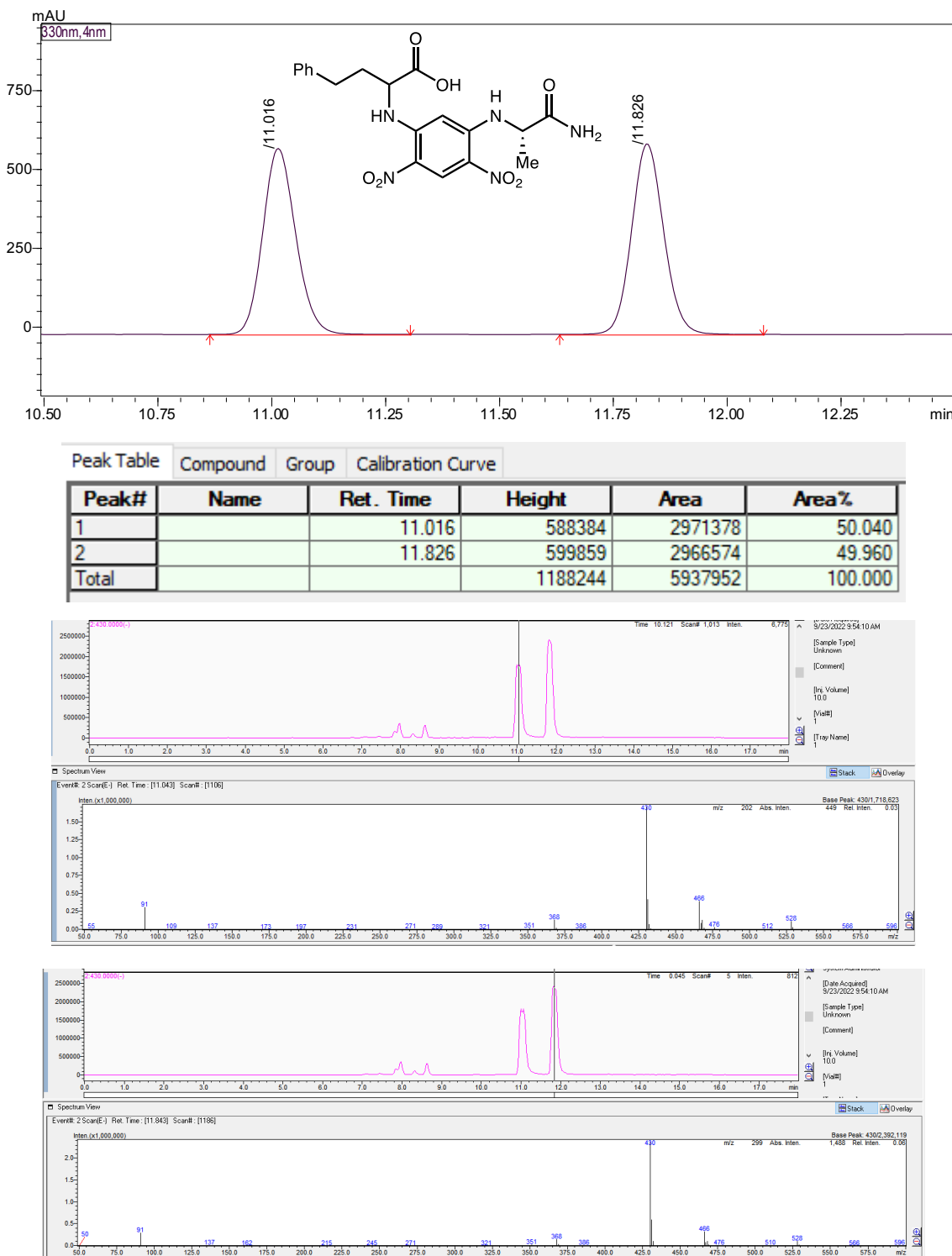




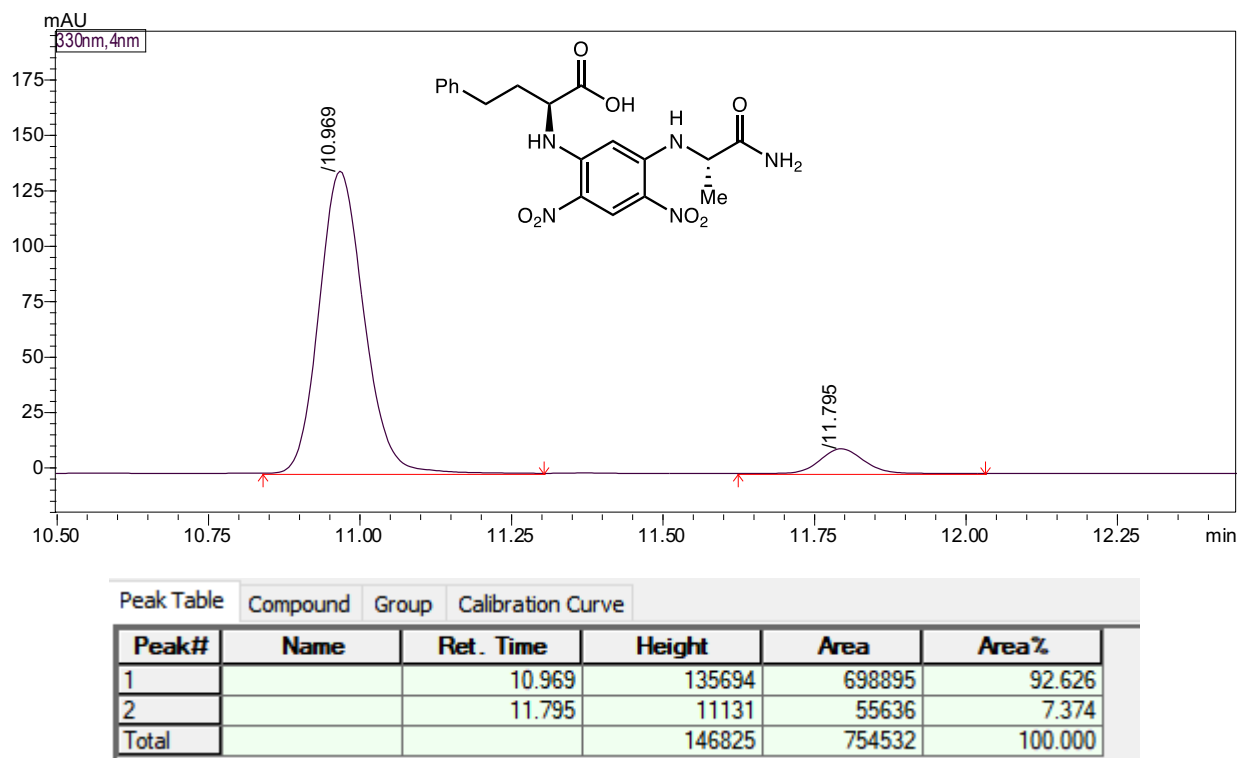
XV. HPLC traces for Marfey's analysis

2-Amino-4-phenylbutanoic acid (3a)

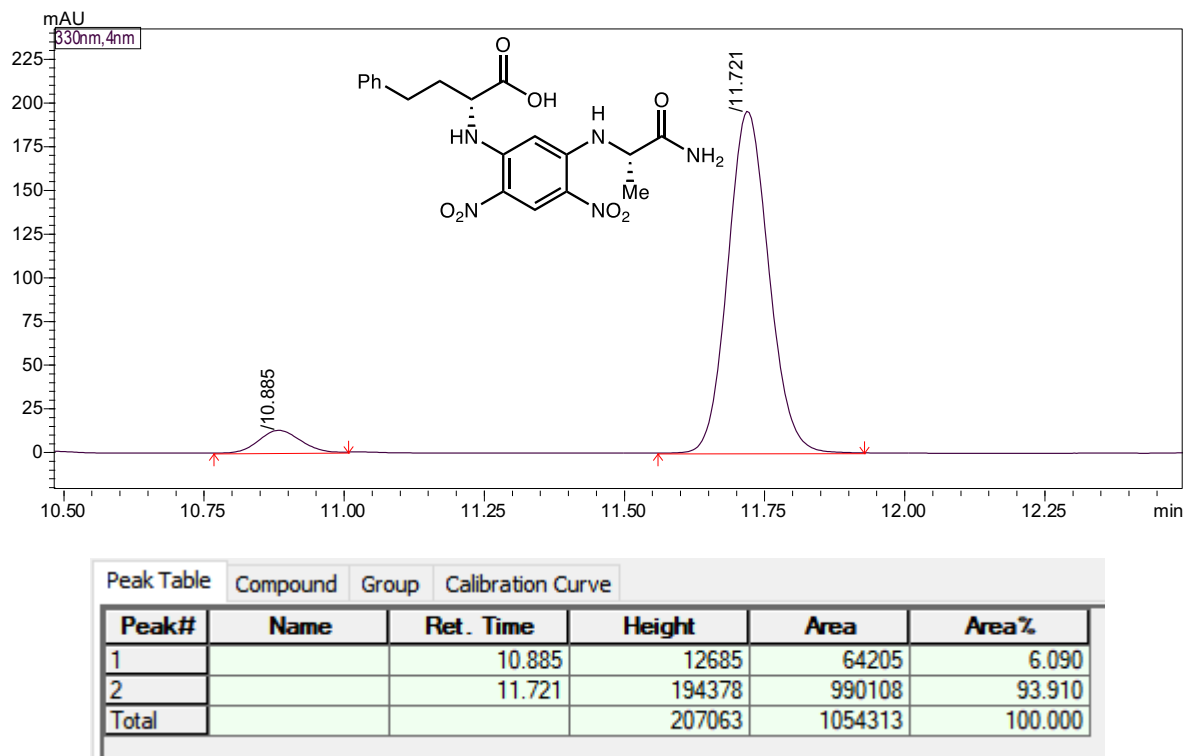
Marfey's analysis of (*rac*)-3a



Marfey's analysis of L-3a

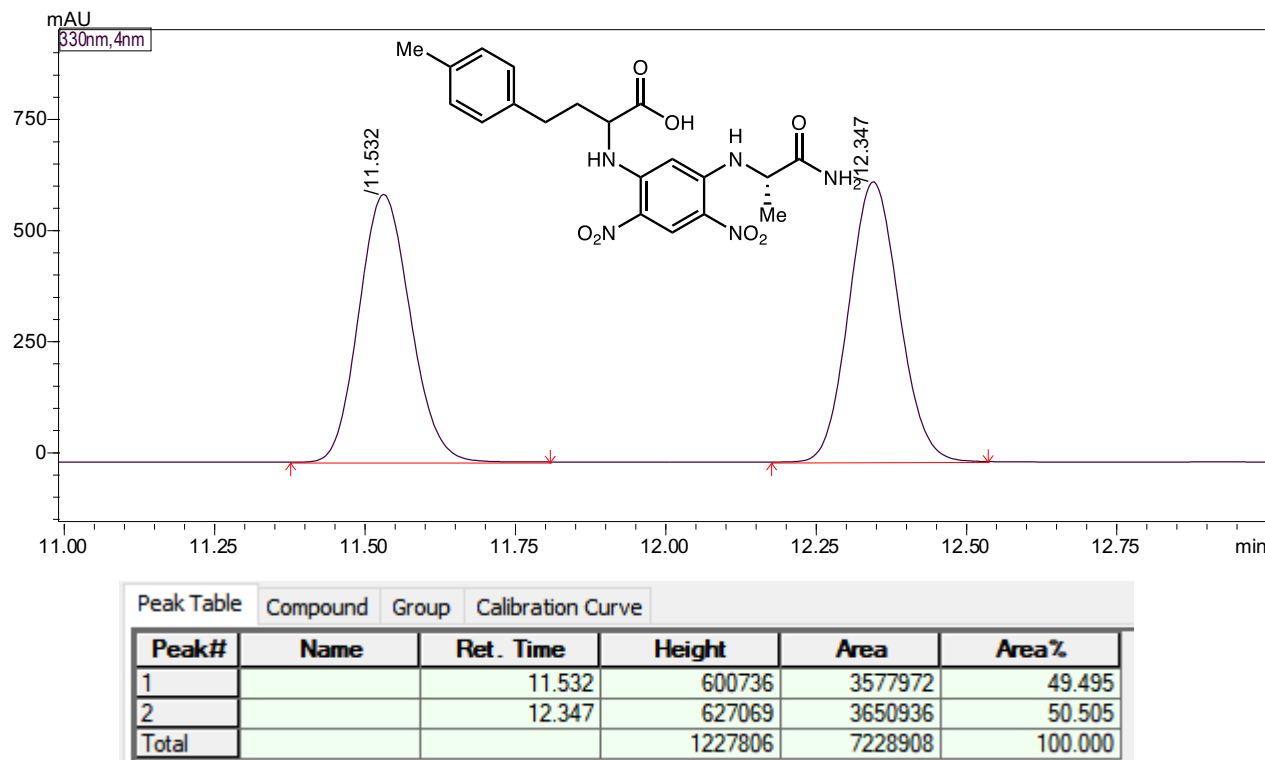


Marfey's analysis of D-3a

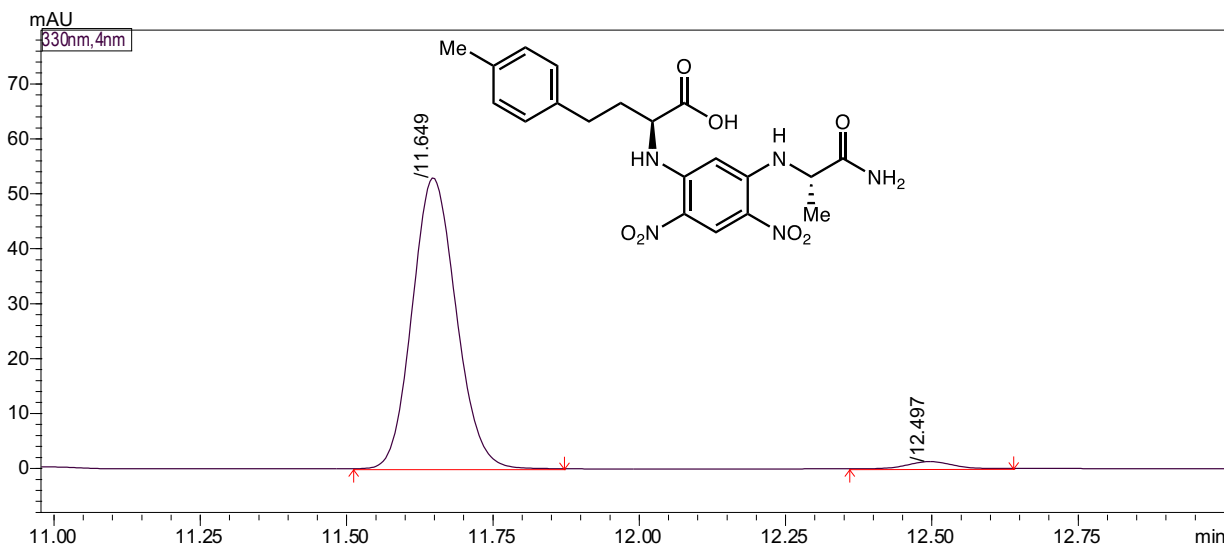


2-Amino-4-(p-tolyl) butanoic acid (3b)

Marfey's analysis for (*rac*)-3b

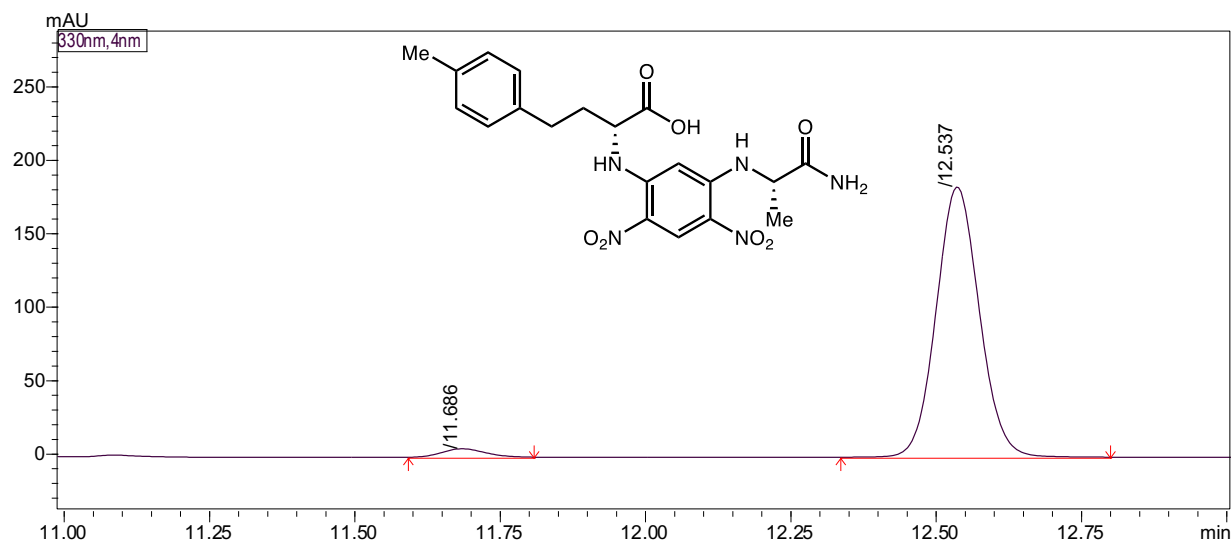


Marfey's analysis for L-3b



Peak Table	Compound	Group	Calibration Curve		
Peak#	Name	Ret. Time	Height	Area	Area%
1		11.649	52625	275964	97.698
2		12.497	1276	6503	2.302
Total			53901	282467	100.000

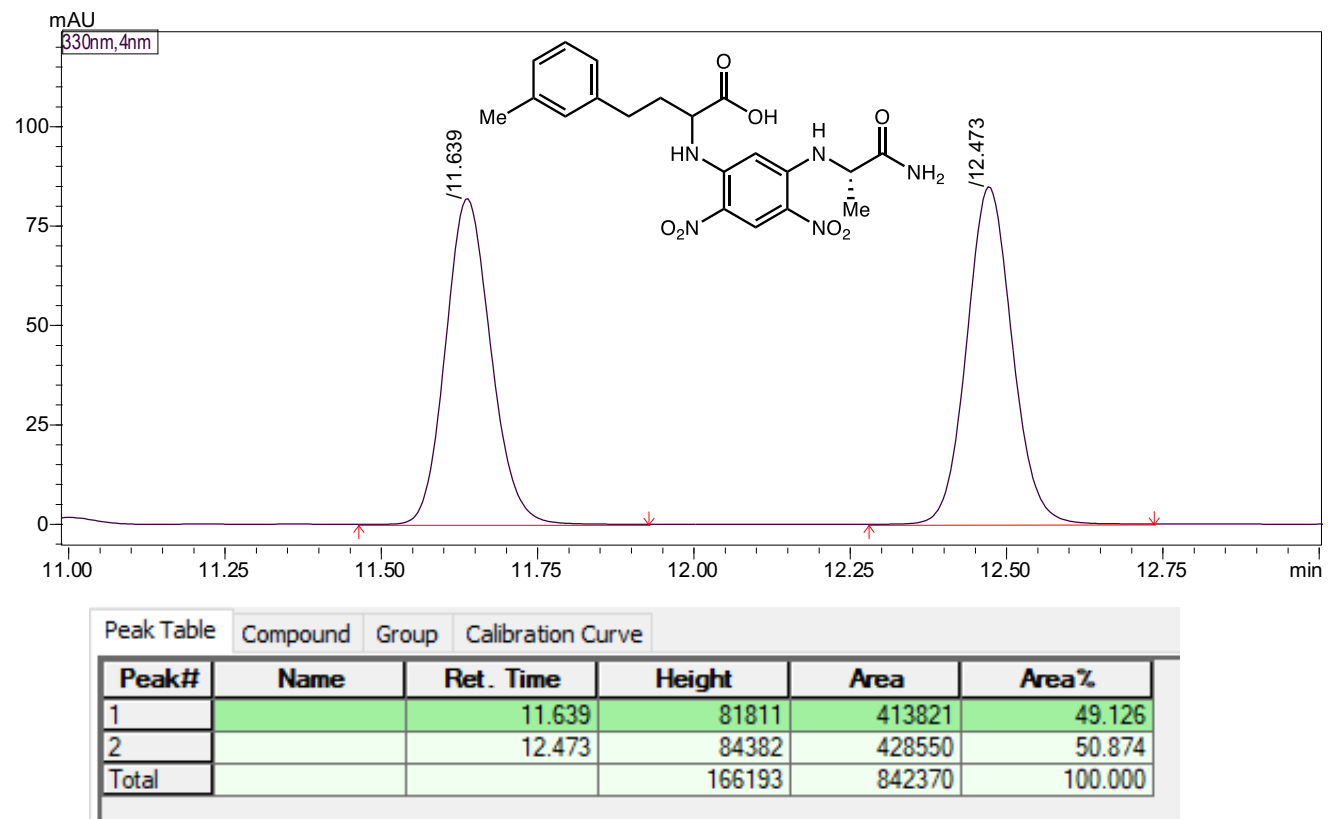
Marfey's analysis for D-3b



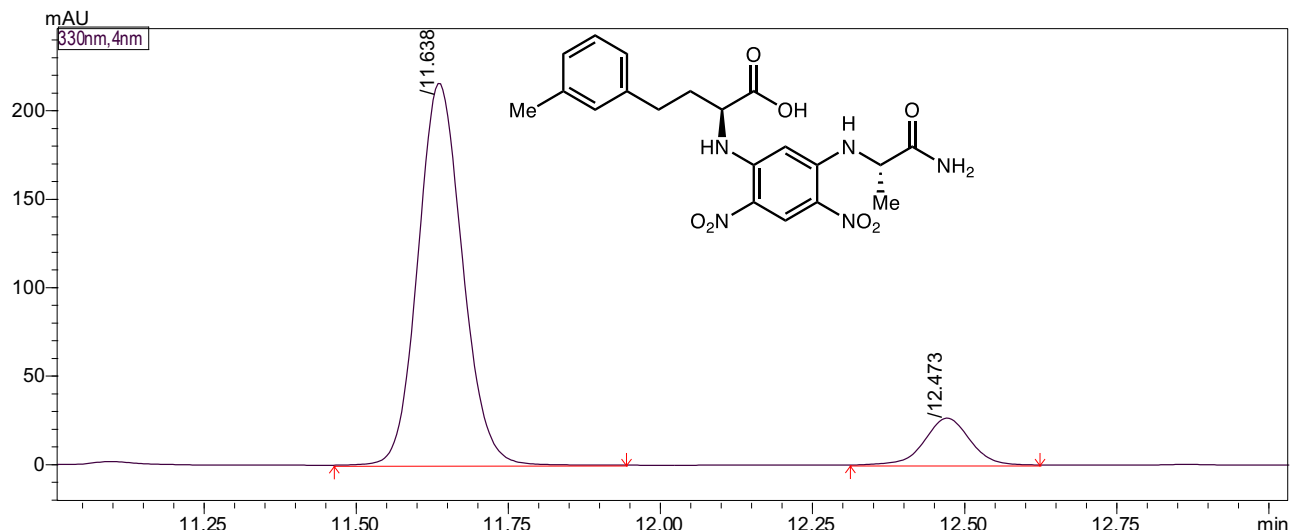
Peak Table	Compound	Group	Calibration Curve		
Peak#	Name	Ret. Time	Height	Area	Area%
1		11.686	5787	29853	3.047
2		12.537	182811	949808	96.953
Total			188598	979661	100.000

2-Amino-4-(m-tolyl) butanoic acid (**3c**)

Marfey's analysis for (*rac*)-**3c**

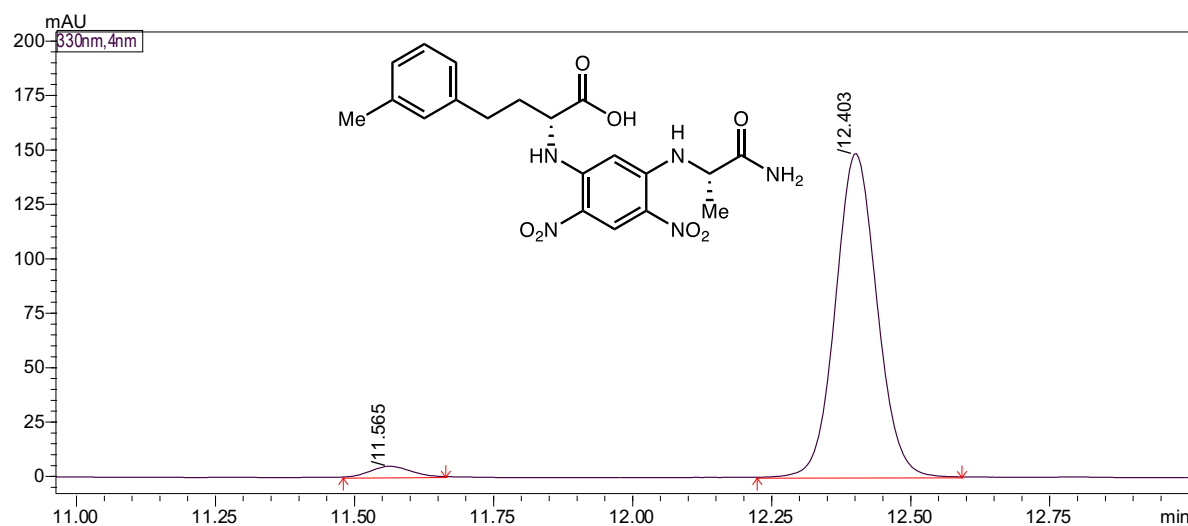


Marfey's analysis for L-**3c**



Peak Table	Compound	Group	Calibration Curve		
Peak#	Name	Ret. Time	Height	Area	Area%
1		11.638	215630	1094107	88.846
2		12.473	26355	137356	11.154
Total			241985	1231463	100.000

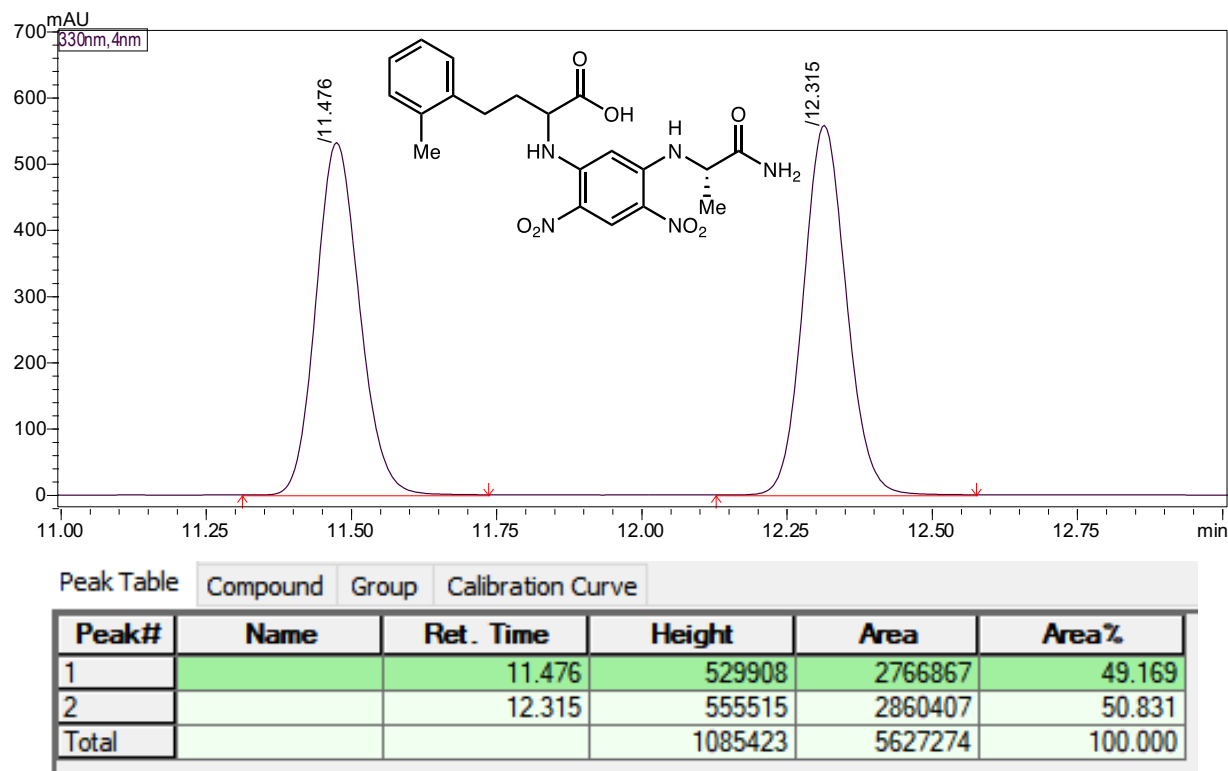
Marfey's analysis for D-3c



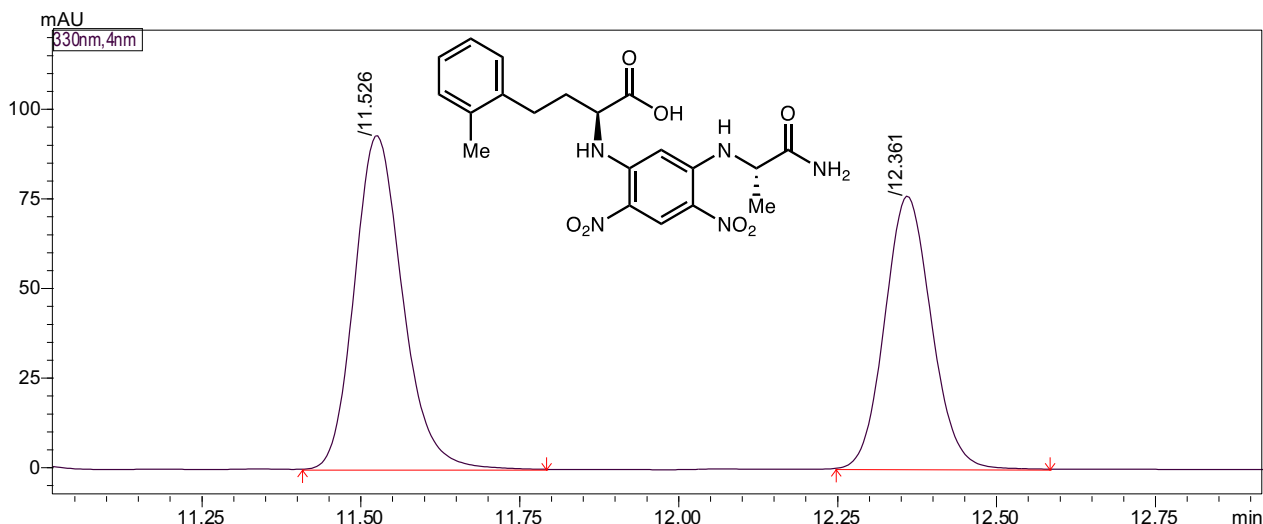
Peak Table	Compound	Group	Calibration Curve		
Peak#	Name	Ret. Time	Height	Area	Area%
1		11.565	4838	23785	2.997
2		12.403	147749	769928	97.003
Total			152588	793713	100.000

2-Amino-4-(o-tolyl) butanoic acid (3d)

Marfey's analysis for (*rac*)-3d

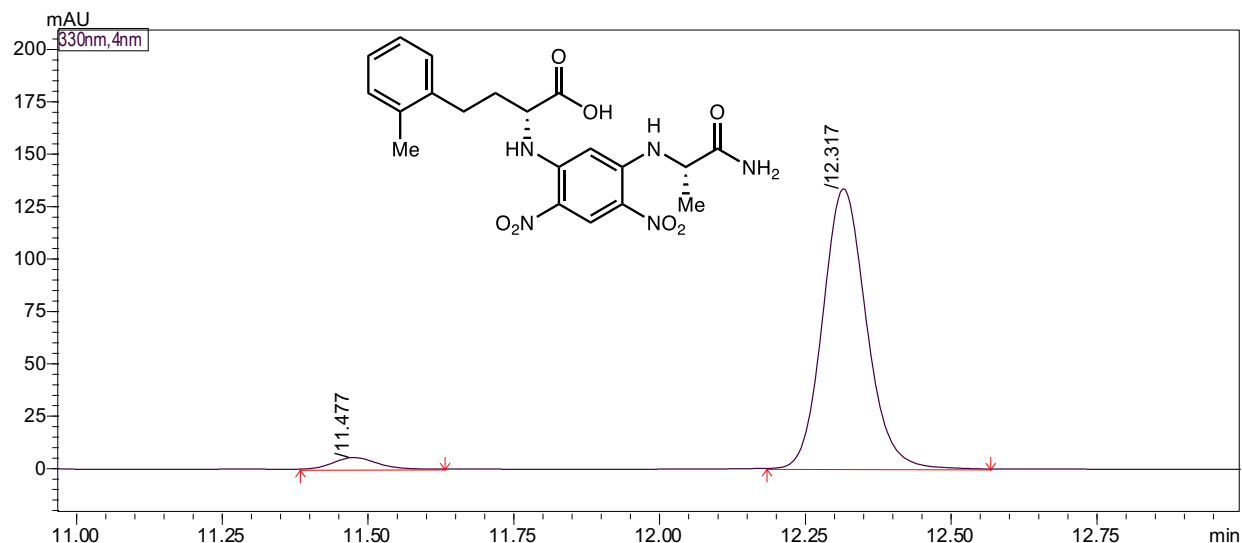


Marfey's analysis for L-3d



Peak Table	Compound	Group	Calibration Curve		
Peak#	Name	Ret. Time	Height	Area	Area%
1		11.526	93004	491223	55.894
2		12.361	75634	387624	44.106
Total			168638	878847	100.000

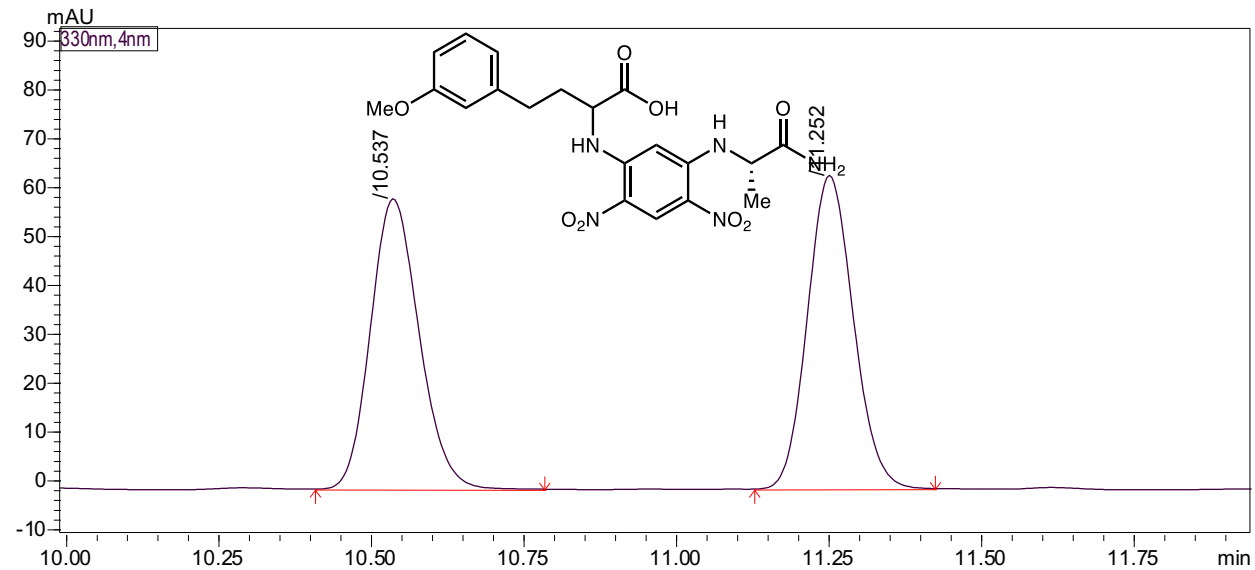
Marfey's analysis for D-3d



Peak Table	Compound	Group	Calibration Curve		
Peak#	Name	Ret. Time	Height	Area	Area%
1		11.477	5518	28403	3.940
2		12.317	133287	692398	96.060
Total			138805	720801	100.000

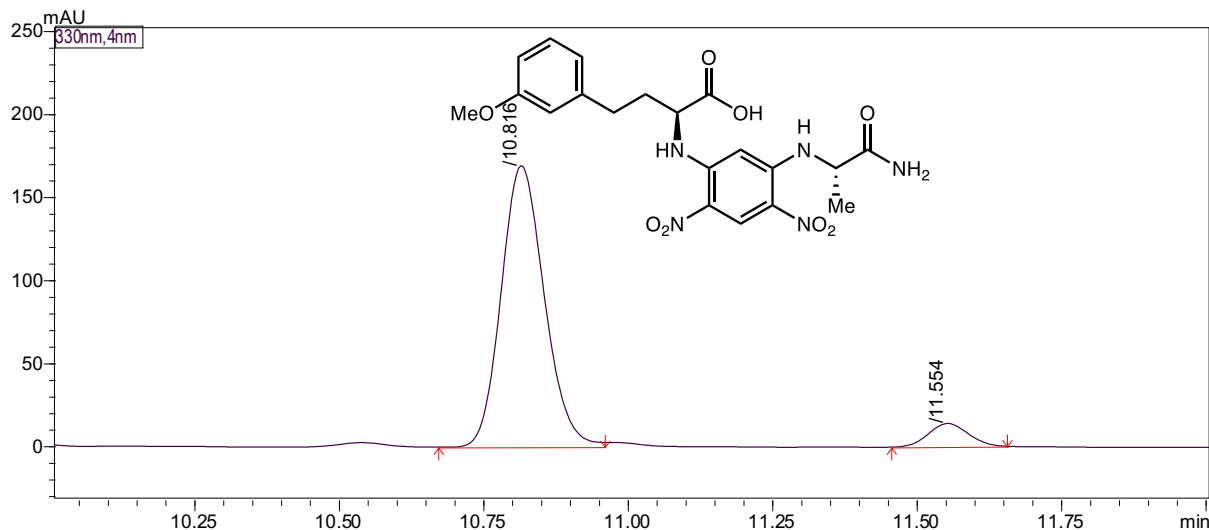
2-Amino-4-(3-methoxyphenyl) butanoic acid (**3e**)

Marfey's analysis of (*rac*)-**3e**



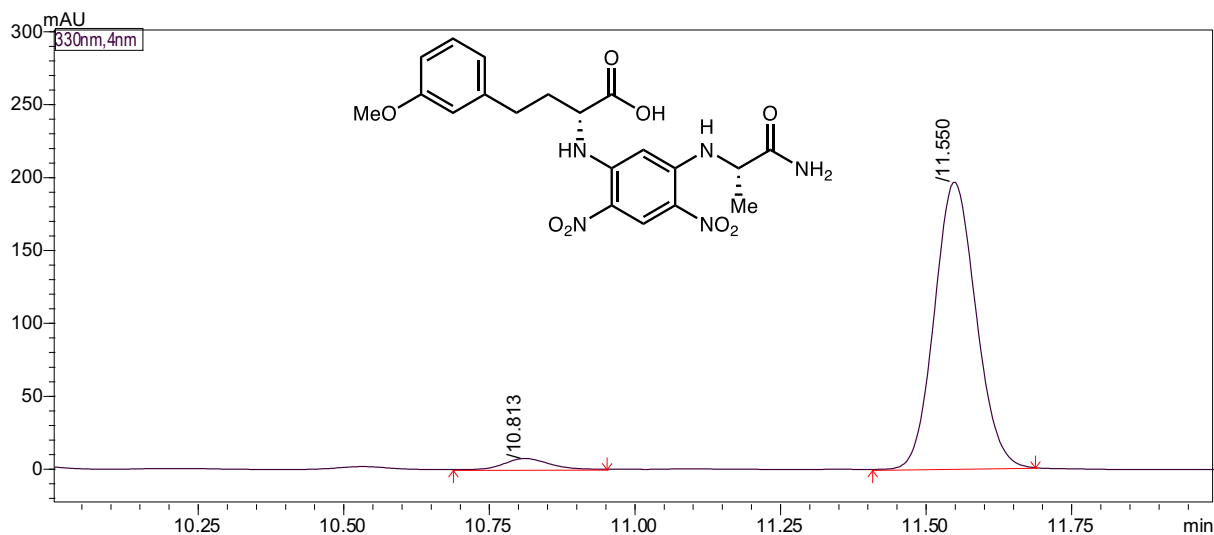
Peak Table					
Peak#	Name	Ret. Time	Height	Area	Area%
1		10.537	59117	328592	49.505
2		11.252	63922	335159	50.495
Total			123039	663751	100.000

Marfey's analysis of L-**3e**



Peak Table	Compound	Group	Calibration Curve		
Peak#	Name	Ret. Time	Height	Area	Area%
1		10.816	168750	877991	92.944
2		11.554	13802	66658	7.056
Total			182553	944649	100.000

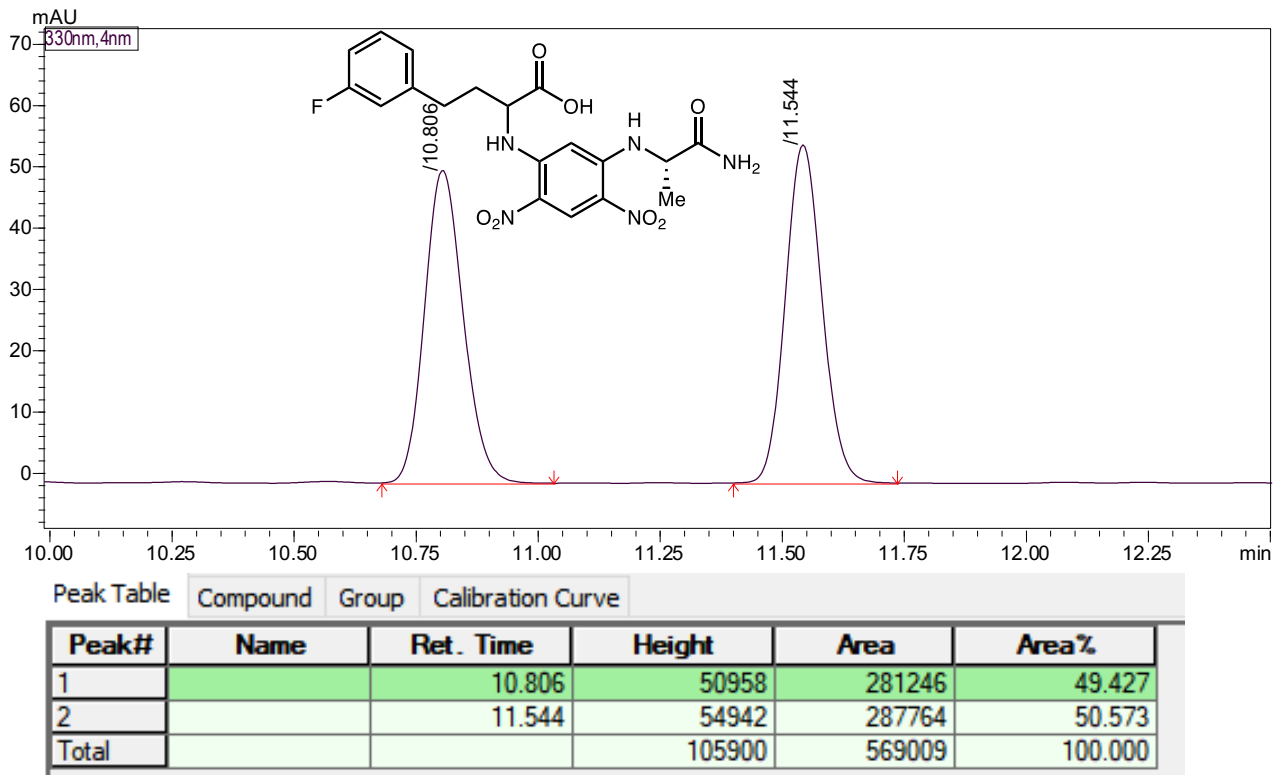
Marfey's analysis of D-3e



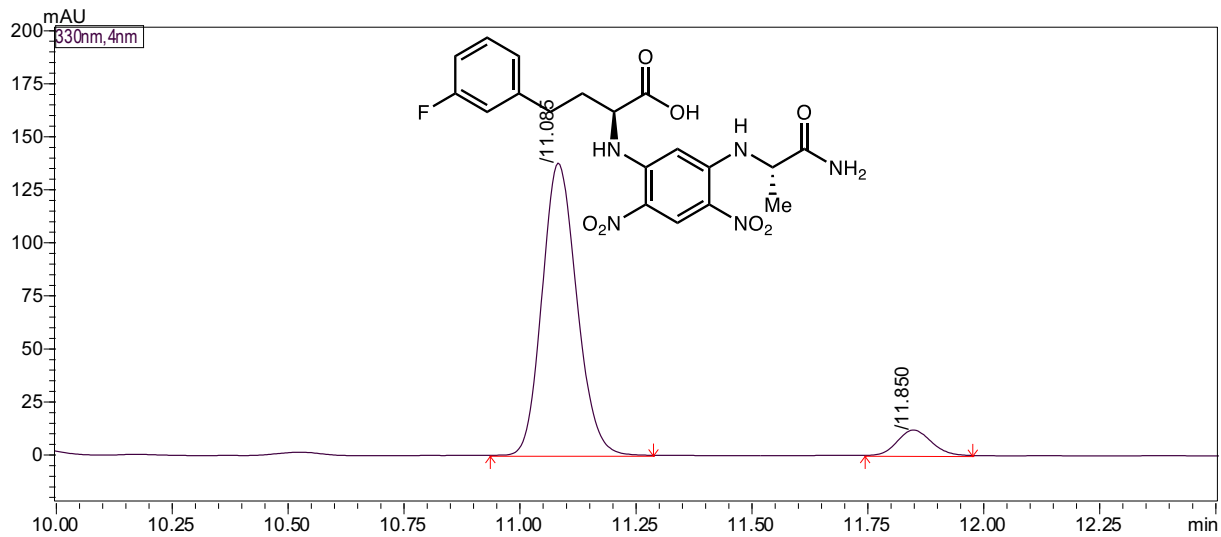
Peak Table	Compound	Group	Calibration Curve			
Peak#	Name	Ret. Time	Height	Area	Area%	
1		10.813	7451	38527	3.816	
2		11.550	196209	971220	96.184	
Total			203660	1009747	100.000	

2-Amino-4-(3-fluorophenyl) butanoic acid (3f)

Marfey's analysis of (*rac*)-3f

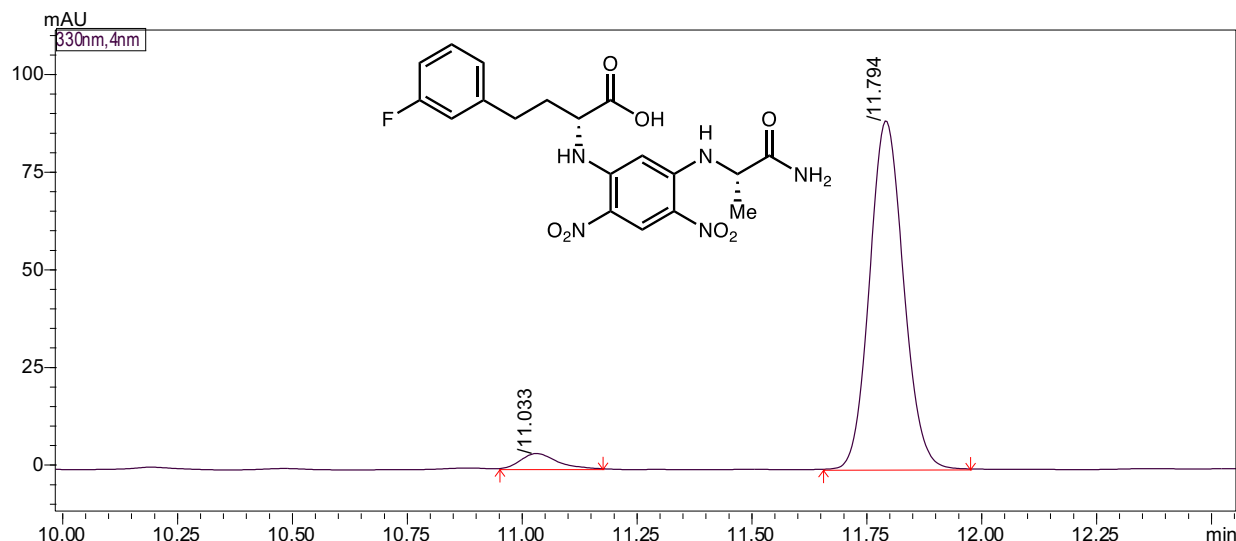


Marfey's analysis of L-3f



Peak Table					
	Compound	Group	Calibration Curve		
Peak#	Name	Ret. Time	Height	Area	Area%
1		11.085	137347	714594	92.231
2		11.850	11883	60193	7.769
Total			149230	774787	100.000

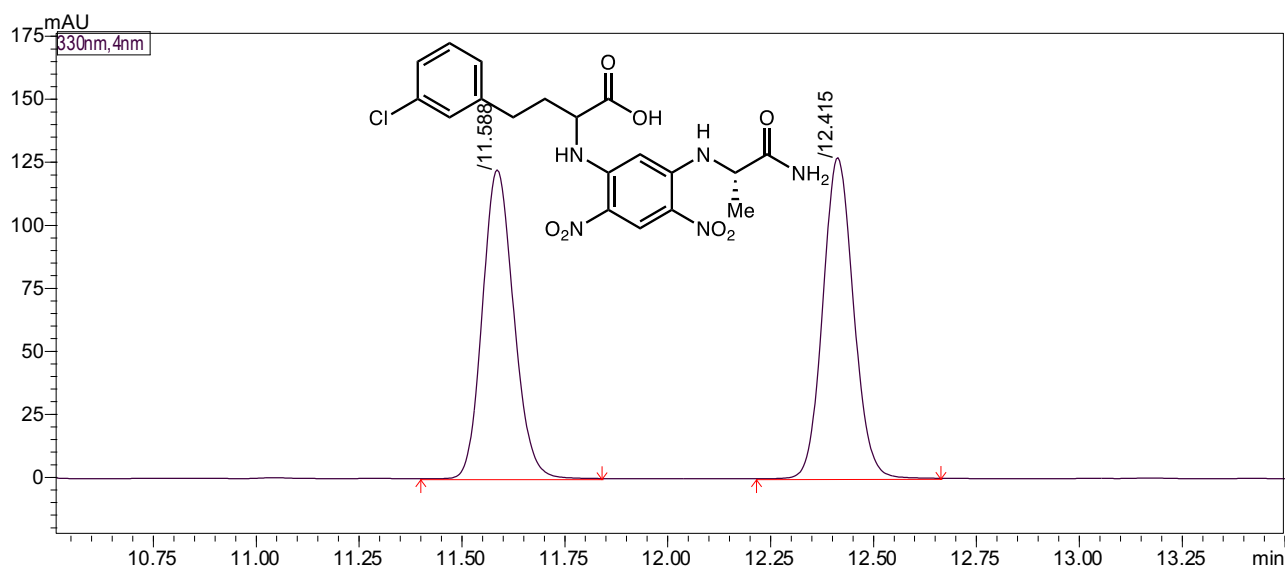
Marfey's analysis of D-3f



Peak Table					
	Compound	Group	Calibration Curve		
Peak#	Name	Ret. Time	Height	Area	Area%
1		11.033	3855	20659	4.324
2		11.794	88561	457146	95.676
Total			92416	477804	100.000

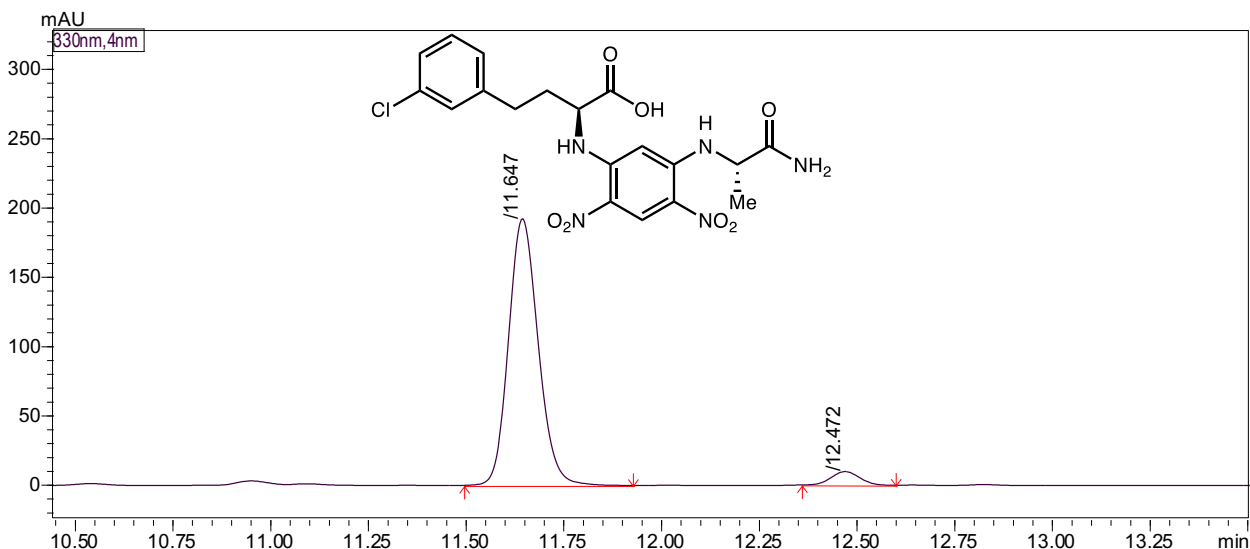
2-Amino-4-(3-chlorophenyl) butanoic acid (3g)

Marfey's analysis of (*rac*)-3g



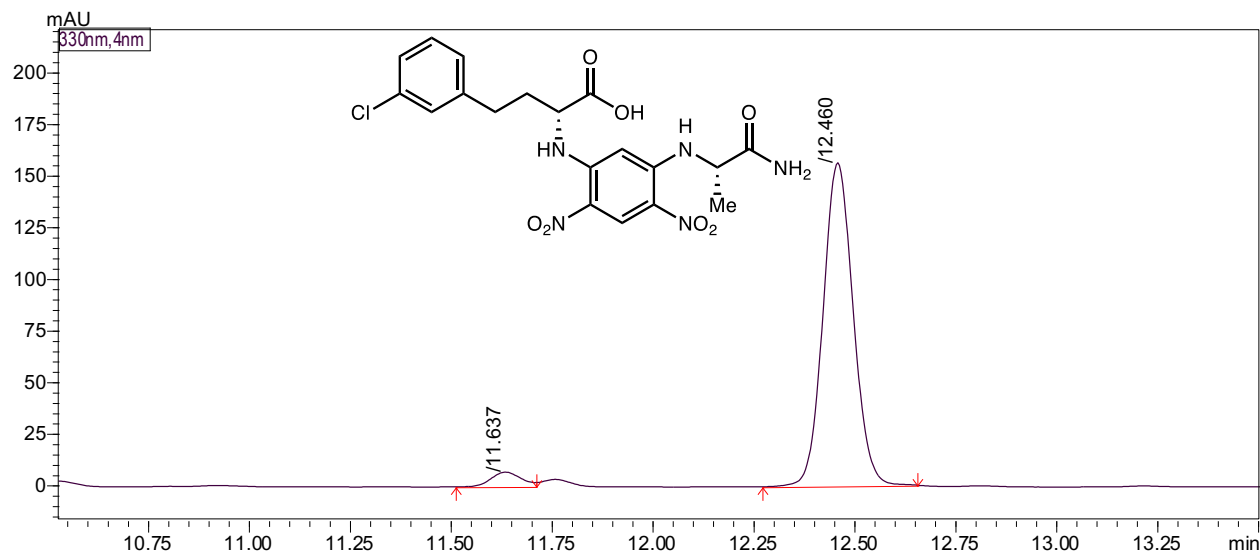
Peak Table					
Peak#	Name	Ret. Time	Height	Area	Area%
1		11.588	122088	648177	49.568
2		12.415	127087	659480	50.432
Total			249176	1307657	100.000

Marfey's analysis of L-3g



Peak Table	Compound	Group	Calibration Curve		
Peak#	Name	Ret. Time	Height	Area	Area%
1		11.647	192127	1011844	95.404
2		12.472	9734	48749	4.596
Total			201861	1060593	100.000

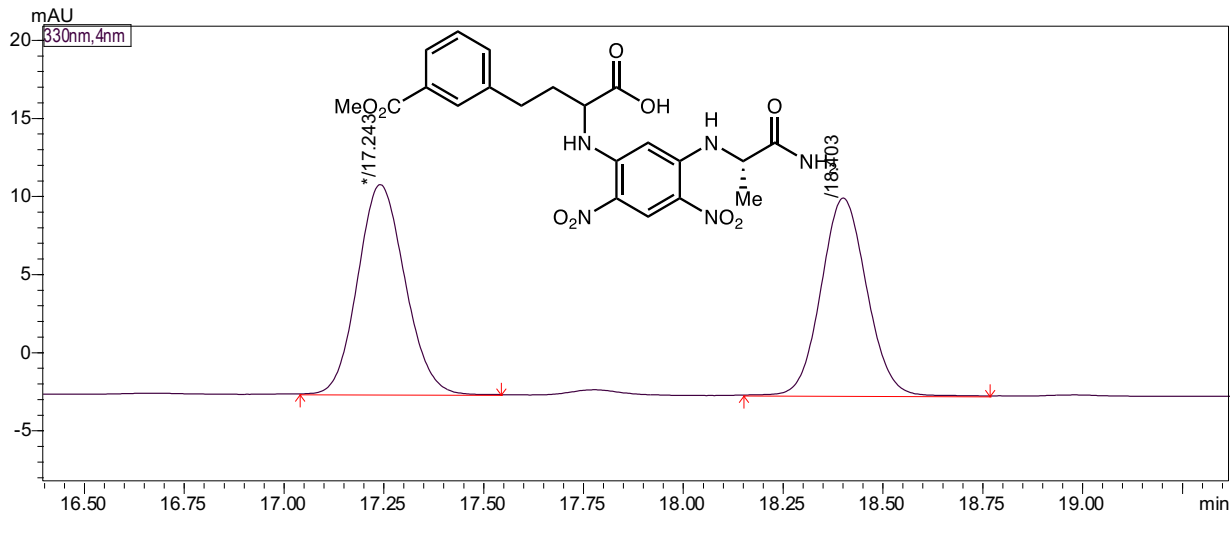
Marfey's analysis of D-3g



Peak Table	Compound	Group	Calibration Curve		
Peak#	Name	Ret. Time	Height	Area	Area%
1		11.637	7042	36895	4.354
2		12.460	155863	810419	95.646
Total			162905	847314	100.000

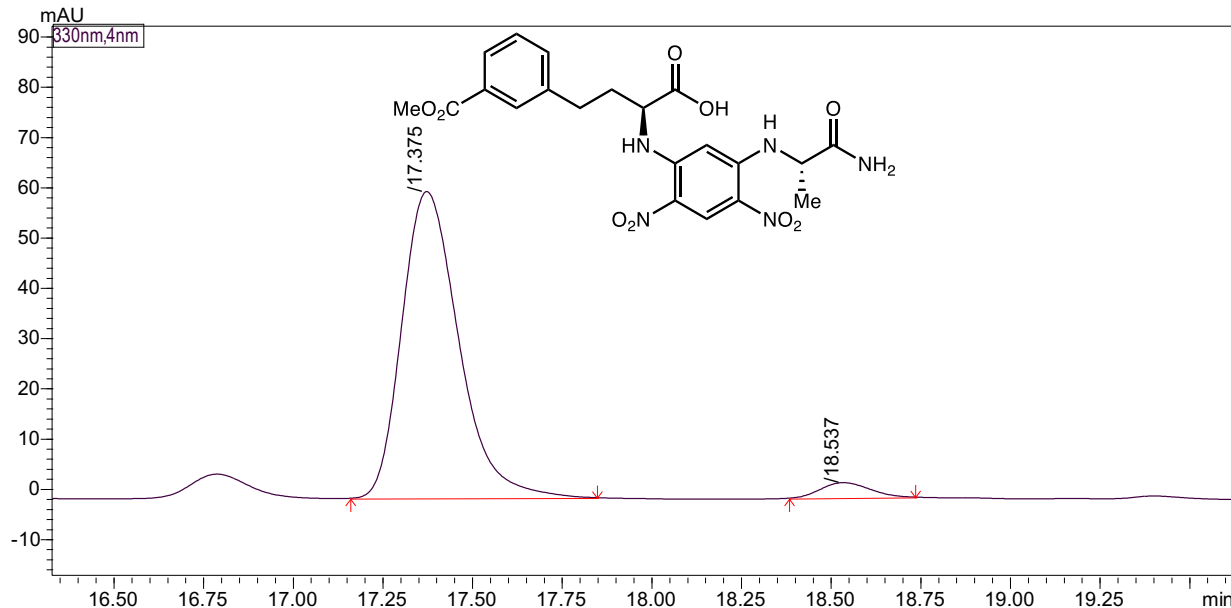
2-Amino-4-(3-(methoxycarbonyl) phenyl) butanoic acid (**3h**)

Marfey's analysis of (*rac*)-**3h**



Peak Table	Compound	Group	Calibration Curve		
Peak#	Name	Ret. Time	Height	Area	Area%
1		17.243	13395	110122	52.438
2		18.403	12601	99881	47.562
Total			25996	210002	100.000

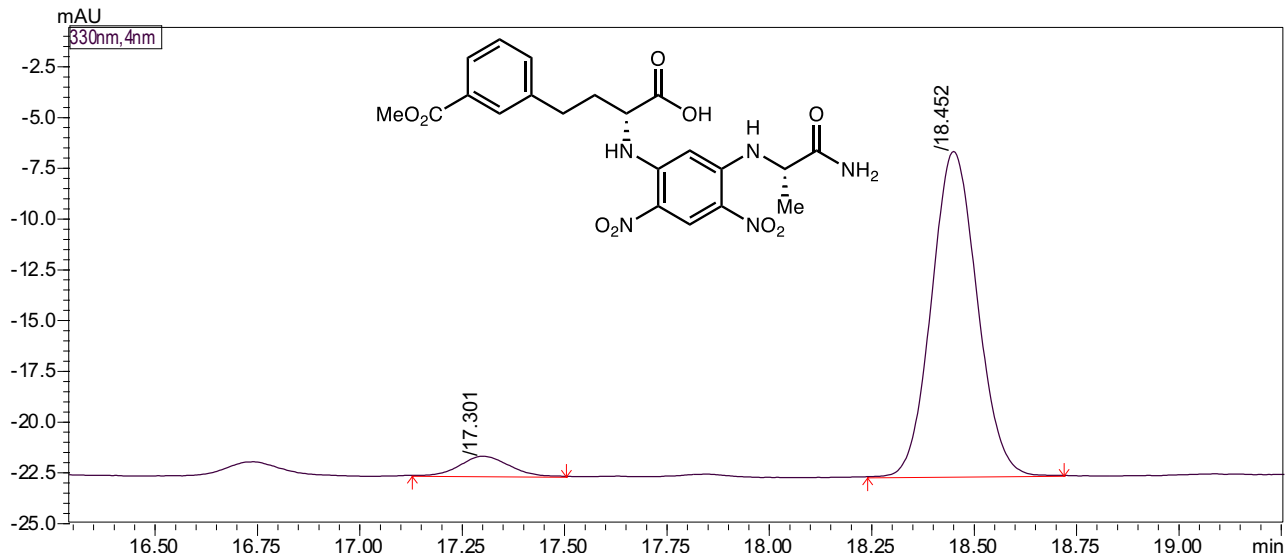
Marfey's analysis of L-**3h**



Peak Table Compound Group Calibration Curve

Peak#	Name	Ret. Time	Height	Area	Area%
1		17.375	60960	672890	95.965
2		18.537	2996	28295	4.035
Total			63956	701186	100.000

Marfey's analysis of D-3h

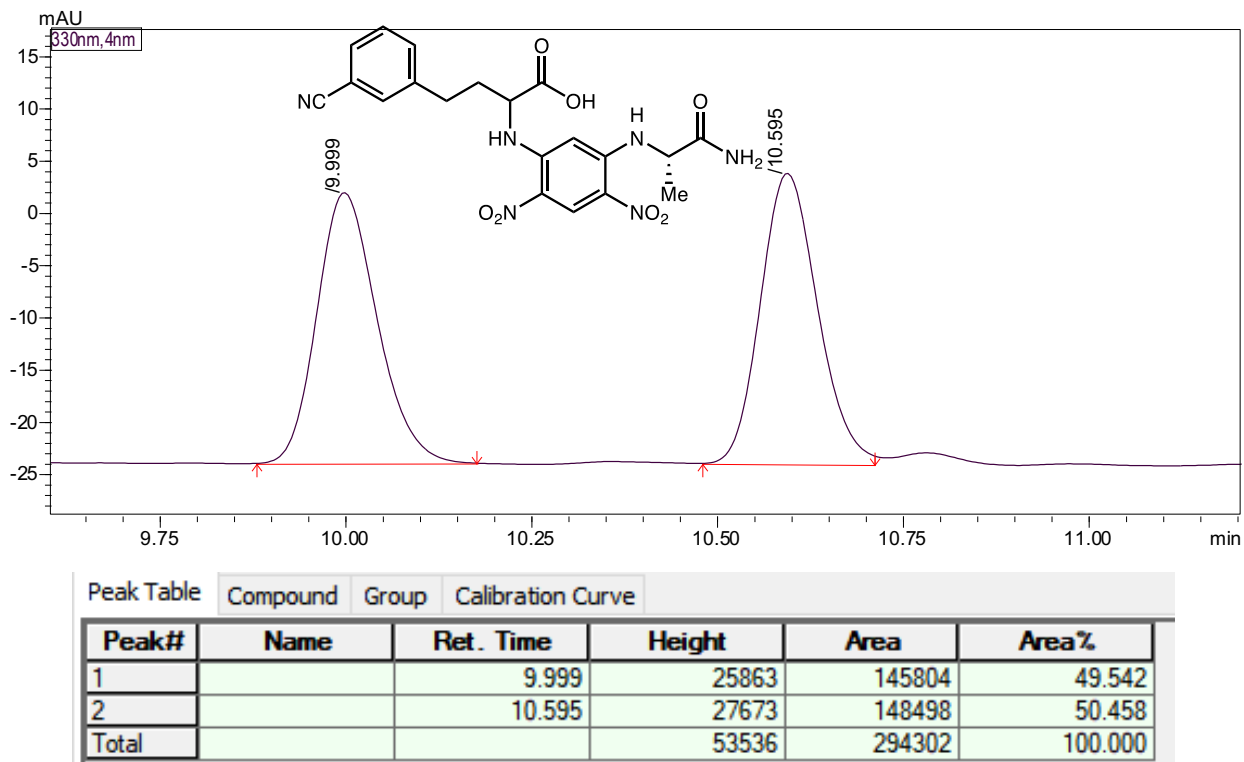


Peak Table Compound Group Calibration Curve

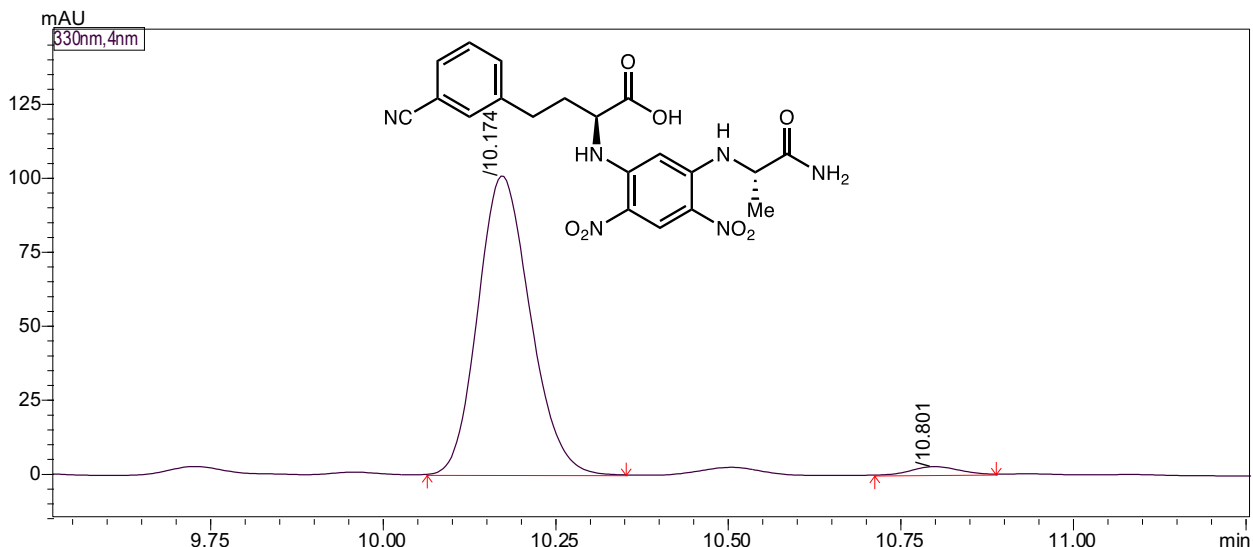
Peak#	Name	Ret. Time	Height	Area	Area%
1		17.301	966	7800	5.945
2		18.452	15981	123404	94.055
Total			16946	131204	100.000

2-Amino-4-(3-cyanophenyl) butanoic acid (3i)

Marfey's analysis of (*rac*)-3i

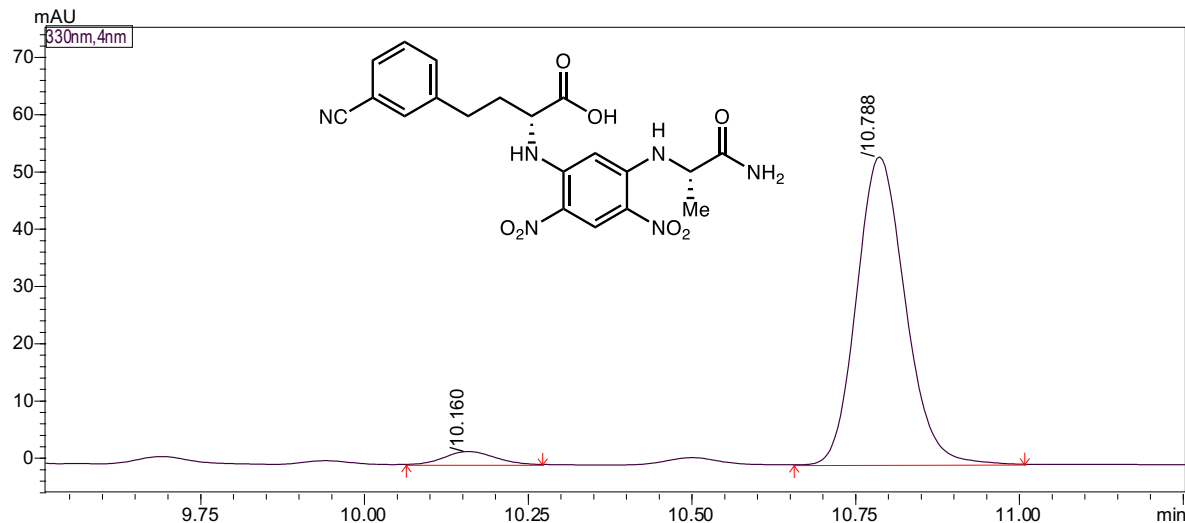


Marfey's analysis of L-3i



Peak Table	Compound	Group	Calibration Curve		
Peak#	Name	Ret. Time	Height	Area	Area%
1		10.174	100776	530680	97.704
2		10.801	2695	12471	2.296
Total			103471	543150	100.000

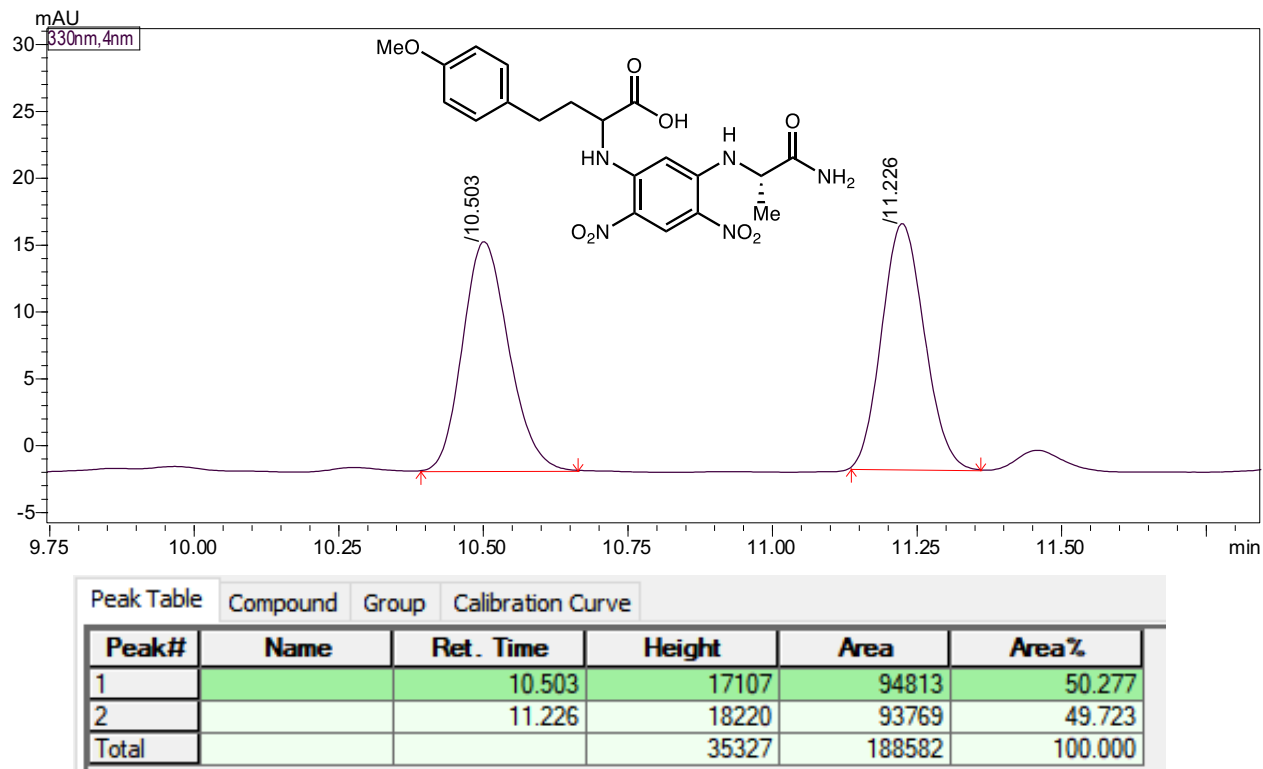
Marfey's analysis of D-3i



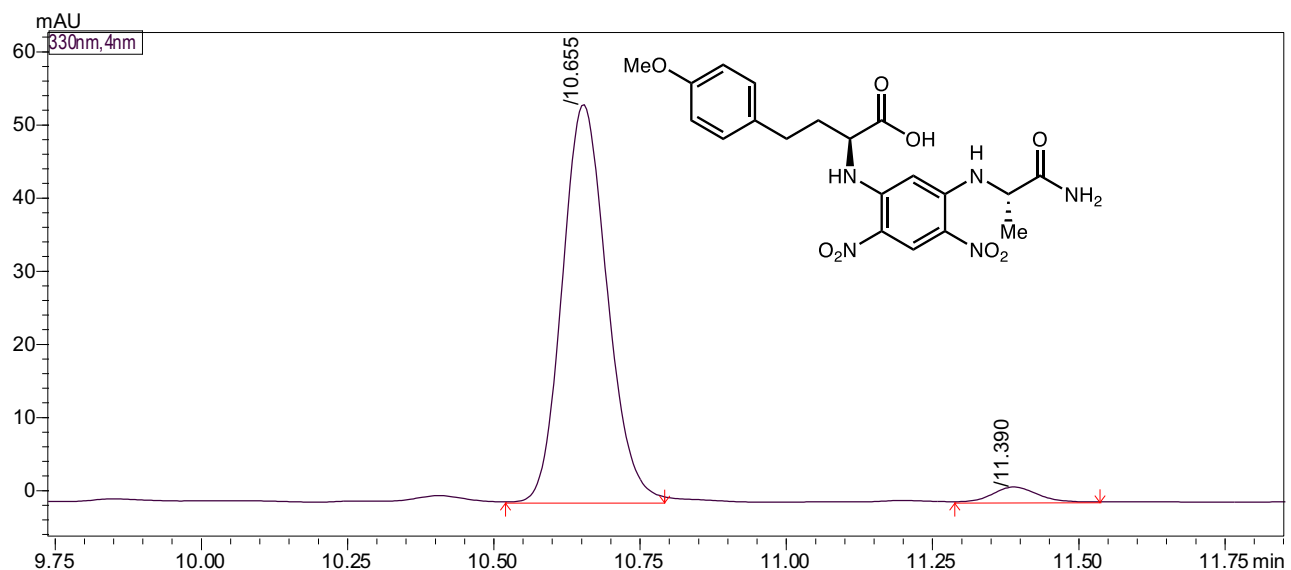
Peak Table	Compound	Group	Calibration Curve		
Peak#	Name	Ret. Time	Height	Area	Area%
1		10.160	2252	11782	4.083
2		10.788	53515	276817	95.917
Total			55767	288599	100.000

2-Amino-4-(4-methoxyphenyl) butanoic acid (**3j**)

Marfey's analysis of (*rac*)-**3j**

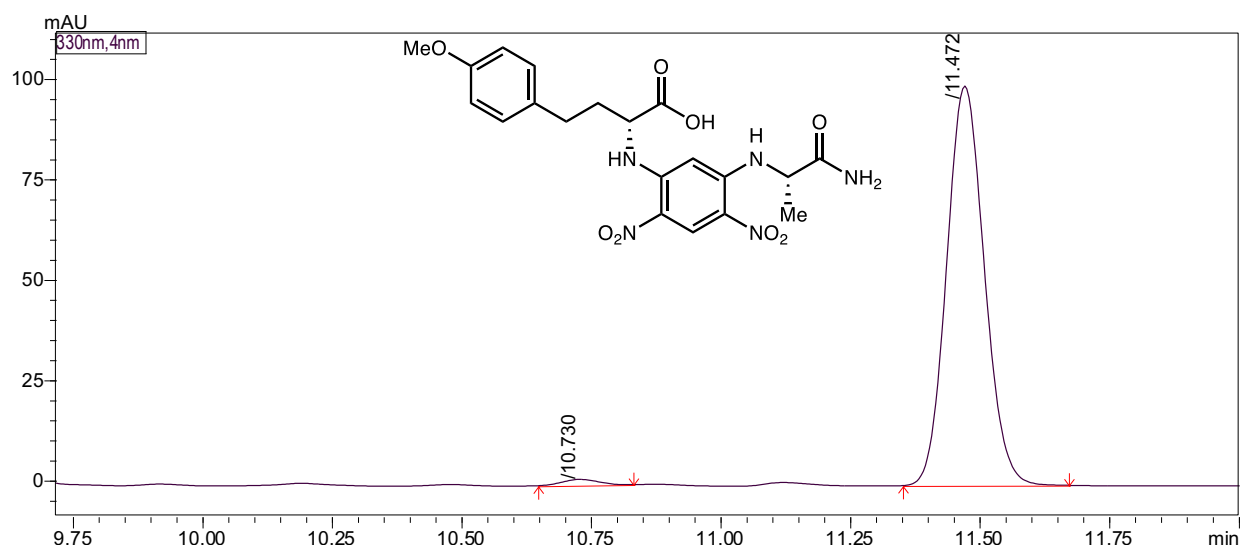


Marfey's analysis of L-**3j**



Peak#	Name	Ret. Time	Height	Area	Area%
1		10.655	54275	289282	96.496
2		11.390	2038	10505	3.504
Total			56314	299787	100.000

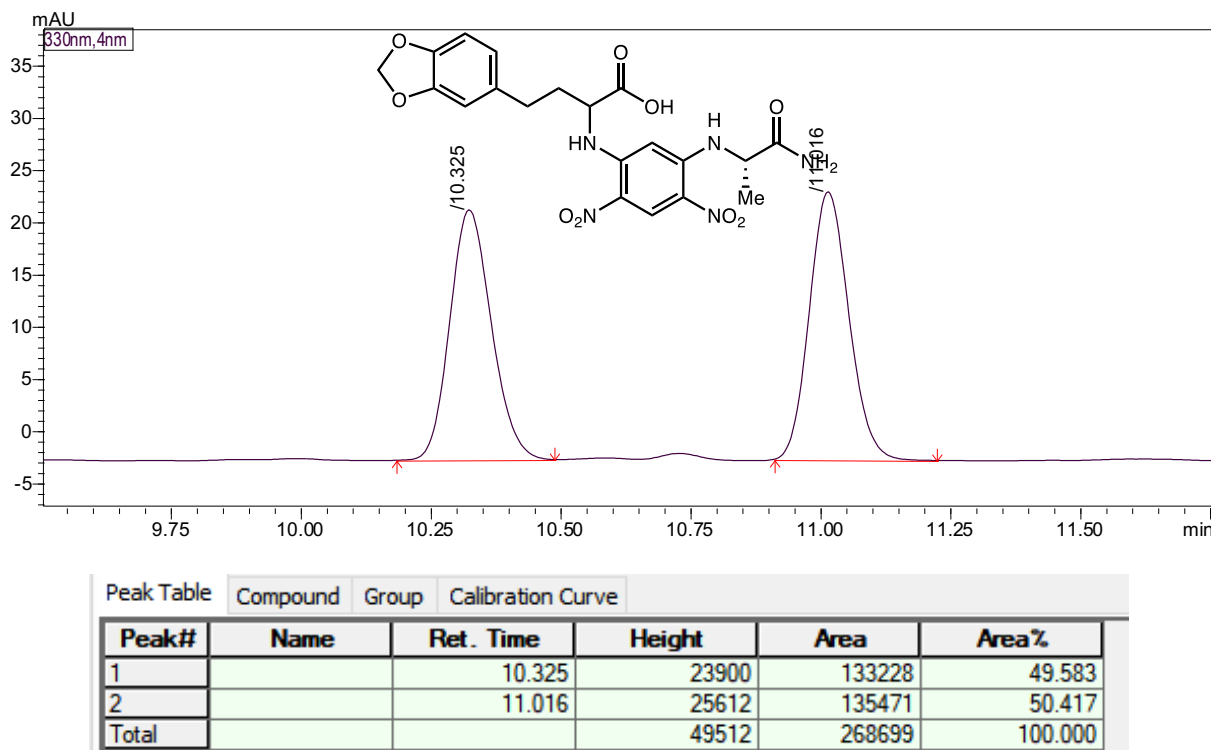
Marfey's analysis of D-3j



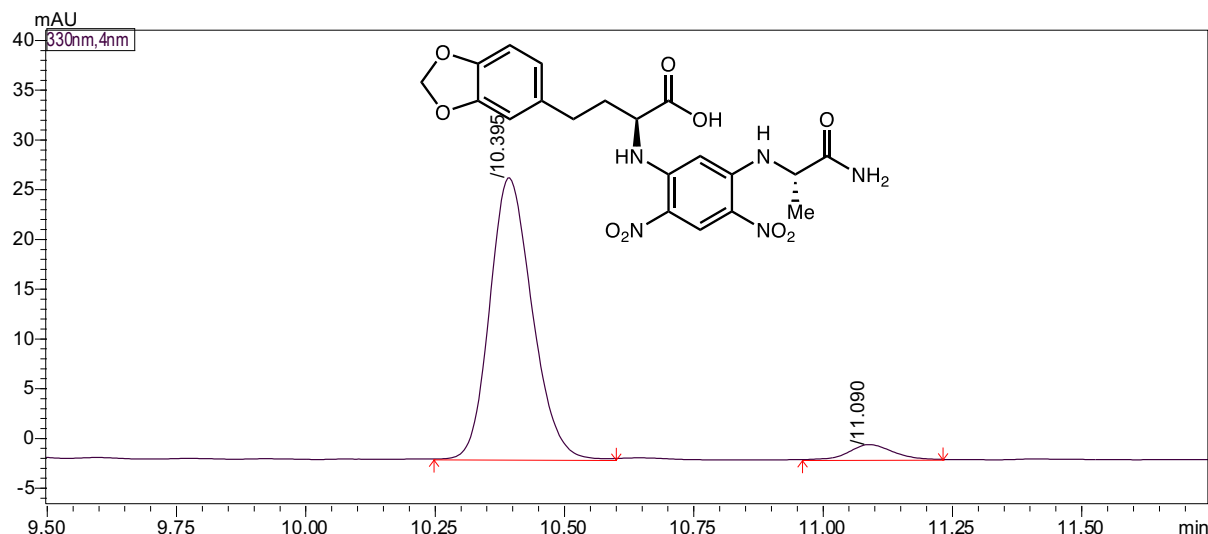
Peak Table	Compound	Group	Calibration Curve		
Peak#	Name	Ret. Time	Height	Area	Area%
1		10.730	1462	7099	1.393
2		11.472	99153	502505	98.607
Total			100615	509604	100.000

2-Amino-4-(benzo[d][1,3]dioxol-5-yl)butanoic acid (**3k**)

Marfey's analysis of (*rac*)-**3k**

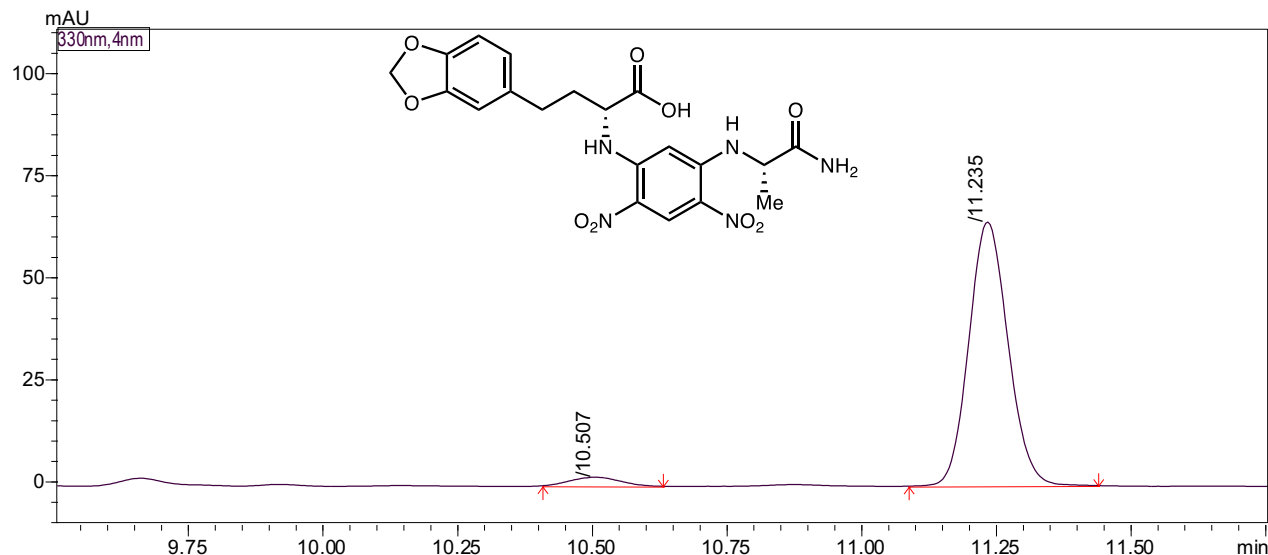


Marfey's analysis of L-**3k**



Peak Table	Compound	Group	Calibration Curve		
Peak#	Name	Ret. Time	Height	Area	Area%
1		10.395	28130	160626	94.924
2		11.090	1494	8590	5.076
Total			29624	169215	100.000

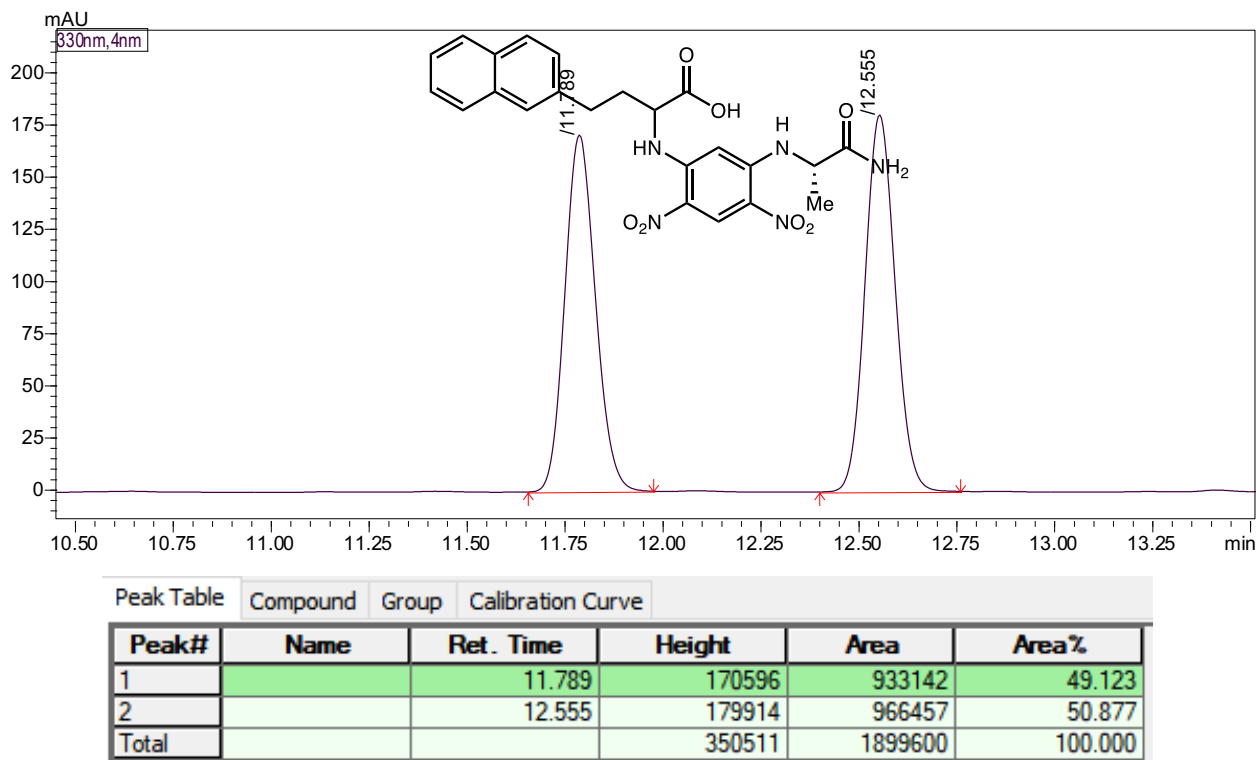
Marfey's analysis of D-3k



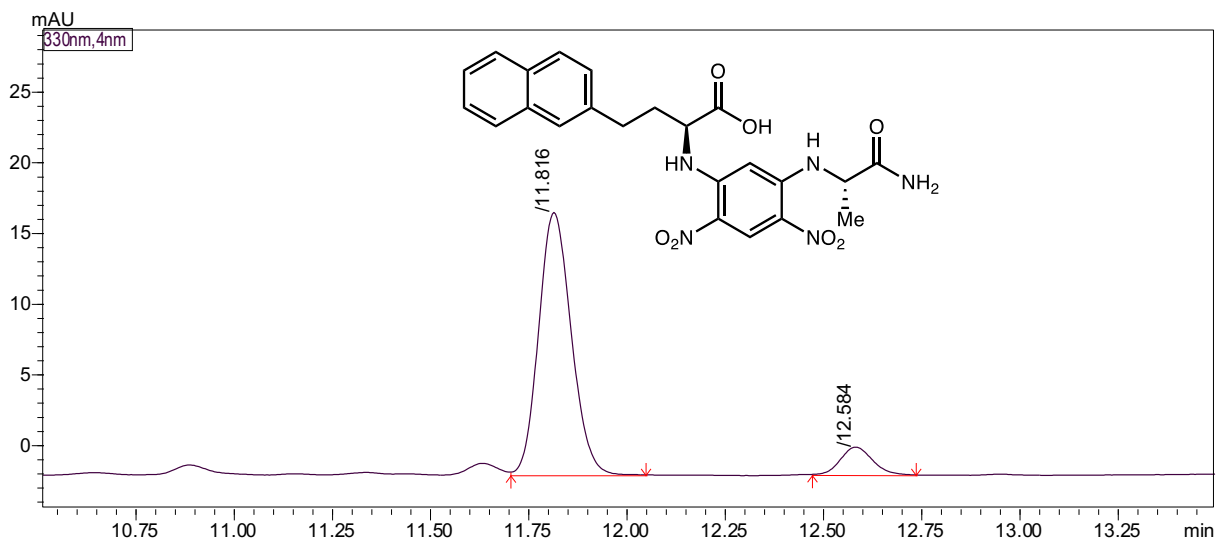
Peak Table	Compound	Group	Calibration Curve		
Peak#	Name	Ret. Time	Height	Area	Area%
1		10.507	2133	13670	4.011
2		11.235	64364	327131	95.989
Total			66497	340802	100.000

2-Amino-4-(naphthalen-2-yl)butanoic acid (**3l**)

Marfey's analysis of (*rac*)-**3l**

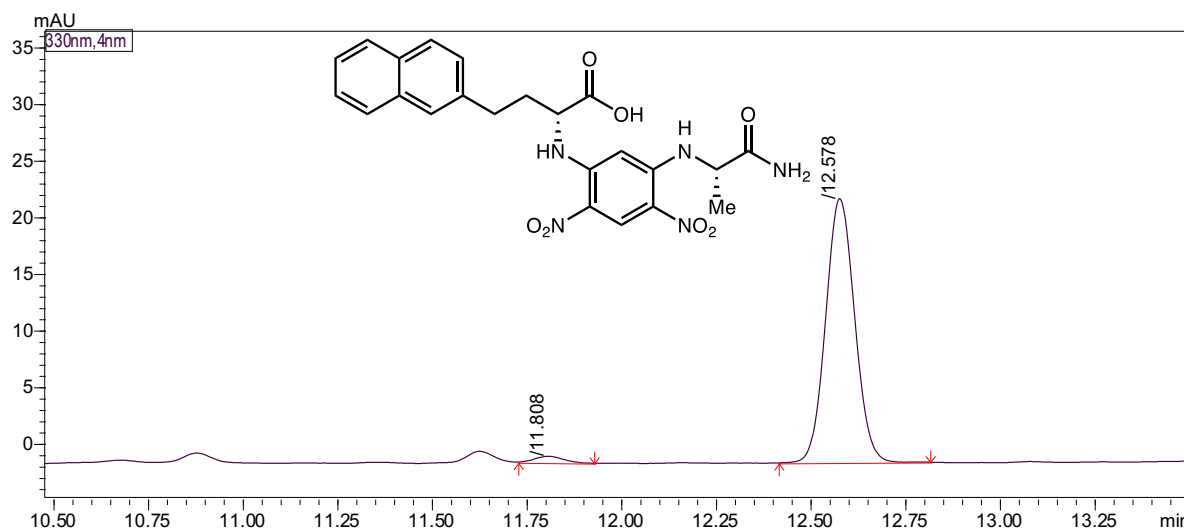


Marfey's analysis of L-**3l**



Peak Table	Compound	Group	Calibration Curve		
Peak#	Name	Ret. Time	Height	Area	Area%
1		11.816	18511	106800	90.773
2		12.584	1940	10856	9.227
Total			20452	117656	100.000

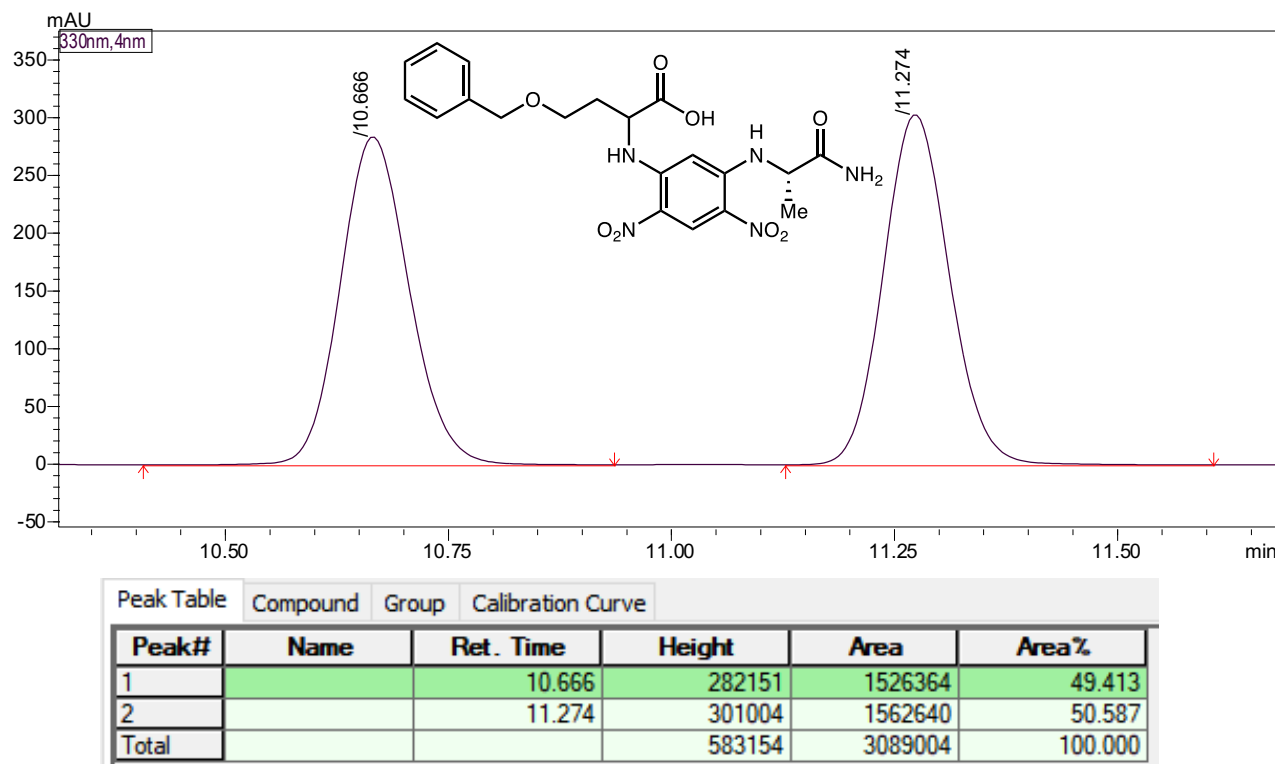
Marfey's analysis of D-3I



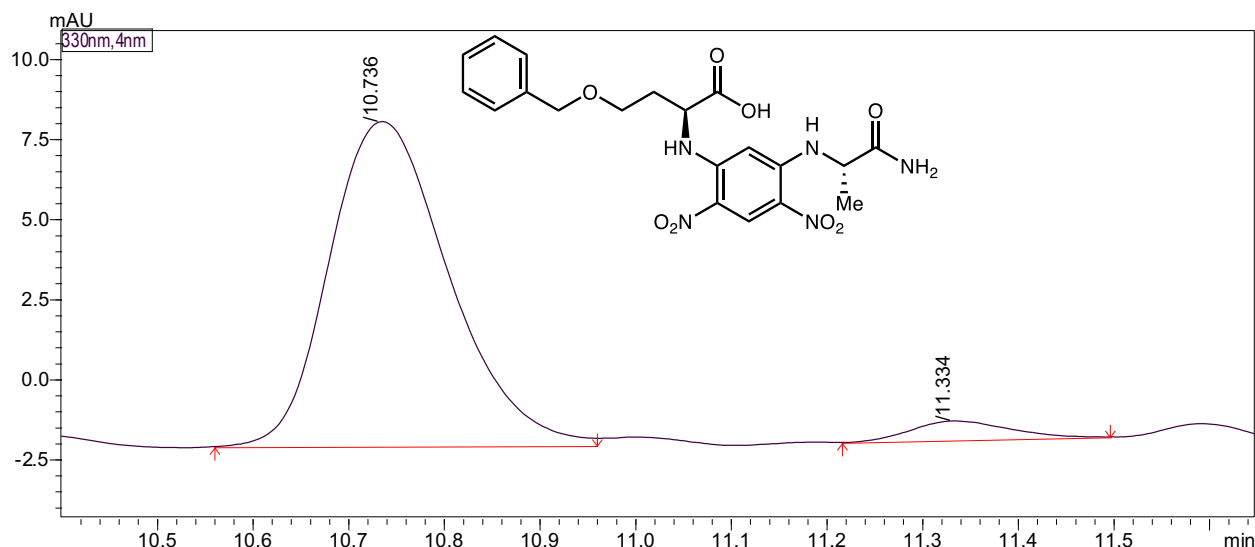
Peak Table	Compound	Group	Calibration Curve		
Peak#	Name	Ret. Time	Height	Area	Area%
1		11.808	576	3023	2.378
2		12.578	23141	124093	97.622
Total			23717	127116	100.000

O-benzyl-L-homoserine (**3m**)

Marfey's analysis of (*rac*)-**3m**

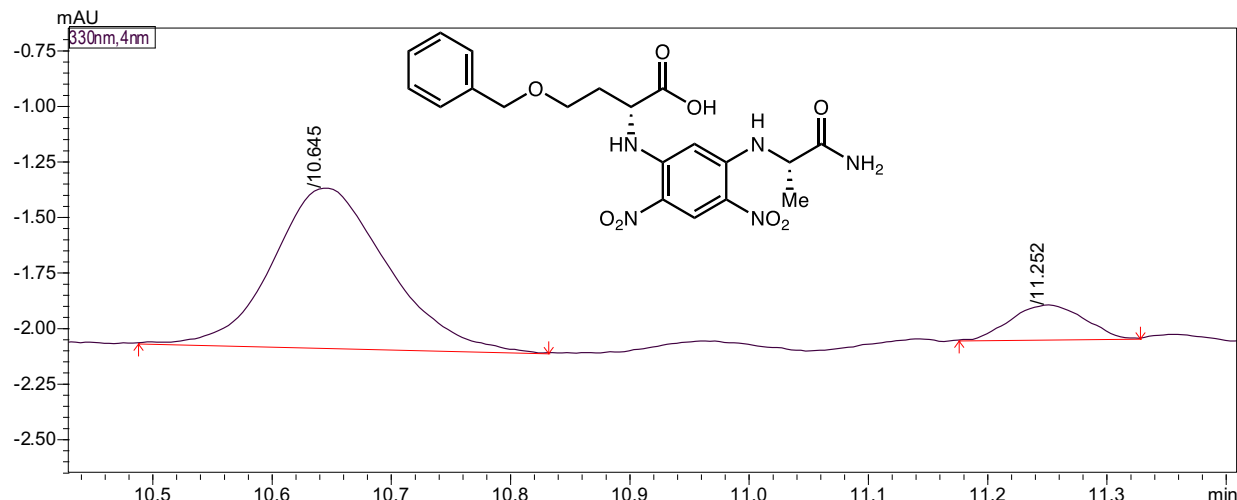


Marfey's analysis of L-**3m**



Peak Table	Compound	Group	Calibration Curve			
Peak#	Name	Ret. Time	Height	Area	Area%	
1		10.736	10130	87952	95.429	
2		11.334	598	4212	4.571	
Total			10728	92164	100.000	

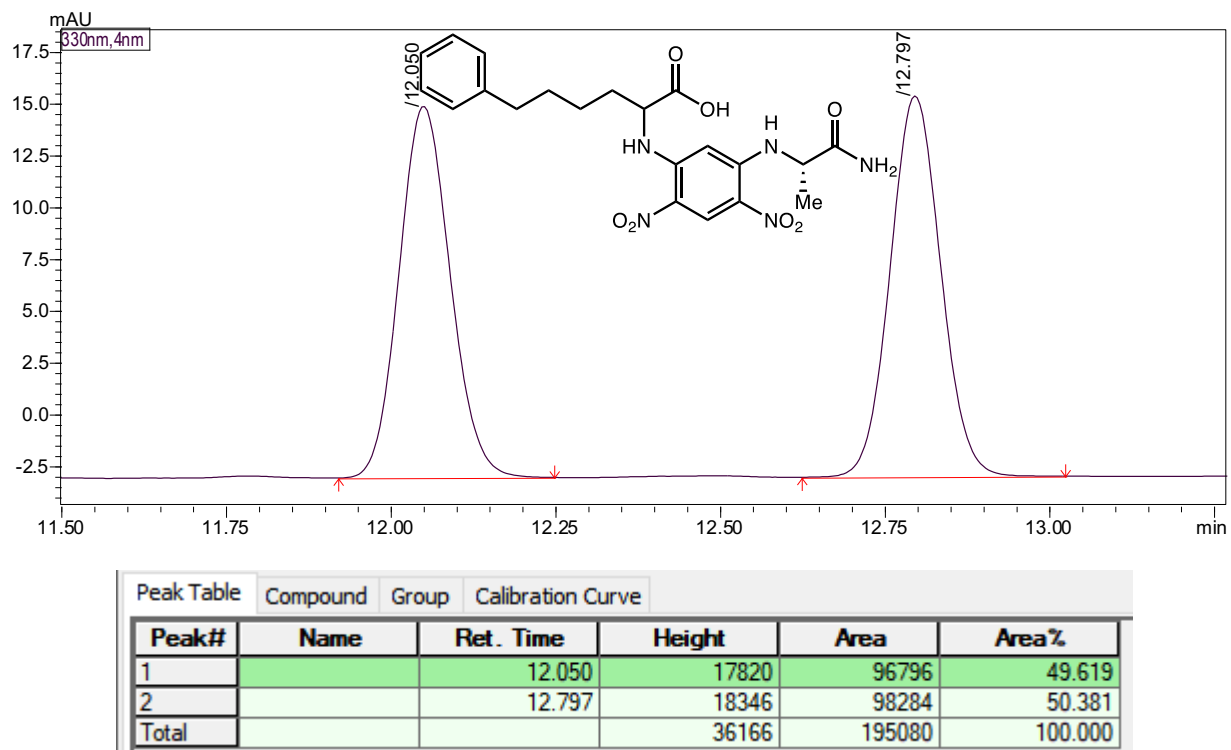
Marfey's analysis of D-3m



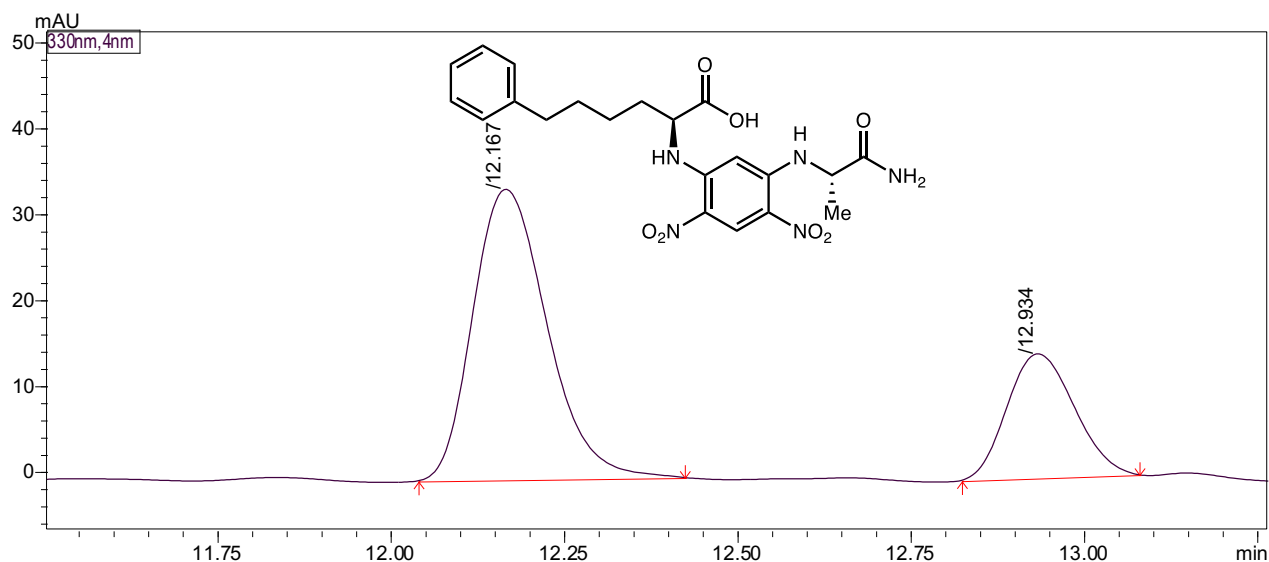
Peak Table	Compound	Group	Calibration Curve			
Peak#	Name	Ret. Time	Height	Area	Area%	
1		10.645	717	4772	88.026	
2		11.252	153	649	11.974	
Total			869	5421	100.000	

2-amino-6-phenylhexanoic acid (**3n**)

Marfey's analysis of (*rac*)-**3n**



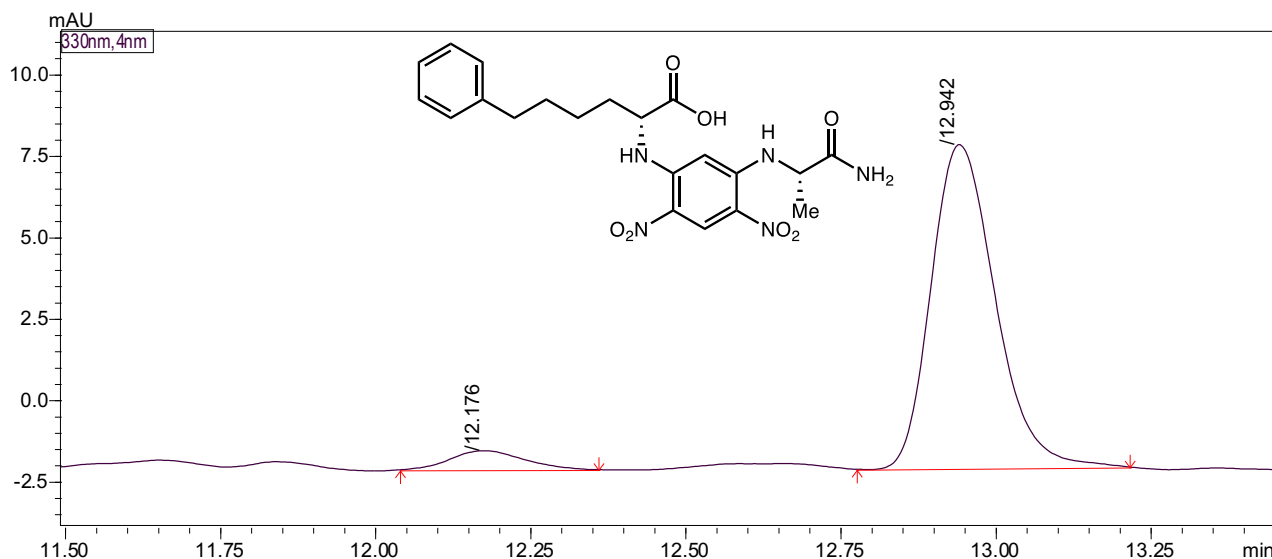
Marfey's analysis of L-**3n**



Peak Table | Compound | Group | Calibration Curve

Peak#	Name	Ret. Time	Height	Area	Area%
1		12.167	33807	251362	72.065
2		12.934	14435	97438	27.935
Total			48242	348800	100.000

Marfey's analysis of D-3n

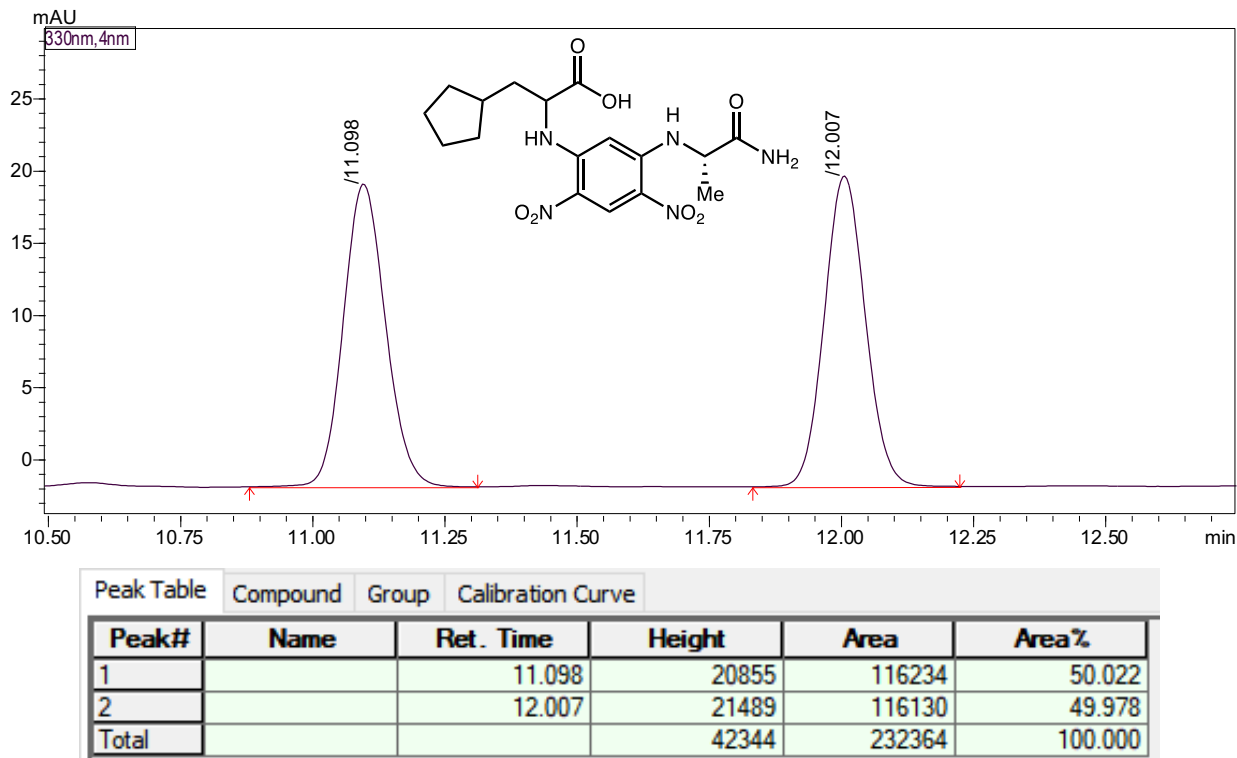


Peak Table | Compound | Group | Calibration Curve

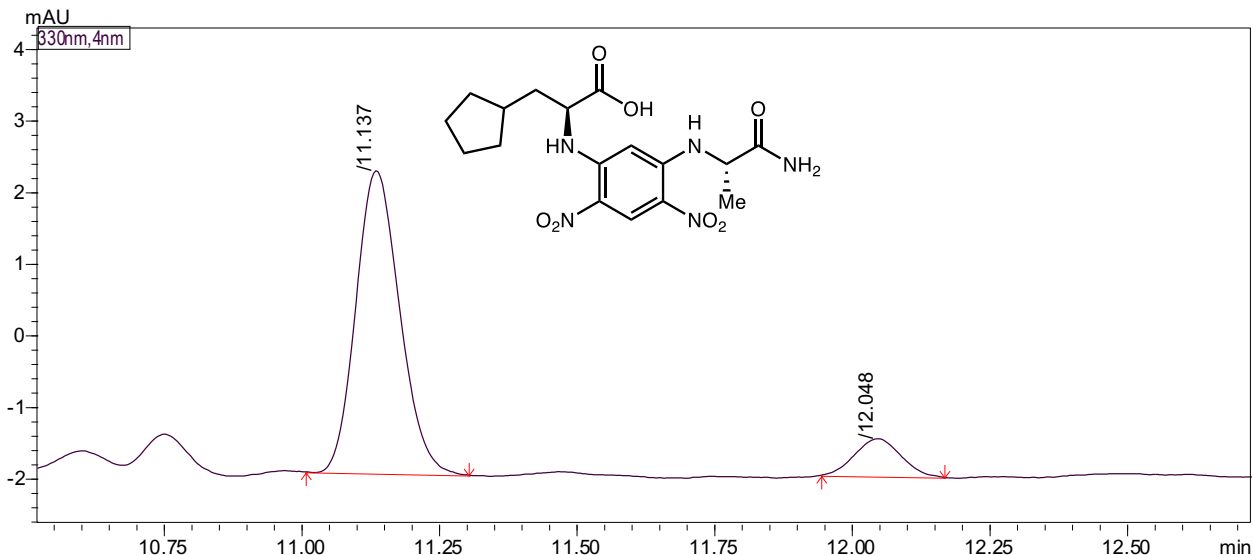
Peak#	Name	Ret. Time	Height	Area	Area%
1		12.176	583	4798	6.306
2		12.942	9934	71287	93.694
Total			10517	76085	100.000

2-amino-3-cyclopentylpropanoic acid (**3o**)

Marfey's analysis of (*rac*)-**3o**



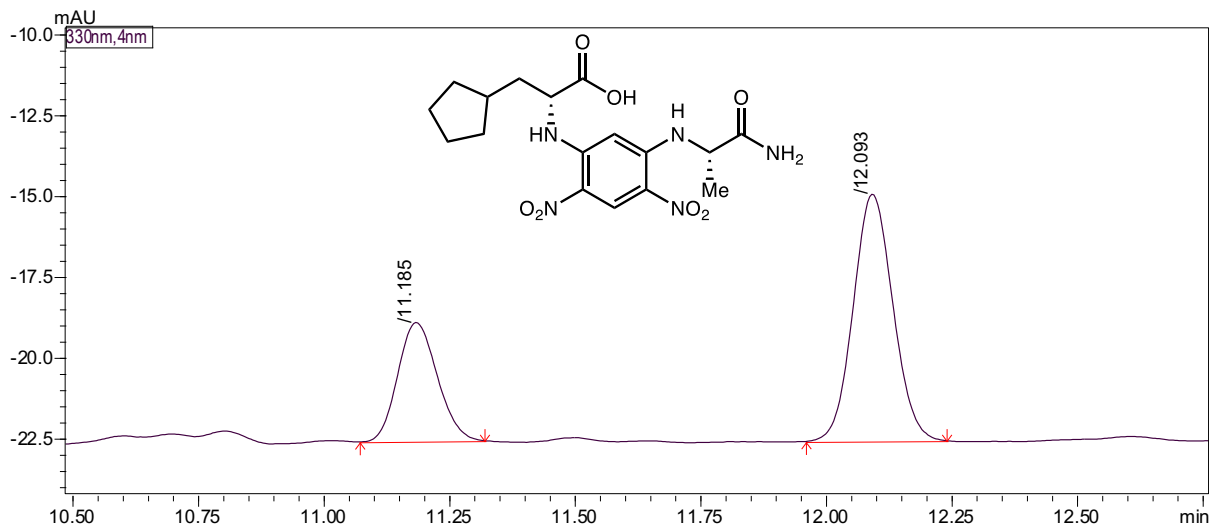
Marfey's analysis of L-**3o**



Peak Table Compound Group Calibration Curve

Peak#	Name	Ret. Time	Height	Area	Area%
1		11.137	4208	23303	88.460
2		12.048	523	3040	11.540
Total			4731	26344	100.000

Marfey's analysis of D-3o

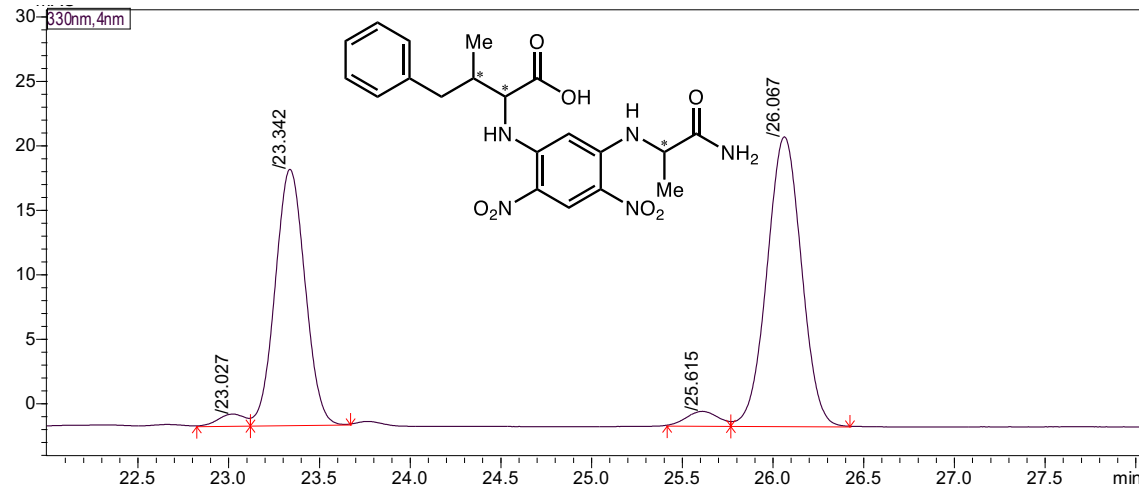


Peak Table Compound Group Calibration Curve

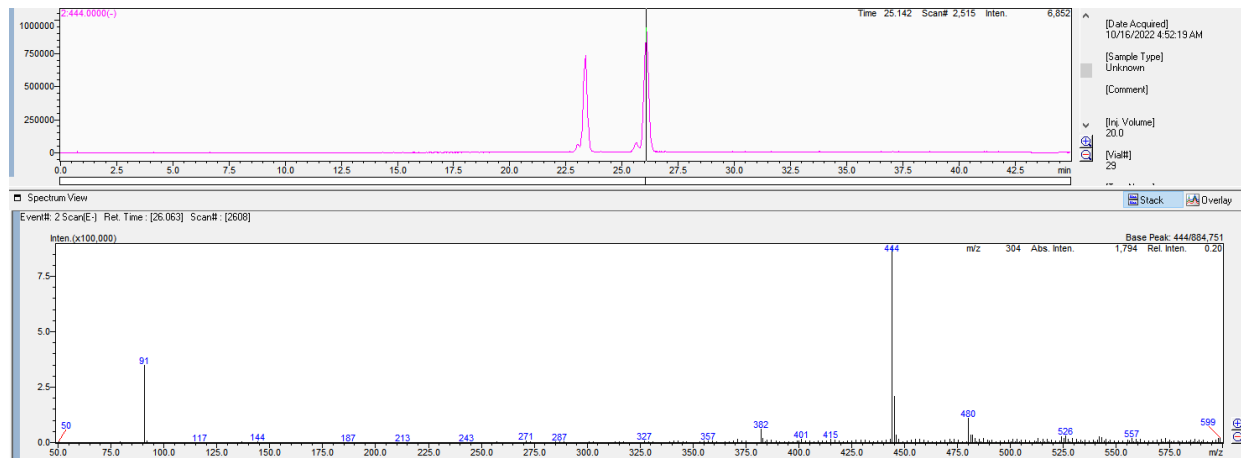
Peak#	Name	Ret. Time	Height	Area	Area%
1		11.185	3656	20017	32.320
2		12.093	7623	41916	67.680
Total			11279	61933	100.000

(2S, 3S)-2-amino-3-methyl-4-phenylbutanoic acid (4a)

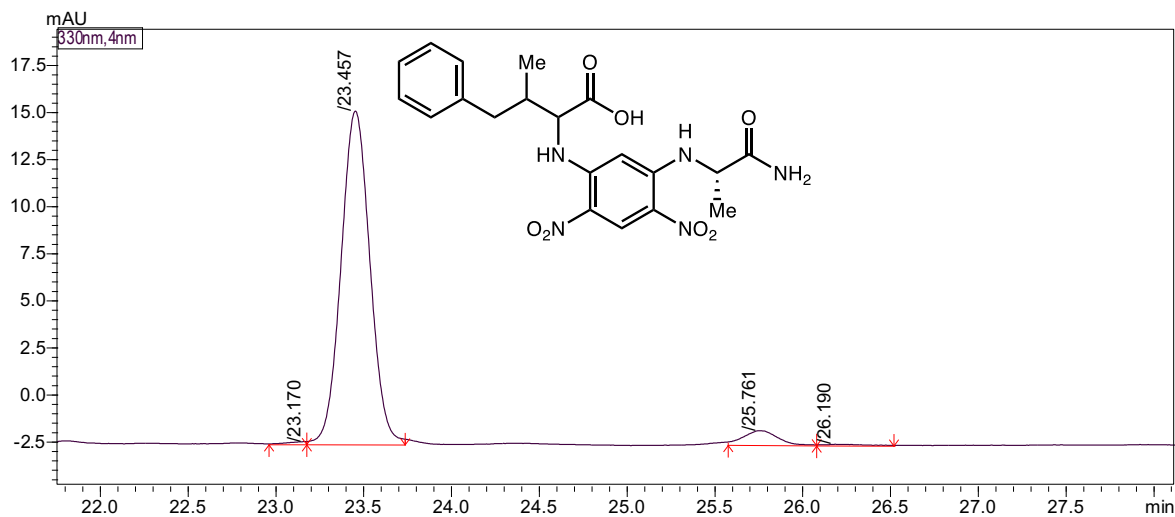
Marfey's analysis of **4a** with (*rac*)-Marfey's reagent



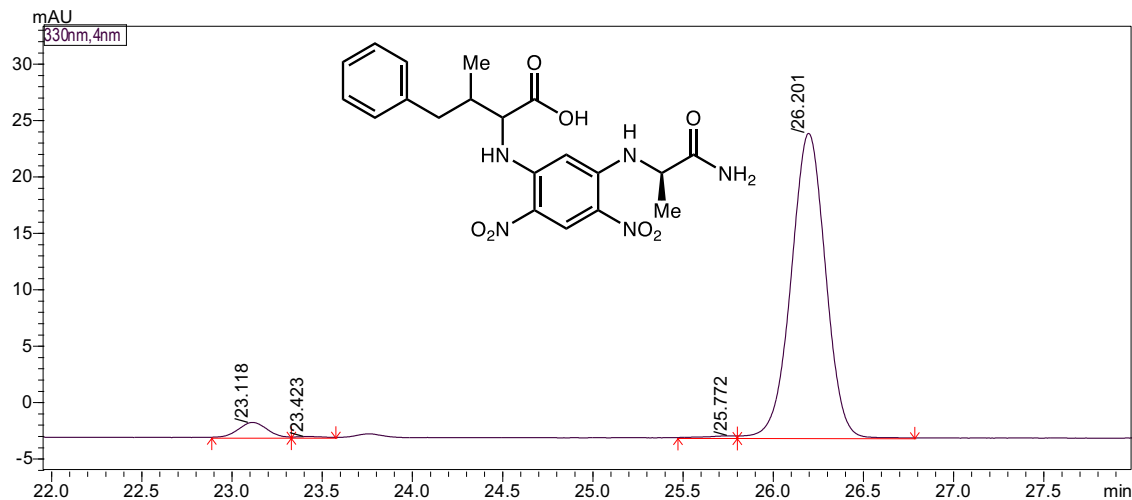
Peak#	Name	Ret. Time	Height	Area	Area%
1		23.027	884	8791	1.620
2		23.342	19813	225874	41.621
3		25.615	1095	13048	2.404
4		26.067	22399	294985	54.355
Total			44192	542698	100.000



Marfey's analysis of **4a** with (*S*)-Marfey's reagent

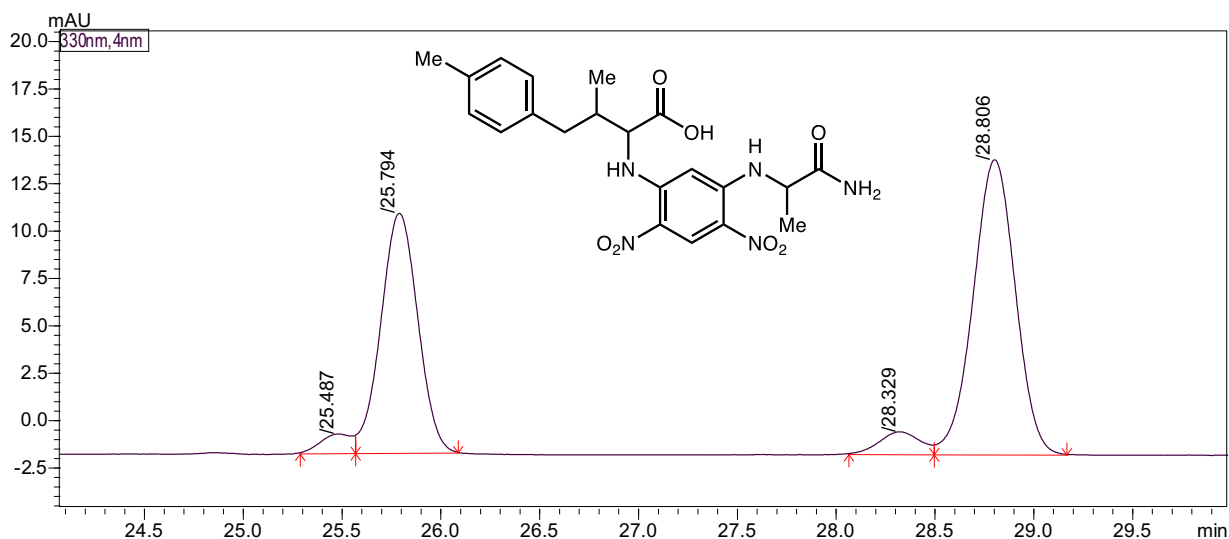


Marfey's analysis of 4a with (R)-Marfey's reagent



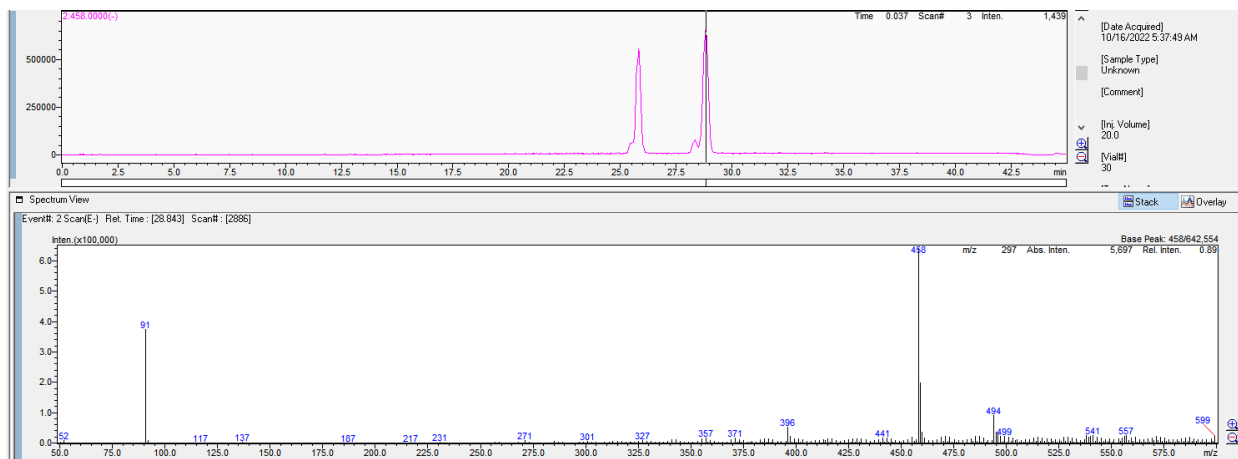
(2S, 3S)-2-amino-3-methyl-4-(p-tolyl)butanoic acid (4b)

Marfey's analysis of **4b** with (*rac*)-Marfey's reagent

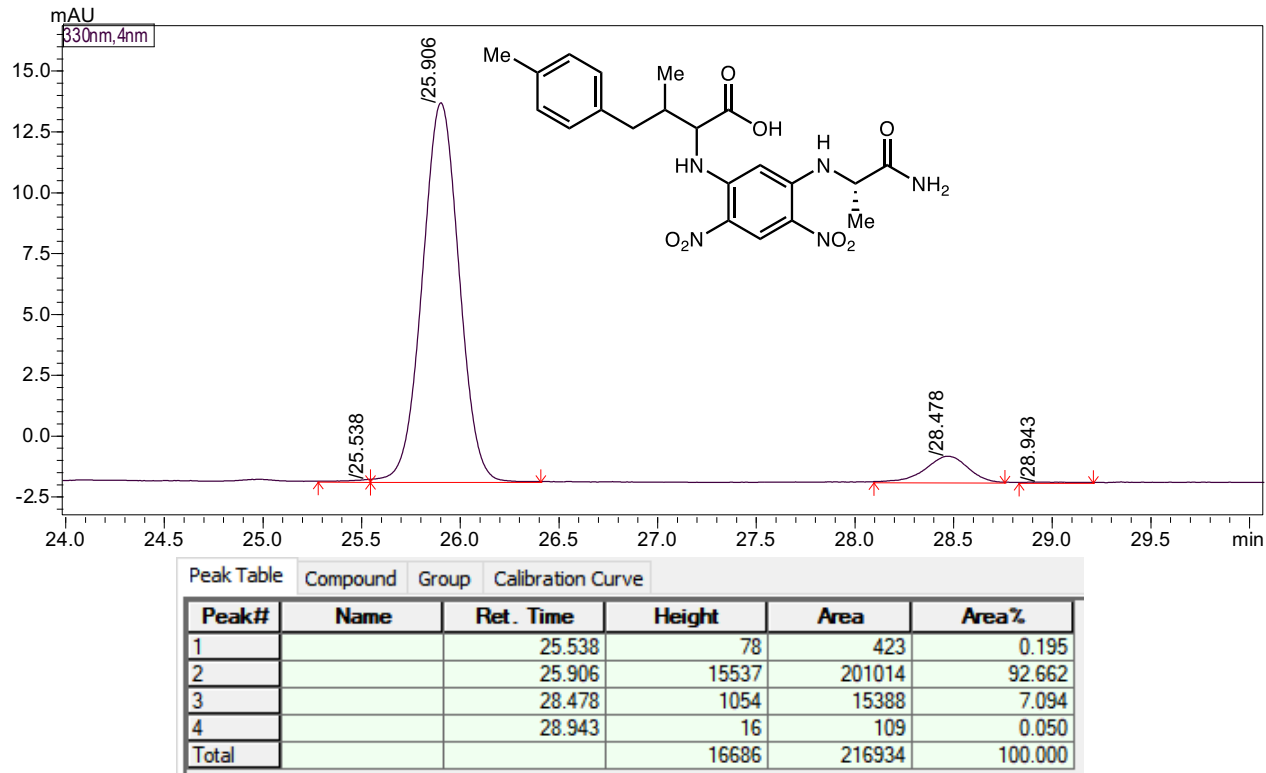


Peak Table

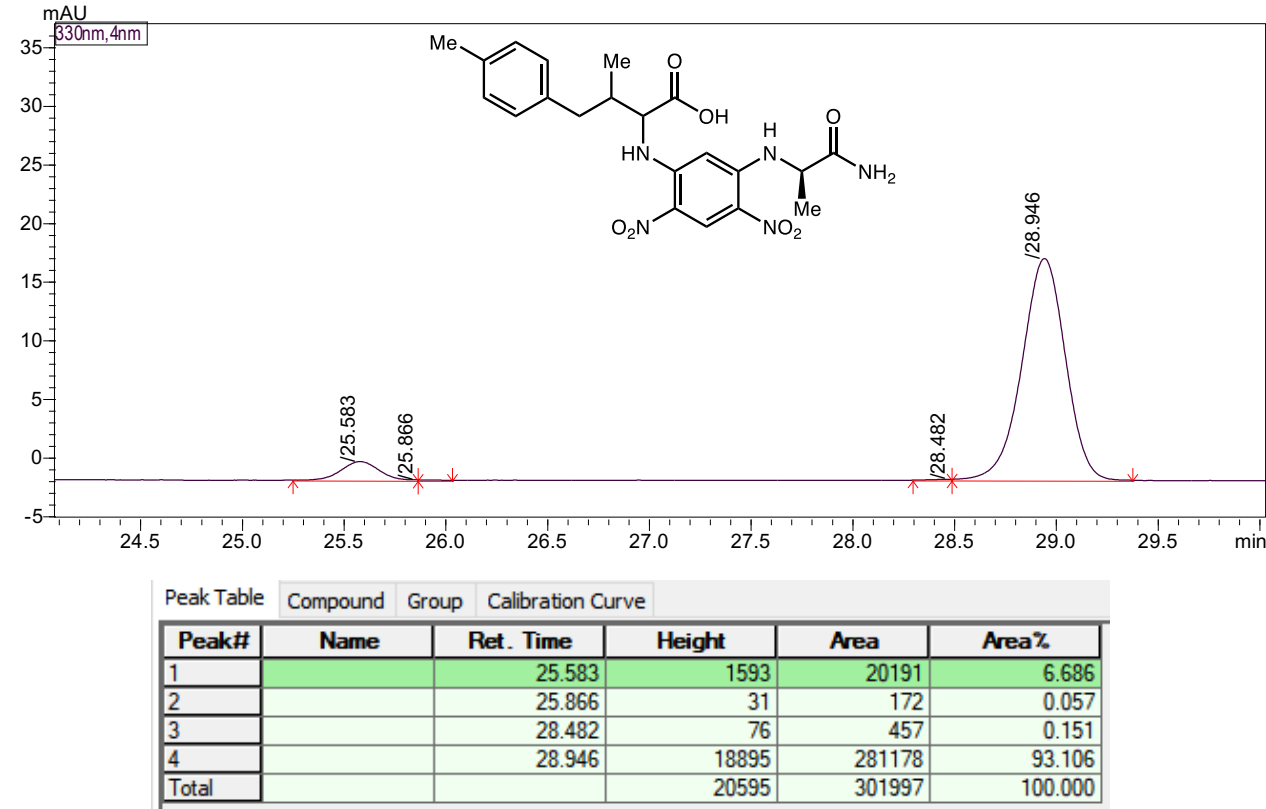
Peak#	Name	Ret. Time	Height	Area	Area%
1		25.487	989	10715	2.543
2		25.794	12599	164013	38.927
3		28.329	1158	16399	3.892
4		28.806	15528	230211	54.638
Total			30273	421337	100.000



Marfey's analysis of **4b** with (*S*)-Marfey's reagent

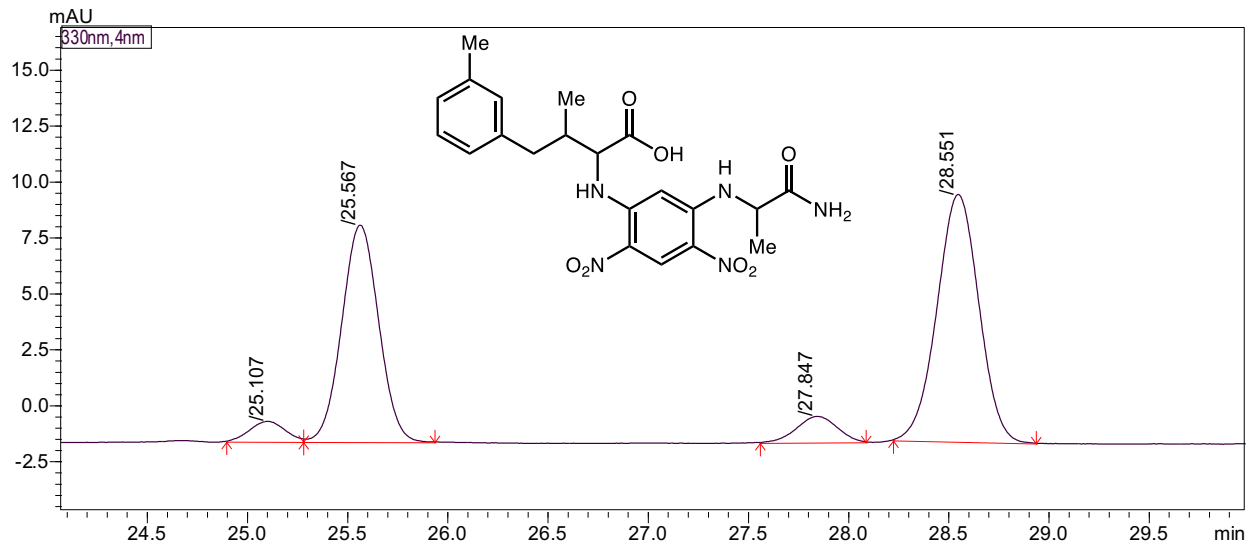


Marfey's analysis of **4b** with (*R*)-Marfey's reagent

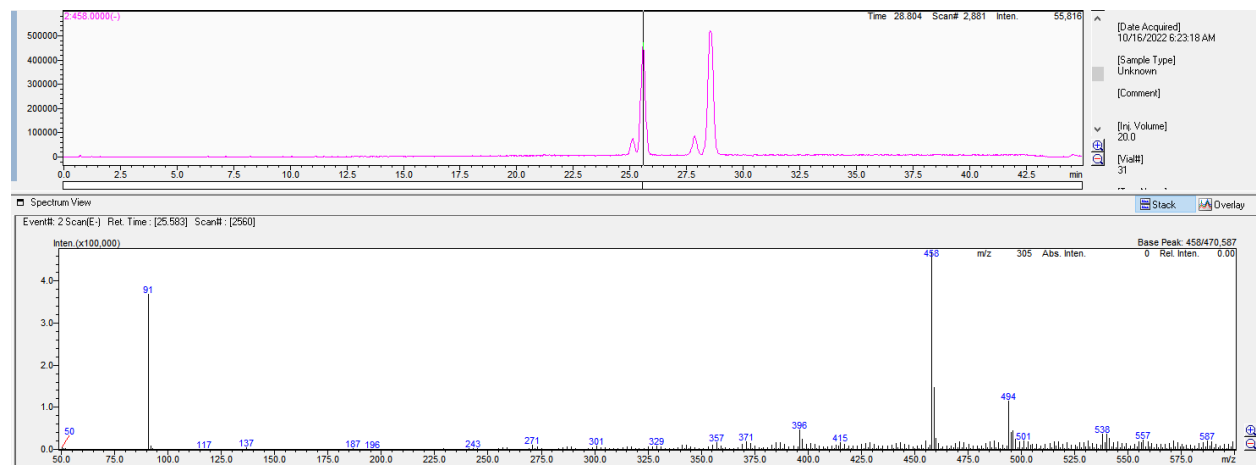


(2S, 3S)-2-amino-3-methyl-4-(m-tolyl)butanoic acid (4c)

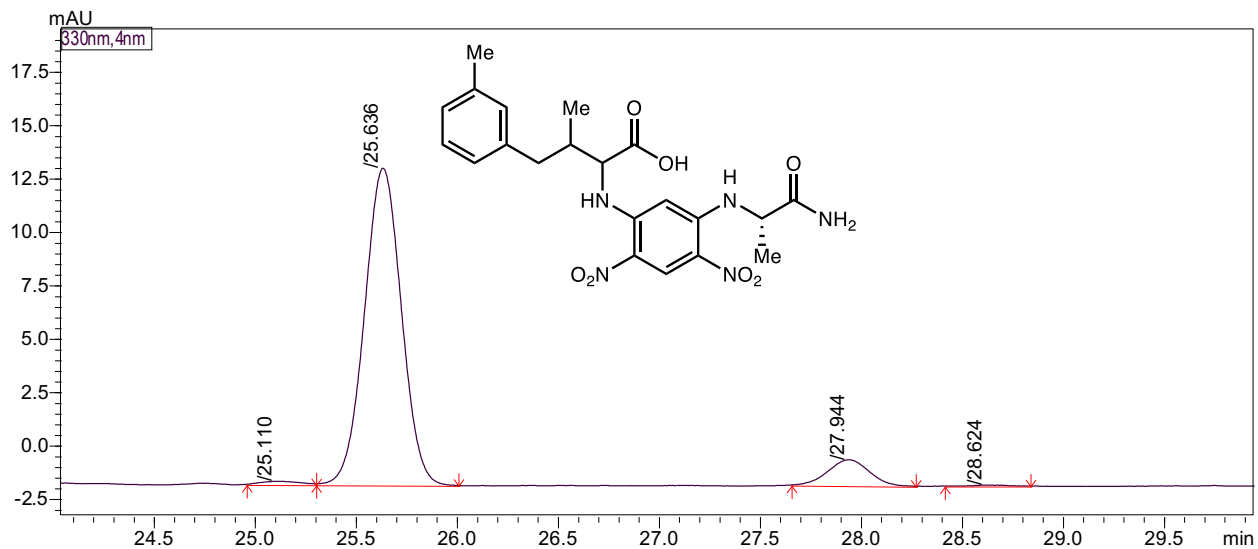
Marfey's analysis of **4c** with (*rac*)-Marfey's reagent



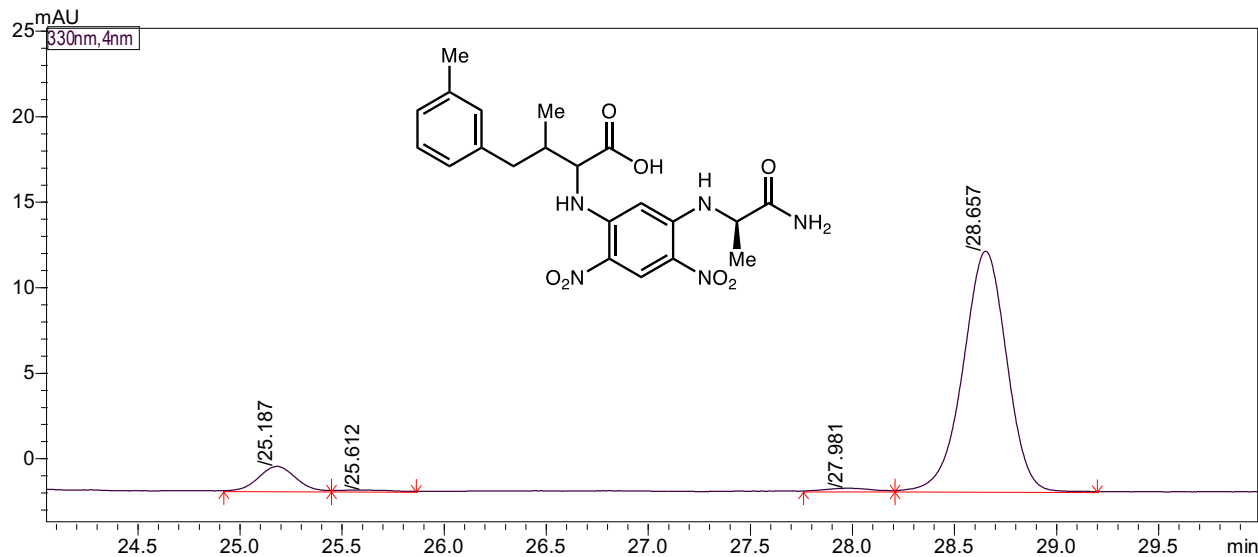
Peak#	Name	Ret. Time	Height	Area	Area%
1		25.107	901	10892	3.507
2		25.567	9678	123681	39.825
3		27.847	1145	15783	5.082
4		28.551	11037	160201	51.585
Total			22761	310558	100.000



Marfey's analysis of **4c** with (*S*)-Marfey's reagent

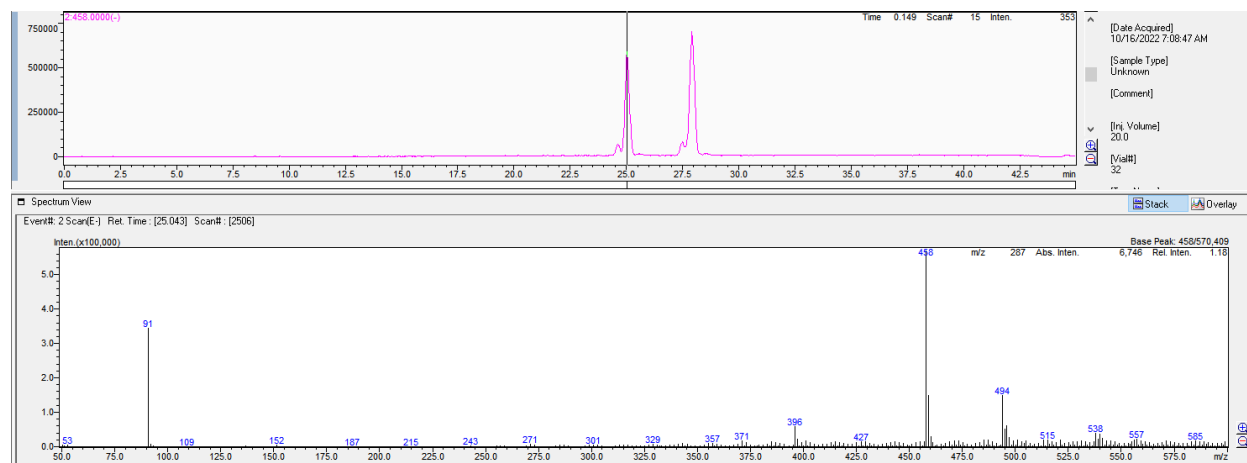
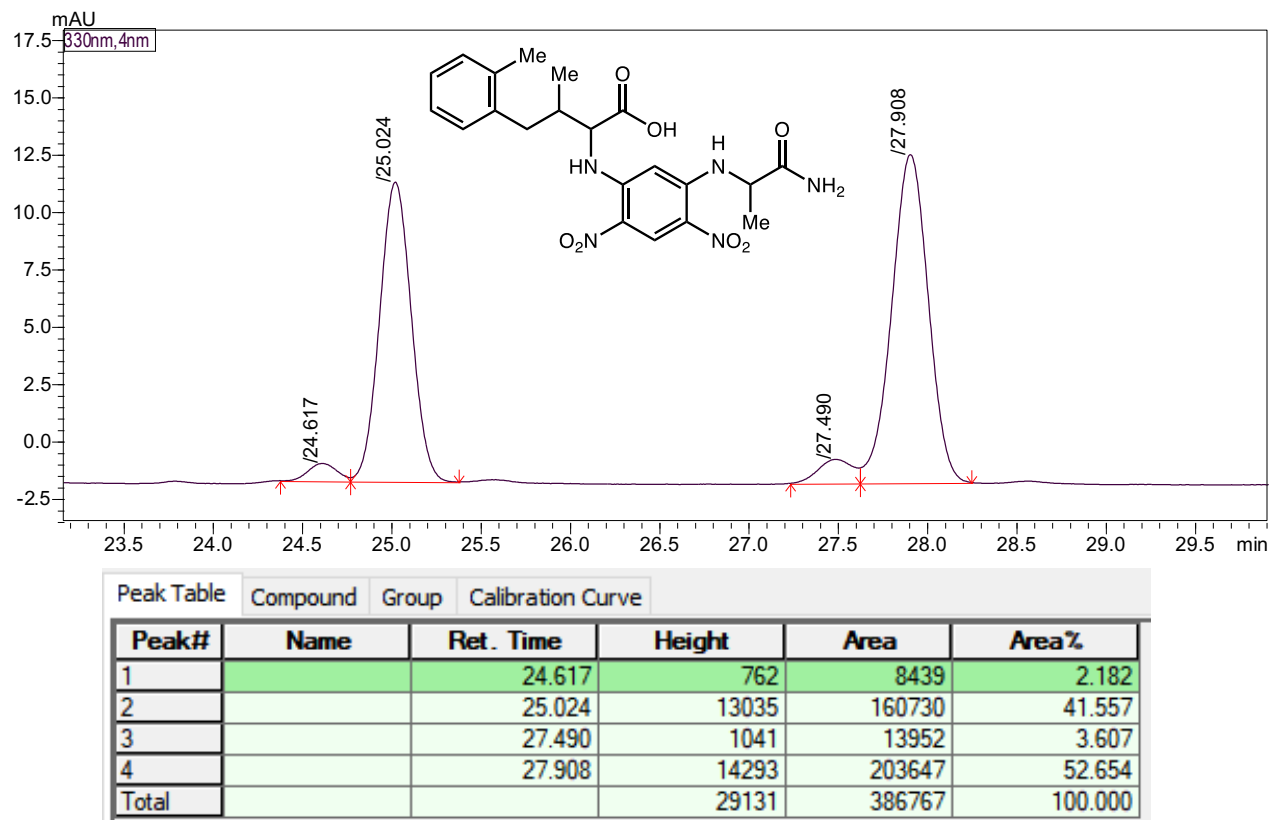


Marfey's analysis of **4c** with (*R*)-Marfey's reagent

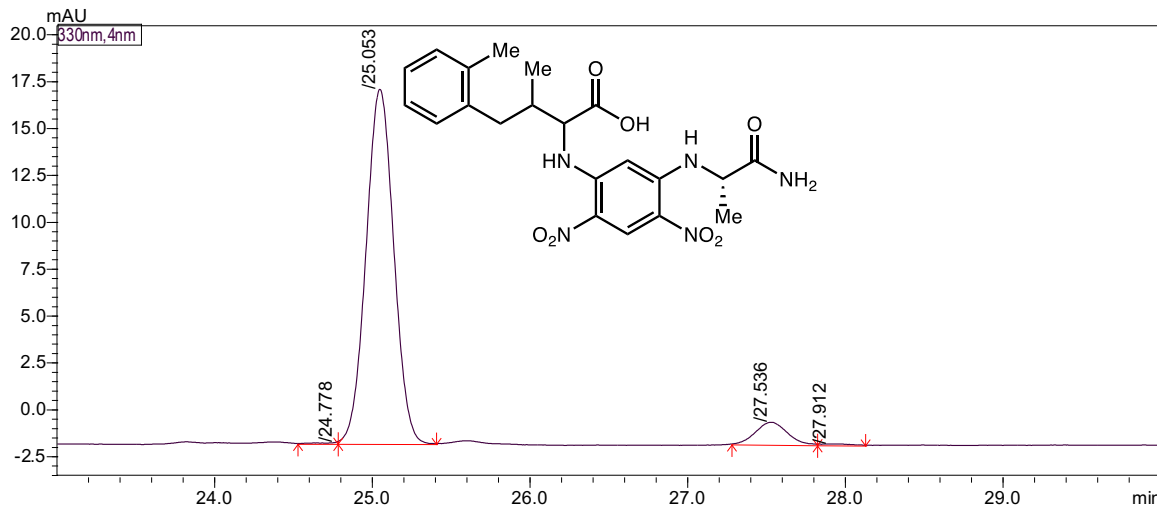


(2S, 3S)-2-amino-3-methyl-4-(o-tolyl)butanoic acid (4d)

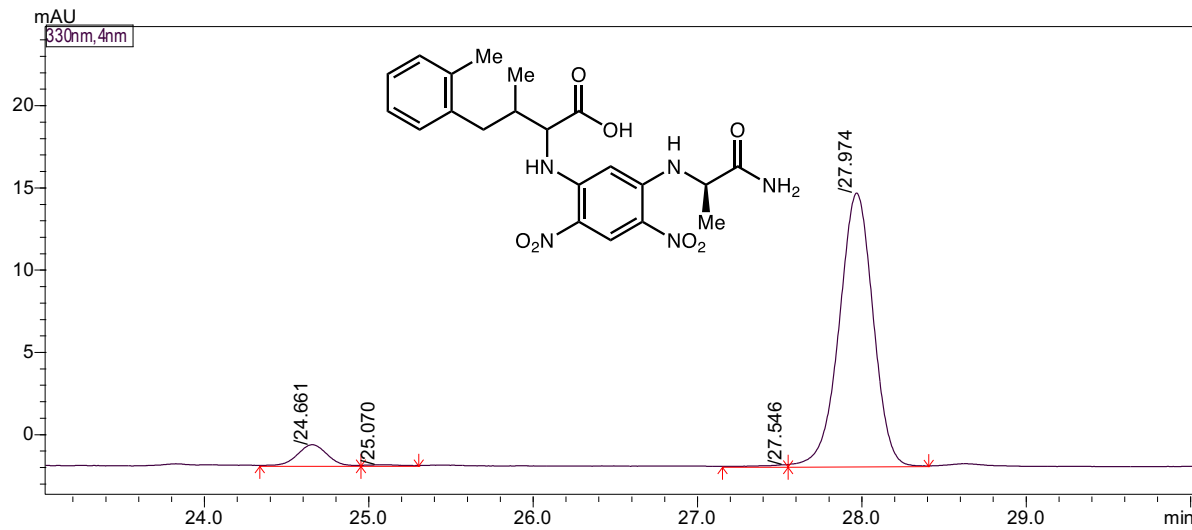
Marfey's analysis of **4d** with (*rac*)-Marfey's reagent



Marfey's analysis of **4d** with (*S*)-Marfey's reagent

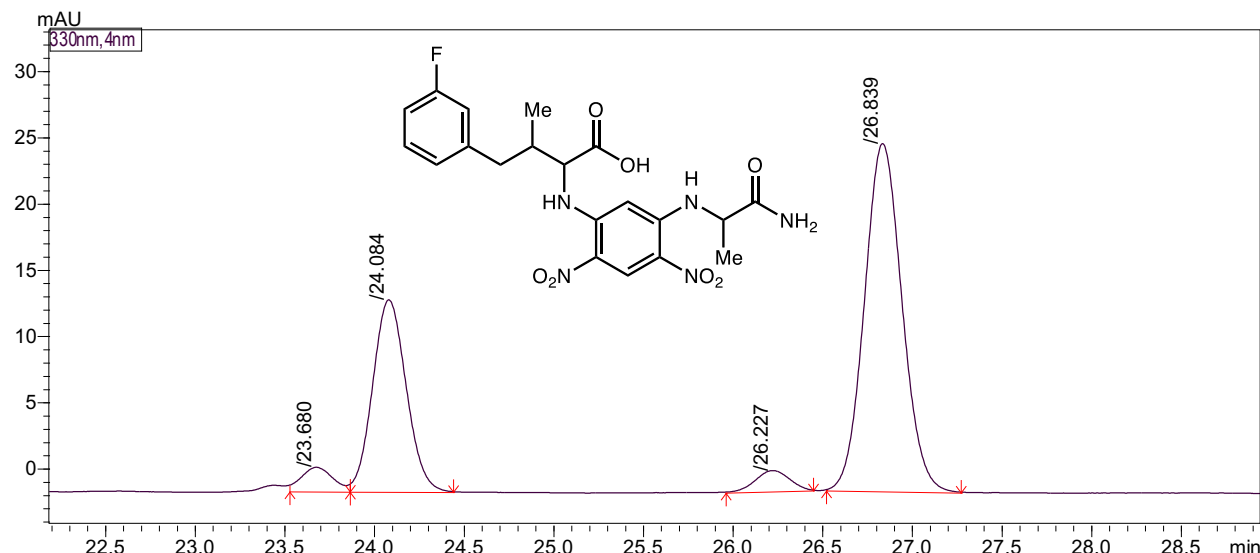


Marfey's analysis of **4d** with (*R*)-Marfey's reagent



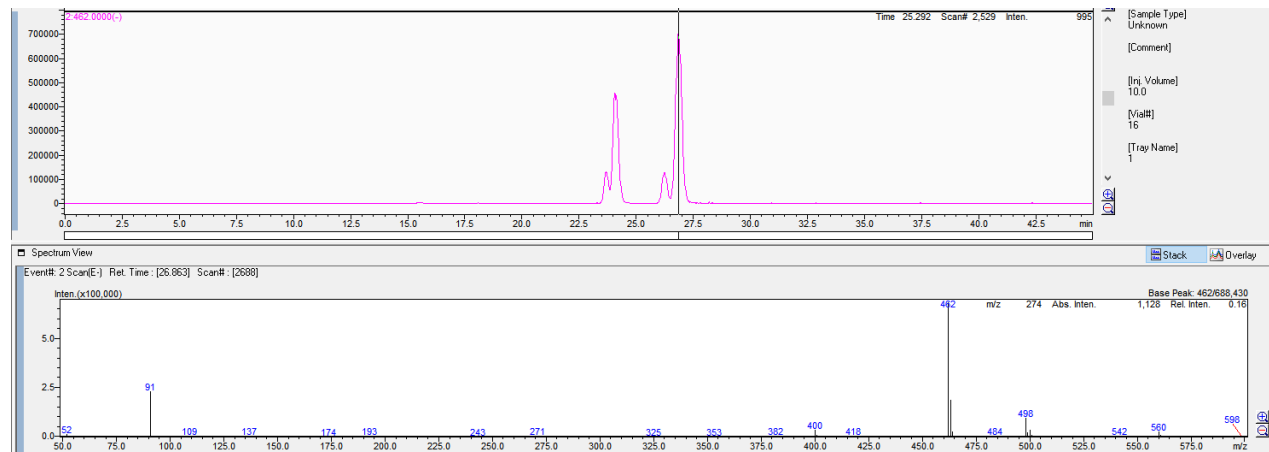
(2*S*, 3*S*)-2-amino-4-(3-fluorophenyl)-3-methylbutanoic acid (4e**)**

Marfey's analysis of **4e** with (*rac*)-Marfey's reagent

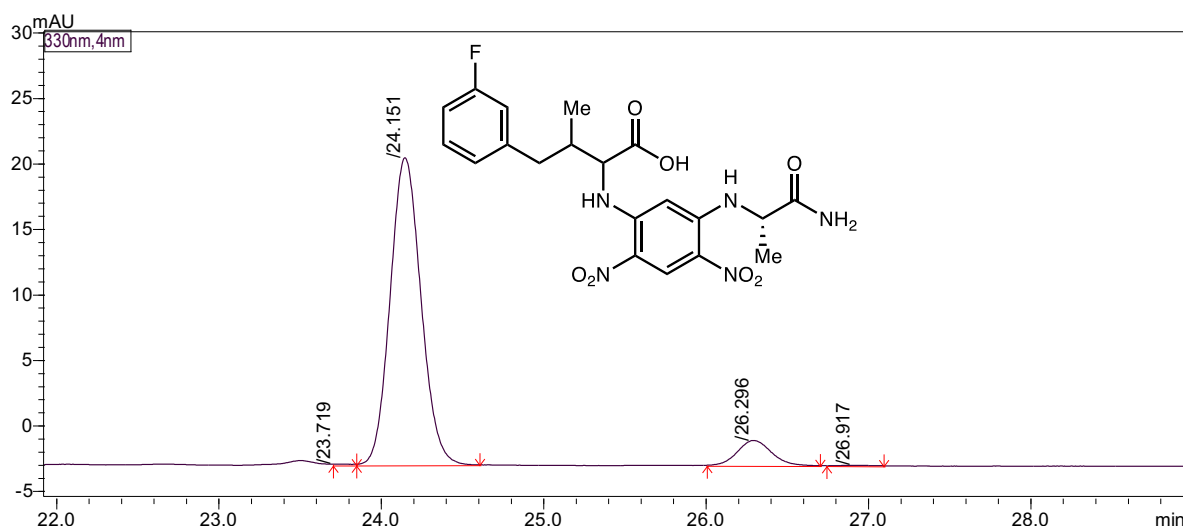


Peak Table

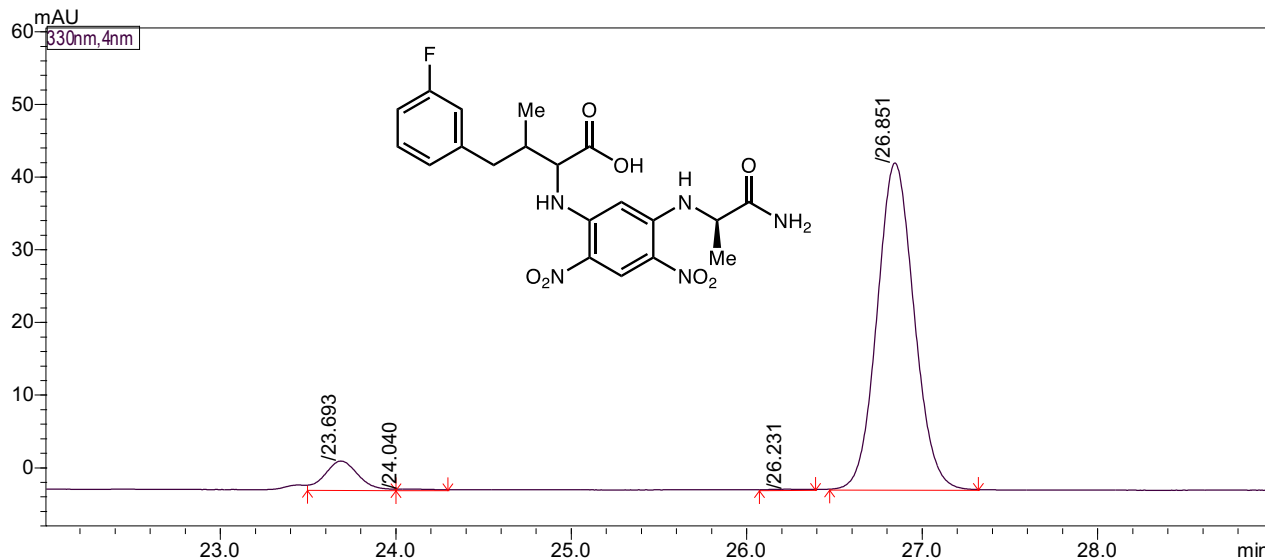
Peak#	Name	Ret. Time	Height	Area	Area%
1		23.680	1797	22008	3.608
2		24.084	14452	187493	30.738
3		26.227	1536	19848	3.254
4		26.839	26207	380625	62.400
Total			43993	609974	100.000



Marfey's analysis of **4e** with (*S*)-Marfey's reagent



Marfey's analysis of 4e with (R)-Marfey's reagent

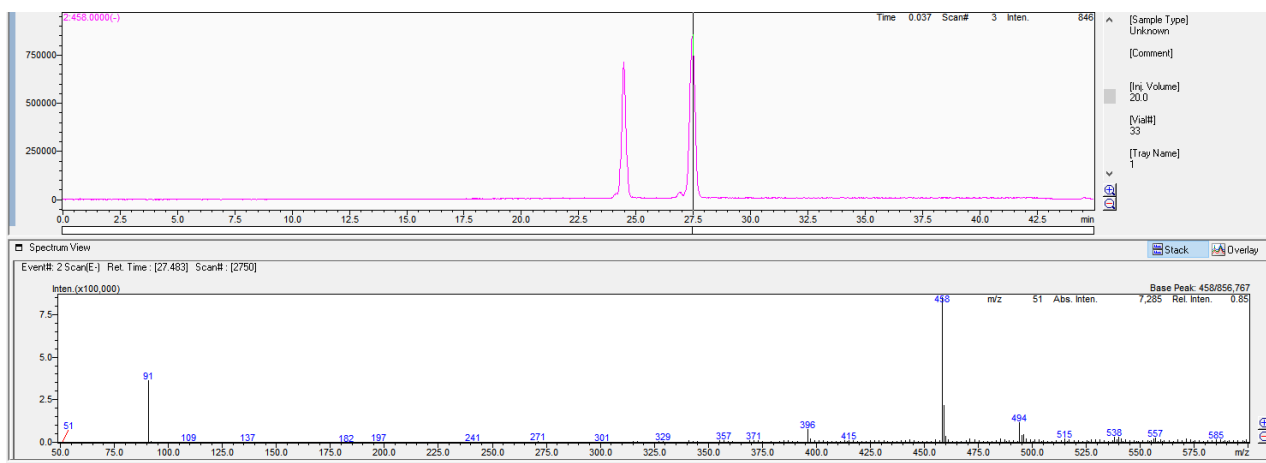
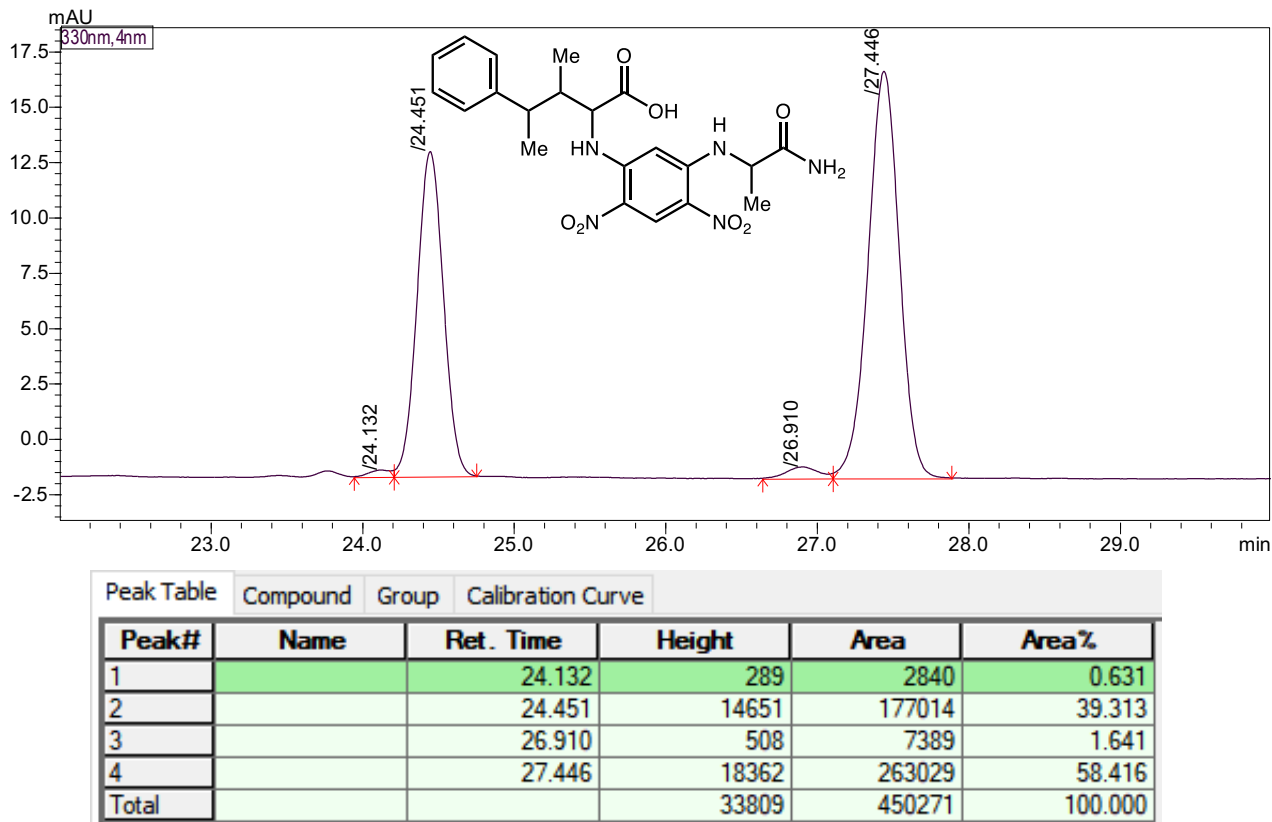


Peak Table:

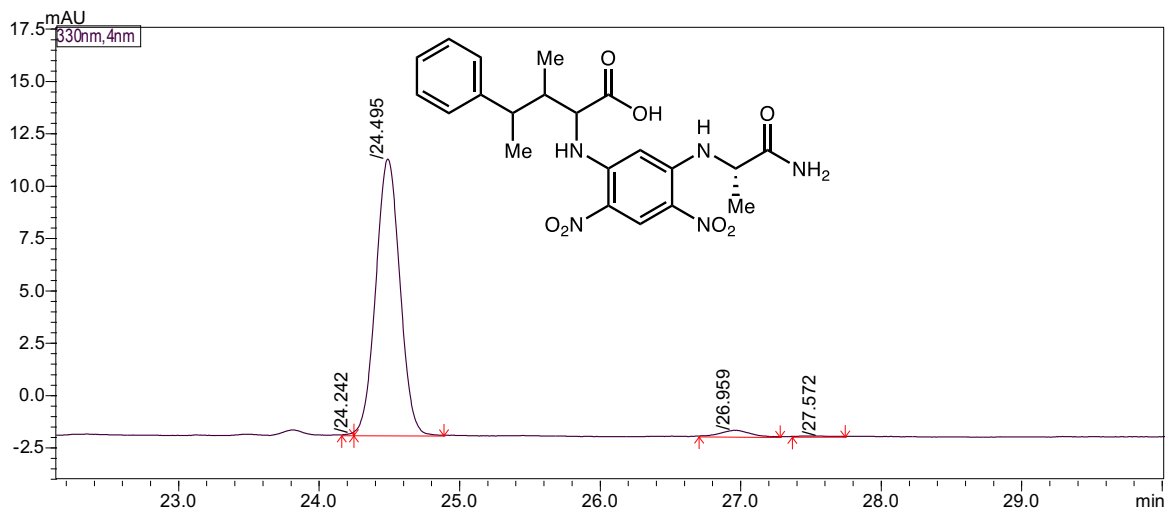
Peak#	Name	Ret. Time	Height	Area	Area%
1		23.693	3923	50617	7.149
2		24.040	75	846	0.120
3		26.231	66	677	0.096
4		26.851	44876	655859	92.636
Total			48940	707999	100.000

(2*S*, 3*S*, 4*S*)-2-amino-4-(3-fluorophenyl)-3-methylbutanoic acid (5a**)**

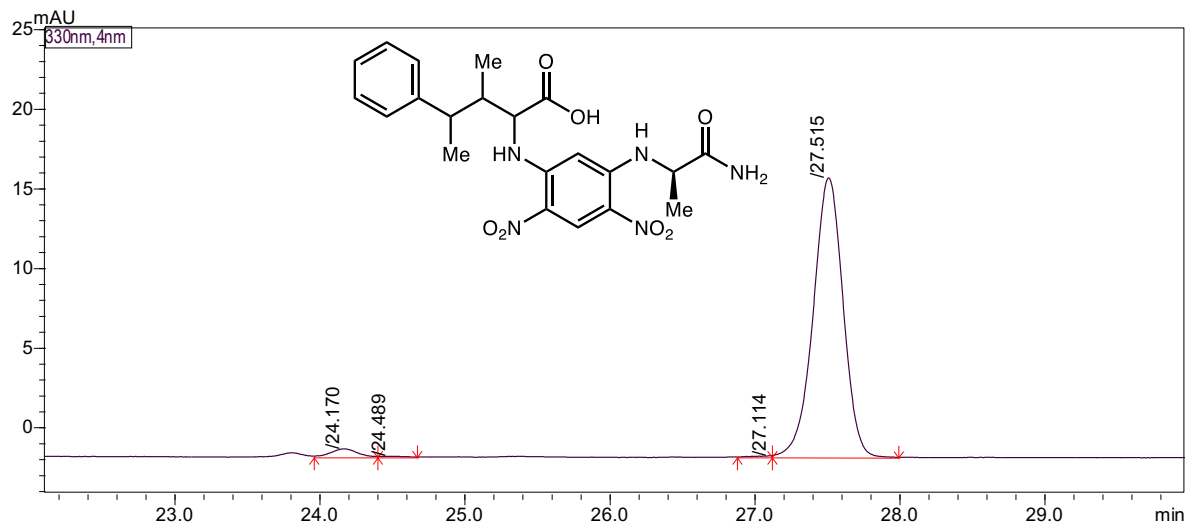
Marfey's analysis of **5a** with (*rac*)-Marfey's reagent



Marfey's analysis of **5a** with (*S*)-Marfey's reagent



Marfey's analysis of 5a with (R)-Marfey's reagent



XVI. Computational Studies and Marcus theory calculations

Computational details of theozyme model calculations

The "theozyme"(56, 81) model used to describe the enzyme active site in the density functional theory (DFT) calculations were obtained from the crystal structure of L-*Pf*PLP β that contains the PLP cofactor from the RCSB Protein Data Bank (PDB ID: 5VM5). The theozyme model includes the PLP cofactor and amino acid residues within 3 Å of the PLP cofactor, namely the side chains and C α atoms of K82, T105, S185, N231, D300, E345, and S371. Main chain atoms of these amino acid residues were replaced with C–H bonds (Fig. S15). In addition, because a glycine residue G298 is in proximity to the PLP cofactor, the entire G298 residue, and key atoms from the polypeptide backbone of the neighboring P297 and L299 residues (*i.e.*, the C α atom and the carbonyl group of P297; the C α atom and the amino group of L299) were also included in this theozyme model. The side chains of P297 and L299 were not included, as they are more than 3 Å away from the cofactor. The protonation state of polar functional groups in the theozyme model is determined based on the protonation states of the catalytically active form of the enzyme. An aspartate residue D300 in proximity to the β -hydroxyl group of the external aldimine **IX** likely serves as the proton source to promote the dehydration (59). Therefore, the protonated carboxylic acid of D300 is studied in the external aldimine **7**. The conversion of internal aldimine **VII** to external aldimine **IX** generates a neutral amino group on the lysine residue (K82). In conventional PLP enzymology, this unprotonated amino group serves as the general base to deprotonate the external aldimine **IX**, leading to quinonoid **X** (see Fig. 2 and TS1 in Fig. 5(A) from the manuscript). Thus, the uncharged amino group of K82 in the external aldimine (**7**) was used in our calculations. Protonation states of other residues were assigned according to their most likely protonation states under the experimental pH (pH = 6–8). These assignments were further confirmed by the protonation state of the entire enzyme assigned using the H++ server (82).

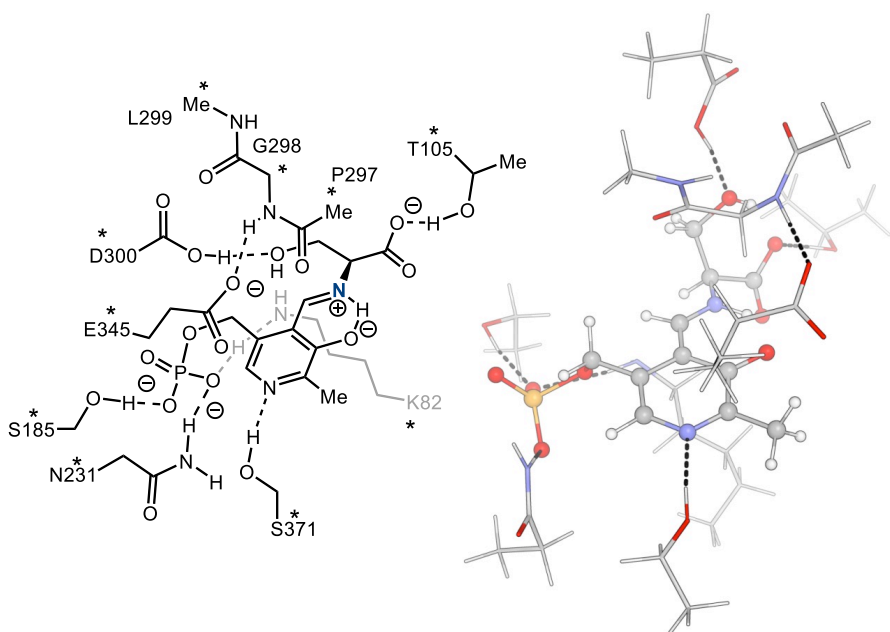


Fig. S15. Theozyme model for DFT calculations. Asterisks indicate carbon atoms on the backbone that were fixed during geometry optimizations.

The DFT calculations were performed using the Gaussian 16 software (83) on Pitt CRC and XSEDE/ACCESS (84) supercomputers. Geometries of intermediates and transition states were optimized using the dispersion-corrected (85) B3LYP-D3 functional (86, 87) with the 6-31G(d) basis set. C^a atoms of all residues included in the theozyme were fixed during geometry optimization to maintain the locations of amino acid residues as in the protein crystal structure (PDB ID: 5VM5). In addition, the hydrogen atoms attached to C^a of all residues except P297, G298, and L299 were fixed to ensure that the side chain orientations resemble those in the protein crystal structure. Vibrational frequency calculations were performed at the same level of theory as their respective geometry optimizations to confirm that the obtained transition states connect their respective minima. Single-point energy calculations were carried out using the ωB97X-D functional (88) with the 6-311+G(2d,2p) basis set for other atoms. Solvation energy corrections were calculated in the single-point energy calculations using the SMD solvation model (89). Chlorobenzene solvent ($\epsilon = 5.60$) was used to mimic the actual dielectric constant within enzyme active site (90, 91). Due to the applied constraints during the geometry optimization of the theozyme (*vide supra*), the computed Gibbs free energies may have reduced accuracy originating

from issues in vibrational entropy calculations, particularly contributions from low vibrational frequency modes. On the other hand, the geometrical constraints are expected to have minimal effects on the computed electronic energies and enthalpies (92). In light of these considerations, only the computed enthalpy values (ΔH) are reported in the manuscript. Indeed, previous computational studies using theozymes typically reported either electronic energies or enthalpies rather than free energies (59, 93).

Conversion between internal aldimine **14** and external aldimine **7**

The conversion of internal aldimine **14** to external aldimine **7** starts with the nucleophilic addition of the amino group of amino acid **2a** to the internal aldimine **14** to form an aminal intermediate **15** (Fig. S16). The barrier of this nucleophilic addition step (TS-5) is found to be 16.1 kcal/mol. From **15**, a proton transfer step takes place to give a more stable aminal **16**. This proton transfer may be further facilitated by H₂O (94). Aminal **16** then collapses to give external aldimine **7** and a free lysine K82. This step (TS-6) shows a low activation barrier of 1.7 kcal/mol relative to **16**.

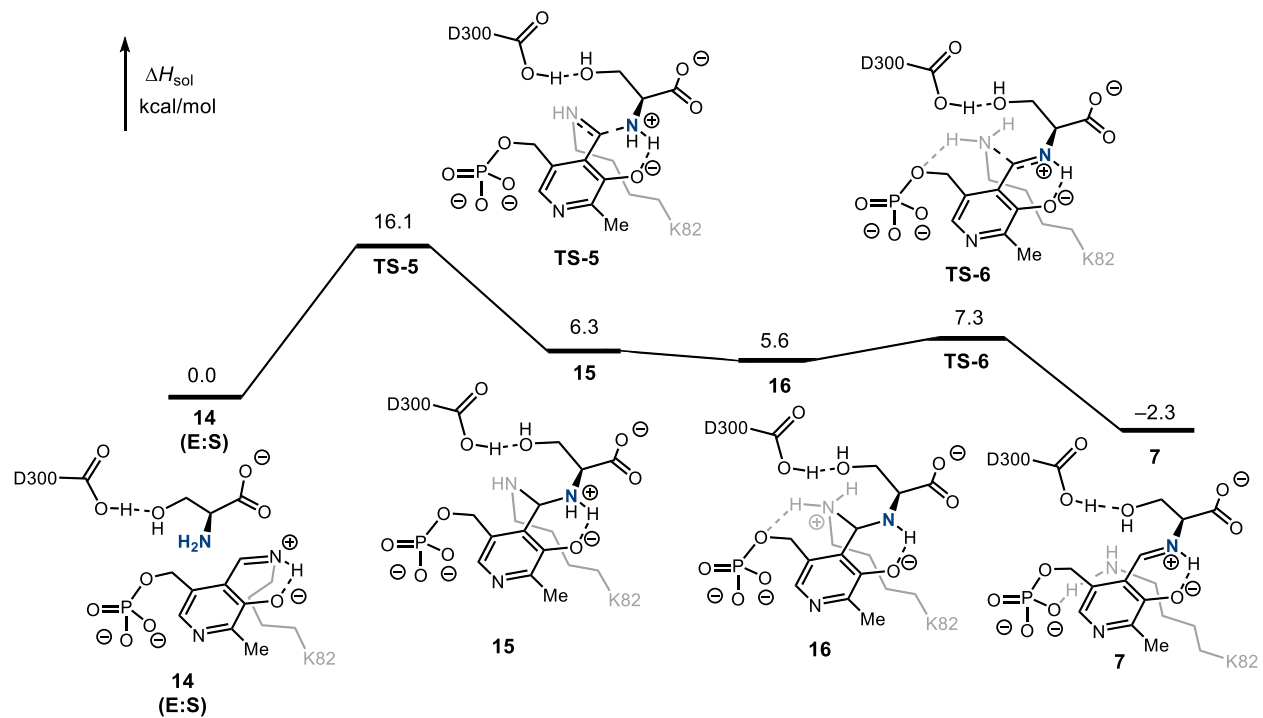


Fig. S16. Computed energy profile for the conversion between internal aldimine 14 and external aldimine 7. Enthalpy values (in kcal/mol) are relative to 14. Some active site residues are omitted for clarity. See **Fig. S15** for all active site residues included in the theozyme calculations.

Azaallyl radical intermediate 11

Mulliken spin density of the azaallyl radical intermediate 11 is computed using the theozyme model and shown in **Fig. S17**. The unpaired electron is largely located at the C^a atom, which has a spin density of 0.57. The C2 atom (pyridoxal aldehyde carbon) has a spin density of 0.26. In contrast, the spin density of each atom in the pyridine ring is small, from 0.01 to 0.06, with the total spin density of the pyridine ring of 0.15. Together, these calculations revealed a substantial radical character on C^a of the azaallyl radical intermediate.

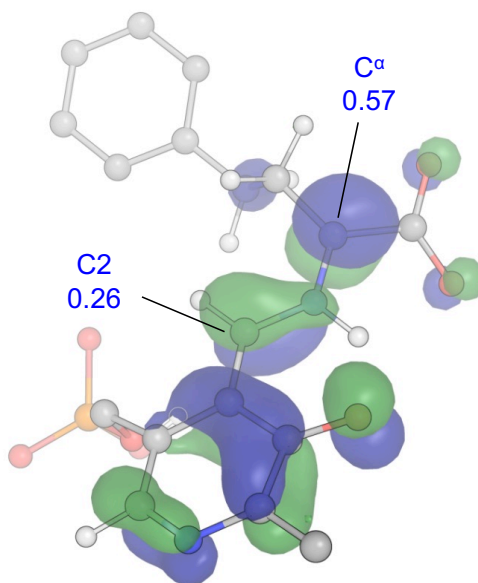


Fig. S17. Singly occupied molecular orbital (SOMO) of azaallyl radical intermediate 11 obtained from theozyme model. Active site residues are omitted for clarity. The Mulliken spin densities are shown in blue.

Radical addition transition states computed in the absence of enzyme active site

To have better understanding on the impact of active site residues on the regioselectivity of the radical addition step, we performed DFT calculations for the radical addition transition state using a free PLP cofactor model in the absence of active site residues (**Fig. S18**). In these DFT calculations, geometry optimizations were performed without any constraints. The calculations were performed at the same level of theory as that in the theozyme model. The computed barriers of the radical addition step to the **C1** atom (*via* **TS-3A**) and the **C2** atom (*via* **TS-3A'**) of the aminoacrylate intermediate are nearly identical ($\Delta H^\ddagger = 8.3$ and 8.1 kcal/mol, respectively, with respect to the van der Waals complex between the aminoacrylate intermediate and the benzyl radical, **10A**). The lack of regioselectivity is due to a combination of electronic effects favoring the more electron-deficient **C2** possessing a larger LUMO coefficient and steric effects favoring the more exposed β -position (**C1**).

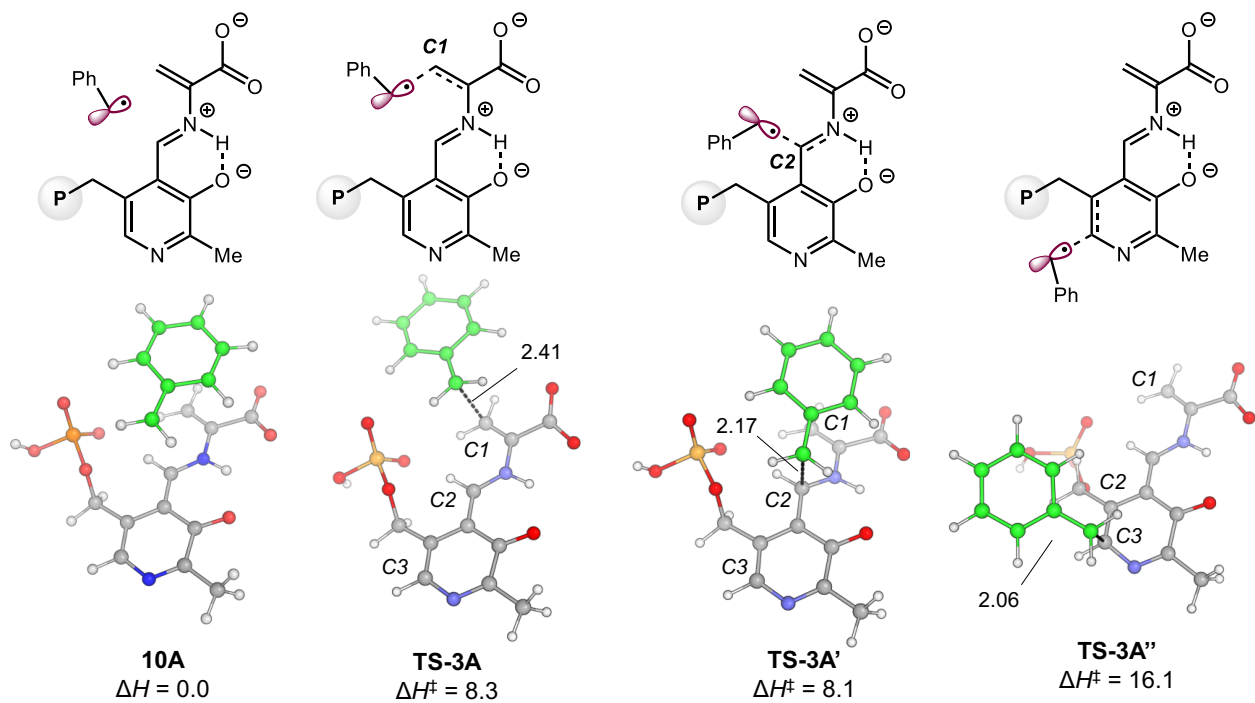
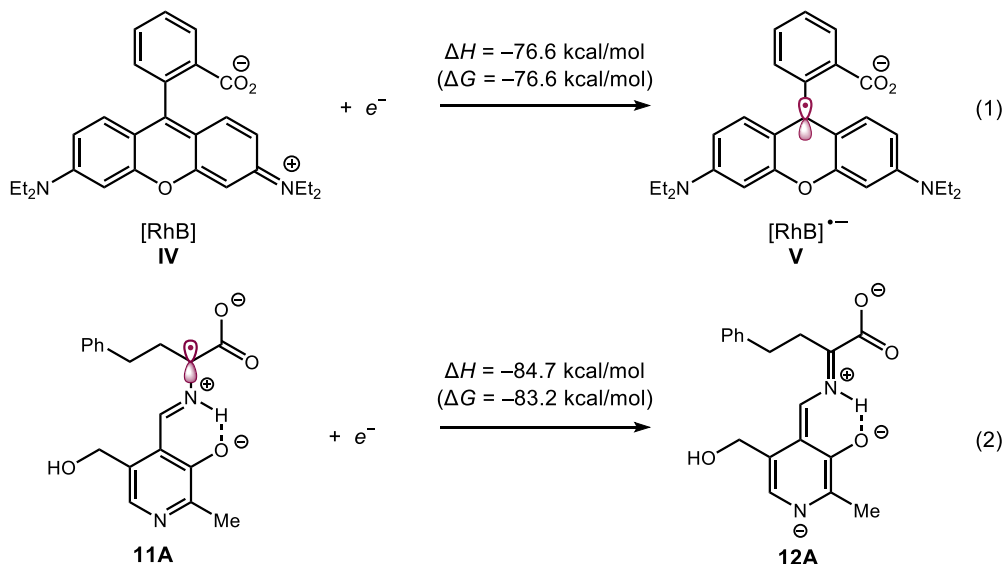


Fig. S18. Optimized structures of radical addition transition states in the absence of active site residues. Enthalpies (in kcal/mol) are relative to the aminoacrylate complex **10A**.

Gibbs free energies of the electron transfer from $[\text{RhB}]^{\cdot-}$ to the azaallyl radical

The radical anion of the photocatalyst rhodamine B, $[\text{RhB}]^{\cdot-}$, often serves as a single electron reductant (42). The reaction Gibbs free energy of the electron transfer between $[\text{RhB}]^{\cdot-}$ and azaallyl radical **11** was calculated based on the computed redox potentials of $E_{1/2}^{\circ}([\text{RhB}]/[\text{RhB}]^{\cdot-})$ and $E_{1/2}^{\circ}(\mathbf{11A}/\mathbf{12A})$ in aqueous solution. In the redox potential calculations, simplified cofactor models **11A** and **12A** were used. The zwitterionic form of RhB was found to be more stable than the spirolactone form in aqueous solution (95, 96). The zwitterionic form of RhB and the corresponding acyclic form of $[\text{RhB}]^{\cdot-}$ were used in the reaction energy calculations. Gibbs free energies and enthalpies of half-reactions (1) and (2) were computed using DFT at the $\omega\text{B97X-D}/6-311+\text{G}(2\text{d},2\text{p})/\text{SMD}(\text{H}_2\text{O})//\text{B3LYP-D3}/6-31\text{G}(\text{d})/\text{SMD}(\text{H}_2\text{O})$ level of theory. The Gibbs free energy of electron is -0.867 kcal/mol (97, 98).



From the half-reaction Gibbs free energies (ΔG), reduction potentials $E_{1/2}^\circ$ can be calculated as (99):

$$E_{1/2}^\circ = -\frac{\Delta G}{n_e F} - E_{1/2}^{\circ, \text{SHE}} + E_{1/2}^{\circ, \text{SCE}}$$

where n_e is the number of electron being transferred (one), F is the Faraday constant, $E_{1/2}^{\circ, \text{SHE}}$ is the absolute potential of the standard hydrogen electrode (SHE, 4.281 V), and $E_{1/2}^{\circ, \text{SCE}}$ is the potential of the saturated calomel electrode (SCE) relative to SHE in aqueous solution (-0.241 V).

Therefore,

$$E_{1/2}^\circ([\text{RhB}/[\text{RhB}]^{\bullet-}]) = -1.20 \text{ V vs SCE}$$

$$E_{1/2}^\circ(\mathbf{11A}/\mathbf{12A}) = -0.91 \text{ V vs SCE}$$

The computed reduction potential $E_{1/2}^\circ([\text{RhB}/[\text{RhB}]^{\bullet-}]) = -1.20 \text{ V vs SCE}$ is in agreement with the experimental standard reduction potential $E^\circ(\text{RhB}/\text{RhB}^\bullet)$ in aqueous solution (-0.87 V vs SHE, which corresponds to -1.11 V vs SCE) (100).

From the computed reaction energies of half-reactions (1) and (2), the Gibbs free energy and enthalpy of the following ET reaction were derived (**Fig. S19**).

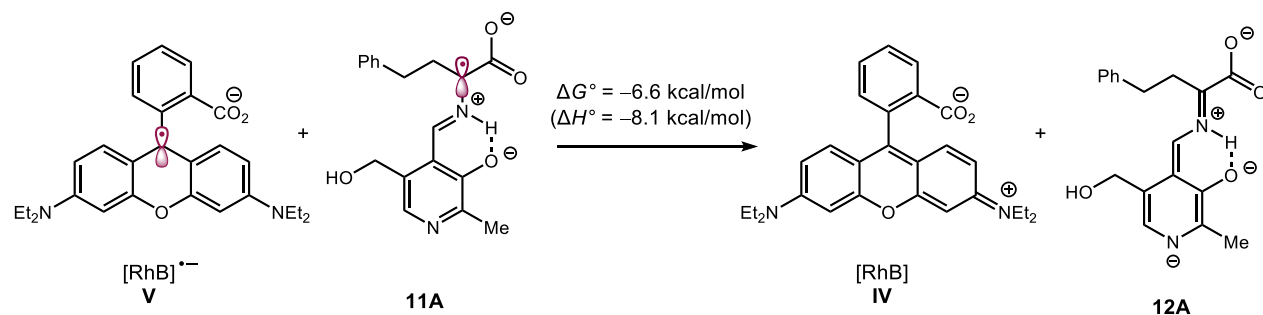


Fig. S19. Computed reaction Gibbs free energy of ET from $[\text{RhB}]^{\bullet-}$ **V** to azaallyl radical **11A**. Gibbs free energy and enthalpy were computed using simplified cofactor model at the $\omega\text{B97X-D}/6-311+\text{G}(2\text{d},2\text{p})/\text{SMD}(\text{H}_2\text{O})/\text{B3LYP-D3}/6-31\text{G}(\text{d})/\text{SMD}(\text{H}_2\text{O})$ level of theory.

Based on the DFT-computed redox potentials in aqueous solution, the ET from $[\text{RhB}]^{\bullet-}$ to **11A** is exergonic by 6.6 kcal/mol. When the experimental reduction potential of RhB (-1.11 V vs SCE) is used instead of the DFT-computed Gibbs free energy, the driving force for the ET reaction is lowered to $\Delta G^\circ = -0.20 \text{ eV}$ (-4.5 kcal/mol). Using the computed reaction enthalpy of this ET step ($\Delta H = -8.1 \text{ kcal/mol}$) and the reaction enthalpy of the proceeding PT step from **12** to **13** computed ($\Delta H = -4.8 \text{ kcal/mol}$, computed using the theozyme model, see **Fig. 5(A)** from the manuscript), the overall reaction of the ET/PT or PCET step is exothermic by 12.9 kcal/mol. It should be noted that the reaction energy of the ET step is affected by the polarity of the environment as well as hydrogen bonding and electrostatic interactions. Because the PLP cofactor in the active site is in a less polar environment, the electron affinity of **11** may be smaller than the value computed in aqueous solution. Nonetheless, considering the exothermicity of the PT step (**12** to **13**, $\Delta H = -4.8 \text{ kcal/mol}$), the overall ET/PT process is expected to be thermodynamically favorable.

Estimation of Electron Transfer Rate using Marcus Theory

Rate constants of long-range electron transfer (ET) processes in protein can be calculated using the Marcus theory (**Eq. S1**) (101-103).

$$k_{\text{ET}} = \frac{1}{\hbar} |H_{\text{AB}}|^2 \sqrt{\frac{\pi}{\lambda k_{\text{B}} T}} \exp \left[-\frac{(\Delta G^{\circ} + \lambda)^2}{4\lambda k_{\text{B}} T} \right] \quad (\text{Eq. S1})$$

where ΔG° is the reaction Gibbs free energy of the ET progress, λ is the reorganization energy, and H_{AB} is the electronic coupling between the reactant and product diabatic states. Here, we use **Eq. S1** to estimate the rate constants of ET from $[\text{RhB}]^{\cdot-}$ to the azaallyl radical (**Fig. S19**).

Based on our DFT calculations using the simplified cofactor model (**Fig. S19**), the Gibbs free energy of ET (ΔG°) is -0.29 eV ($= -6.6$ kcal/mol). Because the reorganization energy (λ) for this ET process is unknown, an estimated λ of 1.0 eV (104, 105) was used in our calculation, considering λ for ET in proteins is usually in the range of 0.5 – 1.5 eV (102, 106-109). The electronic coupling matrix element (H_{AB}) decays exponentially with the distance (R) between the electron donor (D) and the acceptor (A) (**Eq. S2**).

$$|H_{\text{AB}}| = |H_{\text{AB}}^0| \exp \left[-\frac{\beta}{2} (R - R^0) \right] \quad (\text{Eq. S2})$$

where R^0 is the distance between D and A in close contact and H_{AB}^0 is the maximum electronic coupling when the donor and acceptor are in close contact. An exponential decay factor β of 1.4 Å⁻¹ (101) is used in our calculations. The maximum electronic coupling (H_{AB}^0) is calculated using the fragment-charge difference (FCD) method (110) implemented in Q-Chem 5.3 (111). First, the most stable conformer of the van der Waals complex between $[\text{RhB}]^{\cdot-}$ and the azaallyl radical **11A** at open-shell singlet spin state was located at the ωB97X-D/6-311+G(2d,2p)/SMD(H₂O)//B3LYP-D3/6-31G(d) level of theory. The D–A distance in close contact ($R^0 = 4.37$ Å, see **Fig. S20**) was calculated from the distance between the C10' atom of the xanthene moiety of $[\text{RhB}]^{\cdot-}$, which has the largest SOMO coefficient and spin density, and the C^a atom of the azaallyl radical in the van der Waals complex. Next, the maximum electronic coupling (H_{AB}^0) was calculated using the FCD algorithm using the TD-B3LYP-D3/6-31+G(d,p)/SMD(H₂O) level of theory at singlet spin state

with 30 CI-singles excited state roots. The computed maximum electronic coupling H_{AB}^0 is 6.32×10^{-2} eV ($= 509.5$ cm $^{-1}$). This value corresponds to an electronic coupling prefactor term $\left(\frac{1}{\hbar} |H_{AB}^0|^2 \sqrt{\frac{\pi}{\lambda k_B T}}\right)$ of 4.4×10^{11} s $^{-1}$, which indicates the maximum ET rate constant when $\Delta G^0 = -\lambda$ and D/A are in close contact. This result is consistent with previously reported maximum ET rate constants of 10^{12-13} s $^{-1}$ at close contact distances (101, 106, 112, 113).

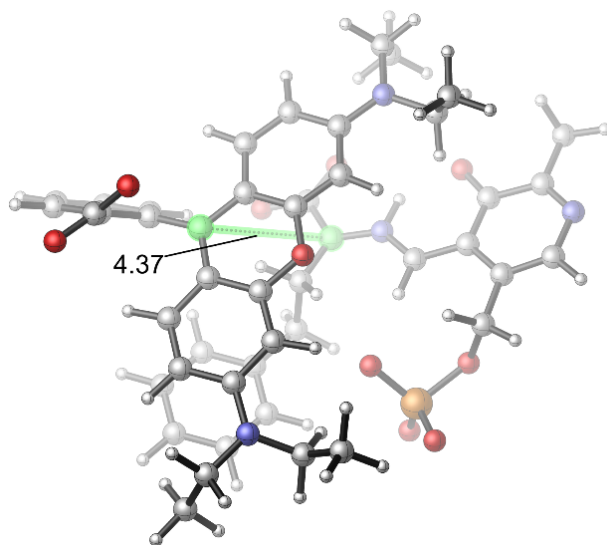


Fig. S20. Optimized geometry of the van der Waals complex of $[\text{RhB}]^{\bullet-}$ and azaallyl radical used in FCD electronic coupling calculations. The distance between the C10' atom of the xanthene moiety of $[\text{RhB}]^{\bullet-}$ and the C $^{\alpha}$ atom of the azaallyl radical is 4.37 Å.

The distance dependence of the ET rate constant (k_{ET}) is shown in **Fig. S21**. These calculations indicate that the long-range ET is relatively fast ($k_{\text{ET}} > 10^2$ s $^{-1}$) when the D–A distance (R) is smaller than 16.8 Å.

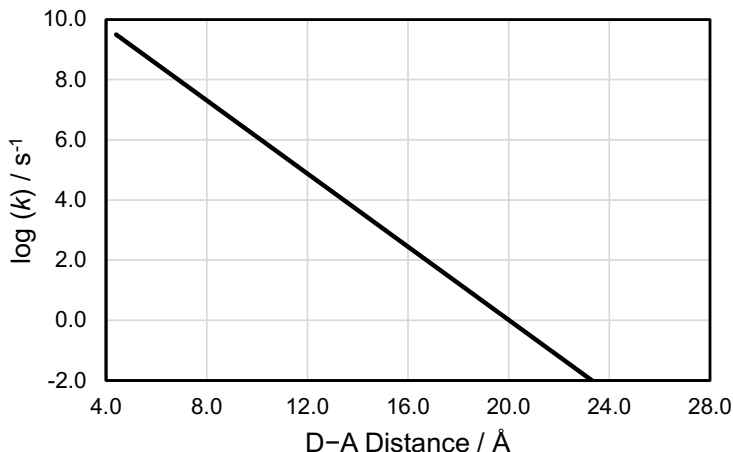


Fig. S21. Distance dependence of the ET rate constant using DFT-calculated reaction Gibbs free energy. $\Delta G^0 = -0.29$ eV, $H_{\text{AB}}^0 = 6.32 \times 10^{-2}$ eV, $\lambda = 1.0$ eV, $\beta = 1.4 \text{ \AA}^{-1}$, and $R^0 = 4.37 \text{ \AA}$ were used in the calculations.

When the experimental reduction potential of RhB is used instead of the DFT-computed Gibbs free energy, the driving force for the reaction is lowered to $\Delta G^0 = -0.20$ eV (*vide supra*). The distance dependence of the ET rate constant is shown in **Fig. S22**. These calculations indicate that the long-range ET is possible ($k_{\text{ET}} > 10^2 \text{ s}^{-1}$) when R (donor-acceptor distance) is smaller than 15.9 Å.

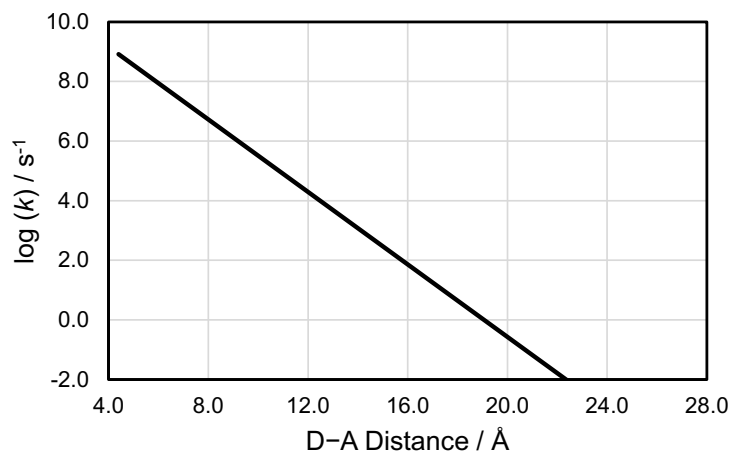


Fig. S22. Distance dependence of the ET rate constant calculated using experimental reduction potential of RhB, which indicates a driving force of $\Delta G^0 = -0.20$ eV.

To investigate the distance between the RhB radical anion $[\text{RhB}]^{\cdot-}$ and the azaallyl radical in the enzyme active site, we performed enhanced sampling simulations using ligand Gaussian accelerated molecular dynamics (LiGaMD) (114) implemented in Amber 20 (115). The starting structure of L-*Pf*PLP $^{\beta}$ was obtained from RCSB Protein Data Bank (PDB ID: 5VM5). The PLP cofactor was modified to the azaallyl radical. The initial geometry of the azaallyl radical and RhB radical anion were optimized using the B3LYP functional (87, 116) and 6-31G(d) basis set in *Gaussian 16* (83). Force field parameters for azaallyl radical and RhB radical anion were generated using the general Amber force field (gaff) (117). Using the Merz-Singh-Kollman scheme (118, 119), RESP charge fitting (120) on electrostatic potential generated at the B3LYP/6-31G(d) level of theory was performed to generate partial charges for azaallyl radical and RhB radical anion. Protonation states of enzyme residues were determined using the H++ server (82). The initial position of the RhB radical anion was identified using blind docking algorithm with CB-Dock2 server (121). The complex was then put into the solvated cuboid box with the periodic boundary condition using the TIP3P water model (122). The minimum distance between the enzyme surface and the edge of water box was set to 10 Å. Water molecules were treated with the SHAKE algorithm (123). The system was neutralized by adding counterions (Na^+ and Cl^-). Long-range electrostatic was calculated using the particle-mesh-Ewald method (124). Lennard-Jones and electrostatic interaction cut-offs were set to 12 Å.

We first performed energy minimization with positional restraints for protein by applying a force constant of $500 \text{ kcal}\cdot\text{mol}^{-1}\cdot\text{\AA}^{-2}$ in 30,000 steps. Next, the system was gradually heated from 0 K to 300 K in a 200 ps equilibration and then relaxed using the isothermal-isobaric ensemble (NPT) in the next 500 ps without any constraints. In our LiGaMD simulations, both non-bonded potential energy of $[\text{RhB}]^{\cdot-}$, which was defined as the ligand, and potential energy of the rest of the system were boosted. The upper limit of the standard deviation of the first and second potential boosts are 6 kcal/mol. The LiGaMD simulation was initiated with a short conventional MD simulation of 2 ns to collect potential energy statistics, which is followed by 48 ns LiGaMD equilibration after adding the boot potential. Finally, three independent sets of 800 ns LiGaMD production simulations with randomized initial atomic velocities were carried out. The reweighted

potential of the mean force (PMF) was obtained using cumulant expansion to the second order ("Gaussian approximation").

The ligand binding free energies were calculated using the potential of mean force (PMF) free energy profile. From the computed 1D PMF profile (**Fig. S23(A)**), the distance between the C10' atom of the xanthene moiety of $[\text{RhB}]^{\cdot-}$ and the C^{α} atom of the azaallyl radical is 16.1 Å, which suggests that the ET rate constant is on the order of $10^2 - 10^3 \text{ s}^{-1}$ based on the distance-dependent k_{ET} estimations (see **Fig. S21**). This rate constant is comparable to those observed in other long-range ET processes in proteins (101, 106, 112, 113).

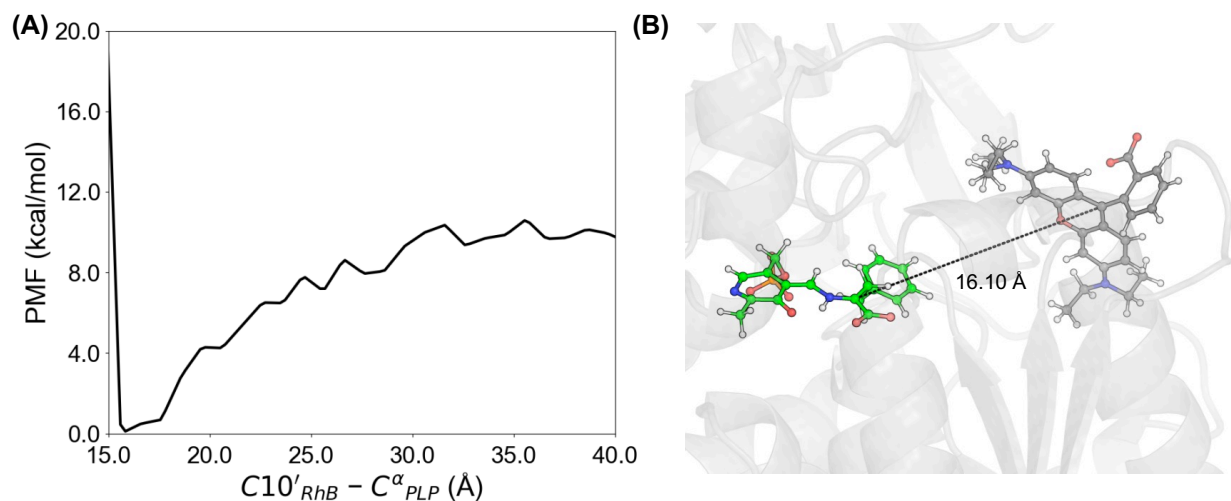


Fig. S23. Ligand Gaussian accelerated molecular dynamics (LiGaMD) simulations on the donor–acceptor distance between the RhB radical anion $[\text{RhB}]^{\cdot-}$ and the azaallyl radical in the enzyme active site. (A) The 1D potential of the mean force (PMF) profile and (B) a representative snapshot calculated from the LiGaMD simulation.

Binding poses of RBF₃K

The alkyltrifluoroborate anion (**1a**) was docked to the L-*P*fPLP^β enzyme (PDB ID: 5VM5) using AutoDock4 software (125) with the Lamarckian genetic algorithm. The dimensions of the grid box were set to 60 Å, 70 Å, and 60 Å. Docking parameters were set as follows: genetic algorithm run of 30, population size of 150, and 25 million energy evaluations. The enzyme position was fixed during docking calculations. The docking calculations suggested that the

preferred binding site of alkyltrifluoroborate is close to the PLP cofactor (with the C···O distance of 8.36 Å, **Fig. S24**). This suggests that once the benzyl radical is formed, it can enter the active site due to its relatively short distance from the PLP cofactor. Furthermore, the alkyltrifluoroborate binding site is exposed to solvent and close to the preferred RhB binding site indicated by the LiGaMD simulations (**Fig. S23**). These results suggest that the photocatalyst can be placed at a relatively short distance from the alkyltrifluoroborate to enable the SET to generate the benzyl radical.

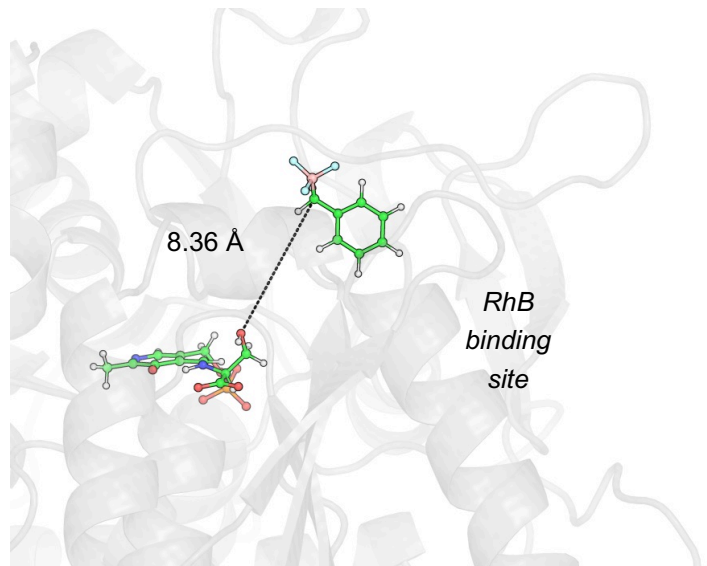


Fig. S24. The binding site of alkyltrifluoroborate from docking studies. RhB binding site was identified from LiGaMD simulation (see **Fig. S23**).

Cartesian Coordinates

7

B3LYP-D3 SCF energy (au):	-3517.39449856
B3LYP-D3 enthalpy (au):	-3516.15309056
wB97X-D SCF energy (au):	-3517.96271794
wB97X-D enthalpy (au):	-3516.72130994

Cartesian coordinates

ATOM	X	Y	Z
C	-3.062609	-35.918356	-13.162440
H	-2.432563	-36.054106	-12.284711
N	-3.996383	-36.818720	-13.377400
H	-4.509376	-36.698221	-14.263048
C	-4.218765	-37.993460	-12.523930
H	-3.250918	-38.211041	-12.048138
C	-4.574105	-39.229196	-13.429549
O	-5.517786	-39.988767	-12.985826
O	-3.927253	-39.382301	-14.470852
C	-5.243189	-37.725758	-11.403441
H	-5.149738	-36.700888	-11.039011
H	-5.026143	-38.426302	-10.581838
O	-6.600562	-37.884713	-11.830864
H	-6.594767	-38.781535	-12.254832
C	-2.768977	-34.854629	-14.064074
C	-1.690661	-33.955129	-13.794070
C	-1.332300	-33.060324	-14.780919
H	-0.503534	-32.374098	-14.624826
N	-1.958756	-32.962854	-15.992233
C	-3.003122	-33.728792	-16.246155
C	-3.739711	-33.567138	-17.547491

H	-3.164767	-32.929560	-18.227057
H	-3.925938	-34.544715	-18.007871
H	-4.725569	-33.110895	-17.378428
C	-3.506616	-34.729934	-15.303797
O	-4.518399	-35.439410	-15.599515
C	-0.976416	-33.903282	-12.459995
H	-1.701466	-33.664359	-11.665116
H	-0.267727	-33.067100	-12.495346
O	-0.316448	-35.118618	-12.170776
P	0.939021	-34.942766	-10.977533
O	2.125495	-34.374329	-11.803576
O	1.132941	-36.417349	-10.543817
O	0.382662	-33.987478	-9.939038
C	-4.743527	-29.178383	-16.052359
H	-5.256604	-28.431472	-15.427190
H	-3.786557	-28.740898	-16.371915
H	-5.352839	-29.355453	-16.942233
C	-4.516249	-30.485285	-15.285985
H	-3.659272	-30.373587	-14.607475
H	-4.233331	-31.267139	-15.994748
C	-5.723980	-30.946071	-14.470096
H	-5.960472	-30.206197	-13.688357
H	-5.470073	-31.867085	-13.927512
C	-7.032155	-31.218287	-15.251021
O	-8.021197	-31.560489	-14.498894
O	-7.052820	-31.111323	-16.490351
C	1.335444	-39.216885	-8.628360
H	1.921873	-38.789271	-9.448486
H	1.981222	-39.319487	-7.742823
H	0.985147	-40.220259	-8.922051

C	0.174656	-38.255278	-8.332546
H	-0.421617	-38.646396	-7.487282
H	-0.488555	-38.218086	-9.211225
O	0.647320	-36.980989	-7.992096
H	0.847676	-36.554611	-8.885507
C	4.537876	-32.972379	-13.022258
H	5.275139	-33.623446	-13.515828
H	4.011594	-33.558914	-12.262709
H	5.082817	-32.141577	-12.551176
C	3.506375	-32.457717	-14.041086
H	2.885112	-33.308073	-14.349959
H	3.978812	-32.022579	-14.929883
C	2.577918	-31.382174	-13.465717
O	2.442963	-30.278438	-14.021876
N	1.971779	-31.750554	-12.322027
H	1.975100	-32.772209	-12.001879
H	1.266187	-31.125064	-11.955925
C	1.913713	-31.307258	-18.620270
H	2.941937	-31.534854	-18.308149
H	1.897319	-30.267159	-18.968556
H	1.658165	-31.949516	-19.472978
C	0.945722	-31.573568	-17.461014
H	1.101534	-32.608759	-17.113139
H	1.204787	-30.923076	-16.607472
O	-0.385612	-31.379314	-17.903040
H	-0.986206	-31.839589	-17.261174
C	2.340083	-39.587954	-16.840800
H	2.825638	-39.495025	-15.862297
H	2.514075	-38.649302	-17.382468
H	2.848521	-40.390160	-17.395883

C	0.839535	-39.871333	-16.687074
H	0.388452	-39.918931	-17.690329
H	0.705259	-40.871641	-16.247281
C	0.065675	-38.850763	-15.833029
H	0.257076	-37.835365	-16.209975
H	-1.007841	-39.030011	-15.980828
C	0.339994	-38.896035	-14.317949
H	1.342203	-38.516563	-14.074604
H	0.307829	-39.948630	-13.985342
C	-0.732228	-38.100057	-13.541465
H	-0.631979	-37.036465	-13.779843
H	-1.709955	-38.431997	-13.916594
N	-0.715831	-38.206983	-12.081081
H	-0.059668	-37.539155	-11.648548
H	-0.434551	-39.143791	-11.793972
C	-6.906389	-43.022757	-12.704509
H	-6.140702	-42.484679	-12.135411
H	-7.829908	-42.444932	-12.591198
H	-7.034339	-44.028345	-12.278039
C	-6.516284	-43.047880	-14.189653
H	-5.496343	-43.481518	-14.265647
C	-7.459651	-43.938877	-15.003798
H	-8.488077	-43.567389	-14.911069
H	-7.427992	-44.982860	-14.660788
H	-7.183074	-43.904283	-16.064040
O	-6.572949	-41.770962	-14.763904
H	-6.084010	-41.117256	-14.181310
C	-9.371823	-34.160173	-9.022073
H	-9.969700	-33.251502	-8.869533
H	-9.030036	-34.511915	-8.040084

H	-8.490751	-33.899636	-9.611583
C	-10.196707	-35.232555	-9.749521
H	-10.497434	-34.858795	-10.736849
H	-11.105090	-35.494685	-9.193941
C	-9.459609	-36.532627	-10.050820
O	-9.989861	-37.631381	-9.991096
O	-8.202297	-36.303055	-10.403697
H	-7.747557	-37.088600	-10.827347
C	-10.504067	-33.649964	-14.664010
H	-11.432153	-33.467144	-14.112247
H	-10.755903	-34.214194	-15.571560
H	-10.029301	-32.705327	-14.950674
C	-9.578461	-34.497739	-13.785679
O	-10.029210	-35.338519	-12.999499
N	-8.266985	-34.258487	-14.014976
H	-8.066021	-33.378077	-14.502456
C	-7.188266	-34.823536	-13.225133
H	-6.311552	-34.959527	-13.870174
H	-7.475650	-35.806760	-12.852307
C	-6.749658	-33.996532	-12.006555
O	-5.965013	-34.471798	-11.187223
N	-7.287936	-32.742528	-11.889446
H	-7.661197	-32.289475	-12.735819
C	-6.864124	-31.873124	-10.808064
H	-7.728582	-31.352222	-10.374364
H	-6.140466	-31.120878	-11.154004
H	-6.383662	-32.487434	-10.044018

8

B3LYP-D3 SCF energy (au): -3517.39139332

B3LYP-D3 enthalpy (au):	-3516.15612132
wB97X-D SCF energy (au):	-3517.95262450
wB97X-D enthalpy (au):	-3516.71735250

Cartesian coordinates

ATOM	X	Y	Z
C	-3.352666	-35.901585	-13.066525
H	-3.361990	-35.717700	-11.998062
N	-4.036344	-36.969930	-13.518245
H	-3.935078	-37.087675	-14.557528
C	-4.795330	-37.879849	-12.877164
H	-1.528303	-37.315007	-12.094886
C	-5.093238	-39.121359	-13.627681
O	-5.866360	-39.992657	-13.022191
O	-4.610987	-39.292786	-14.766658
C	-5.069946	-37.688657	-11.407395
H	-5.334782	-36.642079	-11.199413
H	-4.159321	-37.899073	-10.804806
O	-6.137641	-38.521599	-10.924109
H	-6.229982	-39.230676	-11.642806
C	-2.597518	-35.061243	-13.955089
C	-1.662541	-34.101511	-13.481398
C	-1.047637	-33.236676	-14.386941
H	-0.329204	-32.498354	-14.035142
N	-1.271385	-33.262621	-15.717422
C	-2.070753	-34.226874	-16.203311
C	-2.264833	-34.312850	-17.694607
H	-1.724918	-33.505897	-18.200393
H	-1.913900	-35.283838	-18.073015
H	-3.331470	-34.265588	-17.953415

C	-2.725736	-35.217071	-15.395909
O	-3.388721	-36.173286	-15.937790
C	-1.268229	-34.037405	-12.025258
H	-2.141974	-33.894604	-11.375030
H	-0.591268	-33.191717	-11.865684
O	-0.638588	-35.264022	-11.591806
P	0.934236	-35.294006	-11.056587
O	1.761628	-34.319955	-11.883338
O	1.300665	-36.828002	-11.449772
O	0.969003	-35.133940	-9.547061
C	-4.743540	-29.178243	-16.052410
H	-5.223408	-28.383098	-15.463690
H	-3.754649	-28.817027	-16.369201
H	-5.352792	-29.355571	-16.942231
C	-4.613747	-30.476731	-15.240458
H	-3.730058	-30.416349	-14.589872
H	-4.414529	-31.311709	-15.923314
C	-5.823378	-30.816006	-14.361539
H	-5.983761	-30.001662	-13.632871
H	-5.596237	-31.705613	-13.762017
C	-7.184724	-31.046357	-15.066854
O	-8.043493	-31.684493	-14.349686
O	-7.380203	-30.591985	-16.207554
C	1.335436	-39.216853	-8.628398
H	1.936717	-38.803595	-9.446285
H	1.981222	-39.319500	-7.742807
H	0.985152	-40.220273	-8.922032
C	0.198053	-38.236788	-8.304770
H	-0.511410	-38.717252	-7.608131
H	-0.358660	-38.012110	-9.226958

O	0.691975	-37.067874	-7.695311
H	0.816951	-36.374776	-8.406349
C	4.537885	-32.972389	-13.022289
H	5.272132	-33.628690	-13.509854
H	4.011590	-33.558906	-12.262696
H	5.082809	-32.141575	-12.551162
C	3.517633	-32.444620	-14.049224
H	2.848862	-33.264977	-14.335207
H	4.012981	-32.059031	-14.946565
C	2.680744	-31.292169	-13.490350
O	2.784826	-30.138624	-13.927337
N	1.871615	-31.641445	-12.465942
H	1.738035	-32.634732	-12.180002
H	1.237790	-30.933383	-12.122753
C	1.913668	-31.307230	-18.620329
H	2.969382	-31.517082	-18.382595
H	1.897332	-30.267171	-18.968521
H	1.658185	-31.949536	-19.472952
C	1.082394	-31.589592	-17.368052
H	1.300614	-32.618694	-17.036300
H	1.445319	-30.927755	-16.558536
O	-0.294441	-31.426807	-17.605208
H	-0.743000	-31.993763	-16.906022
C	2.340092	-39.587966	-16.840859
H	2.769904	-39.503765	-15.837849
H	2.514066	-38.649295	-17.382440
H	2.848519	-40.390158	-17.395853
C	0.834376	-39.904186	-16.817133
H	0.492990	-39.990076	-17.860089
H	0.680508	-40.897320	-16.367204

C	-0.046064	-38.884660	-16.083666
H	0.178906	-37.870529	-16.443823
H	-1.095673	-39.065257	-16.349143
C	0.072637	-38.920788	-14.554308
H	1.066408	-38.595418	-14.216426
H	-0.057054	-39.959853	-14.206820
C	-0.993902	-38.032447	-13.917323
H	-0.831727	-36.994127	-14.218266
H	-1.983757	-38.325809	-14.290295
N	-0.927487	-38.063996	-12.443866
H	0.513029	-37.338826	-11.822544
H	-1.320298	-38.939797	-12.099215
C	-6.906491	-43.022919	-12.704454
H	-6.134628	-42.473097	-12.158105
H	-7.829893	-42.444871	-12.591217
H	-7.034260	-44.028258	-12.278077
C	-6.568472	-43.061029	-14.204241
H	-5.516876	-43.406000	-14.310455
C	-7.456854	-44.064120	-14.949960
H	-8.512105	-43.792985	-14.814735
H	-7.306459	-45.091529	-14.586992
H	-7.235695	-44.030274	-16.023401
O	-6.766418	-41.818206	-14.812108
H	-6.350980	-41.101731	-14.236732
C	-9.371529	-34.160474	-9.021787
H	-10.160039	-33.415734	-9.184429
H	-9.087841	-34.174554	-7.963541
H	-8.490770	-33.899171	-9.611993
C	-9.816776	-35.561352	-9.489636
H	-10.120863	-35.526963	-10.538755

H	-10.664379	-35.915752	-8.883580
C	-8.679363	-36.574230	-9.324371
O	-8.169666	-36.817340	-8.240846
O	-8.353625	-37.145578	-10.478310
H	-7.495806	-37.690255	-10.465193
C	-10.504048	-33.649954	-14.664057
H	-11.513417	-33.484580	-14.275285
H	-10.583312	-34.187594	-15.618322
H	-9.987583	-32.699832	-14.845503
C	-9.733544	-34.501726	-13.661507
O	-10.316610	-35.208205	-12.834426
N	-8.385021	-34.433180	-13.819490
H	-8.053536	-33.618844	-14.342827
C	-7.463733	-35.030457	-12.868441
H	-6.554365	-35.361951	-13.383511
H	-7.929229	-35.908237	-12.418863
C	-7.038297	-34.117643	-11.712034
O	-6.480065	-34.592313	-10.717089
N	-7.312276	-32.793556	-11.832402
H	-7.637197	-32.389278	-12.727858
C	-6.864277	-31.873388	-10.807900
H	-6.691759	-30.894522	-11.267161
H	-5.936290	-32.238267	-10.357169
H	-7.606513	-31.759588	-10.003544

9

B3LYP-D3 SCF energy (au):	-270.922367356
B3LYP-D3 enthalpy (au):	-270.800741356
wB97X-D SCF energy (au):	-270.901263491
wB97X-D enthalpy (au):	-270.779637491

Cartesian coordinates

ATOM	X	Y	Z
C	0.467711	0.187671	0.192969
H	1.028195	-0.632544	-0.243397
H	1.027552	0.971561	0.692371
C	-0.936566	0.233194	0.113973
C	-1.677112	-0.795213	-0.541623
C	-1.677941	1.309621	0.686263
C	-3.060460	-0.745102	-0.616262
H	-1.136422	-1.627039	-0.986296
C	-3.061282	1.349121	0.605437
H	-1.137882	2.106432	1.191676
C	-3.765275	0.324817	-0.044981
H	-3.601738	-1.540942	-1.121197
H	-3.603197	2.180050	1.049497
H	-4.849159	0.359928	-0.105896

10

B3LYP-D3 SCF energy (au):	-3711.93118398
B3LYP-D3 enthalpy (au):	-3710.59626098
wB97X-D SCF energy (au):	-3712.44097488
wB97X-D enthalpy (au):	-3711.10605188

Cartesian coordinates

ATOM	X	Y	Z
C	-2.936645	-35.979724	-13.391167
H	-2.506877	-36.046678	-12.396755
N	-3.726469	-36.982933	-13.748867
H	-4.031043	-36.973003	-14.733377

C	-4.000986	-38.160163	-13.008775
H	-0.932002	-37.695787	-11.543094
C	-4.303339	-39.379034	-13.908094
O	-4.832919	-40.375324	-13.329631
O	-3.965995	-39.253683	-15.104918
C	-3.927295	-38.237484	-11.673909
H	-4.151098	-39.194107	-11.218025
H	-3.700134	-37.398388	-11.026657
C	-2.575436	-34.907711	-14.229572
C	-1.567469	-33.966855	-13.830564
C	-1.191276	-32.995163	-14.720857
H	-0.417299	-32.275830	-14.464352
N	-1.720316	-32.865049	-15.978947
C	-2.661378	-33.684131	-16.390195
C	-3.230828	-33.511084	-17.767611
H	-2.516880	-32.968420	-18.395756
H	-3.466413	-34.487054	-18.203202
H	-4.167394	-32.933497	-17.739880
C	-3.176508	-34.780528	-15.549007
O	-4.062349	-35.560459	-15.985010
C	-0.858953	-34.060345	-12.504716
H	-1.564310	-34.236587	-11.685308
H	-0.346301	-33.112711	-12.304517
O	0.100121	-35.132151	-12.560314
P	1.099825	-35.328634	-11.241736
O	2.103775	-34.195837	-11.194802
O	1.853371	-36.688087	-11.699488
O	0.195785	-35.585976	-10.044966
C	-4.743113	-29.178078	-16.052547
H	-5.329112	-28.606256	-15.317550

H	-3.846256	-28.600805	-16.312459
H	-5.353005	-29.355620	-16.942166
C	-4.408641	-30.588922	-15.546122
H	-3.863760	-30.554451	-14.591866
H	-3.734572	-31.054893	-16.270432
C	-5.648775	-31.483690	-15.382652
H	-6.321763	-31.079737	-14.611955
H	-5.317175	-32.453760	-14.993814
C	-6.496009	-31.755063	-16.663289
O	-7.631389	-32.303068	-16.472712
O	-6.012440	-31.432563	-17.775015
C	1.335359	-39.216821	-8.628677
H	1.925151	-38.791459	-9.448292
H	1.981244	-39.319515	-7.742734
H	0.985193	-40.220283	-8.921874
C	0.165611	-38.286296	-8.296168
H	-0.450966	-38.742261	-7.503632
H	-0.484418	-38.171501	-9.174475
O	0.620588	-37.030503	-7.839375
H	0.591814	-36.421182	-8.629022
C	4.537749	-32.972367	-13.022225
H	5.275788	-33.627818	-13.504600
H	4.011654	-33.558948	-12.262713
H	5.082867	-32.141563	-12.551186
C	3.528602	-32.455406	-14.063303
H	2.907323	-33.293966	-14.405038
H	4.029029	-32.028396	-14.938453
C	2.599215	-31.361535	-13.533977
O	2.486236	-30.274104	-14.109011
N	1.935587	-31.674653	-12.395282

H	1.957094	-32.613425	-11.956643
H	1.251487	-31.003466	-12.074194
C	1.913706	-31.307292	-18.620248
H	2.944203	-31.538180	-18.315329
H	1.897275	-30.267155	-18.968549
H	1.658178	-31.949514	-19.472984
C	0.956775	-31.536189	-17.453211
H	1.042182	-32.586905	-17.125232
H	1.277891	-30.918740	-16.595035
O	-0.360011	-31.234972	-17.863783
H	-0.959006	-31.669281	-17.202571
C	2.340087	-39.587893	-16.840638
H	2.815950	-39.502503	-15.857576
H	2.514072	-38.649355	-17.382521
H	2.848518	-40.390155	-17.395967
C	0.840819	-39.901983	-16.722136
H	0.401106	-39.905884	-17.729792
H	0.719424	-40.925324	-16.335206
C	0.043483	-38.943259	-15.826909
H	0.191134	-37.908400	-16.168017
H	-1.028313	-39.152593	-15.945098
C	0.392559	-39.038504	-14.333480
H	1.414326	-38.689910	-14.132369
H	0.345544	-40.094693	-14.018914
C	-0.589372	-38.216512	-13.503170
H	-0.486505	-37.159358	-13.760921
H	-1.608507	-38.528910	-13.756019
N	-0.313286	-38.325592	-12.056234
H	1.168415	-37.420863	-11.763885
H	-0.542069	-39.263630	-11.728571

C	-6.906046	-43.022003	-12.704284
H	-6.119765	-42.485685	-12.163405
H	-7.830054	-42.445325	-12.591166
H	-7.034558	-44.028560	-12.278233
C	-6.531380	-43.130318	-14.193700
H	-5.555735	-43.660551	-14.248321
C	-7.557009	-43.969821	-14.962759
H	-8.542623	-43.491520	-14.900804
H	-7.634131	-44.989701	-14.560154
H	-7.276027	-44.024704	-16.020852
O	-6.471017	-41.886485	-14.829901
H	-5.797882	-41.311461	-14.355157
C	-9.371865	-34.160869	-9.022176
H	-9.088949	-34.891609	-8.257989
H	-10.081990	-34.650275	-9.698841
H	-8.490028	-33.899697	-9.611392
C	-9.998628	-32.934781	-8.345644
H	-10.399176	-32.234330	-9.093011
H	-9.215350	-32.372643	-7.808614
C	-11.138395	-33.228843	-7.295419
O	-11.857752	-32.233691	-7.006141
O	-11.186375	-34.397754	-6.830652
C	-10.504270	-33.649851	-14.664236
H	-11.190087	-33.063985	-14.044618
H	-11.039210	-34.545752	-15.001237
H	-10.185246	-33.069468	-15.536199
C	-9.320784	-34.085741	-13.800855
O	-9.517148	-34.550880	-12.664573
N	-8.099451	-33.952006	-14.352535
H	-7.939026	-33.335698	-15.191284

C	-6.908277	-34.414576	-13.654838
H	-6.122955	-34.624445	-14.384779
H	-7.145461	-35.347438	-13.128689
C	-6.333698	-33.429451	-12.623416
O	-5.121931	-33.233188	-12.509349
N	-7.259339	-32.813803	-11.841007
H	-8.197607	-33.207754	-11.829269
C	-6.864182	-31.873381	-10.808384
H	-7.764331	-31.435425	-10.370523
H	-6.237900	-31.088415	-11.244802
H	-6.289602	-32.363269	-10.011048
C	-6.525180	-35.850872	-9.915747
H	-7.332646	-36.483556	-9.563426
H	-6.765752	-35.137406	-10.691950
C	-5.236963	-35.935647	-9.361015
C	-4.167199	-35.100581	-9.815731
C	-4.938504	-36.886678	-8.339391
C	-2.891714	-35.233784	-9.285521
H	-4.365937	-34.377471	-10.604009
C	-3.657825	-37.002067	-7.819057
H	-5.738676	-37.532707	-7.983349
C	-2.619999	-36.181834	-8.285243
H	-2.068052	-34.629232	-9.650283
H	-3.453700	-37.743990	-7.047992
H	-1.611890	-36.277288	-7.895871

11

B3LYP-D3 SCF energy (au):	-3711.96390796
B3LYP-D3 enthalpy (au):	-3710.62615796
wB97X-D SCF energy (au):	-3712.48640104

wB97X-D enthalpy (au): -3711.14865104

Cartesian coordinates

ATOM	X	Y	Z
C	-2.902191	-35.898791	-13.609410
H	-2.809867	-35.801753	-12.536025
N	-3.528844	-37.012152	-14.056577
H	-3.490796	-37.162731	-15.079482
C	-4.175345	-37.951307	-13.345029
H	-0.239516	-37.596487	-11.353586
C	-4.410828	-39.275469	-14.053962
O	-5.091034	-40.122032	-13.389042
O	-3.891670	-39.395957	-15.186956
C	-4.498193	-37.727558	-11.907157
H	-4.724955	-36.670847	-11.714436
H	-5.387358	-38.321303	-11.678732
C	-2.390514	-34.906836	-14.460841
C	-1.517572	-33.876000	-13.973982
C	-1.190169	-32.845410	-14.820687
H	-0.498753	-32.067801	-14.503151
N	-1.685372	-32.708721	-16.086180
C	-2.461271	-33.646720	-16.594596
C	-3.046677	-33.434356	-17.961404
H	-2.394984	-32.777712	-18.547299
H	-3.187757	-34.392885	-18.468236
H	-4.033417	-32.951544	-17.875031
C	-2.785467	-34.876816	-15.868695
O	-3.390453	-35.828520	-16.434094
C	-0.848042	-33.953042	-12.626507
H	-1.526068	-34.293021	-11.835111

H	-0.481773	-32.958769	-12.343292
O	0.269834	-34.862768	-12.724005
P	1.136174	-35.144644	-11.337106
O	1.939528	-33.914788	-10.978772
O	2.143510	-36.293633	-11.882606
O	0.161195	-35.746349	-10.325417
C	-4.743042	-29.178229	-16.052556
H	-5.323025	-28.577092	-15.335845
H	-3.844179	-28.610899	-16.329302
H	-5.353084	-29.355511	-16.942172
C	-4.393067	-30.559446	-15.479979
H	-3.765592	-30.456196	-14.582349
H	-3.788865	-31.093369	-16.218140
C	-5.627167	-31.409627	-15.145481
H	-6.235806	-30.926655	-14.366711
H	-5.296898	-32.363964	-14.708023
C	-6.567027	-31.745792	-16.344627
O	-7.718931	-32.188643	-16.024568
O	-6.134838	-31.561646	-17.505367
C	1.335596	-39.216961	-8.629003
H	1.923400	-38.793677	-9.451170
H	1.981163	-39.319723	-7.742368
H	0.985133	-40.219927	-8.921865
C	0.145848	-38.304931	-8.307720
H	-0.426090	-38.730270	-7.468469
H	-0.542045	-38.293614	-9.163223
O	0.547103	-37.002514	-7.951244
H	0.517069	-36.455852	-8.779142
C	4.537837	-32.972442	-13.022279
H	5.275649	-33.631768	-13.499205

H	4.011610	-33.558892	-12.262719
H	5.082807	-32.141556	-12.551145
C	3.532817	-32.459310	-14.071776
H	2.875340	-33.286125	-14.371734
H	4.040719	-32.089018	-14.968024
C	2.655101	-31.304810	-13.584039
O	2.603402	-30.231623	-14.194952
N	1.964191	-31.544469	-12.445204
H	1.943941	-32.455698	-11.950854
H	1.323070	-30.821436	-12.149199
C	1.913632	-31.307310	-18.620272
H	2.938680	-31.545468	-18.304277
H	1.897304	-30.267135	-18.968512
H	1.658190	-31.949521	-19.472978
C	0.938572	-31.487609	-17.464134
H	0.929956	-32.545474	-17.152379
H	1.301668	-30.910465	-16.594715
O	-0.344069	-31.066147	-17.881165
H	-0.976984	-31.482980	-17.238395
C	2.339965	-39.587841	-16.840813
H	2.833871	-39.502807	-15.866682
H	2.514154	-38.649337	-17.382497
H	2.848515	-40.390199	-17.395812
C	0.838991	-39.888288	-16.686726
H	0.367648	-39.876008	-17.679345
H	0.720509	-40.914673	-16.306948
C	0.077280	-38.933667	-15.750471
H	0.167306	-37.900996	-16.116396
H	-0.994010	-39.175958	-15.783385
C	0.562365	-38.999679	-14.296077

H	1.588100	-38.618807	-14.204178
H	0.588949	-40.054137	-13.971527
C	-0.320963	-38.204936	-13.336264
H	-0.331458	-37.149981	-13.626470
H	-1.355268	-38.573011	-13.400268
N	0.228876	-38.265787	-11.969860
H	1.639234	-37.156380	-11.924106
H	0.102271	-39.192132	-11.565801
C	-6.905120	-43.021139	-12.704093
H	-6.124353	-42.485379	-12.154202
H	-7.830545	-42.445956	-12.591124
H	-7.035006	-44.028628	-12.278415
C	-6.532849	-43.108432	-14.195322
H	-5.527464	-43.577668	-14.259983
C	-7.512279	-44.007372	-14.957427
H	-8.526004	-43.594607	-14.879656
H	-7.517316	-45.032786	-14.561677
H	-7.241446	-44.036329	-16.019071
O	-6.557176	-41.862257	-14.829836
H	-5.938005	-41.230974	-14.354053
C	-9.372156	-34.160644	-9.022242
H	-9.088483	-34.851862	-8.222499
H	-10.067046	-34.693818	-9.682492
H	-8.489603	-33.899970	-9.611230
C	-10.027809	-32.915600	-8.407488
H	-10.446751	-32.263772	-9.188002
H	-9.254594	-32.308261	-7.904860
C	-11.155026	-33.173314	-7.333828
O	-11.905133	-32.183875	-7.110158
O	-11.161676	-34.307196	-6.787764

C	-10.504321	-33.649784	-14.664265
H	-11.052907	-33.042869	-13.933420
H	-11.222730	-34.329652	-15.133470
H	-10.050898	-32.993769	-15.414357
C	-9.462246	-34.483029	-13.915821
O	-9.797801	-35.432792	-13.207953
N	-8.181605	-34.049264	-14.076292
H	-7.964517	-33.309919	-14.787011
C	-7.070302	-34.682736	-13.396726
H	-6.254665	-34.885425	-14.099600
H	-7.406734	-35.637161	-12.980251
C	-6.471860	-33.865968	-12.239976
O	-5.430576	-34.219672	-11.685866
N	-7.194578	-32.769229	-11.895143
H	-8.016109	-32.591644	-12.457102
C	-6.864154	-31.873383	-10.808608
H	-7.714055	-31.761072	-10.125943
H	-6.565344	-30.885062	-11.185249
H	-6.023706	-32.311171	-10.264838
C	-3.337143	-38.205130	-10.989840
H	-2.396975	-37.763626	-11.332728
H	-3.245876	-39.291266	-11.120797
C	-3.541606	-37.855658	-9.535369
C	-2.757649	-36.869979	-8.921638
C	-4.521538	-38.508340	-8.773441
C	-2.928063	-36.566609	-7.569394
H	-1.984599	-36.355950	-9.488677
C	-4.708173	-38.191289	-7.428291
H	-5.143273	-39.266267	-9.246227
C	-3.904929	-37.222517	-6.819149

H	-2.275423	-35.829730	-7.109826
H	-5.482263	-38.698104	-6.855256
H	-4.045900	-36.978908	-5.767810

12

B3LYP-D3 SCF energy (au):	-3711.76399448
B3LYP-D3 enthalpy (au):	-3710.43259448
wB97X-D SCF energy (au):	-3712.54498111
wB97X-D enthalpy (au):	-3711.21358111

Cartesian coordinates

ATOM	X	Y	Z
C	-2.460847	-36.585237	-13.912956
H	-2.538439	-36.349054	-12.860231
N	-2.968780	-37.769298	-14.302562
H	-2.815149	-37.973020	-15.312056
C	-3.659986	-38.675281	-13.589497
H	0.215282	-37.915636	-11.147355
C	-3.914779	-39.994496	-14.228432
O	-4.689406	-40.791571	-13.566137
O	-3.377724	-40.241502	-15.338795
C	-4.118010	-38.333535	-12.207446
H	-4.468291	-37.290317	-12.153489
H	-4.962844	-38.985442	-11.969603
C	-1.859286	-35.657148	-14.807192
C	-1.173107	-34.502416	-14.336901
C	-0.838544	-33.501836	-15.245667
H	-0.347947	-32.590261	-14.903463
N	-1.090714	-33.582397	-16.562479
C	-1.599553	-34.728056	-17.053336

C	-1.787970	-34.833118	-18.543169
H	-1.551683	-33.875330	-19.022303
H	-1.143314	-35.617031	-18.969992
H	-2.816473	-35.130289	-18.790914
C	-1.943487	-35.858009	-16.250066
O	-2.327222	-36.964665	-16.775650
C	-0.678059	-34.371087	-12.922822
H	-1.370448	-34.768849	-12.174583
H	-0.491838	-33.315614	-12.683589
O	0.583676	-35.096272	-12.815678
P	1.303165	-35.246241	-11.344260
O	2.004716	-33.952865	-10.971571
O	2.442247	-36.349939	-11.709729
O	0.287243	-35.855647	-10.376170
C	-4.743059	-29.178151	-16.052442
H	-4.705143	-28.088458	-15.899899
H	-3.724070	-29.515176	-16.283685
H	-5.353062	-29.355586	-16.942228
C	-5.257639	-29.871683	-14.783618
H	-4.516060	-29.703058	-13.989204
H	-5.289349	-30.958451	-14.931585
C	-6.641230	-29.395816	-14.290173
H	-6.716431	-28.304534	-14.410553
H	-6.736555	-29.629589	-13.222543
C	-7.805688	-30.081030	-15.052357
O	-8.243290	-31.152152	-14.503351
O	-8.190597	-29.561324	-16.119128
C	1.335578	-39.216937	-8.629061
H	1.926389	-38.790449	-9.445876
H	1.981163	-39.319720	-7.742358

H	0.985139	-40.219937	-8.921833
C	0.156196	-38.295202	-8.292640
H	-0.402545	-38.713173	-7.439740
H	-0.548160	-38.280832	-9.132737
O	0.581826	-36.996956	-7.950443
H	0.565783	-36.468422	-8.794604
C	4.537833	-32.972442	-13.022307
H	5.268401	-33.628968	-13.514087
H	4.011605	-33.558883	-12.262710
H	5.082803	-32.141561	-12.551128
C	3.513270	-32.441307	-14.045861
H	2.839008	-33.256615	-14.337890
H	4.003804	-32.058468	-14.946835
C	2.676642	-31.284249	-13.495644
O	2.726071	-30.152726	-13.996104
N	1.914611	-31.592629	-12.423742
H	1.890585	-32.524569	-11.962067
H	1.316345	-30.860439	-12.067750
C	1.913602	-31.307327	-18.620340
H	2.953969	-31.527172	-18.331671
H	1.897353	-30.267100	-18.968516
H	1.658233	-31.949512	-19.472938
C	0.979210	-31.515962	-17.436879
H	1.124158	-32.532014	-17.042329
H	1.275411	-30.823340	-16.626517
O	-0.361349	-31.329971	-17.822443
H	-0.824491	-32.137649	-17.425574
C	2.339957	-39.587850	-16.840842
H	2.860256	-39.502833	-15.880573
H	2.514157	-38.649328	-17.382495

H	2.848516	-40.390196	-17.395790
C	0.854450	-39.924069	-16.636561
H	0.316358	-39.827314	-17.588748
H	0.783885	-40.986064	-16.350914
C	0.139448	-39.090921	-15.563737
H	0.051398	-38.046044	-15.884495
H	-0.892150	-39.457492	-15.477228
C	0.836264	-39.164188	-14.197236
H	1.822916	-38.681172	-14.224772
H	1.013191	-40.222921	-13.930020
C	0.019599	-38.490271	-13.105711
H	-0.127750	-37.440840	-13.364591
H	-0.971747	-38.957739	-13.056658
N	0.718675	-38.515633	-11.805663
H	1.998118	-37.241192	-11.804075
H	0.712765	-39.457900	-11.417317
C	-6.905159	-43.021190	-12.704118
H	-6.090570	-42.478516	-12.218024
H	-7.830542	-42.445929	-12.591122
H	-7.034977	-44.028618	-12.278394
C	-6.595943	-43.198206	-14.207394
H	-5.630947	-43.747508	-14.273540
C	-7.666989	-44.064906	-14.885339
H	-8.643147	-43.567858	-14.808116
H	-7.744579	-45.063688	-14.428971
H	-7.432428	-44.178024	-15.950788
O	-6.543874	-41.993682	-14.900089
H	-5.769832	-41.464851	-14.484188
C	-9.371967	-34.160812	-9.022096
H	-9.129341	-35.008113	-8.372499

H	-10.152617	-34.504906	-9.710906
H	-8.489912	-33.899794	-9.611397
C	-9.866629	-32.976295	-8.177535
H	-10.166230	-32.137978	-8.825214
H	-9.033353	-32.580675	-7.572625
C	-11.055951	-33.247469	-7.178985
O	-11.538734	-32.208447	-6.644011
O	-11.387126	-34.447451	-6.992812
C	-10.504328	-33.649786	-14.664238
H	-11.251972	-33.599742	-13.865155
H	-10.975490	-34.140106	-15.525773
H	-10.185759	-32.637292	-14.933598
C	-9.349164	-34.513635	-14.163039
O	-9.553098	-35.635106	-13.699354
N	-8.124581	-33.936542	-14.296041
H	-8.095137	-32.957121	-14.600634
C	-6.956998	-34.474219	-13.621764
H	-6.071426	-34.378820	-14.261938
H	-7.118135	-35.536180	-13.432969
C	-6.625761	-33.831057	-12.261869
O	-5.952091	-34.451983	-11.442499
N	-7.093978	-32.566045	-12.061238
H	-7.562532	-32.061037	-12.818227
C	-6.864062	-31.873366	-10.808595
H	-7.810095	-31.634728	-10.305686
H	-6.305497	-30.940195	-10.972491
H	-6.278056	-32.532232	-10.165154
C	-3.012028	-38.540355	-11.128251
H	-2.110120	-37.998816	-11.425668
H	-2.758202	-39.609338	-11.126541

C	-3.406668	-38.095378	-9.741653
C	-2.807945	-36.974474	-9.147279
C	-4.386255	-38.791098	-9.016220
C	-3.162103	-36.577184	-7.856591
H	-2.033497	-36.428297	-9.682533
C	-4.751484	-38.387698	-7.732070
H	-4.867905	-39.652267	-9.475766
C	-4.135389	-37.279366	-7.143448
H	-2.663733	-35.719591	-7.411516
H	-5.524011	-38.933382	-7.191704
H	-4.421657	-36.960651	-6.142344

13

B3LYP-D3 SCF energy (au):	-3711.76261904
B3LYP-D3 enthalpy (au):	-3710.42807704
wB97X-D SCF energy (au):	-3712.55578739
wB97X-D enthalpy (au):	-3711.22124539

Cartesian coordinates

ATOM	X	Y	Z
C	-3.041658	-36.335978	-13.024534
H	-2.376532	-36.423176	-12.168274
N	-3.926792	-37.304799	-13.156034
H	-4.528458	-37.296860	-13.987235
C	-4.009212	-38.448773	-12.226089
H	-2.987092	-38.680316	-11.905315
C	-4.602340	-39.740146	-12.889937
O	-4.480072	-40.779064	-12.197986
O	-5.170309	-39.616771	-14.013394
C	-4.836169	-38.116526	-10.965810

H	-4.933850	-39.064572	-10.426405
H	-5.843781	-37.791377	-11.255390
C	-2.808714	-35.261471	-13.928807
C	-1.762408	-34.318947	-13.659357
C	-1.432758	-33.412243	-14.643087
H	-0.623811	-32.703888	-14.480709
N	-2.068843	-33.317687	-15.853540
C	-3.102421	-34.102271	-16.095777
C	-3.878529	-33.918139	-17.371435
H	-3.269968	-33.376889	-18.104762
H	-4.193220	-34.888437	-17.771385
H	-4.793724	-33.334876	-17.188731
C	-3.565395	-35.144242	-15.159176
O	-4.547709	-35.886701	-15.445488
C	-1.053260	-34.238570	-12.323165
H	-1.798264	-34.111886	-11.520925
H	-0.442569	-33.329034	-12.317902
O	-0.263822	-35.386467	-12.076182
P	1.109467	-35.094052	-11.057513
O	2.174127	-34.553525	-12.053415
O	1.400042	-36.528200	-10.546537
O	0.659843	-34.077587	-10.025516
C	-4.743593	-29.178647	-16.052238
H	-5.328173	-28.573753	-15.343332
H	-3.861721	-28.589254	-16.346396
H	-5.352770	-29.355492	-16.942325
C	-4.334826	-30.523247	-15.434379
H	-3.500070	-30.376448	-14.734804
H	-3.956304	-31.180732	-16.222980
C	-5.479964	-31.214789	-14.690987

H	-5.774136	-30.623116	-13.812228
H	-5.131255	-32.177532	-14.291160
C	-6.758639	-31.496916	-15.517358
O	-7.792902	-31.767194	-14.807385
O	-6.700665	-31.462512	-16.764584
C	1.335453	-39.216831	-8.628340
H	1.926803	-38.794123	-9.447591
H	1.981225	-39.319538	-7.742811
H	0.985138	-40.220249	-8.922063
C	0.194835	-38.232284	-8.332321
H	-0.408384	-38.599611	-7.482505
H	-0.468399	-38.181340	-9.209587
O	0.711157	-36.971800	-7.993106
H	0.980933	-36.578532	-8.879287
C	4.537838	-32.972357	-13.022274
H	5.287235	-33.628088	-13.493580
H	4.011599	-33.558919	-12.262688
H	5.082840	-32.141589	-12.551168
C	3.529037	-32.482853	-14.072845
H	2.954016	-33.354598	-14.408491
H	4.022198	-32.020228	-14.936842
C	2.547429	-31.447537	-13.511957
O	2.471146	-30.300131	-13.987585
N	1.836733	-31.912103	-12.472818
H	1.887759	-32.940016	-12.192223
H	1.129206	-31.314245	-12.068641
C	1.913724	-31.307284	-18.620238
H	2.948308	-31.526222	-18.321952
H	1.897249	-30.267175	-18.968558
H	1.658179	-31.949518	-19.472971

C	0.971278	-31.622464	-17.445241
H	1.229876	-32.626371	-17.069550
H	1.168623	-30.926262	-16.612429
O	-0.376288	-31.576611	-17.883238
H	-0.939605	-32.052044	-17.225385
C	2.340045	-39.587934	-16.840696
H	2.831257	-39.497484	-15.865083
H	2.514079	-38.649307	-17.382508
H	2.848532	-40.390160	-17.395922
C	0.843576	-39.872764	-16.674046
H	0.365038	-39.856804	-17.665429
H	0.712906	-40.895876	-16.288887
C	0.115679	-38.900012	-15.732784
H	0.272430	-37.865981	-16.070971
H	-0.963640	-39.083542	-15.824677
C	0.495870	-39.016517	-14.245110
H	1.482372	-38.576909	-14.045580
H	0.559364	-40.085026	-13.971954
C	-0.562120	-38.334660	-13.353448
H	-0.579555	-37.265055	-13.580024
H	-1.539696	-38.746369	-13.651888
N	-0.405171	-38.455269	-11.911468
H	0.230107	-37.739498	-11.525915
H	-0.048487	-39.373989	-11.653744
C	-6.906838	-43.022367	-12.704691
H	-6.134079	-42.476096	-12.150399
H	-7.829727	-42.445115	-12.591183
H	-7.034183	-44.028544	-12.277873
C	-6.501688	-43.037506	-14.190134
H	-5.450297	-43.385313	-14.244890

C	-7.362259	-44.016981	-14.999152
H	-8.415857	-43.713540	-14.940009
H	-7.271780	-45.045843	-14.620740
H	-7.065951	-43.997589	-16.055324
O	-6.657208	-41.785933	-14.804418
H	-6.051695	-41.084228	-14.409405
C	-9.371877	-34.161375	-9.023416
H	-9.065889	-34.169490	-7.967737
H	-9.627766	-35.192388	-9.308795
H	-8.490413	-33.898179	-9.610405
C	-10.573897	-33.223380	-9.233075
H	-11.501394	-33.724375	-8.919567
H	-10.680552	-33.026362	-10.311328
C	-10.504769	-31.846107	-8.488142
O	-9.380017	-31.275310	-8.469095
O	-11.592918	-31.434444	-7.994138
C	-10.504160	-33.649856	-14.663973
H	-11.235006	-33.214016	-13.972952
H	-11.062293	-34.224955	-15.414258
H	-9.932534	-32.849675	-15.144556
C	-9.615493	-34.602567	-13.860585
O	-10.103749	-35.519273	-13.194714
N	-8.293013	-34.336085	-13.979931
H	-8.035013	-33.471718	-14.476762
C	-7.289337	-34.929875	-13.120119
H	-6.388316	-35.161411	-13.703144
H	-7.679324	-35.868182	-12.721327
C	-6.881903	-34.079507	-11.901995
O	-6.303963	-34.630671	-10.957028
N	-7.174687	-32.760197	-11.931121

H	-7.527813	-32.346565	-12.796505
C	-6.864358	-31.873115	-10.808087
H	-7.738009	-31.703344	-10.162763
H	-6.507114	-30.915353	-11.204680
H	-6.072044	-32.336449	-10.215505
C	-4.202274	-37.052502	-10.041914
H	-4.337740	-36.060323	-10.482957
H	-3.124521	-37.241926	-9.955082
C	-4.833451	-37.087250	-8.666803
C	-6.060270	-36.449559	-8.418150
C	-4.230856	-37.803981	-7.621885
C	-6.665649	-36.534448	-7.163138
H	-6.519943	-35.869867	-9.213069
C	-4.835347	-37.889826	-6.365384
H	-3.270945	-38.286117	-7.797782
C	-6.059143	-37.257441	-6.131243
H	-7.610649	-36.021164	-6.997322
H	-4.342547	-38.444497	-5.566609
H	-6.530682	-37.317233	-5.149915

14

B3LYP-D3 SCF energy (au):	-3517.38642504
B3LYP-D3 enthalpy (au):	-3516.14844604
wB97X-D SCF energy (au):	-3517.95567798
wB97X-D enthalpy (au):	-3516.71769898

Cartesian coordinates

ATOM	X	Y	Z
C	-1.567961	-36.416059	-13.665726
H	-1.165623	-36.475767	-12.653566

N	-5.617297	-37.515500	-12.098204
H	-5.716785	-36.787502	-11.388216
C	-5.165697	-38.780235	-11.519139
H	-4.107543	-38.702473	-11.245950
C	-5.329764	-39.901618	-12.578003
O	-6.533976	-39.984938	-13.036045
O	-4.385767	-40.659059	-12.861153
C	-5.953311	-39.214075	-10.257414
H	-5.931087	-38.419061	-9.501813
H	-5.494549	-40.118583	-9.823790
O	-7.336052	-39.478818	-10.550827
H	-7.337938	-39.737467	-11.515889
C	-1.587182	-35.151971	-14.319341
C	-1.215433	-33.961767	-13.621808
C	-1.112303	-32.800168	-14.364890
H	-0.791899	-31.873722	-13.897452
N	-1.368571	-32.724884	-15.703108
C	-1.738474	-33.804121	-16.369709
C	-2.035864	-33.710906	-17.843401
H	-1.655730	-32.773327	-18.254741
H	-1.588936	-34.563631	-18.368086
H	-3.118147	-33.774890	-18.024251
C	-1.880785	-35.102315	-15.738548
O	-2.222306	-36.117735	-16.437272
C	-1.069153	-33.903768	-12.103278
H	-2.096614	-33.835861	-11.700393
H	-0.569137	-32.968242	-11.823700
O	-0.432652	-35.009419	-11.514880
P	1.114944	-34.688492	-10.758984
O	2.020500	-34.358087	-11.977284

O	1.405468	-36.057417	-10.117721
O	0.863017	-33.496850	-9.850198
C	-4.743730	-29.168439	-16.052184
H	-5.250694	-28.406887	-15.441847
H	-3.776033	-28.755758	-16.370257
H	-5.352701	-29.355457	-16.942316
C	-4.547688	-30.474247	-15.267183
H	-3.674515	-30.379649	-14.607265
H	-4.299954	-31.280942	-15.967534
C	-5.748542	-30.890852	-14.411856
H	-5.972594	-30.097519	-13.678421
H	-5.485968	-31.772158	-13.812551
C	-7.075831	-31.201258	-15.146885
O	-7.963533	-31.763704	-14.398411
O	-7.220120	-30.888909	-16.340061
C	1.335603	-39.216635	-8.628692
H	1.935633	-38.789037	-9.439564
H	1.981076	-39.319598	-7.742767
H	0.985134	-40.220365	-8.921833
C	0.197821	-38.232624	-8.307188
H	-0.466078	-38.680126	-7.544047
H	-0.407944	-38.080893	-9.215756
O	0.696717	-37.022908	-7.811971
H	0.976104	-36.496072	-8.641498
C	4.547882	-32.972448	-13.032299
H	5.291106	-33.627463	-13.513199
H	4.021614	-33.558919	-12.262708
H	5.092741	-32.141543	-12.561128
C	3.529873	-32.466355	-14.070001
H	2.889007	-33.310323	-14.352425

H	4.020905	-32.069555	-14.966825
C	2.640786	-31.344832	-13.519871
O	2.634642	-30.209638	-14.031027
N	1.932363	-31.719202	-12.445081
H	1.907711	-32.739749	-12.136511
H	1.309845	-31.047528	-12.018634
C	1.923782	-31.307584	-18.620042
H	2.965893	-31.544590	-18.358136
H	1.917213	-30.267012	-18.968701
H	1.668184	-31.949373	-19.473041
C	1.057906	-31.485989	-17.378843
H	1.019434	-32.553661	-17.111935
H	1.541635	-30.970549	-16.531780
O	-0.243675	-30.973684	-17.611567
H	-0.794416	-31.365378	-16.884443
C	2.349776	-39.597751	-16.839700
H	2.889311	-39.497286	-15.888026
H	2.524186	-38.659564	-17.382850
H	2.868672	-40.400085	-17.396523
C	0.884490	-39.954808	-16.556918
H	0.288782	-39.904161	-17.479559
H	0.853295	-41.007622	-16.235296
C	0.228720	-39.092744	-15.466217
H	0.920809	-38.989606	-14.617876
H	0.054301	-38.078722	-15.845925
C	-1.095299	-39.683472	-14.957397
H	-0.936806	-40.707069	-14.589545
H	-1.809488	-39.763535	-15.790016
C	-1.748553	-38.872022	-13.826073
H	-2.698165	-39.337281	-13.535655

H	-1.099134	-38.839446	-12.943449
N	-1.964320	-37.506552	-14.280455
H	-6.541106	-37.671421	-12.494267
H	-2.288441	-37.322573	-15.252884
C	-6.905723	-43.021640	-12.704429
H	-6.120696	-42.486011	-12.167005
H	-7.830393	-42.445661	-12.601103
H	-7.034650	-44.018553	-12.278178
C	-6.561909	-43.104089	-14.204275
H	-5.482364	-43.335222	-14.291888
C	-7.344437	-44.224354	-14.898572
H	-8.422264	-44.062139	-14.765466
H	-7.083842	-45.212630	-14.493221
H	-7.133377	-44.217503	-15.974994
O	-6.875397	-41.914230	-14.886246
H	-6.655839	-41.153805	-14.275037
C	-9.369963	-34.161544	-9.022751
H	-10.075705	-33.324879	-9.102406
H	-9.079693	-34.292353	-7.974621
H	-8.471301	-33.928948	-9.601529
C	-9.983365	-35.453574	-9.580910
H	-10.222476	-35.347628	-10.641756
H	-10.912499	-35.696935	-9.041901
C	-9.048990	-36.644264	-9.393874
O	-8.541212	-36.939880	-8.323150
O	-8.891461	-37.336746	-10.521202
H	-8.270951	-38.121920	-10.396655
C	-10.504102	-33.649894	-14.674020
H	-11.492653	-33.421922	-14.263381
H	-10.645332	-34.204279	-15.611655

H	-9.947295	-32.731830	-14.893940
C	-9.757507	-34.520440	-13.680211
O	-10.354346	-35.252211	-12.885505
N	-8.407829	-34.438149	-13.806396
H	-8.067624	-33.613093	-14.313416
C	-7.519639	-35.041502	-12.836317
H	-6.617654	-35.425108	-13.326081
H	-8.034573	-35.884469	-12.371302
C	-7.068255	-34.132565	-11.685944
O	-6.542973	-34.643426	-10.689582
N	-7.297888	-32.802431	-11.823512
H	-7.602120	-32.411176	-12.731599
C	-6.884158	-31.853166	-10.808105
H	-7.747606	-31.454070	-10.255307
H	-6.352004	-31.017954	-11.277471
H	-6.219827	-32.358125	-10.102907

15

B3LYP-D3 SCF energy (au):	-3517.36717341
B3LYP-D3 enthalpy (au):	-3516.12608641
wB97X-D SCF energy (au):	-3517.94867357
wB97X-D enthalpy (au):	-3516.70758657

Cartesian coordinates

ATOM	X	Y	Z
C	-2.393708	-36.365149	-13.353618
H	-1.884532	-36.231233	-12.397876
N	-3.918578	-36.635953	-12.992496
H	-4.276040	-35.814156	-12.477805
C	-4.155102	-37.868200	-12.159773

H	-3.267944	-37.971413	-11.525936
C	-4.289213	-39.224432	-12.966656
O	-5.482083	-39.535322	-13.325106
O	-3.267407	-39.907520	-13.125943
C	-5.366000	-37.663766	-11.239635
H	-5.296561	-36.708602	-10.711260
H	-5.354556	-38.478206	-10.495244
O	-6.593300	-37.653051	-11.957458
H	-6.504712	-38.418665	-12.595086
C	-2.330461	-35.089742	-14.174540
C	-1.258591	-34.195528	-14.042470
C	-1.155920	-33.168528	-14.994968
H	-0.331549	-32.458989	-14.928024
N	-2.011544	-32.984755	-16.013008
C	-3.077776	-33.791344	-16.103535
C	-4.058243	-33.579476	-17.225655
H	-3.724044	-32.758504	-17.868977
H	-4.177423	-34.493789	-17.823812
H	-5.059217	-33.345867	-16.837689
C	-3.322771	-34.870119	-15.189615
O	-4.384928	-35.618358	-15.318739
C	-0.185855	-34.135663	-12.961320
H	-0.379382	-33.208005	-12.394805
H	0.779318	-33.977203	-13.467983
O	-0.084451	-35.212266	-12.069193
P	0.992596	-34.832528	-10.738860
O	2.261921	-34.311772	-11.478243
O	1.184424	-36.220412	-10.099300
O	0.277140	-33.766297	-9.929923
C	-4.743598	-29.178309	-16.052235

H	-5.056561	-28.217257	-15.620843
H	-3.698409	-29.081667	-16.377409
H	-5.352783	-29.355508	-16.942258
C	-4.874050	-30.313893	-15.031215
H	-3.999914	-30.291832	-14.366293
H	-4.814455	-31.279556	-15.547510
C	-6.130617	-30.274589	-14.147489
H	-6.183036	-29.288895	-13.654006
H	-6.012153	-31.019878	-13.357049
C	-7.489894	-30.500274	-14.858156
O	-8.284070	-31.330082	-14.274521
O	-7.732989	-29.855319	-15.894729
C	1.335409	-39.216837	-8.628463
H	1.897213	-38.748988	-9.442176
H	1.981223	-39.319480	-7.742805
H	0.985160	-40.220289	-8.921996
C	0.156241	-38.300271	-8.256442
H	-0.461976	-38.804248	-7.487691
H	-0.476341	-38.163642	-9.148745
O	0.592353	-37.073433	-7.745921
H	0.837183	-36.545541	-8.588831
C	4.537887	-32.972463	-13.022355
H	5.271298	-33.619018	-13.527497
H	4.011609	-33.558892	-12.262691
H	5.082759	-32.141540	-12.551098
C	3.507066	-32.433809	-14.027016
H	2.918719	-33.277774	-14.412335
H	3.978189	-31.937514	-14.884671
C	2.516821	-31.421245	-13.433802
O	2.217233	-30.390181	-14.062536

N	2.043257	-31.748385	-12.217541
H	2.105522	-32.752378	-11.836877
H	1.266414	-31.191396	-11.883440
C	1.913737	-31.307526	-18.620131
H	2.938544	-31.536739	-18.299158
H	1.897198	-30.267050	-18.968646
H	1.658227	-31.949414	-19.473008
C	0.928895	-31.578944	-17.474005
H	1.081246	-32.614833	-17.127822
H	1.169292	-30.932924	-16.612618
O	-0.395725	-31.389036	-17.942235
H	-1.015142	-31.847637	-17.318444
C	2.339880	-39.587874	-16.840492
H	2.820559	-39.487661	-15.860120
H	2.514131	-38.649356	-17.382540
H	2.848619	-40.390176	-17.396081
C	0.838393	-39.867659	-16.691333
H	0.407577	-40.071954	-17.684860
H	0.696553	-40.789729	-16.107353
C	0.056749	-38.724009	-16.031831
H	0.475150	-38.489543	-15.046096
H	0.179818	-37.810164	-16.632354
C	-1.439126	-39.033794	-15.886394
H	-1.586850	-39.896680	-15.221852
H	-1.850715	-39.322805	-16.866780
C	-2.265927	-37.859773	-15.353559
H	-2.142857	-36.993712	-16.010799
H	-3.332556	-38.129452	-15.389794
N	-1.808260	-37.485811	-14.017033
H	-4.395895	-36.547092	-13.946390

H	-1.806136	-38.305753	-13.413268
C	-6.906151	-43.021711	-12.704280
H	-6.156106	-42.498837	-12.097403
H	-7.830143	-42.445556	-12.591221
H	-7.034456	-44.028606	-12.278200
C	-6.458768	-43.001575	-14.173296
H	-5.432691	-43.418762	-14.221692
C	-7.362683	-43.873785	-15.048482
H	-8.395084	-43.506974	-14.991474
H	-7.341629	-44.924180	-14.726944
H	-7.040558	-43.814562	-16.094296
O	-6.509697	-41.708308	-14.720825
H	-5.996623	-41.047560	-14.179900
C	-9.369900	-34.161418	-9.022398
H	-9.932719	-33.245636	-8.798614
H	-9.028517	-34.594928	-8.074055
H	-8.491516	-33.898976	-9.611795
C	-10.228745	-35.153294	-9.819764
H	-10.530990	-34.698217	-10.772223
H	-11.136453	-35.445635	-9.279209
C	-9.501167	-36.428405	-10.225053
O	-10.029199	-37.528549	-10.239347
O	-8.246001	-36.171037	-10.569166
H	-7.808637	-36.924736	-11.061458
C	-10.504074	-33.649944	-14.664064
H	-11.453360	-33.679274	-14.120362
H	-10.658529	-34.108889	-15.649520
H	-10.165860	-32.616897	-14.805876
C	-9.472629	-34.463992	-13.883586
O	-9.812383	-35.389044	-13.139862

N	-8.191629	-34.101613	-14.147700
H	-8.072848	-33.165698	-14.549617
C	-7.052290	-34.659127	-13.443031
H	-6.196796	-34.743404	-14.127214
H	-7.294769	-35.668420	-13.106950
C	-6.591651	-33.893670	-12.197196
O	-5.682563	-34.361969	-11.500577
N	-7.242091	-32.726974	-11.921497
H	-7.757132	-32.269467	-12.689067
C	-6.864134	-31.873181	-10.808090
H	-7.751527	-31.582235	-10.230605
H	-6.359403	-30.963191	-11.157392
H	-6.178508	-32.430307	-10.165390

16

B3LYP-D3 SCF energy (au):	-3517.37712829
B3LYP-D3 enthalpy (au):	-3516.13283929
wB97X-D SCF energy (au):	-3517.95305525
wB97X-D enthalpy (au):	-3516.70876625

Cartesian coordinates

ATOM	X	Y	Z
C	-3.019094	-36.176144	-13.210090
H	-2.579670	-35.991461	-12.228082
N	-4.277177	-36.774285	-13.101980
H	-4.822449	-36.725705	-13.964577
C	-4.465295	-37.880562	-12.163114
H	-3.600927	-37.856159	-11.485470
C	-4.404671	-39.280972	-12.869127
O	-5.500880	-39.942260	-12.945026

O	-3.295328	-39.651413	-13.313914
C	-5.694883	-37.707142	-11.259396
H	-5.741972	-36.675312	-10.905930
H	-5.579708	-38.387717	-10.396235
O	-6.937399	-37.977513	-11.919444
H	-6.765304	-38.833142	-12.387184
C	-2.874266	-34.997167	-14.138566
C	-1.753517	-34.158152	-13.981054
C	-1.454496	-33.247787	-14.993057
H	-0.585380	-32.598801	-14.901538
N	-2.185325	-33.114182	-16.122400
C	-3.286356	-33.855985	-16.259023
C	-4.136353	-33.672652	-17.488106
H	-3.590720	-33.092396	-18.241185
H	-4.432119	-34.647097	-17.895785
H	-5.067905	-33.139700	-17.247262
C	-3.716733	-34.858627	-15.293172
O	-4.749846	-35.586986	-15.524234
C	-0.885490	-34.152259	-12.742541
H	-1.483756	-33.851409	-11.870622
H	-0.121372	-33.379916	-12.878487
O	-0.260832	-35.407083	-12.471134
P	1.016459	-35.222559	-11.253266
O	2.206803	-34.712278	-12.107310
O	1.153851	-36.659256	-10.720412
O	0.469658	-34.180009	-10.292248
C	-4.743465	-29.178187	-16.052331
H	-5.293275	-28.493877	-15.387795
H	-3.818583	-28.669240	-16.361568
H	-5.352852	-29.355549	-16.942228

C	-4.431623	-30.508423	-15.358487
H	-3.574360	-30.386398	-14.682092
H	-4.111762	-31.233662	-16.109505
C	-5.600991	-31.077767	-14.553275
H	-5.824758	-30.423962	-13.695590
H	-5.304974	-32.041356	-14.115544
C	-6.929595	-31.309159	-15.310588
O	-7.915472	-31.630032	-14.543983
O	-6.972793	-31.196074	-16.549428
C	1.335385	-39.216853	-8.628439
H	1.923151	-38.800802	-9.453471
H	1.981255	-39.319485	-7.742806
H	0.985159	-40.220270	-8.922010
C	0.182863	-38.239125	-8.364179
H	-0.402846	-38.573276	-7.487892
H	-0.489530	-38.253524	-9.236424
O	0.662392	-36.946643	-8.113752
H	0.872154	-36.595816	-9.036864
C	4.537861	-32.972459	-13.022345
H	5.269599	-33.623460	-13.522543
H	4.011629	-33.558908	-12.262689
H	5.082762	-32.141537	-12.551099
C	3.487853	-32.455350	-14.018855
H	2.917991	-33.320609	-14.380098
H	3.936478	-31.935164	-14.873784
C	2.500719	-31.480747	-13.364980
O	2.317958	-30.337945	-13.815252
N	1.908225	-31.989796	-12.268056
H	1.962458	-33.025837	-12.065399
H	1.151266	-31.467860	-11.848067

C	1.913726	-31.307487	-18.620166
H	2.936017	-31.535792	-18.291797
H	1.897234	-30.267053	-18.968636
H	1.658205	-31.949432	-19.472979
C	0.913327	-31.597337	-17.486877
H	1.106091	-32.616799	-17.113313
H	1.103209	-30.920458	-16.635778
O	-0.406245	-31.478242	-17.988988
H	-1.029638	-31.957457	-17.385926
C	2.339846	-39.587822	-16.840465
H	2.854132	-39.487202	-15.875891
H	2.514148	-38.649372	-17.382549
H	2.848623	-40.390198	-17.396091
C	0.842109	-39.809793	-16.620177
H	0.336157	-39.915336	-17.592148
H	0.672577	-40.753873	-16.082369
C	0.202685	-38.648477	-15.843305
H	0.642489	-38.586902	-14.838522
H	0.466756	-37.704409	-16.342926
C	-1.323835	-38.748338	-15.754016
H	-1.640513	-39.603110	-15.144757
H	-1.721628	-38.924292	-16.765519
C	-2.003583	-37.479938	-15.237425
H	-1.605084	-36.592841	-15.734161
H	-3.075273	-37.516203	-15.448341
N	-1.881888	-37.264379	-13.772920
H	-0.984211	-36.847997	-13.447065
H	-2.098218	-38.165396	-13.309529
C	-6.906191	-43.021707	-12.704339
H	-6.147868	-42.488742	-12.119535

H	-7.830151	-42.445561	-12.591193
H	-7.034416	-44.028606	-12.278169
C	-6.468871	-43.059622	-14.174316
H	-5.485773	-43.576516	-14.213811
C	-7.448059	-43.862299	-15.035821
H	-8.443916	-43.405294	-14.983076
H	-7.518470	-44.906798	-14.700789
H	-7.124701	-43.846381	-16.083221
O	-6.390794	-41.778315	-14.739464
H	-5.923554	-41.153325	-14.114761
C	-9.369982	-34.161403	-9.022378
H	-9.887164	-33.229797	-8.751060
H	-9.017212	-34.629675	-8.094427
H	-8.491471	-33.898976	-9.611783
C	-10.330324	-35.086593	-9.785058
H	-10.581917	-34.643039	-10.756485
H	-11.265499	-35.236192	-9.231249
C	-9.796435	-36.468666	-10.139135
O	-10.494404	-37.471598	-10.154267
O	-8.507154	-36.426038	-10.441021
H	-8.173582	-37.232905	-10.923469
C	-10.504117	-33.649975	-14.664067
H	-11.423266	-33.410513	-14.118772
H	-10.781629	-34.235146	-15.550784
H	-9.994834	-32.734477	-14.984677
C	-9.612872	-34.498913	-13.756494
O	-10.101637	-35.306274	-12.956511
N	-8.294579	-34.301374	-13.968534
H	-8.054272	-33.448289	-14.485300
C	-7.249900	-34.862549	-13.128666

H	-6.342864	-34.978181	-13.734435
H	-7.540704	-35.853193	-12.783082
C	-6.907144	-34.021099	-11.892434
O	-6.299648	-34.494637	-10.930357
N	-7.302245	-32.715231	-11.903996
H	-7.565169	-32.264518	-12.794616
C	-6.864131	-31.873229	-10.808091
H	-7.415569	-32.091541	-9.884828
H	-7.041867	-30.828136	-11.083574
H	-5.797978	-32.017750	-10.595462

H₂O

B3LYP-D3 SCF energy (au):	-76.4089621570
B3LYP-D3 enthalpy (au):	-76.3840231570
wB97X-D SCF energy (au):	-76.4413268604
wB97X-D enthalpy (au):	-76.4163878604

Cartesian coordinates

ATOM	X	Y	Z
O	0.292106	-1.065535	0.000000
H	1.259590	-1.016173	0.000000
H	0.015685	-0.137067	0.000000

TS-1

B3LYP-D3 SCF energy (au):	-3517.36201881
B3LYP-D3 enthalpy (au):	-3516.12719681
wB97X-D SCF energy (au):	-3517.92646527
wB97X-D enthalpy (au):	-3516.69164327

Cartesian coordinates

ATOM	X	Y	Z
C	-3.368175	-35.685724	-13.249825
H	-3.025860	-35.679090	-12.222552
N	-4.047042	-36.747786	-13.609067
H	-4.295030	-36.798980	-14.605815
C	-4.258598	-37.913872	-12.781336
H	-2.677051	-38.110662	-12.473182
C	-4.685675	-39.091343	-13.617886
O	-5.467394	-39.960448	-13.042249
O	-4.259660	-39.191656	-14.792423
C	-5.041446	-37.675530	-11.506631
H	-4.941022	-36.644532	-11.161323
H	-4.682562	-38.351411	-10.715730
O	-6.472061	-37.897747	-11.665392
H	-6.497767	-38.777825	-12.121362
C	-2.949085	-34.631308	-14.127075
C	-1.893348	-33.773106	-13.717300
C	-1.410060	-32.836494	-14.616019
H	-0.572624	-32.194802	-14.351421
N	-1.894658	-32.693034	-15.879512
C	-2.885820	-33.475712	-16.288212
C	-3.397533	-33.319894	-17.695001
H	-2.735549	-32.665481	-18.271421
H	-3.477212	-34.300652	-18.179231
H	-4.412347	-32.896903	-17.697602
C	-3.482329	-34.522867	-15.466158
O	-4.384622	-35.289219	-15.928407
C	-1.210987	-33.969729	-12.378197
H	-1.921544	-33.825538	-11.547347
H	-0.426785	-33.214236	-12.267625

O	-0.672955	-35.279352	-12.339297
P	0.703434	-35.627015	-11.381145
O	1.837696	-34.775534	-12.000125
O	0.777024	-37.150818	-11.639256
O	0.333665	-35.241257	-9.939303
C	-4.743513	-29.178267	-16.052323
H	-5.119665	-28.268905	-15.564131
H	-3.709443	-28.993726	-16.376583
H	-5.352837	-29.355541	-16.942244
C	-4.797650	-30.387437	-15.107545
H	-3.908934	-30.381006	-14.461530
H	-4.713033	-31.309875	-15.694796
C	-6.034393	-30.471083	-14.201391
H	-6.088849	-29.554065	-13.588672
H	-5.894498	-31.301859	-13.503127
C	-7.413804	-30.625892	-14.896067
O	-8.240377	-31.405772	-14.293772
O	-7.641902	-29.970719	-15.930697
C	1.335428	-39.216831	-8.628486
H	1.948279	-38.830916	-9.451764
H	1.981218	-39.319521	-7.742772
H	0.985162	-40.220272	-8.921991
C	0.204778	-38.204791	-8.393702
H	-0.496905	-38.605981	-7.634358
H	-0.351477	-38.090539	-9.334106
O	0.718686	-36.971622	-7.958697
H	0.623854	-36.317266	-8.727737
C	4.537867	-32.972428	-13.022304
H	5.270277	-33.624954	-13.517528
H	4.011606	-33.558881	-12.262701

H	5.082806	-32.141562	-12.551141
C	3.479127	-32.471436	-14.018590
H	2.921268	-33.340200	-14.389452
H	3.922169	-31.939108	-14.867414
C	2.493419	-31.511336	-13.347731
O	2.392662	-30.329082	-13.707458
N	1.809657	-32.062187	-12.323243
H	1.779669	-33.107947	-12.140185
H	1.098879	-31.480239	-11.900108
C	1.913736	-31.307288	-18.620238
H	2.946206	-31.538302	-18.321775
H	1.897294	-30.267155	-18.968575
H	1.658161	-31.949496	-19.472986
C	0.967905	-31.547471	-17.438578
H	1.069095	-32.598618	-17.117775
H	1.302323	-30.934674	-16.581268
O	-0.359472	-31.251162	-17.815470
H	-0.954787	-31.657411	-17.123059
C	2.340008	-39.587967	-16.840747
H	2.767138	-39.500532	-15.836749
H	2.514104	-38.649291	-17.382478
H	2.848554	-40.390162	-17.395922
C	0.832912	-39.886110	-16.821345
H	0.504331	-40.003074	-17.865658
H	0.656079	-40.860424	-16.340937
C	-0.049985	-38.827994	-16.142329
H	0.241827	-37.824681	-16.484536
H	-1.081474	-38.977348	-16.487820
C	-0.067024	-38.870492	-14.605705
H	0.865174	-38.511340	-14.153168

H	-0.202285	-39.920123	-14.292290
C	-1.239125	-38.043083	-14.076903
H	-1.049014	-36.974118	-14.194770
H	-2.159296	-38.312155	-14.605746
N	-1.497774	-38.251077	-12.625220
H	-0.767742	-37.691273	-12.076196
H	-1.343306	-39.233232	-12.388639
C	-6.906306	-43.022712	-12.704505
H	-6.147235	-42.483319	-12.126757
H	-7.829946	-42.444969	-12.591189
H	-7.034386	-44.028351	-12.278046
C	-6.501865	-43.022928	-14.186840
H	-5.474797	-43.444802	-14.256115
C	-7.423558	-43.922900	-15.018039
H	-8.458163	-43.566636	-14.932901
H	-7.381007	-44.969975	-14.683879
H	-7.137018	-43.874240	-16.075201
O	-6.574452	-41.744743	-14.745336
H	-6.076013	-41.075267	-14.170752
C	-9.371671	-34.160253	-9.021948
H	-10.007116	-33.269921	-8.925676
H	-9.039420	-34.456541	-8.018389
H	-8.490829	-33.899601	-9.611707
C	-10.124248	-35.298115	-9.728927
H	-10.428032	-34.966121	-10.730415
H	-11.023902	-35.599602	-9.179266
C	-9.298167	-36.558202	-9.975494
O	-9.748574	-37.685325	-9.829422
O	-8.074051	-36.261513	-10.382293
H	-7.558566	-37.045763	-10.758452

C	-10.504072	-33.649975	-14.664061
H	-11.477352	-33.627946	-14.164086
H	-10.630682	-34.127478	-15.644670
H	-10.116144	-32.635678	-14.813693
C	-9.543155	-34.487029	-13.813446
O	-9.957754	-35.362373	-13.047339
N	-8.236225	-34.204086	-14.042760
H	-8.057078	-33.300684	-14.489596
C	-7.141358	-34.777382	-13.276168
H	-6.277350	-34.923018	-13.935808
H	-7.429390	-35.759293	-12.895538
C	-6.678835	-33.949165	-12.068546
O	-5.800964	-34.375471	-11.320032
N	-7.311268	-32.749763	-11.871538
H	-7.767303	-32.294088	-12.675938
C	-6.864139	-31.873126	-10.808043
H	-7.712097	-31.289595	-10.427895
H	-6.084172	-31.174505	-11.145779
H	-6.447504	-32.484499	-10.004616

TS-2

B3LYP-D3 SCF energy (au):	-3517.36481748
B3LYP-D3 enthalpy (au):	-3516.13175748
wB97X-D SCF energy (au):	-3517.92321837
wB97X-D enthalpy (au):	-3516.69015837

Cartesian coordinates

ATOM	X	Y	Z
C	-3.215147	-35.849375	-13.254987
H	-3.139096	-35.688664	-12.184396

N	-3.860450	-36.937612	-13.637966
H	-3.852365	-37.087352	-14.661829
C	-4.471662	-37.923643	-12.868281
H	-1.297816	-37.366986	-11.895226
C	-4.675149	-39.233511	-13.548908
O	-5.567574	-40.008639	-13.014461
O	-4.005405	-39.489795	-14.579764
C	-5.119595	-37.617134	-11.650143
H	-5.054751	-36.601035	-11.267863
H	-5.118375	-38.390783	-10.886939
O	-6.872884	-37.668945	-11.921086
H	-6.950622	-38.620135	-12.147682
C	-2.631339	-34.909879	-14.166275
C	-1.685514	-33.942479	-13.728149
C	-1.220040	-32.997027	-14.629989
H	-0.478065	-32.261342	-14.325729
N	-1.613690	-32.944012	-15.926115
C	-2.447437	-33.873436	-16.385829
C	-2.834670	-33.837967	-17.839674
H	-2.265096	-33.066213	-18.366861
H	-2.658125	-34.817096	-18.302250
H	-3.909811	-33.641148	-17.953383
C	-2.968116	-34.961325	-15.577963
O	-3.665871	-35.887368	-16.099040
C	-1.029142	-34.027944	-12.371965
H	-1.734751	-34.224624	-11.556201
H	-0.525051	-33.078575	-12.148993
O	-0.061210	-35.094348	-12.434420
P	0.993161	-35.312837	-11.170438
O	2.099381	-34.273165	-11.242888

O	1.597968	-36.750759	-11.621095
O	0.168423	-35.427219	-9.899039
C	-4.743500	-29.178246	-16.052342
H	-5.137279	-28.284514	-15.549443
H	-3.713571	-28.966731	-16.374222
H	-5.352847	-29.355557	-16.942231
C	-4.776127	-30.402876	-15.125479
H	-3.888987	-30.388894	-14.476391
H	-4.674467	-31.314736	-15.728259
C	-6.013780	-30.519317	-14.224011
H	-6.074856	-29.619683	-13.586729
H	-5.874374	-31.364860	-13.542846
C	-7.394453	-30.663102	-14.920919
O	-8.243406	-31.390147	-14.287861
O	-7.599127	-30.047705	-15.984979
C	1.335368	-39.216873	-8.628373
H	1.935825	-38.801060	-9.445697
H	1.981244	-39.319484	-7.742812
H	0.985181	-40.220281	-8.922054
C	0.182600	-38.254358	-8.315918
H	-0.483172	-38.716330	-7.563749
H	-0.417234	-38.097459	-9.224054
O	0.667528	-37.030638	-7.815141
H	0.573515	-36.368140	-8.556367
C	4.537892	-32.972388	-13.022282
H	5.274518	-33.626600	-13.508890
H	4.011571	-33.558894	-12.262707
H	5.082815	-32.141581	-12.551169
C	3.521953	-32.450779	-14.054261
H	2.909919	-33.290421	-14.408476

H	4.016721	-32.000550	-14.921242
C	2.584288	-31.378484	-13.495033
O	2.495975	-30.260721	-14.017143
N	1.893289	-31.745961	-12.391980
H	1.908384	-32.704977	-11.988911
H	1.200832	-31.090787	-12.056331
C	1.913750	-31.307343	-18.620220
H	2.951562	-31.533694	-18.333964
H	1.897264	-30.267133	-18.968572
H	1.658161	-31.949482	-19.472998
C	0.989795	-31.547076	-17.427240
H	1.098048	-32.596125	-17.102776
H	1.335566	-30.928052	-16.579129
O	-0.345772	-31.262549	-17.780413
H	-0.906109	-31.746855	-17.107666
C	2.340127	-39.587979	-16.840725
H	2.794974	-39.500670	-15.848244
H	2.514067	-38.649301	-17.382510
H	2.848488	-40.390134	-17.395910
C	0.838851	-39.909403	-16.761898
H	0.448683	-39.979300	-17.788480
H	0.710723	-40.910462	-16.322021
C	-0.014886	-38.910761	-15.968988
H	0.153342	-37.893543	-16.351538
H	-1.074207	-39.131275	-16.154349
C	0.211197	-38.927258	-14.449661
H	1.211335	-38.559261	-14.181889
H	0.142963	-39.966588	-14.087069
C	-0.850271	-38.074639	-13.755182
H	-0.735266	-37.030316	-14.057510

H	-1.844350	-38.417588	-14.068554
N	-0.707586	-38.103965	-12.282011
H	0.828763	-37.375270	-11.803058
H	-1.089973	-38.979175	-11.924198
C	-6.906358	-43.022689	-12.704511
H	-6.140897	-42.478921	-12.140947
H	-7.829925	-42.444977	-12.591196
H	-7.034365	-44.028374	-12.278034
C	-6.518308	-43.050045	-14.190570
H	-5.497877	-43.487923	-14.264158
C	-7.460912	-43.949332	-14.999047
H	-8.490240	-43.580106	-14.905808
H	-7.426282	-44.992983	-14.653004
H	-7.186772	-43.917263	-16.060311
O	-6.576100	-41.779016	-14.765916
H	-6.100918	-41.113632	-14.167752
C	-9.371354	-34.160596	-9.021678
H	-10.016247	-33.271032	-8.951963
H	-9.032333	-34.409928	-8.005991
H	-8.491034	-33.899254	-9.612062
C	-10.113457	-35.339165	-9.667508
H	-10.409660	-35.061217	-10.688285
H	-11.027918	-35.584339	-9.109744
C	-9.287452	-36.638784	-9.830638
O	-9.849124	-37.730304	-9.646188
O	-8.068569	-36.439038	-10.192962
H	-7.457180	-37.303996	-11.054010
C	-10.504062	-33.649991	-14.664067
H	-11.465773	-33.619887	-14.142286
H	-10.667471	-34.106695	-15.649611

H	-10.104650	-32.639370	-14.804887
C	-9.549727	-34.527650	-13.855145
O	-9.966370	-35.462047	-13.169976
N	-8.239994	-34.200923	-14.024697
H	-8.065581	-33.276828	-14.428876
C	-7.179083	-34.796809	-13.232467
H	-6.320408	-35.049427	-13.865132
H	-7.544137	-35.727971	-12.796036
C	-6.662400	-33.936799	-12.075486
O	-5.725801	-34.321041	-11.374441
N	-7.320043	-32.757238	-11.856819
H	-7.804426	-32.310440	-12.645995
C	-6.864095	-31.873158	-10.807952
H	-7.688087	-31.217392	-10.503357
H	-6.016146	-31.245915	-11.124457
H	-6.539313	-32.473171	-9.954736

TS-3

B3LYP-D3 SCF energy (au):	-3711.91646765
B3LYP-D3 enthalpy (au):	-3710.58374165
wB97X-D SCF energy (au):	-3712.42978679
wB97X-D enthalpy (au):	-3711.09706079

Cartesian coordinates

ATOM	X	Y	Z
C	-3.007839	-35.882341	-13.570554
H	-2.929209	-35.804422	-12.490926
N	-3.668119	-36.937513	-14.032203
H	-3.635992	-37.072138	-15.052788
C	-4.389050	-37.886781	-13.301130

H	-0.363134	-37.512103	-11.434128
C	-4.409618	-39.278670	-13.939171
O	-5.082577	-40.155122	-13.309962
O	-3.745511	-39.408327	-14.992448
C	-4.923867	-37.604778	-12.077547
H	-4.981742	-36.589145	-11.694987
H	-5.574867	-38.354074	-11.647816
C	-2.447489	-34.892813	-14.406783
C	-1.546072	-33.893598	-13.908721
C	-1.182258	-32.869317	-14.746905
H	-0.468229	-32.115164	-14.424787
N	-1.669023	-32.716011	-16.016440
C	-2.476798	-33.617617	-16.530963
C	-3.045133	-33.390350	-17.902392
H	-2.390766	-32.721794	-18.470803
H	-3.170644	-34.343690	-18.423429
H	-4.038825	-32.920391	-17.825707
C	-2.849943	-34.841890	-15.808104
O	-3.493045	-35.758746	-16.383470
C	-0.877899	-33.996836	-12.561283
H	-1.548380	-34.375826	-11.781798
H	-0.536332	-33.002631	-12.247261
O	0.258863	-34.875578	-12.689318
P	1.152634	-35.153794	-11.316452
O	1.994962	-33.938420	-10.999886
O	2.115235	-36.337727	-11.864501
O	0.179630	-35.704102	-10.276680
C	-4.743088	-29.178152	-16.052501
H	-5.323645	-28.577593	-15.335803
H	-3.844455	-28.610254	-16.328685

H	-5.353032	-29.355576	-16.942205
C	-4.393018	-30.559121	-15.480490
H	-3.770321	-30.457204	-14.579507
H	-3.784251	-31.089299	-16.217233
C	-5.627769	-31.411968	-15.154936
H	-6.237095	-30.935392	-14.372979
H	-5.297546	-32.369883	-14.725309
C	-6.565287	-31.736558	-16.359279
O	-7.724433	-32.165069	-16.046980
O	-6.123406	-31.557802	-17.517387
C	1.335597	-39.216963	-8.629014
H	1.926329	-38.795374	-9.450151
H	1.981161	-39.319719	-7.742366
H	0.985133	-40.219926	-8.921860
C	0.156912	-38.290732	-8.304274
H	-0.424831	-38.716767	-7.471497
H	-0.526905	-38.254240	-9.162513
O	0.588543	-37.002654	-7.931127
H	0.544237	-36.440395	-8.746812
C	4.537846	-32.972447	-13.022288
H	5.277188	-33.631023	-13.498191
H	4.011607	-33.558887	-12.262718
H	5.082800	-32.141556	-12.551139
C	3.535351	-32.461099	-14.074851
H	2.884637	-33.290894	-14.381190
H	4.045946	-32.084753	-14.967096
C	2.647553	-31.313786	-13.588444
O	2.596896	-30.236676	-14.192775
N	1.944361	-31.565932	-12.460205
H	1.939225	-32.476196	-11.963862

H	1.302861	-30.845457	-12.159131
C	1.913604	-31.307322	-18.620279
H	2.941778	-31.543811	-18.312560
H	1.897305	-30.267127	-18.968509
H	1.658211	-31.949523	-19.472978
C	0.954067	-31.494330	-17.451891
H	0.954512	-32.553696	-17.144478
H	1.327860	-30.919379	-16.585827
O	-0.337291	-31.076170	-17.845429
H	-0.955708	-31.484497	-17.184940
C	2.339962	-39.587846	-16.840817
H	2.825683	-39.502702	-15.862722
H	2.514155	-38.649334	-17.382497
H	2.848516	-40.390198	-17.395809
C	0.837566	-39.890747	-16.703235
H	0.383899	-39.898709	-17.704449
H	0.716209	-40.910650	-16.307314
C	0.055465	-38.922135	-15.799607
H	0.158673	-37.894902	-16.177881
H	-1.014998	-39.162390	-15.852679
C	0.499521	-38.968912	-14.331984
H	1.527256	-38.599345	-14.216099
H	0.501996	-40.017805	-13.989773
C	-0.404658	-38.148297	-13.413535
H	-0.384892	-37.096826	-13.715685
H	-1.441430	-38.501299	-13.511142
N	0.102665	-38.200913	-12.028946
H	1.565148	-37.171949	-11.931944
H	-0.066054	-39.115413	-11.613262
C	-6.905154	-43.021178	-12.704105

H	-6.124681	-42.485653	-12.153669
H	-7.830537	-42.445936	-12.591125
H	-7.034985	-44.028619	-12.278404
C	-6.524546	-43.113662	-14.192025
H	-5.533068	-43.613251	-14.248794
C	-7.522913	-43.979789	-14.967085
H	-8.524326	-43.536708	-14.898005
H	-7.562702	-45.005801	-14.574861
H	-7.242499	-44.014063	-16.026166
O	-6.503202	-41.864681	-14.821351
H	-5.892135	-41.248996	-14.316143
C	-9.372138	-34.160655	-9.022268
H	-9.086661	-34.844246	-8.216662
H	-10.063135	-34.702292	-9.679664
H	-8.489643	-33.899989	-9.611185
C	-10.035108	-32.914171	-8.418463
H	-10.455421	-32.270199	-9.204738
H	-9.266032	-32.299425	-7.918466
C	-11.163594	-33.169799	-7.345561
O	-11.919292	-32.182689	-7.131044
O	-11.165535	-34.299748	-6.791430
C	-10.504324	-33.649786	-14.664263
H	-11.052484	-33.052712	-13.925067
H	-11.219696	-34.334483	-15.130954
H	-10.064946	-32.984771	-15.414812
C	-9.446123	-34.476531	-13.930466
O	-9.764213	-35.436722	-13.228977
N	-8.172891	-34.022943	-14.095028
H	-7.969608	-33.279441	-14.805623
C	-7.045153	-34.649245	-13.435900

H	-6.236848	-34.835348	-14.151537
H	-7.361095	-35.613190	-13.025010
C	-6.444035	-33.832861	-12.280309
O	-5.379379	-34.163355	-11.754749
N	-7.191260	-32.765352	-11.899961
H	-8.027729	-32.602205	-12.444133
C	-6.864126	-31.873351	-10.808630
H	-7.712140	-31.775961	-10.121783
H	-6.578597	-30.878823	-11.179412
H	-6.015649	-32.304862	-10.272323
C	-3.255520	-38.419911	-10.629103
H	-2.414994	-38.096602	-11.229507
H	-3.645305	-39.407160	-10.851444
C	-3.484057	-37.803534	-9.363312
C	-2.732592	-36.669504	-8.953870
C	-4.480237	-38.291554	-8.476901
C	-2.951203	-36.084009	-7.714182
H	-1.951359	-36.274579	-9.598695
C	-4.704288	-37.685032	-7.247990
H	-5.080564	-39.145961	-8.783216
C	-3.938159	-36.580072	-6.852962
H	-2.337140	-35.237900	-7.417863
H	-5.485485	-38.066368	-6.593070
H	-4.117104	-36.106786	-5.890118

TS-3'

B3LYP-D3 SCF energy (au):	-3711.91957950
B3LYP-D3 enthalpy (au):	-3710.58574150
wB97X-D SCF energy (au):	-3712.42591860
wB97X-D enthalpy (au):	-3711.09208060

Cartesian coordinates

ATOM	X	Y	Z
C	-2.399953	-36.253292	-13.368867
H	-1.808441	-36.402723	-12.471323
N	-3.006661	-37.367969	-13.854131
H	-3.333615	-37.323797	-14.826067
C	-3.346302	-38.522199	-13.148859
H	0.504555	-37.879714	-11.130091
C	-3.818152	-39.673423	-14.071375
O	-4.382561	-40.651798	-13.496190
O	-3.565271	-39.521112	-15.285551
C	-3.227178	-38.678789	-11.816361
H	-2.848002	-37.911316	-11.150040
H	-3.531536	-39.627868	-11.393976
C	-2.056498	-35.149123	-14.233132
C	-1.101774	-34.158190	-13.859511
C	-0.892961	-33.088441	-14.711094
H	-0.156132	-32.326667	-14.465095
N	-1.566176	-32.890472	-15.879550
C	-2.473631	-33.769557	-16.258827
C	-3.252927	-33.525066	-17.519212
H	-2.736968	-32.785443	-18.139320
H	-3.385008	-34.461713	-18.069957
H	-4.260560	-33.148400	-17.286662
C	-2.767756	-34.984522	-15.494492
O	-3.602389	-35.820410	-15.938696
C	-0.298153	-34.208009	-12.583974
H	-0.874621	-34.616611	-11.757622
H	-0.015162	-33.187326	-12.309261

O	0.897482	-35.003945	-12.748525
P	1.683270	-35.339880	-11.321108
O	2.423629	-34.106193	-10.854495
O	2.747553	-36.443644	-11.852524
O	0.666915	-36.003852	-10.396013
C	-4.743443	-29.178375	-16.052434
H	-5.351200	-28.615436	-15.328779
H	-3.904190	-28.532046	-16.349088
H	-5.352906	-29.355492	-16.942165
C	-4.230323	-30.490166	-15.443181
H	-3.374052	-30.278059	-14.786816
H	-3.848711	-31.128919	-16.242951
C	-5.288889	-31.249054	-14.638775
H	-5.602585	-30.660725	-13.764685
H	-4.850393	-32.174527	-14.234987
C	-6.557688	-31.661876	-15.426812
O	-7.578703	-31.923629	-14.693180
O	-6.491474	-31.728757	-16.668676
C	1.335476	-39.216791	-8.629015
H	1.936105	-38.795922	-9.440970
H	1.981140	-39.319542	-7.742660
H	0.985201	-40.220296	-8.921687
C	0.149510	-38.292040	-8.304963
H	-0.428478	-38.725743	-7.474223
H	-0.529338	-38.251276	-9.171987
O	0.558993	-37.001343	-7.913785
H	0.711403	-36.499757	-8.758598
C	4.538108	-32.972651	-13.022430
H	5.261938	-33.624212	-13.528008
H	4.011610	-33.558841	-12.262755

H	5.082563	-32.141462	-12.551000
C	3.489363	-32.451123	-14.021559
H	2.876893	-33.296315	-14.366241
H	3.941155	-31.988171	-14.905481
C	2.521243	-31.413757	-13.450577
O	2.160596	-30.436012	-14.113844
N	2.094802	-31.636767	-12.179632
H	2.212122	-32.544796	-11.696120
H	1.333045	-31.046064	-11.872400
C	1.913934	-31.307485	-18.620135
H	2.947542	-31.538204	-18.325226
H	1.897229	-30.267098	-18.968617
H	1.658014	-31.949350	-19.472997
C	0.975763	-31.537645	-17.439877
H	1.053514	-32.593255	-17.127758
H	1.317604	-30.938162	-16.578805
O	-0.349373	-31.216156	-17.816967
H	-0.925061	-31.640417	-17.130802
C	2.340039	-39.588013	-16.840794
H	2.865357	-39.504589	-15.884354
H	2.514078	-38.649277	-17.382423
H	2.848561	-40.390153	-17.395935
C	0.847972	-39.883280	-16.633939
H	0.312063	-39.769391	-17.585733
H	0.728731	-40.937143	-16.340361
C	0.195874	-39.002271	-15.557532
H	0.291176	-37.942986	-15.837157
H	-0.881503	-39.211816	-15.508256
C	0.832482	-39.215370	-14.179029
H	1.900825	-38.963892	-14.193605

H	0.765846	-40.283563	-13.909834
C	0.185330	-38.375924	-13.091067
H	0.231792	-37.319287	-13.371117
H	-0.867398	-38.654127	-12.989644
N	0.917392	-38.515201	-11.819758
H	2.285749	-37.330738	-11.888288
H	0.820214	-39.464558	-11.462589
C	-7.115304	-42.523673	-12.920132
H	-6.342225	-41.991045	-12.356814
H	-7.888419	-41.790360	-13.176151
H	-7.545129	-43.321074	-12.295852
C	-6.497525	-43.130307	-14.191594
H	-5.705808	-43.839225	-13.861497
C	-7.532916	-43.934563	-14.984705
H	-8.348953	-43.271696	-15.297945
H	-7.954813	-44.755304	-14.387758
H	-7.072189	-44.351924	-15.888167
O	-5.980992	-42.166578	-15.066409
H	-5.327876	-41.590800	-14.567087
C	-9.372639	-34.158488	-9.021807
H	-9.097885	-34.912502	-8.277362
H	-10.104652	-34.620657	-9.696631
H	-8.490715	-33.900397	-9.611490
C	-9.966367	-32.933335	-8.310829
H	-10.374596	-32.215461	-9.037091
H	-9.158335	-32.390083	-7.789814
C	-11.077329	-33.210238	-7.229085
O	-11.788149	-32.208588	-6.931890
O	-11.120003	-34.368872	-6.739695
C	-10.504022	-33.650038	-14.664008

H	-11.264184	-33.179395	-14.030687
H	-11.030408	-34.212898	-15.444855
H	-9.874153	-32.878563	-15.118103
C	-9.706407	-34.617478	-13.795129
O	-10.262643	-35.486584	-13.122685
N	-8.364577	-34.421314	-13.860650
H	-8.031227	-33.596430	-14.379065
C	-7.455515	-35.027911	-12.916085
H	-6.571866	-35.417768	-13.435455
H	-7.959330	-35.872886	-12.442951
C	-6.977484	-34.121053	-11.766523
O	-6.435164	-34.638479	-10.786400
N	-7.180718	-32.786892	-11.896619
H	-7.453594	-32.395623	-12.805685
C	-6.864241	-31.873365	-10.808130
H	-7.714707	-31.755460	-10.124724
H	-6.603083	-30.897072	-11.230515
H	-6.014747	-32.264561	-10.241302
C	-3.981415	-35.265743	-12.181063
H	-4.408150	-36.218121	-11.885497
H	-4.472007	-34.770250	-13.010696
C	-3.323338	-34.464046	-11.190811
C	-2.729528	-35.067740	-10.056749
C	-3.133108	-33.075190	-11.382120
C	-1.925585	-34.340035	-9.190222
H	-2.867933	-36.132624	-9.895575
C	-2.360994	-32.339858	-10.488715
H	-3.588896	-32.593323	-12.242312
C	-1.737767	-32.968926	-9.404026
H	-1.406078	-34.854117	-8.386439

H	-2.220922	-31.273670	-10.654181
H	-1.093309	-32.399092	-8.739032

TS-3''

B3LYP-D3 SCF energy (au):	-3711.88591703
B3LYP-D3 enthalpy (au):	-3710.55083603
wB97X-D SCF energy (au):	-3712.41544583
wB97X-D enthalpy (au):	-3711.08036483

Cartesian coordinates

ATOM	X	Y	Z
C	-3.050064	-36.109903	-13.373831
H	-3.149508	-35.821204	-12.330804
N	-3.703322	-37.184784	-13.751894
H	-3.530919	-37.503352	-14.715317
C	-4.537220	-38.052945	-12.996505
H	-0.486572	-37.702274	-11.381757
C	-4.477753	-39.479271	-13.565372
O	-5.302185	-40.308496	-13.085754
O	-3.619263	-39.670000	-14.464325
C	-5.297308	-37.636096	-11.974405
H	-5.356405	-36.602411	-11.642330
H	-5.935052	-38.346488	-11.462718
C	-2.274265	-35.320570	-14.274597
C	-1.339442	-34.348047	-13.823773
C	-0.857549	-33.383074	-14.747733
H	0.050185	-32.844998	-14.485695
N	-1.014240	-33.570285	-16.125098
C	-1.759645	-34.537711	-16.573004
C	-1.929692	-34.699687	-18.059177

H	-1.436189	-33.876438	-18.584036
H	-1.511909	-35.659292	-18.388943
H	-2.994779	-34.728801	-18.317164
C	-2.430558	-35.525810	-15.707159
O	-3.072095	-36.468499	-16.237083
C	-0.715998	-34.373076	-12.454835
H	-1.342100	-34.851513	-11.697548
H	-0.507049	-33.353845	-12.112909
O	0.526247	-35.107906	-12.586764
P	1.395034	-35.436826	-11.205918
O	2.391987	-34.321218	-10.962514
O	2.205553	-36.753408	-11.705989
O	0.380636	-35.806279	-10.134834
C	-4.743181	-29.178377	-16.052328
H	-4.840231	-28.112731	-15.794922
H	-3.693325	-29.357983	-16.322418
H	-5.353011	-29.355516	-16.942243
C	-5.132338	-30.052306	-14.852711
H	-4.375437	-29.906349	-14.072062
H	-5.061395	-31.112034	-15.131186
C	-6.526774	-29.794243	-14.245657
H	-6.718183	-28.709595	-14.230847
H	-6.532507	-30.150496	-13.209663
C	-7.667854	-30.494821	-15.027911
O	-8.229082	-31.473281	-14.421868
O	-7.926658	-30.062611	-16.170146
C	1.335456	-39.216737	-8.628752
H	1.909390	-38.773892	-9.449351
H	1.981175	-39.319567	-7.742724
H	0.985177	-40.220292	-8.921822

C	0.166759	-38.298355	-8.244262
H	-0.414831	-38.776081	-7.437942
H	-0.515157	-38.178620	-9.098270
O	0.625137	-37.050419	-7.780508
H	0.641635	-36.464012	-8.583869
C	4.537779	-32.972492	-13.022406
H	5.269222	-33.622245	-13.520667
H	4.011701	-33.558875	-12.262670
H	5.082757	-32.141528	-12.551053
C	3.499532	-32.456568	-14.036311
H	2.971862	-33.318703	-14.468649
H	3.962127	-31.908302	-14.864419
C	2.418299	-31.530551	-13.464034
O	2.050900	-30.524693	-14.088263
N	1.900360	-31.890875	-12.269275
H	2.075178	-32.808663	-11.820240
H	1.069489	-31.391889	-11.974901
C	1.913738	-31.307310	-18.620219
H	2.961620	-31.520807	-18.357188
H	1.897277	-30.267147	-18.968578
H	1.658165	-31.949485	-19.472988
C	1.033885	-31.560368	-17.406331
H	1.224053	-32.581214	-17.040887
H	1.326173	-30.883772	-16.587237
O	-0.334724	-31.415526	-17.742227
H	-0.773174	-32.119452	-17.200182
C	2.340078	-39.587907	-16.840709
H	2.824899	-39.502434	-15.862140
H	2.514073	-38.649342	-17.382496
H	2.848527	-40.390158	-17.395930

C	0.838243	-39.891028	-16.701363
H	0.377354	-39.864810	-17.699400
H	0.716149	-40.922957	-16.338517
C	0.067089	-38.952134	-15.758761
H	0.189246	-37.909679	-16.087017
H	-1.006246	-39.169906	-15.833858
C	0.488367	-39.074867	-14.287023
H	1.513169	-38.710554	-14.132803
H	0.480867	-40.139270	-13.997613
C	-0.446307	-38.294797	-13.363833
H	-0.411764	-37.235946	-13.632809
H	-1.474925	-38.653303	-13.504378
N	0.007736	-38.383628	-11.960759
H	1.535024	-37.495699	-11.799438
H	-0.201862	-39.302880	-11.574325
C	-6.906349	-43.022733	-12.704541
H	-6.119603	-42.480664	-12.173912
H	-7.829924	-42.444950	-12.591193
H	-7.034365	-44.028354	-12.278017
C	-6.545421	-43.157636	-14.193165
H	-5.571819	-43.694761	-14.247129
C	-7.577300	-44.007496	-14.943402
H	-8.565132	-43.535675	-14.868910
H	-7.640450	-45.026694	-14.535454
H	-7.311383	-44.066863	-16.005862
O	-6.480353	-41.925074	-14.851899
H	-5.952626	-41.299948	-14.270066
C	-9.372277	-34.159605	-9.022185
H	-10.113710	-33.350977	-9.134532
H	-9.075858	-34.199833	-7.963111

H	-8.490345	-33.900201	-9.611287
C	-9.893038	-35.522942	-9.496899
H	-10.178972	-35.447103	-10.554284
H	-10.776437	-35.820947	-8.912243
C	-8.779224	-36.620890	-9.363226
O	-8.983606	-37.521902	-8.509960
O	-7.779625	-36.446930	-10.116540
C	-10.504077	-33.649984	-14.664068
H	-11.419044	-33.471037	-14.089088
H	-10.796108	-34.154829	-15.595094
H	-10.007757	-32.702844	-14.899990
C	-9.618024	-34.587188	-13.847287
O	-10.093721	-35.534703	-13.224879
N	-8.291435	-34.284346	-13.917210
H	-8.059077	-33.393939	-14.364920
C	-7.296821	-34.896845	-13.052306
H	-6.522941	-35.415946	-13.627736
H	-7.783595	-35.628065	-12.389286
C	-6.612602	-33.911727	-12.107919
O	-5.539414	-34.187297	-11.560944
N	-7.311190	-32.772120	-11.844654
H	-7.887807	-32.375207	-12.588546
C	-6.864237	-31.872994	-10.808147
H	-7.687630	-31.200228	-10.545547
H	-5.993846	-31.270190	-11.106756
H	-6.583865	-32.456505	-9.927085
C	-2.030823	-31.662419	-14.565698
H	-2.906382	-32.074073	-15.059784
H	-1.436319	-30.997564	-15.188831
C	-2.152906	-31.364786	-13.158253

C	-3.103994	-32.050128	-12.365406
C	-1.250061	-30.492547	-12.505215
C	-3.137496	-31.892738	-10.983147
H	-3.807061	-32.736069	-12.828173
C	-1.298684	-30.326585	-11.122162
H	-0.485695	-29.988174	-13.094519
C	-2.235577	-31.029054	-10.351254
H	-3.866392	-32.469451	-10.421297
H	-0.590330	-29.655026	-10.637633
H	-2.252175	-30.913904	-9.269718

TS-4

B3LYP-D3 SCF energy (au):	-3711.72726555
B3LYP-D3 enthalpy (au):	-3710.40061555
wB97X-D SCF energy (au):	-3712.51466913
wB97X-D enthalpy (au):	-3711.18801913

Cartesian coordinates

ATOM	X	Y	Z
C	-3.446749	-35.795178	-13.474849
H	-3.306081	-35.697023	-12.406127
N	-3.998168	-36.917714	-13.873837
H	-4.063519	-37.044906	-14.894210
C	-4.288916	-38.058660	-13.057134
H	-2.689064	-38.184699	-12.580130
C	-4.535697	-39.282652	-13.896748
O	-5.178288	-40.250002	-13.329036
O	-4.064093	-39.321794	-15.067446
C	-5.243981	-37.827318	-11.894844
H	-4.957021	-36.951290	-11.300839

H	-5.168300	-38.700245	-11.239908
C	-2.913820	-34.783272	-14.345382
C	-1.939936	-33.878232	-13.845807
C	-1.407805	-32.926113	-14.704230
H	-0.630154	-32.246312	-14.362962
N	-1.772204	-32.810185	-16.007729
C	-2.657303	-33.667819	-16.511640
C	-3.014336	-33.563171	-17.970792
H	-2.376461	-32.826657	-18.470771
H	-2.908861	-34.542566	-18.454934
H	-4.068796	-33.279038	-18.100026
C	-3.258343	-34.752882	-15.752795
O	-4.014949	-35.604613	-16.314779
C	-1.386812	-34.023328	-12.438026
H	-2.180414	-33.859864	-11.690561
H	-0.624531	-33.252972	-12.275688
O	-0.845840	-35.324960	-12.280062
P	0.605465	-35.610744	-11.424460
O	1.676613	-34.751537	-12.144562
O	0.704373	-37.137981	-11.651789
O	0.355496	-35.202816	-9.962337
C	-4.743568	-29.178265	-16.052334
H	-4.566089	-28.093160	-15.995342
H	-3.774434	-29.664916	-16.223232
H	-5.352828	-29.355546	-16.942260
C	-5.363327	-29.684484	-14.742676
H	-4.629547	-29.512070	-13.942053
H	-5.505270	-30.771212	-14.783548
C	-6.706838	-29.026802	-14.361686
H	-6.679356	-27.953875	-14.603932

H	-6.855377	-29.130926	-13.278603
C	-7.910899	-29.698829	-15.075883
O	-8.296229	-30.788444	-14.527235
O	-8.370425	-29.153417	-16.099909
C	1.335465	-39.216793	-8.628500
H	1.957439	-38.841838	-9.450600
H	1.981198	-39.319543	-7.742766
H	0.985154	-40.220274	-8.921983
C	0.219258	-38.184370	-8.412359
H	-0.489678	-38.560228	-7.646922
H	-0.331925	-38.077180	-9.355946
O	0.759539	-36.953632	-8.001253
H	0.645461	-36.298968	-8.769767
C	4.537827	-32.972400	-13.022275
H	5.267238	-33.624930	-13.522386
H	4.011632	-33.558914	-12.262701
H	5.082825	-32.141565	-12.551157
C	3.472436	-32.461179	-14.007370
H	2.896763	-33.321172	-14.368822
H	3.917111	-31.933737	-14.858827
C	2.528166	-31.479515	-13.305911
O	2.586419	-30.259301	-13.529195
N	1.710416	-32.063492	-12.411908
H	1.640558	-33.119086	-12.267306
H	1.058812	-31.459046	-11.929681
C	1.913782	-31.307283	-18.620230
H	2.948330	-31.538032	-18.325979
H	1.897283	-30.267160	-18.968595
H	1.658151	-31.949491	-19.472983
C	0.973189	-31.534236	-17.434124

H	1.052457	-32.586377	-17.113131
H	1.332308	-30.928714	-16.580013
O	-0.348354	-31.207572	-17.793293
H	-0.939397	-31.687108	-17.133431
C	2.340012	-39.587976	-16.840652
H	2.757284	-39.501859	-15.832759
H	2.514102	-38.649299	-17.382440
H	2.848504	-40.390154	-17.395992
C	0.837268	-39.903115	-16.841309
H	0.521362	-40.015827	-17.890354
H	0.668361	-40.883743	-16.370365
C	-0.059414	-38.864200	-16.161115
H	0.197280	-37.857028	-16.520186
H	-1.094280	-39.045772	-16.478447
C	-0.039923	-38.890757	-14.624874
H	0.899189	-38.523631	-14.193552
H	-0.167382	-39.937509	-14.298549
C	-1.211665	-38.061852	-14.106811
H	-1.016246	-36.992612	-14.205404
H	-2.111160	-38.327228	-14.668310
N	-1.523826	-38.288070	-12.668925
H	-0.838849	-37.705775	-12.091511
H	-1.352699	-39.266271	-12.429095
C	-6.906306	-43.022612	-12.704482
H	-6.123509	-42.480940	-12.164731
H	-7.830003	-42.445031	-12.591194
H	-7.034357	-44.028331	-12.278075
C	-6.528029	-43.127159	-14.195177
H	-5.535388	-43.634577	-14.240696
C	-7.524123	-44.020578	-14.949356

H	-8.528370	-43.582657	-14.883102
H	-7.556028	-45.042133	-14.540172
H	-7.248719	-44.070360	-16.010034
O	-6.512570	-41.899968	-14.847596
H	-5.917679	-41.240194	-14.330248
C	-9.371657	-34.160375	-9.021850
H	-9.339931	-33.543887	-8.108436
H	-9.271939	-35.201543	-8.704347
H	-8.490975	-33.899361	-9.611721
C	-10.714510	-33.963890	-9.737917
H	-10.724398	-34.586646	-10.644986
H	-10.835449	-32.920004	-10.057029
C	-11.929418	-34.369593	-8.831254
O	-12.831631	-33.503622	-8.665527
O	-11.880509	-35.536293	-8.343648
C	-10.504073	-33.650005	-14.664061
H	-11.243004	-33.786334	-13.869413
H	-10.850382	-34.196073	-15.550782
H	-10.404139	-32.586397	-14.907615
C	-9.178277	-34.254764	-14.186062
O	-9.151900	-35.321574	-13.574678
N	-8.070241	-33.547314	-14.539263
H	-8.191684	-32.565456	-14.814896
C	-6.759508	-33.929237	-14.036013
H	-5.991722	-33.463772	-14.664614
H	-6.626129	-35.008097	-14.111426
C	-6.484143	-33.539536	-12.571253
O	-5.793177	-34.252541	-11.844866
N	-7.022922	-32.351072	-12.169653
H	-7.517182	-31.770465	-12.852326

C	-6.864103	-31.873090	-10.808044
H	-7.839423	-31.677405	-10.345771
H	-6.263966	-30.951100	-10.774581
H	-6.347531	-32.651085	-10.243033
C	-6.729318	-37.656969	-12.348151
H	-6.924646	-36.609645	-12.587973
H	-6.861344	-38.239399	-13.266419
C	-7.749228	-38.151732	-11.347270
C	-7.769221	-39.516367	-11.005735
C	-8.704253	-37.304817	-10.767040
C	-8.711359	-40.009237	-10.102497
H	-7.040762	-40.170601	-11.481450
C	-9.655702	-37.790484	-9.860338
H	-8.716198	-36.256516	-11.052384
C	-9.653514	-39.148303	-9.525364
H	-8.713832	-41.072106	-9.852713
H	-10.391920	-37.113109	-9.422613
H	-10.390384	-39.533414	-8.819436

TS-5

B3LYP-D3 SCF energy (au):	-3517.35436041
B3LYP-D3 enthalpy (au):	-3516.11735641
wB97X-D SCF energy (au):	-3517.92897921
wB97X-D enthalpy (au):	-3516.69197521

Cartesian coordinates

ATOM	X	Y	Z
C	-2.230758	-36.353007	-13.426834
H	-1.860091	-36.352591	-12.405170
N	-4.164911	-36.654058	-13.094353

H	-4.562209	-35.833360	-12.629215
C	-4.533948	-37.916061	-12.405028
H	-3.644366	-38.243205	-11.849855
C	-4.868756	-39.067896	-13.425243
O	-5.721187	-39.934648	-12.994745
O	-4.295983	-39.072455	-14.519229
C	-5.645429	-37.747557	-11.356703
H	-5.599546	-36.760226	-10.891730
H	-5.507834	-38.516026	-10.582041
O	-6.951096	-37.871242	-11.930328
H	-6.918718	-38.760309	-12.366093
C	-2.224627	-35.049101	-14.126088
C	-1.510804	-33.958731	-13.591488
C	-1.279459	-32.869610	-14.435063
H	-0.678529	-32.030523	-14.092300
N	-1.712252	-32.807806	-15.715530
C	-2.452421	-33.803075	-16.204963
C	-2.924716	-33.713877	-17.632877
H	-2.307640	-33.004830	-18.194834
H	-2.889695	-34.705682	-18.098660
H	-3.973574	-33.384718	-17.688008
C	-2.782770	-34.990493	-15.448063
O	-3.492191	-35.941019	-15.941884
C	-0.997528	-33.916117	-12.160445
H	-1.862554	-33.828924	-11.478614
H	-0.419619	-32.994001	-12.027634
O	-0.232013	-35.057407	-11.827580
P	1.027935	-34.773818	-10.656253
O	2.188367	-34.219382	-11.532291
O	1.290223	-36.204889	-10.139812

O	0.450130	-33.767399	-9.677219
C	-4.743376	-29.178060	-16.052217
H	-5.129770	-28.278974	-15.553084
H	-3.713212	-28.975845	-16.376407
H	-5.353044	-29.355389	-16.942105
C	-4.779560	-30.397379	-15.120426
H	-3.889900	-30.389071	-14.476683
H	-4.687060	-31.313218	-15.718060
C	-6.012719	-30.497490	-14.211132
H	-6.071748	-29.586297	-13.590466
H	-5.864652	-31.330074	-13.516297
C	-7.395418	-30.656728	-14.895002
O	-8.235349	-31.396365	-14.252203
O	-7.622745	-30.052083	-15.956967
C	1.333896	-39.216881	-8.628450
H	1.910374	-38.764058	-9.441385
H	1.981694	-39.318935	-7.742961
H	0.985773	-40.220581	-8.922027
C	0.172613	-38.270387	-8.279480
H	-0.462742	-38.745783	-7.506696
H	-0.452071	-38.135514	-9.178446
O	0.638754	-37.048431	-7.789325
H	0.906774	-36.535075	-8.636899
C	4.537767	-32.972924	-13.022508
H	5.275466	-33.620343	-13.521196
H	4.011801	-33.559147	-12.262871
H	5.081968	-32.141278	-12.550716
C	3.505312	-32.450623	-14.038227
H	2.871041	-33.291624	-14.347226
H	3.979418	-32.025868	-14.931344

C	2.590833	-31.356914	-13.471224
O	2.468821	-30.260821	-14.049213
N	1.981494	-31.695484	-12.323384
H	2.005557	-32.699334	-11.926619
H	1.306922	-31.036855	-11.956691
C	1.912714	-31.308151	-18.619444
H	2.951811	-31.533171	-18.338434
H	1.896582	-30.267026	-18.968512
H	1.658999	-31.949380	-19.473299
C	1.005944	-31.559695	-17.410754
H	1.127445	-32.611292	-17.100077
H	1.361108	-30.949392	-16.562447
O	-0.342178	-31.278867	-17.737694
H	-0.894207	-31.673288	-17.007271
C	2.339158	-39.586063	-16.840312
H	2.905943	-39.484896	-15.903797
H	2.514176	-38.649902	-17.383196
H	2.848769	-40.390754	-17.395348
C	0.884989	-39.907414	-16.500679
H	0.246714	-39.856643	-17.394000
H	0.841547	-40.952671	-16.156119
C	0.330207	-39.000260	-15.394280
H	1.109139	-38.837445	-14.635614
H	0.094314	-38.007156	-15.793044
C	-0.898955	-39.586685	-14.696444
H	-0.640469	-40.564886	-14.263062
H	-1.713755	-39.767275	-15.411379
C	-1.439972	-38.689222	-13.584543
H	-2.253163	-39.226239	-13.088450
H	-0.661740	-38.470593	-12.841391

N	-1.872768	-37.429541	-14.162545
H	-4.408382	-36.657862	-14.092961
H	-2.350668	-37.462791	-15.063636
C	-6.905607	-43.020245	-12.703323
H	-6.141920	-42.481028	-12.133203
H	-7.830172	-42.445902	-12.591138
H	-7.035017	-44.028971	-12.279079
C	-6.525714	-43.046052	-14.191949
H	-5.489575	-43.438420	-14.272438
C	-7.438327	-43.985293	-14.986653
H	-8.481268	-43.659805	-14.883834
H	-7.355111	-45.023744	-14.636094
H	-7.176573	-43.947021	-16.050409
O	-6.640145	-41.780431	-14.784270
H	-6.203773	-41.091321	-14.202574
C	-9.369072	-34.163500	-9.023676
H	-9.877739	-33.235773	-8.727096
H	-9.025336	-34.666736	-8.111514
H	-8.491530	-33.896883	-9.611100
C	-10.312942	-35.058972	-9.835719
H	-10.560979	-34.574485	-10.788831
H	-11.250474	-35.256740	-9.302987
C	-9.714753	-36.400774	-10.227944
O	-10.354753	-37.439317	-10.268715
O	-8.427276	-36.277633	-10.520166
H	-8.059275	-37.075059	-11.003658
C	-10.503277	-33.650426	-14.663996
H	-11.472941	-33.668813	-14.157282
H	-10.627929	-34.092737	-15.661158
H	-10.141196	-32.622501	-14.782126

C	-9.517503	-34.488741	-13.859227
O	-9.891877	-35.395299	-13.112147
N	-8.222163	-34.161723	-14.106700
H	-8.077938	-33.224219	-14.499368
C	-7.121454	-34.726277	-13.356190
H	-6.247862	-34.816606	-14.012525
H	-7.386139	-35.730629	-13.018647
C	-6.672674	-33.941218	-12.115440
O	-5.793997	-34.419396	-11.389482
N	-7.286149	-32.747787	-11.889088
H	-7.762814	-32.285472	-12.681573
C	-6.863089	-31.873776	-10.808625
H	-7.731798	-31.527764	-10.233256
H	-6.329061	-30.998218	-11.199768
H	-6.191611	-32.432468	-10.153089

TS-6

B3LYP-D3 SCF energy (au):	-3517.37640495
B3LYP-D3 enthalpy (au):	-3516.13487795
wB97X-D SCF energy (au):	-3517.94764859
wB97X-D enthalpy (au):	-3516.70612159

Cartesian coordinates

ATOM	X	Y	Z
C	-3.095539	-36.115021	-13.099847
H	-2.592893	-36.019441	-12.139541
N	-4.282396	-36.783915	-13.057065
H	-4.841539	-36.688046	-13.911046
C	-4.477856	-37.902225	-12.133541
H	-3.605285	-37.902316	-11.468197

C	-4.442425	-39.289184	-12.876451
O	-5.556579	-39.922591	-12.959944
O	-3.345056	-39.674696	-13.324250
C	-5.703237	-37.726371	-11.224279
H	-5.739500	-36.699660	-10.854109
H	-5.592072	-38.421023	-10.372216
O	-6.946129	-37.972781	-11.889122
H	-6.780097	-38.821337	-12.375667
C	-2.916515	-34.975253	-14.031762
C	-1.786898	-34.140261	-13.875047
C	-1.469908	-33.257674	-14.902174
H	-0.596886	-32.613677	-14.814670
N	-2.185719	-33.140297	-16.046537
C	-3.292872	-33.868861	-16.181750
C	-4.129277	-33.699701	-17.421852
H	-3.569939	-33.139035	-18.179391
H	-4.430914	-34.678135	-17.815167
H	-5.057405	-33.153330	-17.198921
C	-3.748210	-34.841790	-15.195935
O	-4.799131	-35.547432	-15.414254
C	-0.938192	-34.109336	-12.621900
H	-1.557349	-33.806711	-11.764449
H	-0.186819	-33.323486	-12.754701
O	-0.301398	-35.349750	-12.330312
P	1.000498	-35.132798	-11.153982
O	2.165803	-34.624773	-12.046071
O	1.174831	-36.562533	-10.611029
O	0.470826	-34.083657	-10.191173
C	-4.743526	-29.178311	-16.052266
H	-5.296138	-28.499025	-15.385030

H	-3.822281	-28.662678	-16.361290
H	-5.352825	-29.355505	-16.942267
C	-4.422460	-30.508068	-15.361474
H	-3.565089	-30.381586	-14.686084
H	-4.099398	-31.229711	-16.114624
C	-5.587235	-31.085914	-14.555446
H	-5.815154	-30.433716	-13.697820
H	-5.284593	-32.047662	-14.117980
C	-6.913444	-31.326708	-15.313838
O	-7.901600	-31.641260	-14.547907
O	-6.951385	-31.227190	-16.554140
C	1.335392	-39.216860	-8.628472
H	1.920321	-38.793063	-9.451407
H	1.981246	-39.319468	-7.742808
H	0.985159	-40.220276	-8.921988
C	0.181865	-38.244613	-8.345541
H	-0.412292	-38.607538	-7.486100
H	-0.482951	-38.230007	-9.223890
O	0.661306	-36.962712	-8.048556
H	0.881535	-36.581856	-8.961133
C	4.537877	-32.972478	-13.022352
H	5.272376	-33.623829	-13.518829
H	4.011632	-33.558916	-12.262696
H	5.082734	-32.141525	-12.551089
C	3.494856	-32.457896	-14.027909
H	2.912362	-33.321007	-14.373919
H	3.952799	-31.961802	-14.892235
C	2.521725	-31.453837	-13.397748
O	2.362188	-30.316826	-13.873076
N	1.914048	-31.929984	-12.295740

H	1.953787	-32.965580	-12.064396
H	1.173621	-31.377593	-11.885131
C	1.913735	-31.307520	-18.620144
H	2.938860	-31.533690	-18.298740
H	1.897215	-30.267044	-18.968642
H	1.658211	-31.949413	-19.472992
C	0.927101	-31.603163	-17.476654
H	1.134552	-32.619883	-17.103357
H	1.119463	-30.922618	-16.629375
O	-0.400120	-31.499771	-17.963893
H	-1.010780	-31.974143	-17.346530
C	2.339825	-39.587776	-16.840362
H	2.847104	-39.488420	-15.872204
H	2.514161	-38.649417	-17.382582
H	2.848645	-40.390202	-17.396162
C	0.841345	-39.811664	-16.636814
H	0.346148	-39.915656	-17.614577
H	0.665128	-40.756157	-16.101800
C	0.200290	-38.650694	-15.865636
H	0.625019	-38.598537	-14.853942
H	0.479711	-37.705559	-16.355543
C	-1.325218	-38.732983	-15.792275
H	-1.654525	-39.607926	-15.218253
H	-1.723404	-38.857965	-16.811813
C	-1.974504	-37.480088	-15.201295
H	-1.600470	-36.580337	-15.697684
H	-3.054595	-37.516334	-15.373693
N	-1.786111	-37.306593	-13.755049
H	-0.912755	-36.858279	-13.437103
H	-1.992925	-38.191406	-13.277059

C	-6.906119	-43.021715	-12.704321
H	-6.147128	-42.487912	-12.121411
H	-7.830174	-42.445556	-12.591182
H	-7.034449	-44.028596	-12.278190
C	-6.475560	-43.059177	-14.176480
H	-5.485494	-43.561894	-14.220061
C	-7.448284	-43.878908	-15.029365
H	-8.450764	-43.437204	-14.970970
H	-7.500367	-44.923614	-14.691621
H	-7.132197	-43.860438	-16.078935
O	-6.419645	-41.778894	-14.746630
H	-5.962229	-41.143849	-14.124627
C	-9.369961	-34.161443	-9.022419
H	-9.882367	-33.228774	-8.745345
H	-9.016346	-34.634584	-8.097285
H	-8.491488	-33.898947	-9.611787
C	-10.336825	-35.079613	-9.784192
H	-10.587710	-34.634990	-10.755228
H	-11.272020	-35.224578	-9.229146
C	-9.807741	-36.463015	-10.137538
O	-10.509413	-37.462960	-10.162419
O	-8.514901	-36.424676	-10.425147
H	-8.179673	-37.231082	-10.907357
C	-10.504092	-33.649941	-14.664069
H	-11.423193	-33.403326	-14.121841
H	-10.783127	-34.237289	-15.548865
H	-9.989886	-32.738301	-14.987721
C	-9.619167	-34.499121	-13.751811
O	-10.112012	-35.303002	-12.950912
N	-8.300276	-34.305519	-13.961345

H	-8.055478	-33.456334	-14.482487
C	-7.258731	-34.867614	-13.119846
H	-6.354265	-34.985969	-13.728520
H	-7.552752	-35.855873	-12.769941
C	-6.908091	-34.024528	-11.888182
O	-6.291895	-34.498236	-10.931422
N	-7.304237	-32.719253	-11.899971
H	-7.565822	-32.271023	-12.792182
C	-6.864122	-31.873165	-10.808085
H	-7.414353	-32.088187	-9.883346
H	-7.042081	-30.829142	-11.087109
H	-5.797649	-32.017010	-10.596605

Cartesian coordinates of structures computed using the free PLP cofactor model in the absence of active site residues

10A (free PLP cofactor model)

B3LYP-D3 SCF energy (au):	-1674.32907938
B3LYP-D3 enthalpy (au):	-1673.95861738
wB97X-D SCF energy (au):	-1674.50700065
wB97X-D enthalpy (au):	-1674.13653865

Cartesian coordinates

ATOM	X	Y	Z
N	-1.682560	0.330184	0.464201
H	-2.574112	-0.183421	0.359317
C	-0.547849	-0.301615	0.237738
H	0.354666	0.304550	0.269950
C	-0.439242	-1.695746	-0.025555
C	0.843950	-2.307200	-0.192731

C	0.905437	-3.665893	-0.413767
C	-1.375907	-3.959192	-0.349665
C	-1.624561	-2.532001	-0.111628
H	1.871941	-4.151906	-0.544520
N	-0.181239	-4.490270	-0.489429
O	-2.805291	-2.108951	0.009273
C	-2.588715	-4.847627	-0.434277
H	-3.182545	-4.784043	0.487109
H	-3.257619	-4.514611	-1.238633
H	-2.284096	-5.884359	-0.609813
C	2.128715	-1.516582	-0.113623
H	2.983830	-2.209162	-0.112446
H	2.170406	-0.940734	0.819699
O	2.240728	-0.633188	-1.229445
P	2.940971	0.860475	-0.969434
O	2.931563	1.534749	-2.313664
O	2.383504	1.436861	0.302287
O	4.524844	0.401978	-0.646239
H	4.932849	0.328347	-1.523102
C	-1.863603	1.701391	0.779543
C	-3.364080	2.106721	0.779624
O	-4.140695	1.182151	0.411316
O	-3.620159	3.286744	1.104609
C	-0.862213	2.561375	1.004906
H	0.195564	2.317845	0.935614
H	-1.156981	3.584203	1.209444
C	-0.503622	0.564823	-2.753015
H	-1.198350	-0.263735	-2.652636
H	0.549742	0.339566	-2.874617
C	-0.944522	1.892133	-2.596552

C	-2.305685	2.200303	-2.299251
C	-0.018945	2.977672	-2.684502
C	-2.714634	3.510505	-2.100738
H	-3.009234	1.391205	-2.122010
C	-0.451493	4.282828	-2.506718
H	1.033529	2.747493	-2.832917
C	-1.796950	4.563088	-2.218983
H	-3.733071	3.706892	-1.779774
H	0.271265	5.096233	-2.558573
H	-2.117944	5.587821	-2.041585

TS-3A (free PLP cofactor model)

B3LYP-D3 SCF energy (au):	-1674.32343142
B3LYP-D3 enthalpy (au):	-1673.95330342
wB97X-D SCF energy (au):	-1674.49351661
wB97X-D enthalpy (au):	-1674.12338861

Cartesian coordinates

ATOM	X	Y	Z
N	-2.280825	-0.064310	-0.125884
H	-3.086478	-0.676472	-0.334191
C	-1.074161	-0.608003	-0.032365
H	-0.259309	0.082137	0.155845
C	-0.790020	-1.988266	-0.173901
C	0.559352	-2.460704	-0.082236
C	0.795858	-3.809792	-0.232457
C	-1.421211	-4.346482	-0.549087
C	-1.851808	-2.950892	-0.420769
H	1.814367	-4.193125	-0.173905
N	-0.171038	-4.748020	-0.458863

O	-3.072635	-2.649644	-0.514802
C	-2.501865	-5.364876	-0.799400
H	-3.056362	-5.124723	-1.716011
H	-3.246345	-5.349288	0.007666
H	-2.064390	-6.365000	-0.881199
C	1.714885	-1.537995	0.231753
H	1.541926	-1.049265	1.200613
H	2.640462	-2.126376	0.314364
O	1.880567	-0.541937	-0.780051
P	2.347770	0.976773	-0.283030
O	2.444935	1.806844	-1.526327
O	3.884504	0.644203	0.312155
H	3.795456	0.824387	1.260802
O	1.528919	1.366592	0.929484
C	-2.593662	1.297416	-0.044162
C	-4.032953	1.632053	-0.502965
O	-4.798587	0.637376	-0.579362
O	-4.251381	2.843838	-0.753617
C	-1.686739	2.260003	0.286347
H	-2.081529	3.264731	0.356699
H	-0.687738	2.065401	0.669006
C	-0.853661	2.865636	-1.888849
H	-0.038421	2.151449	-1.943404
H	-1.829013	2.581644	-2.262919
C	-0.564162	4.247227	-1.701148
C	0.768841	4.699469	-1.498997
C	-1.612995	5.208573	-1.676067
C	1.030098	6.053878	-1.327103
H	1.565821	3.958131	-1.480827
C	-1.332418	6.557408	-1.498230

H	-2.637687	4.848006	-1.746019
C	-0.009760	6.996115	-1.333388
H	2.057628	6.384984	-1.180641
H	-2.149249	7.278173	-1.476579
H	0.205285	8.054931	-1.195885

TS-3A' (free PLP cofactor model)

B3LYP-D3 SCF energy (au):	-1674.31958855
B3LYP-D3 enthalpy (au):	-1673.94942155
wB97X-D SCF energy (au):	-1674.49387210
wB97X-D enthalpy (au):	-1674.12370510

Cartesian coordinates

ATOM	X	Y	Z
N	-1.789448	0.073574	0.534185
H	-2.637194	-0.512674	0.500234
C	-0.642461	-0.452039	0.038469
H	0.219554	0.207634	0.069628
C	-0.404799	-1.886198	0.014532
C	0.912870	-2.408845	-0.041772
C	1.079577	-3.785049	-0.078604
C	-1.175909	-4.217682	-0.054675
C	-1.522412	-2.801923	-0.023106
H	2.084735	-4.207222	-0.103949
N	0.061796	-4.683110	-0.079149
O	-2.736284	-2.431178	-0.045569
C	-2.322556	-5.194048	-0.074874
H	-2.971036	-5.054061	0.800429
H	-2.966446	-5.019033	-0.947383
H	-1.943287	-6.221191	-0.095128

C	2.132206	-1.519766	-0.015326
H	3.038907	-2.137248	0.066842
H	2.104404	-0.854860	0.857133
O	2.211645	-0.731626	-1.209266
P	2.846576	0.807583	-1.067317
O	2.836444	1.365487	-2.464687
O	2.234338	1.472634	0.132837
O	4.437886	0.443698	-0.675850
H	4.864024	0.287321	-1.533052
C	-2.023287	1.408438	0.850466
C	-3.537714	1.744460	1.011357
O	-4.306428	0.787336	0.721709
O	-3.807057	2.911212	1.370882
C	-1.052543	2.341255	0.976798
H	0.008277	2.158588	0.822772
H	-1.390203	3.344972	1.206927
C	-0.937007	-0.189901	-2.098334
H	-1.713428	-0.949393	-2.101571
H	0.065940	-0.502013	-2.370643
C	-1.322923	1.174996	-2.313982
C	-2.662448	1.584249	-2.096242
C	-0.362732	2.154181	-2.676737
C	-3.028875	2.917550	-2.242985
H	-3.387686	0.866260	-1.723088
C	-0.748647	3.479153	-2.839141
H	0.679847	1.865284	-2.798952
C	-2.078155	3.868532	-2.625761
H	-4.046204	3.218607	-2.008716
H	0.000297	4.221202	-3.109165
H	-2.363796	4.914409	-2.726661

TS-3A'' (free PLP cofactor model)

B3LYP-D3 SCF energy (au):	-1674.29917686
B3LYP-D3 enthalpy (au):	-1673.92943286
wB97X-D SCF energy (au):	-1674.48065756
wB97X-D enthalpy (au):	-1674.11091356

Cartesian coordinates

ATOM	X	Y	Z
N	-2.272451	0.568602	0.336707
H	-3.082960	-0.050779	0.161667
C	-1.061663	0.063544	0.453213
H	-0.253980	0.775043	0.626665
C	-0.749465	-1.327884	0.372797
C	0.597610	-1.769180	0.411484
C	0.857572	-3.159984	0.234777
C	-1.375100	-3.730982	0.466528
C	-1.809549	-2.323547	0.299191
H	1.858628	-3.502968	0.493368
N	-0.135252	-4.122142	0.479491
O	-3.030006	-2.063536	0.176597
C	-2.471320	-4.747253	0.654029
H	-3.094398	-4.491612	1.520144
H	-3.145960	-4.742516	-0.210805
H	-2.038987	-5.743615	0.785684
C	1.762197	-0.818608	0.551437
H	1.706325	-0.021963	-0.199787
H	2.702121	-1.358383	0.373682
O	1.776349	-0.247821	1.864145
P	2.240857	1.356761	1.977052

O	2.339186	1.656454	3.442550
O	3.798787	1.260516	1.356428
H	4.342623	0.994510	2.114082
O	1.435395	2.146724	0.978070
C	-2.658314	1.934541	0.392493
C	-4.175756	2.119134	0.093050
O	-4.783020	1.035785	-0.128150
O	-4.598548	3.295095	0.105138
C	-1.821344	2.944856	0.662973
H	-0.758656	2.837799	0.873065
H	-2.268378	3.933297	0.662313
C	1.067152	-3.490520	-1.785997
H	0.091034	-3.085930	-2.047275
H	1.092390	-4.578224	-1.754719
C	2.227769	-2.822691	-2.322945
C	2.182697	-1.453116	-2.686451
C	3.482211	-3.474317	-2.420424
C	3.321325	-0.781259	-3.116071
H	1.238554	-0.921059	-2.600725
C	4.617024	-2.800765	-2.859353
H	3.548617	-4.524328	-2.139029
C	4.549460	-1.446998	-3.212234
H	3.255018	0.275422	-3.364693
H	5.566235	-3.331527	-2.923039
H	5.439728	-0.916816	-3.542271

Cartesian coordinates of computed structures in the electron transfer step

11A

B3LYP-D3 SCF energy (au): -1107.33595008

B3LYP-D3 enthalpy (au):	-1106.97972708
B3LYP-D3 free energy (au):	-1107.05669808
wB97X-D SCF energy (au):	-1107.28399933
wB97X-D enthalpy (au):	-1106.92777633
wB97X-D free energy (au):	-1107.00474733
wB97X-D free energy (quasi-harmonic) (au):	-1106.99958325

Cartesian coordinates

ATOM	X	Y	Z
N	-2.875478	0.062098	-0.136793
H	-3.348574	-0.859883	-0.159410
C	-1.529700	0.006389	-0.037478
H	-1.004069	0.948072	0.012485
C	-0.818020	-1.204752	0.019419
C	0.616905	-1.195774	0.029054
C	1.275091	-2.398541	0.114611
C	-0.658398	-3.667395	0.159179
C	-1.501101	-2.484945	0.060164
H	2.362195	-2.422595	0.119465
N	0.660725	-3.618044	0.186449
O	-2.774242	-2.599635	0.016917
C	-1.344767	-5.001186	0.226471
H	-2.029864	-5.046589	1.082540
H	-1.956391	-5.172515	-0.668649
H	-0.610720	-5.806035	0.313965
C	1.400547	0.083341	-0.118509
H	1.096283	0.601963	-1.039463
H	2.469393	-0.151655	-0.206637
O	1.168107	0.938022	1.018410
C	-3.654164	1.151687	-0.217978

C	-5.127202	0.892637	-0.416857
O	-5.498714	-0.318282	-0.371289
O	-5.849516	1.909304	-0.619759
C	-3.049138	2.511130	-0.203321
H	-3.829157	3.241477	0.018433
H	-2.296036	2.574085	0.592572
C	-2.379400	2.874572	-1.564252
H	-1.794428	2.019347	-1.921130
H	-3.169961	3.055198	-2.299463
C	-1.476304	4.078077	-1.434826
C	-1.893609	5.351366	-1.842352
C	-0.200892	3.939361	-0.863108
C	-1.057090	6.461180	-1.689986
H	-2.879539	5.472559	-2.285228
C	0.636144	5.044906	-0.708474
H	0.134537	2.958449	-0.531781
C	0.210617	6.311365	-1.123034
H	-1.396184	7.441152	-2.015636
H	1.621660	4.918351	-0.267604
H	0.862710	7.172640	-1.005600
H	1.578569	1.794716	0.812310

12A

B3LYP-D3 SCF energy (au):	-1107.45474555
B3LYP-D3 enthalpy (au):	-1107.09956855
B3LYP-D3 free energy (au):	-1107.17464255
wB97X-D SCF energy (au):	-1107.41788933
wB97X-D enthalpy (au):	-1107.06271233
wB97X-D free energy (au):	-1107.13778633
wB97X-D free energy (quasi-harmonic) (au):	-1107.13354078

Cartesian coordinates

ATOM	X	Y	Z
N	-2.931902	0.068205	-0.166833
H	-3.355637	-0.880752	-0.133583
C	-1.594393	0.041766	-0.045370
H	-1.079041	0.989760	-0.031639
C	-0.863300	-1.179725	0.094284
C	0.559063	-1.172170	0.093306
C	1.237992	-2.374245	0.266715
C	-0.705177	-3.601856	0.397238
C	-1.533268	-2.453340	0.222685
H	2.327927	-2.377228	0.269904
N	0.640394	-3.570276	0.423931
O	-2.837334	-2.565121	0.184147
C	-1.384876	-4.936491	0.557527
H	-2.068095	-4.939534	1.418008
H	-2.000830	-5.181808	-0.318816
H	-0.646209	-5.731590	0.696353
C	1.338412	0.090928	-0.155473
H	0.986118	0.576533	-1.078136
H	2.401548	-0.150980	-0.293083
O	1.185156	1.010326	0.951005
C	-3.767193	1.114729	-0.305122
C	-5.198293	0.810865	-0.482061
O	-5.567007	-0.415614	-0.419443
O	-5.991423	1.793217	-0.690004
C	-3.188175	2.489955	-0.356059
H	-3.983470	3.223343	-0.201732
H	-2.462328	2.624771	0.461924

C	-2.465294	2.801680	-1.702109
H	-1.856511	1.935721	-1.988136
H	-3.226045	2.932607	-2.479437
C	-1.581316	4.021450	-1.611271
C	-2.007084	5.270626	-2.083453
C	-0.319592	3.934806	-0.998490
C	-1.196422	6.402258	-1.955481
H	-2.981771	5.354861	-2.559193
C	0.492604	5.062338	-0.867906
H	0.027418	2.976481	-0.616955
C	0.057276	6.302183	-1.347073
H	-1.544167	7.360720	-2.332536
H	1.467138	4.973119	-0.394221
H	0.689837	7.180267	-1.248015
H	1.587767	1.850075	0.672517

RhB

B3LYP-D3 SCF energy (au):	-1420.33486748
B3LYP-D3 enthalpy (au):	-1419.77521548
B3LYP-D3 free energy (au):	-1419.87011848
wB97X-D SCF energy (au):	-1420.22018213
wB97X-D enthalpy (au):	-1419.66053013
wB97X-D free energy (au):	-1419.75543313
wB97X-D free energy (quasi-harmonic) (au):	-1419.74792565

Cartesian coordinates

ATOM	X	Y	Z
C	-7.597490	-4.588117	0.054910
C	-6.183550	-4.470850	0.042316
C	-5.593281	-3.224615	0.068631

C	-6.332698	-2.010687	0.102549
C	-7.749339	-2.145793	0.108228
C	-8.361950	-3.369784	0.087044
C	-5.647188	-0.776692	0.138491
C	-4.237550	-0.783677	0.097022
C	-3.539894	-2.023306	0.056301
C	-2.164900	-2.116379	0.015399
H	-1.727557	-3.103702	-0.042817
C	-1.371740	-0.939550	0.024023
C	-2.059859	0.322849	0.083156
C	-3.426319	0.386462	0.119071
H	-5.534747	-5.334548	-0.008694
H	-8.358178	-1.249077	0.141067
H	-9.442733	-3.408155	0.115628
H	-1.496997	1.245638	0.125194
H	-3.911899	1.354329	0.176241
O	-4.223899	-3.208622	0.044548
N	-0.017298	-0.998154	-0.014094
N	-8.208810	-5.799529	0.038022
C	0.823294	0.203264	-0.137279
H	1.729882	-0.101184	-0.668025
H	0.324589	0.932724	-0.779921
C	1.186375	0.818235	1.213794
H	1.839017	1.685833	1.065678
H	0.290447	1.146443	1.751295
H	1.716530	0.091984	1.839941
C	0.710347	-2.274211	0.052034
H	0.190568	-2.952376	0.733726
H	1.679812	-2.061872	0.511663
C	0.908874	-2.919384	-1.319467

H	1.475807	-3.851090	-1.214529
H	-0.051846	-3.150820	-1.791243
H	1.466597	-2.250441	-1.984285
C	-9.668146	-5.946387	-0.077823
H	-9.849547	-6.897361	-0.586758
H	-10.061557	-5.168813	-0.736887
C	-10.378308	-5.930182	1.275324
H	-10.223076	-4.976227	1.790391
H	-11.454970	-6.076707	1.133964
H	-10.003439	-6.733774	1.919008
C	-7.452168	-7.056567	0.131805
H	-6.601705	-6.917317	0.804015
H	-8.108485	-7.785859	0.615325
C	-6.994997	-7.582036	-1.229031
H	-6.323717	-6.871181	-1.722229
H	-6.461500	-8.530648	-1.102230
H	-7.854780	-7.756234	-1.885481
C	-6.397907	0.508579	0.058481
C	-6.430096	1.158071	-1.184726
C	-7.097861	1.052780	1.152799
C	-7.149117	2.341908	-1.349166
H	-5.892777	0.725591	-2.023837
C	-7.823273	2.235865	0.965519
C	-7.849231	2.883224	-0.268870
H	-7.162022	2.835066	-2.316875
H	-8.363914	2.645993	1.812419
H	-8.410564	3.805785	-0.387716
C	-7.054339	0.400863	2.531563
O	-6.117817	-0.423848	2.742459
O	-7.946948	0.740736	3.359328

[RhB]⁻

B3LYP-D3 SCF energy (au):	-1420.44048507
B3LYP-D3 enthalpy (au):	-1419.88378607
B3LYP-D3 free energy (au):	-1419.98118607
wB97X-D SCF energy (au):	-1420.33923634
wB97X-D enthalpy (au):	-1419.78253734
wB97X-D free energy (au):	-1419.87993734
wB97X-D free energy (quasi-harmonic) (au):	-1419.87130527

Cartesian coordinates

ATOM	X	Y	Z
C	-7.604736	-4.575156	0.092348
C	-6.195398	-4.429766	0.049730
C	-5.612874	-3.174319	0.053721
C	-6.349935	-1.964628	0.096539
C	-7.756622	-2.132698	0.124844
C	-8.366705	-3.377199	0.129815
C	-5.660606	-0.705200	0.068479
C	-4.227511	-0.730120	0.014314
C	-3.540429	-1.969756	-0.016584
C	-2.161907	-2.082728	-0.056610
H	-1.744973	-3.080866	-0.103155
C	-1.339195	-0.928023	-0.052677
C	-2.003147	0.326587	0.000018
C	-3.386093	0.410114	0.033976
H	-5.534016	-5.284915	-0.009262
H	-8.388032	-1.251621	0.159529
H	-9.448082	-3.416776	0.178032
H	-1.433039	1.246622	0.039963

H	-3.843428	1.392308	0.092177
O	-4.228298	-3.172337	-0.011177
N	0.036243	-1.026108	-0.095208
N	-8.200288	-5.819640	0.095218
C	0.891627	0.155412	-0.209092
H	1.809335	-0.156870	-0.718549
H	0.415048	0.887714	-0.868348
C	1.239474	0.792279	1.138699
H	1.897060	1.657492	0.993450
H	0.337004	1.128814	1.660214
H	1.757716	0.072923	1.783328
C	0.723717	-2.310944	0.040191
H	0.174218	-2.948094	0.740683
H	1.693287	-2.114333	0.509711
C	0.933662	-3.034997	-1.291760
H	1.466784	-3.979645	-1.131721
H	-0.023361	-3.257719	-1.775817
H	1.527296	-2.418443	-1.976657
C	-9.649063	-5.981805	-0.033673
H	-9.826531	-6.942224	-0.529098
H	-10.043758	-5.216970	-0.710049
C	-10.389361	-5.947261	1.305301
H	-10.240925	-4.988157	1.813051
H	-11.464990	-6.092766	1.150131
H	-10.027968	-6.743199	1.966729
C	-7.417921	-7.051635	0.195639
H	-6.568272	-6.890018	0.866568
H	-8.050618	-7.799519	0.685347
C	-6.939601	-7.586033	-1.156841
H	-6.289934	-6.862002	-1.660290

H	-6.377456	-8.517561	-1.021255
H	-7.792550	-7.793491	-1.813381
C	-6.401889	0.578764	0.049437
C	-6.272494	1.420132	-1.072659
C	-7.277249	0.974202	1.088995
C	-6.976935	2.618960	-1.173411
H	-5.612656	1.114053	-1.880201
C	-8.007742	2.163427	0.957190
C	-7.855191	2.993492	-0.152850
H	-6.851982	3.248423	-2.050541
H	-8.693280	2.440186	1.753281
H	-8.417763	3.920669	-0.223213
C	-7.436475	0.178668	2.381126
O	-6.384691	-0.261645	2.926582
O	-8.616342	0.052411	2.826113

XVII. ^1H , ^{19}F and ^{13}C NMR spectra of compounds

References

1. K. Chen, F. H. Arnold, Engineering New Catalytic Activities in Enzymes. *Nat. Catal.* **3**, 203-213 (2020).
2. Y. Yang, F. H. Arnold, Navigating the Unnatural Reaction Space: Directed Evolution of Heme Proteins for Selective Carbene and Nitrene Transfer. *Acc. Chem. Res.* **54**, 1209-1225 (2021).
3. O. F. Brandenberg, R. Fasan, F. H. Arnold, Exploiting and Engineering Hemoproteins for Abiological Carbene and Nitrene Transfer Reactions. *Curr. Opin. Biotechnol.* **47**, 102-111 (2017).
4. B. A. Sandoval, T. K. Hyster, Emerging Strategies for Expanding the Toolbox of Enzymes in Biocatalysis. *Curr. Opin. Chem. Biol.* **55**, 45-51 (2020).
5. W. Harrison, X. Huang, H. Zhao, Photobiocatalysis for Abiological Transformations. *Acc. Chem. Res.* **55**, 1087-1096 (2022).
6. C. Klaus, S. C. Hammer, New Catalytic Reactions by Enzyme Engineering. *Trends in Chemistry* **4**, 363-366 (2022).
7. Q. Zhou, M. Chin, Y. Fu, P. Liu, Y. Yang, Stereodivergent Atom-Transfer Radical Cyclization by Engineered Cytochromes P450. *Science* **374**, 1612-1616 (2021).
8. J. Rui *et al.*, Directed Evolution of Nonheme Iron Enzymes to Access Abiological Radical-Relay C(sp³)–H Azidation. *Science* **376**, 869-874 (2022).
9. M. A. Emmanuel, N. R. Greenberg, D. G. Oblinsky, T. K. Hyster, Accessing Non-Natural Reactivity by Irradiating Nicotinamide-Dependent Enzymes with Light. *Nature* **540**, 414-417 (2016).
10. K. F. Biegasiewicz *et al.*, Photoexcitation of Flavoenzymes Enables a Stereoselective Radical Cyclization. *Science* **364**, 1166 (2019).
11. X. Huang *et al.*, Photoenzymatic Enantioselective Intermolecular Radical Hydroalkylation. *Nature* **584**, 69-74 (2020).
12. C. G. Page *et al.*, Quaternary Charge-Transfer Complex Enables Photoenzymatic Intermolecular Hydroalkylation of Olefins. *J. Am. Chem. Soc.* **143**, 97-102 (2021).
13. X. Huang *et al.*, Photoinduced Chemomimetic Biocatalysis for Enantioselective Intermolecular Radical Conjugate Addition. *Nat. Catal.* **5**, 586-593 (2022).

14. Y. Ye *et al.*, Using Enzymes to Tame Nitrogen-Centred Radicals for Enantioselective Hydroamination. *Nat. Chem.* **15**, 206-212 (2023).
15. H. Fu *et al.*, An Asymmetric sp^3 - sp^3 Cross-Electrophile Coupling Using ‘Ene’-Reductases. *Nature* **610**, 302-307 (2022).
16. A. E. Allen, D. W. C. MacMillan, Synergistic Catalysis: A Powerful Synthetic Strategy for New Reaction Development. *Chem. Sci.* **3**, 633-658 (2012).
17. A. C. Eliot, J. F. Kirsch, Pyridoxal Phosphate Enzymes: Mechanistic, Structural, and Evolutionary Considerations. *Annu. Rev. Biochem* **73**, 383-415 (2004).
18. Y.-L. Du, K. S. Ryan, Pyridoxal Phosphate-Dependent Reactions in the Biosynthesis of Natural Products. *Nat. Prod. Rep.* **36**, 430-457 (2019).
19. J. B. Hedges, K. S. Ryan, Biosynthetic Pathways to Nonproteinogenic A-Amino Acids. *Chem. Rev.* **120**, 3161-3209 (2020).
20. Y. Ding *et al.*, Impact of Non-Proteinogenic Amino Acids in the Discovery and Development of Peptide Therapeutics. *Amino Acids* **52**, 1207-1226 (2020).
21. A. Dumas, L. Lercher, C. D. Spicer, B. G. Davis, Designing Logical Codon Reassignment – Expanding the Chemistry in Biology. *Chem. Sci.* **6**, 50-69 (2015).
22. C. Nájera, J. M. Sansano, Catalytic Asymmetric Synthesis of α -Amino Acids. *Chem. Rev.* **107**, 4584-4671 (2007).
23. P. J. Almhjell, C. E. Boville, F. H. Arnold, Engineering Enzymes for Noncanonical Amino Acid Synthesis. *Chem. Soc. Rev.* **47**, 8980-8997 (2018).
24. K. Fesko, G. A. Strohmeier, R. Breinbauer, Expanding the Threonine Aldolase Toolbox for the Asymmetric Synthesis of Tertiary α -Amino Acids. *Appl. Microbiol. Biotechnol.* **99**, 9651-9661 (2015).
25. K. Fesko, M. Uhl, J. Steinreiber, K. Gruber, H. Griengl, Biocatalytic Access to A,A-Dialkyl-A-Amino Acids by a Mechanism-Based Approach. *Angew. Chem. Int. Ed.* **49**, 121-124 (2010).
26. R. S. Phillips, Synthetic Applications of Tryptophan Synthase. *Tetrahedron: Asymmetry* **15**, 2787-2792 (2004).
27. E. Watkins-Dulaney, S. Straathof, F. Arnold, Tryptophan Synthase: Biocatalyst Extraordinaire. *ChemBioChem* **22**, 5-16 (2021).

28. D. Milić *et al.*, Crystallographic Snapshots of Tyrosine Phenol-Lyase Show That Substrate Strain Plays a Role in C–C Bond Cleavage. *J. Am. Chem. Soc.* **133**, 16468-16476 (2011).
29. L. Martínez-Montero, J. H. Schrittwieser, W. Kroutil, Regioselective Biocatalytic Transformations Employing Transaminases and Tyrosine Phenol Lyases. *Top. Catal.* **62**, 1208-1217 (2019).
30. T. H. P. Maier, Semisynthetic Production of Unnatural L- α -Amino Acids by Metabolic Engineering of the Cysteine-Biosynthetic Pathway. *Nat. Biotechnol.* **21**, 422-427 (2003).
31. W. M. Rabeh, P. F. Cook, Structure and Mechanism of O-Acetylserine Sulphydrylase. *J. Biol. Chem.* **279**, 26803-26806 (2004).
32. R. J. M. Goss, P. L. A. Newill, A Convenient Enzymatic Synthesis of L-Halotryptophans. *Chem. Commun.*, 4924-4925 (2006).
33. A. R. Buller *et al.*, Directed Evolution of the Tryptophan Synthase β -Subunit for Stand-Alone Function Recapitulates Allosteric Activation. *Proc. Natl. Acad. Sci. U.S.A.* **112**, 14599-14604 (2015).
34. Y. Hai, M. Chen, A. Huang, Y. Tang, Biosynthesis of Mycotoxin Fusaric Acid and Application of a PLP-Dependent Enzyme for Chemoenzymatic Synthesis of Substituted L-Pipecolic Acids. *J. Am. Chem. Soc.* **142**, 19668-19677 (2020).
35. M. Chen, C.-T. Liu, Y. Tang, Discovery and Biocatalytic Application of a PLP-Dependent Amino Acid γ -Substitution Enzyme That Catalyzes C–C Bond Formation. *J. Am. Chem. Soc.* **142**, 10506-10515 (2020).
36. Q. Wang, Q. Gu, S.-L. You, Enantioselective Carbonyl Catalysis Enabled by Chiral Aldehydes. *Angew. Chem. Int. Ed.* **58**, 6818-6825 (2019).
37. P. A. Frey, G. H. Reed, Pyridoxal-5'-Phosphate as the Catalyst for Radical Isomerization in Reactions of Plp-Dependent Aminomutases. *Biochim. Biophys. Acta* **1814**, 1548-1557 (2011).
38. E. R. Hoffarth, K. W. Rothchild, K. S. Ryan, Emergence of Oxygen- and Pyridoxal Phosphate-Dependent Reactions. *The FEBS Journal* **287**, 1403-1428 (2020).
39. E. R. Hoffarth *et al.*, A Shared Mechanistic Pathway for Pyridoxal Phosphate-Dependent Arginine Oxidases. *Proc. Natl. Acad. Sci. U.S.A.* **118**, e2012591118 (2021).

40. J. M. R. Narayananam, C. R. J. Stephenson, Visible Light Photoredox Catalysis: Applications in Organic Synthesis. *Chem. Soc. Rev.* **40**, 102-113 (2011).
41. C. K. Prier, D. A. Rankic, D. W. C. MacMillan, Visible Light Photoredox Catalysis with Transition Metal Complexes: Applications in Organic Synthesis. *Chem. Rev.* **113**, 5322-5363 (2013).
42. N. A. Romero, D. A. Nicewicz, Organic Photoredox Catalysis. *Chem. Rev.* **116**, 10075-10166 (2016).
43. K. L. Skubi, T. R. Blum, T. P. Yoon, Dual Catalysis Strategies in Photochemical Synthesis. *Chem. Rev.* **116**, 10035-10074 (2016).
44. M. Zhang, L. Wang, S. Shu, A. Sancar, D. Zhong, Bifurcating Electron-Transfer Pathways in DNA Photolyases Determine the Repair Quantum Yield. *Science* **354**, 209-213 (2016).
45. D. Sorigué *et al.*, An Algal Photoenzyme Converts Fatty Acids to Hydrocarbons. *Science* **357**, 903-907 (2017).
46. S. Zhang *et al.*, Structural Basis for Enzymatic Photocatalysis in Chlorophyll Biosynthesis. *Nature* **574**, 722-725 (2019).
47. S. Tang, X. Zhang, J. Sun, D. Niu, J. J. Chruma, 2-Azaallyl Anions, 2-Azaallyl Cations, 2-Azaallyl Radicals, and Azomethine Ylides. *Chem. Rev.* **118**, 10393-10457 (2018).
48. D. R. Weinberg *et al.*, Proton-Coupled Electron Transfer. *Chem. Rev.* **112**, 4016-4093 (2012).
49. R. G. Agarwal *et al.*, Free Energies of Proton-Coupled Electron Transfer Reagents and Their Applications. *Chem. Rev.* **122**, 1-49 (2022).
50. J. C. Tellis, D. N. Primer, G. A. Molander, Single-Electron Transmetalation in Organoboron Cross-Coupling by Photoredox/Nickel Dual Catalysis. *Science* **345**, 433-436 (2014).
51. M. Herger *et al.*, Synthesis of β -Branched Tryptophan Analogues Using an Engineered Subunit of Tryptophan Synthase. *J. Am. Chem. Soc.* **138**, 8388-8391 (2016).
52. A. R. Buller *et al.*, Directed Evolution Mimics Allosteric Activation by Stepwise Tuning of the Conformational Ensemble. *J. Am. Chem. Soc.* **140**, 7256-7266 (2018).
53. G. R. Pettit *et al.*, Antineoplastic Agents. 599. Total Synthesis of Dolastatin 16. *J. Nat. Prod.* **78**, 476-485 (2015).

54. J. Kimura *et al.*, Kulokekahilide-1, a Cytotoxic Depsipeptide from the Cephalaspidean Mollusk *Philinopsis Speciosa*. *J. Org. Chem.* **67**, 1760-1767 (2002).
55. C. J. Easton, M. C. Merrett, Stereoselective Synthesis of (2S,3S)- γ -Hydroxyvaline Utilising an Asymmetric Radical Hydrogen Bromide Addition. *Tetrahedron* **53**, 1151-1156 (1997).
56. D. J. Tantillo, J. Chen, K. N. Houk, Theozymes and Compuzymes: Theoretical Models for Biological Catalysis. *Curr. Opin. Chem. Biol.* **2**, 743-750 (1998).
57. J. Xu *et al.*, Structural Studies Reveal Flexible Roof of Active Site Responsible for Ω -Transaminase Crmg Overcoming by-Product Inhibition. *Commun. Biol.* **3**, 455 (2020).
58. L. Yang *et al.*, Mechanism-Guided Computational Design of ω -Transaminase by Reprograming of High-Energy-Barrier Steps. *Angew. Chem. Int. Ed.* **61**, e202212555 (2022).
59. X. Sheng, F. Himo, Enzymatic Pictet–Spengler Reaction: Computational Study of the Mechanism and Enantioselectivity of Norcoclaurine Synthase. *J. Am. Chem. Soc.* **141**, 11230-11238 (2019).
60. R. Bhushan, H. Brückner, Marfey's Reagent for Chiral Amino Acid Analysis: A Review. *Amino Acids* **27**, 231-247 (2004).
61. D. K. Romney, J. Murciano-Calles, J. E. Wehrmüller, F. H. Arnold, Unlocking Reactivity of TrpB: A General Biocatalytic Platform for Synthesis of Tryptophan Analogues. *J. Am. Chem. Soc.* **139**, 10769-10776 (2017).
62. C. E. Boville *et al.*, Engineered Biosynthesis of β -Alkyl Tryptophan Analogues. *Angew. Chem. Int. Ed.* **57**, 14764-14768 (2018).
63. D. G. Gibson *et al.*, Enzymatic Assembly of DNA Molecules Up to Several Hundred Kilobases. *Nat. Methods* **6**, 343-345 (2009).
64. P. Marfey, Determination of D-Amino Acids. II. Use of a Bifunctional Reagent, 1,5-Difluoro-2,4-Dinitrobenzene. *Carlsberg Res. Commun.* **49**, 591-596 (1984).
65. H. Brückner, C. Keller-Hoehl, HPLC Separation of DL-Amino Acids Derivatized With N^2 -(5-Fluoro-2,4-Dinitrophenyl)-L-Amino Acid Amides. *Chromatographia* **30**, 621-629 (1990).
66. K. H. Nielsen, Paper Chromatographic Determination of Aromatic α -Keto Acids. *J. Chromatogr. A* **10**, 463-472 (1963).

67. G. A. Molander, L. N. Cavalcanti, Oxidation of Organotrifluoroborates via Oxone. *J. Org. Chem.* **76**, 623-630 (2011).
68. I. Romero-Estudillo, V. R. Batchu, A. Boto, One-Pot Conversion of Amino Acids into 2,5-Disubstituted Oxazoles: No Metals Needed. *Adv. Synth. Catal.* **356**, 3742-3748 (2014).
69. E. E. Stache, T. Rovis, A. G. Doyle, Dual Nickel- and Photoredox-Catalyzed Enantioselective Desymmetrization of Cyclic Meso-Anhydrides. *Angew. Chem. Int. Ed.* **56**, 3679-3683 (2017).
70. S. Y. Go *et al.*, A Unified Synthetic Strategy to Introduce Heteroatoms via Electrochemical Functionalization of Alkyl Organoboron Reagents. *J. Am. Chem. Soc.* **144**, 9149-9160 (2022).
71. H. Huang *et al.*, Suzuki-Type Cross-Coupling of Alkyl Trifluoroborates with Acid Fluoride Enabled by NHC/Photoredox Dual Catalysis. *Chem. Sci.* **13**, 2584-2590 (2022).
72. C.-T. Yang *et al.*, Alkylboronic Esters from Copper-Catalyzed Borylation of Primary and Secondary Alkyl Halides and Pseudohalides. *Angew. Chem. Int. Ed.* **51**, 528-532 (2012).
73. A. Giroux, Synthesis of Benzylic Boronates via Palladium-Catalyzed Cross-Coupling Reaction of Bis(pinacolato)diboron with Benzylic Halides. *Tetrahedron Lett.* **44**, 233-235 (2003).
74. J. Huang, W. Yan, C. Tan, W. Wu, H. Jiang, Palladium-Catalyzed Regioselective Hydroboration of Aryl Alkenes with $B_2\text{pin}_2$. *Chem. Comm.* **54**, 1770-1773 (2018).
75. M. V. Pavan *et al.*, New Anthranilic Acid Based Antagonists with High Affinity Andselectivity for the Human Cholecystokinin Receptor 1 (hCCK₁-R). *J. Med. Chem.* **54**, 5769-5785 (2011).
76. B. Kandagatla *et al.*, Practical Synthesis of Fingolimod from Diethyl Acetamidomalonate. *RSC Adv.* **3**, 9687 (2013).
77. A. Mi *et al.*, Amino Acid Anhydride Hydrochlorides as Acylating Agents in Friedel-Crafts Reaction: A Practical Synthesis of L-Homophenylalanine. *Synthesis* **2001**, 1007-1009 (2004).
78. M. F. Oldfield, R. N. Bennett, G. Kiddie, R. M. Wallsgrave, N. P. Botting, Biochemical Characterisation of An Aldoxime-Forming Flavoprotein Involved in 2-

- Phenylethylglucosinolate Biosynthesis in Brassica Species. *Plant Physiol. Biochem.* **37**, 99-108 (1999).
79. M. Sabat, C. R. Johnson, Synthesis of Unnatural Amino Acids via Suzuki Cross-Coupling of Enantiopure Vinyloxazolidine Derivatives. *Org. Lett.* **2**, 1089-1092 (2000).
80. L. Shi *et al.*, Chiral Pyridoxal-Catalyzed Asymmetric Biomimetic Transamination of α -Keto Acids. *Org. Lett.* **17**, 5784-5787 (2015).
81. L. Noodleman, T. Lovell, W.-G. Han, J. Li, F. Himo, Quantum Chemical Studies of Intermediates and Reaction Pathways in Selected Enzymes and Catalytic Synthetic Systems. *Chem. Rev.* **104**, 459-508 (2004).
82. R. Anandakrishnan, B. Aguilar, A. V. Onufriev, H++ 3.0: Automating pK Prediction and the Preparation of Biomolecular Structures for Atomistic Molecular Modeling and Simulations. *Nucleic Acids Res.* **40**, W537-W541 (2012).
83. M. J. Frisch *et al.* (Wallingford, CT, 2016).
84. J. Towns *et al.*, XSEDE: Accelerating Scientific Discovery. *Comput. Sci. Eng.* **16**, 62-74 (2014).
85. S. Grimme, J. Antony, S. Ehrlich, H. Krieg, A Consistent and Accurate *Ab Initio* Parametrization of Density Functional Dispersion Correction (DFT-D) for the 94 Elements H-Pu. *J. Chem. Phys.* **132**, 154104 (2010).
86. C. Lee, W. Yang, R. G. Parr, Development of the Colle-Salvetti Correlation-Energy Formula into a Functional of the Electron Density. *Phys. Rev. B* **37**, 785-789 (1988).
87. A. D. Becke, Density Functional Thermochemistry. III. The Role of Exact Exchange. *J. Chem. Phys.* **98**, 5648-5652 (1993).
88. J.-D. Chai, M. Head-Gordon, Long-Range Corrected Hybrid Density Functionals with Damped Atom–Atom Dispersion Corrections. *Phys. Chem. Chem. Phys.* **10**, 6615-6620 (2008).
89. A. V. Marenich, C. J. Cramer, D. G. Truhlar, Universal Solvation Model Based on Solute Electron Density and on a Continuum Model of the Solvent Defined by the Bulk Dielectric Constant and Atomic Surface Tensions. *J. Phys. Chem. B* **113**, 6378-6396 (2009).

90. C. Li, W. Wu, D. Kumar, S. Shaik, Kinetic Isotope Effect Is a Sensitive Probe of Spin State Reactivity in C–H Hydroxylation of *N,N*-Dimethylaniline by Cytochrome P450. *J. Am. Chem. Soc.* **128**, 394-395 (2006).
91. D. Usharani, D. Janardanan, S. Shaik, Does the Taud Enzyme Always Hydroxylate Alkanes, While an Analogous Synthetic Non-Heme Reagent Always Desaturates Them? *J. Am. Chem. Soc.* **133**, 176-179 (2011).
92. P. E. M. Siegbahn, F. Himo, The Quantum Chemical Cluster Approach for Modeling Enzyme Reactions. *WIREs Comput. Mol. Sci.* **1**, 323-336 (2011).
93. B. Li *et al.*, Mechanism of the Stereoselective Catalysis of Diels–Alderase PyrE3 Involved in Pyrroindomycin Biosynthesis. *J. Am. Chem. Soc.* **144**, 5099-5107 (2022).
94. N. M. F. S. A. Cerqueira, P. A. Fernandes, M. J. Ramos, Computational Mechanistic Studies Addressed to the Transimination Reaction Present in All Pyridoxal 5'-Phosphate-Requiring Enzymes. *J. Chem. Theory Comput.* **7**, 1356-1368 (2011).
95. R. W. Ramette, E. B. Sandell, Rhodamine B Equilibria. *J. Am. Chem. Soc.* **78**, 4872-4878 (1956).
96. W. Chi, Q. Qi, R. Lee, Z. Xu, X. Liu, A Unified Push–Pull Model for Understanding the Ring-Opening Mechanism of Rhodamine Dyes. *J. Phys. Chem. C* **124**, 3793-3801 (2020).
97. J. E. Bartmess, Thermodynamics of the Electron and the Proton. *J. Phys. Chem.* **98**, 6420-6424 (1994).
98. J. E. Bartmess, Thermodynamics of the Electron and the Proton. *J. Phys. Chem.* **99**, 6755-6755 (1995).
99. A. A. Isse, A. Gennaro, Absolute Potential of the Standard Hydrogen Electrode and the Problem of Interconversion of Potentials in Different Solvents. *J. Phys. Chem. B* **114**, 7894-7899 (2010).
100. M. Okada, I. Nishio, F. Takahashi, H. Tatsumi, J. Jin, Cathodic Electrochemiluminescence from Rhodamine B in Aqueous Media Using Peroxydisulfate as Co-Reactant. *Chem. Lett.* **50**, 1659-1661 (2021).
101. C. C. Moser, J. M. Keske, K. Warncke, R. S. Farid, P. L. Dutton, Nature of Biological Electron Transfer. *Nature* **355**, 796-802 (1992).

102. H. B. Gray, J. R. Winkler, Electron Transfer in Proteins. *Annu. Rev. Biochem.* **65**, 537-561 (1996).
103. J. Blumberger, Recent Advances in the Theory and Molecular Simulation of Biological Electron Transfer Reactions. *Chem. Rev.* **115**, 11191-11238 (2015).
104. P. Kyritsis, J. G. Huber, I. Quinkal, J. Gaillard, J.-M. Moulis, Intramolecular Electron Transfer between [4Fe-4S] Clusters Studied by Proton Magnetic Resonance Spectroscopy. *Biochemistry* **36**, 7839-7846 (1997).
105. J. P. Roth, J. P. Klinman, Catalysis of Electron Transfer During Activation of O₂ by the Flavoprotein Glucose Oxidase. *Proc. Natl. Acad. Sci. U.S.A.* **100**, 62-67 (2003).
106. D. S. Wuttke, M. J. Bjerrum, J. R. Winkler, H. B. Gray, Electron-Tunneling Pathways in Cytochrome C. *Science* **256**, 1007-1009 (1992).
107. A. J. Di Bilio *et al.*, Reorganization Energy of Blue Copper: Effects of Temperature and Driving Force on the Rates of Electron Transfer in Ruthenium- and Osmium-Modified Azurins. *J. Am. Chem. Soc.* **119**, 9921-9922 (1997).
108. H. B. Gray, J. R. Winkler, Long-Range Electron Transfer. *Proc. Natl. Acad. Sci. U.S.A.* **102**, 3534-3539 (2005).
109. M. Casella, A. Magistrato, I. Tavernelli, P. Carloni, U. Rothlisberger, Role of Protein Frame and Solvent for the Redox Properties of Azurin from *Pseudomonas aeruginosa*. *Proc. Natl. Acad. Sci. U.S.A.* **103**, 19641-19646 (2006).
110. A. A. Voityuk, N. Rösch, Fragment Charge Difference Method for Estimating Donor-Acceptor Electronic Coupling: Application to DNA π-Stacks. *J. Chem. Phys.* **117**, 5607-5616 (2002).
111. Y. Shao *et al.*, Advances in Molecular Quantum Chemistry Contained in the Q-Chem 4 Program Package. *Mol. Phys.* **113**, 184-215 (2015).
112. H. B. Gray, J. R. Winkler, Electron Flow through Proteins. *Chem. Phys. Lett.* **483**, 1-9 (2009).
113. J. R. Winkler, H. B. Gray, Electron Flow through Metalloproteins. *Chem. Rev.* **114**, 3369-3380 (2014).

114. Y. Miao, A. Bhattacharai, J. Wang, Ligand Gaussian Accelerated Molecular Dynamics (Ligamd): Characterization of Ligand Binding Thermodynamics and Kinetics. *J. Chem. Theory Comput.* **16**, 5526-5547 (2020).
115. D. A. Case *et al.* (University of California, San Francisco, CA, 2020).
116. A. D. Becke, Density-Functional Exchange-Energy Approximation with Correct Asymptotic Behavior. *Phys. Rev. A* **38**, 3098-3100 (1988).
117. J. Wang, R. M. Wolf, J. W. Caldwell, P. A. Kollman, D. A. Case, Development and Testing of A General Amber Force Field. *J. Comput. Chem.* **25**, 1157-1174 (2004).
118. U. C. Singh, P. A. Kollman, An Approach to Computing Electrostatic Charges for Molecules. *J. Comp. Chem.* **5**, 129-145 (1984).
119. B. H. Besler, K. M. Merz Jr, P. A. Kollman, Atomic Charges Derived from Semiempirical Methods. *J. Comp. Chem.* **11**, 431-439 (1990).
120. C. I. Bayly, P. Cieplak, W. Cornell, P. A. Kollman, A Well-Behaved Electrostatic Potential Based Method Using Charge Restraints for Deriving Atomic Charges: The RESP Model. *J. Phys. Chem.* **97**, 10269-10280 (1993).
121. Y. Liu *et al.*, CB-Dock2: Improved Protein–Ligand Blind Docking by Integrating Cavity Detection, Docking and Homologous Template Fitting. *Nucleic Acids Res.* **50**, W159-W164 (2022).
122. W. L. Jorgensen, J. Chandrasekhar, J. D. Madura, R. W. Impey, M. L. Klein, Comparison of Simple Potential Functions for Simulating Liquid Water. *J. Chem. Phys.* **79**, 926-935 (1983).
123. J.-P. Ryckaert, G. Ciccotti, H. J. C. Berendsen, Numerical Integration of the Cartesian Equations of Motion of A System with Constraints: Molecular Dynamics of *N*-Alkanes. *J. Comput. Phys.* **23**, 327-341 (1977).
124. T. Darden, D. York, L. Pedersen, Particle Mesh Ewald: An *N*-Log(*N*) Method for Ewald Sums in Large Systems. *J. Chem. Phys.* **98**, 10089-10092 (1993).
125. G. M. Morris *et al.*, AutoDock4 and AutoDockTools4: Automated Docking with Selective Receptor Flexibility. *J Comput Chem.* **30**, 2785-2791 (2009).